Study of the insulin-sensitizing effect of myo-inositol in mouse : Evaluation of the nutritional interest of a myo-inositol supplementation

Marine Croze

THÈSE

Présentée devant

L'INSTITUT NATIONAL DES SCIENCES APPLIQUÉES DE LYON

pour obtenir

LE GRADE DE DOCTEUR

Ecole Doctorale Interdisciplinaire Science Santé (ED205)
Champ disciplinaire : Biochimie

Study of the insulin-sensitizing effect of *myo*-inositol in mouse

Evaluation of the nutritional interest of *myo*-inositol supplementation

---

Soutenue publiquement le 27 Novembre 2013 par

Marine CROZE

Sous la direction de :

Dr. Christophe SOULAGE et Pr. Michel GUICHARDANT

Membres du Jury :
Dr. Karine COUTURIER, Examinateur
Pr. Michel GUICHARDANT, Directeur de thèse
Pr. Béatrice MORIO, Rapporteur
Pr. Michel NARCE, Rapporteur
Dr. Christophe SOULAGE, Directeur de thèse
Dr. Hubert VIDAL, Président du jury

Thèse réalisée au sein de l'unité INSERM U1060 / INSA de Lyon
"Cardiovasculaire, Métabolisme, Diabétologie et Nutrition"

Preface

This work has been performed in the research institute directed by Hubert Vidal :

"Cardiovascular, Metabolism, Diabetes and Nutrition (CarMeN)"
INSERM U1060 ; UCBL ; INSA-Lyon
IMBL, 11 Av. Jean Capelle
69621 Villeurbanne, France

It has given rise to the redaction of the following articles :

1. Marine L. Croze, Roxane E. Vella, Nicolas, J. Pillon, Hédi A. Soula, Lilas Hadji, Michel Guichardant, Christophe O. Soulage. *« Chronic treatment with myo-inositol reduces white adipose tissue accretion and improves insulin sensitivity in female mice ».* Journal of Nutritional Biochemistry. 2013 ; 24(2):457-66.

2. Marine L. Croze, Christophe O. Soulage. *« Potential role and therapeutic interest of myo-inositol in metabolic diseases ».* Biochimie. 2013 ; 95 : 1811-1827.

3. Marine L. Croze, Michel Guichardant, Christophe O. Soulage. « *myo*-Inositol dietary supplement reduces fat accretion and improves insulin sensitivity in mice fed a high fat diet». In preparation for the British Journal of Nutrition.

And to the presentation of the following communications :

Talk presentations

- Marine L. Croze. *« Use of a high fat diet mouse model of insulin resistance and obesity to test the interest of a nutritional supplementation based on myo-inositol ».* 1st Thematic School of EGID, September 2013 (Cap Hornu).

- Marine L. Croze, Roxane E. Vella, Nicolas, J. Pillon, Hédi A. Soula, Lilas Hadji, Michel Guichardant, Christophe O. Soulage. *« Dietary myo-inositol supplement improves insulin sensitivity in female mice ».* 17th Scientific Day of the EDISS Doctoral School, October 2012 (Lyon).

- Marine L. Croze, Roxane E. Vella, Nicolas, J. Pillon, Hédi A. Soula, Lilas Hadji, Michel Guichardant, Christophe O. Soulage. *« Chronic treatment with myo-inositol reduces white adipose tissue accretion and improves insulin sensitivity in female mice »* Young Researchers in Life Science Congress, may 2011. (Paris)

Poster presentations

- Marine L. Croze, Roxane E. Vella, Nicolas, J. Pillon, Hédi A. Soula, Lilas Hadji, Michel Guichardant, Christophe O. Soulage. *« Chronic treatment with myo-inositol reduces fat accretion and improves insulin sensitivity in mouse ».* Annual SFD ("Société Francophone du Diabète") congress, March 2012 (Nice) and G2L2 congress, march 2012 (Lyon).

- Marine L. Croze, Roxane E. Vella, Nicolas, J. Pillon, Michel Guichardant, Christophe O. Soulage. *« Chronic treatment with myo-inositol improves oxidative stress resistance capacity and insulin sensitivity in mouse ».* Annual G2L2 congress, October 2010 (Lausanne) and SFD ("Société Francophone du Diabète") congress, March 2011 (Geneva).

I also contributed to other research projects which have given rise to the redaction and publication of the following articles:

1. Nicolas J. Pillon, Laurent Soulère, Roxane E. Vella, <u>Marine Croze</u>, Bertrand Caré, Hédi A. Soula, Alain Doutheau, Michel Lagarde, Christophe O. Soulage. *« Quantitative structure-activity relationship for 4-hydroxy-2-alkenal induced cytotoxicity in L6 muscle cells »*. Chemico-biological Interactions. 2010 ; 188(1):171-80

2. Nicolas J. Pillon, <u>Marine L. Croze</u>, Roxane E. Vella, Laurent Soulère, Michel Lagarde, Christophe O. Soulage. *« The lipid peroxidation by-product 4-Hydro-2-Nonenal (4-HNE) induces insulin resistance in skeletal muscle through both carbonyl and oxidative stress »*. Endocrinology. 2012 ; 153(5):2099-111

3. Laetitia Koppe, Nicolas J. Pillon, Roxane E. Vella, <u>Marine L. Croze</u>, Caroline C. Pelletier, Stéphane Chambert, Ziad Massy, Griet Glorieux, Raymond Vanholder, Yann Dugenet, Hedi A. Soula, Denis Fouque, Christophe O. Soulage. *« p-cresyl sulfate promotes insulin resistance associated with Chronic Kidney Disease »*. Journal of the American Society of Nephrology. 2012 ; 24(1):88-99

4. Caroline C. Pelletier, Laetitia Koppe, <u>Marine L. Croze</u>, Emilie Kalbacher, Roxane E. Vella, Fitsum Guebre-Egziabher,Alain Géloën, Lionel Badet, Denis Fouque, Christophe O. Soulage. « *White adipose tissue overproduces the lipid-mobilizing factor zinc α2-glycoprotein in chronic kidney disease* ». Kidney International. 2013 ; 83 : 878-886.

5. Roxane E. Vella, Nicolas J. Pillon, Bader Zarrouki, <u>Marine L. Croze</u>, Laetitia Koppe, Michel Guichardant, Alain Géloën, Christophe O. Soulage. « *Ozone exposure triggers insulin resistance through muscle endoplasmic reticulum stress* ». Diabetes. Submitted (in revision).

And I also presented the following communications :

<u>Talk presentations</u>

- <u>Marine L. Croze,</u> Nicolas J. Pillon, Bader Zarrouki, Roxane Vella, Michel Guichardant, Michel Lagarde, Christophe Soulage. « *Role of advanced lipid peroxydation by-products HHE and HNE in the pathophysiology of insulin resistance* ». Annual G2L2 Congress , march 2013 (Geneva)
- Nicolas J. Pillon, <u>Marine L. Croze,</u> Roxane E. Vella, Laurent Soulère, Michel Lagarde, Christophe O. Soulage. *« The lipid peroxidation by-product 4-Hydro-2-Nonenal (4-HNE) induces insulin resistance in skeletal muscle».* 15th Scientific Day of the EDISS Doctoral School, March 2010 (Lyon).

<u>Posters presentations</u>

- <u>Marine L. Croze</u>, Stéphane Chambert, Louise Grand, Hédi A. Soula, Alain Geloën, Christophe O. Soulage. *« Cirsimaritin inhibits lipogenesis and reduces fat accretion in mouse».* Annual AFERO (Association Française d'Etude et Recherche sur l'Obésité) Congress, January 2013 (Paris) and annual SFD ("Société Francophone du Diabète") Congress, march 2013 (Montpellier).
- Nicolas J. Pillon, Bader Zarrouki, <u>Marine Croze</u>, Roxane Vella, Michel Guichardant, Michel Lagarde et Christophe O. Soulage. *« Role of 4-hydroxy-2-hexenal, the omega-3 fatty acids lipid peroxydation by product, in the pathophysiology of insulin resistance».* Annual SFD ("Société Francophone du Diabète") Congress, march 2012 (Nice).

2

INSA-Lyon related Doctoral Schools

SIGLE	ECOLE DOCTORALE	NOM ET COORDONNEES DU RESPONSABLE
CHIMIE	**CHIMIE DE LYON** **http://www.edchimie-lyon.fr** Insa : R. GOURDON	M. Jean Marc LANCELIN Université de Lyon – Collège Doctoral Bât ESCPE 43 bd du 11 novembre 1918 69622 VILLEURBANNE Cedex Tél : 04.72.43 13 95 directeur@edchimie-lyon.fr
E.E.A.	**ELECTRONIQUE,** **ELECTROTECHNIQUE, AUTOMATIQUE** **http://edeea.ec-lyon.fr** Secrétariat : M.C. HAVGOUDOUKIAN eea@ec-lyon.fr	M. Gérard SCORLETTI Ecole Centrale de Lyon 36 avenue Guy de Collongue 69134 ECULLY Tél : 04.72.18 65 55 Fax : 04 78 43 37 17 Gerard.scorletti@ec-lyon.fr
E2M2	**EVOLUTION, ECOSYSTEME,** **MICROBIOLOGIE, MODELISATION** **http://e2m2.universite-lyon.fr** Insa : H. CHARLES	Mme Gudrun BORNETTE CNRS UMR 5023 LEHNA Université Claude Bernard Lyon 1 Bât Forel 43 bd du 11 novembre 1918 69622 VILLEURBANNE Cédex Tél : 06.07.53.89.13 e2m2@ univ-lyon1.fr
EDISS	**INTERDISCIPLINAIRE SCIENCES-** **SANTE** **http://www.ediss-lyon.fr** Sec : Samia VUILLERMOZ Insa : M. LAGARDE	M. Didier REVEL Hôpital Louis Pradel Bâtiment Central 28 Avenue Doyen Lépine 69677 BRON Tél : 04.72.68.49.09 Fax :04 72 68 49 16 Didier.revel@creatis.uni-lyon1.fr
INFOMATHS	**INFORMATIQUE ET** **MATHEMATIQUES** **http://infomaths.univ-lyon1.fr** Sec :Renée EL MELHEM	Mme Sylvie CALABRETTO Université Claude Bernard Lyon 1 INFOMATHS Bâtiment Braconnier 43 bd du 11 novembre 1918 69622 VILLEURBANNE Cedex Tél : 04.72. 44.82.94 Fax 04 72 43 16 87 infomaths@univ-lyon1.fr
Matériaux	**MATERIAUX DE LYON** **http://ed34.universite-lyon.fr** Secrétariat : M. LABOUNE PM : 71.70 –Fax : 87.12 Bat. Saint Exupéry Ed.materiaux@insa-lyon.fr	M. Jean-Yves BUFFIERE INSA de Lyon MATEIS Bâtiment Saint Exupéry 7 avenue Jean Capelle 69621 VILLEURBANNE Cedex Tél : 04.72.43 83 18 Fax 04 72 43 85 28 Jean-yves.buffiere@insa-lyon.fr
MEGA	**MECANIQUE, ENERGETIQUE, GENIE** **CIVIL, ACOUSTIQUE** **http://mega.ec-lyon.fr** Secrétariat : M. LABOUNE PM : 71.70 –Fax : 87.12 Bat. Saint Exupéry mega@insa-lyon.fr	M. Philippe BOISSE INSA de Lyon Laboratoire LAMCOS Bâtiment Jacquard 25 bis avenue Jean Capelle 69621 VILLEURBANNE Cedex Tél :04.72 .43.71.70 Fax : 04 72 43 72 37 Philippe.boisse@insa-lyon.fr
ScSo	**ScSo*** **http://recherche.univ-lyon2.fr/scso/** Sec : Viviane POLSINELLI Brigitte DUBOIS Insa : J.Y. TOUSSAINT	M. OBADIA Lionel Université Lyon 2 86 rue Pasteur 69365 LYON Cedex 07 Tél : 04.78.77.23.86 Fax : 04.37.28.04.48 Lionel.Obadia@univ-lyon2.fr

*ScSo : Histoire, Géographie, Aménagement, Urbanisme, Archéologie, Science politique, Sociologie, Anthropologie

Table of Contents

Remerciements (acknowledgments)

Je tiens à remercier tout particulièrement **Christophe SOULAGE** pour l'encadrement de ma thèse. Un grand merci donc pour ta disponibilité, ton écoute, la cellule de soutien psychologique dans les moments de déprime ;-) et pour tes conseils scientifiques ou personnels. Merci également de m'avoir soutenue dans mes différentes candidatures et de m'avoir fait confiance, notamment pour l'OT. Enfin, un grand merci aussi pour la bonne ambiance que tu as su mettre dans l'équipe et qui a fait que je suis toujours venue au labo avec plaisir et ce malgré les déceptions occasionnées par certains résultats… Merci aussi pour l'enrichissement de mon vocabulaire ;-)

Merci à **Michel GUICHARDANT** pour les discussions scientifiques, et l'apport de son expertise en biochimie. Merci également pour son soutien, ses conseils et sa disponibilité.

Merci à **Hubert VIDA**L de m'avoir accueillie dans son laboratoire et soutenue dans mes projets post-doctoraux.

Merci à **Hedi SOULA**, pour ses ineffables conversations lors des pauses café, pour ses conseils vestimentaires que je n'ai jamais écoutés et pour ses clips qui me remettent toujours de bonne humeur. Et bien évidemment, merci pour la guitare!

Merci à **Roxane** pour son aide sur les manips et pour son amitié. J'ai beaucoup apprécié le fait qu'on ait fait nos thèses ensemble et qu'on ait pu partager nos problèmes de manips, nos angoisses sur nos avenir professionnels, nos chambres en congrès et le même bureau ! Merci aussi pour un certain midi de Novembre 2012 ;-)

Merci à **Nicolas** de m'avoir formée à la culture cellulaire et au western blot et pour ses conseils rédactionnels.

Merci à **Laetitia**, **Caroline**, **Pascaline**, **Bertrand**, **Fabien**, **Cyril** et les chimistes (**Stéphane, Laurent, Pedro**) pour les conversations et les bons moments aux pauses repas, ou autour d'une boisson chaude ou froide. Merci notamment à Cyril pour les références cinématographiques, et à Fabien pour les conseils écologistes.

Merci à **Michel Narce**, **Béatrice Morio** et **Karine Couturier** d'avoir accepté de participer à mon jury de thèse.

Merci à **l'ensemble des membres de l'unité CarMeN** pour leur aide et/ou leur sympathie, et en particulier merci aux autres doctorants (Bérengère, Manar, Hui, Maud, Mayssa, Manon, Charlotte…) avec qui j'ai pu discuter, partager quelques soirées ou échanger des conseils ou du matériel pour les manips.

Merci à **Bénédicte**, **Blandine**, **Thomas**, **Romain** et **Alexia,** pour leur amitié sur laquelle je peux toujours compter.

Merci à **Simon, mes parents et ma belle-famille** pour leur soutien précieux et permanent, ainsi que pour leur confiance et leur curiosité vis-à-vis de mes travaux de recherche.

8

Abstract

Study of the insulin-sensitizing effect of *myo*-inositol in mouse:
Evaluation of the nutritional interest of a *myo*-inositol supplementation

Insulin resistance is the first step in the development of type 2 diabetes thus finding insulin-sensitizing strategies is challenging for scientists. Some inositol isomers or derivatives have been reported to exert insulin-mimetic activity. *myo*-Inositol being the most abundant stereoisomeric form of inositol in foodstuffs, we tested its insulin-mimetic potential in the long term and as a nutritional strategy for insulin resistance prevention and/or treatment.

This study demonstrates that chronic *myo*-inositol treatment improves insulin sensitivity and reduces white adipose tissue accretion in mouse. The insulin-sensitizing effect seems to be related to a direct effect on insulin signaling pathway. Reduction in adipose tissue mass also probably contribute to the long term effect of *myo*-inositol on insulin sensitivity.

myo-Inositol supplementation also improved insulin sensitivity and reduced white adipose tissue deposition in mice fed a high fat diet, but did not prevent insulin-resistance or obesity development. On one year-old mice with established obesity and altered glycemic control, *myo*-inositol supplementation showed no beneficial effect. *myo*-Inositol apparently acts on adipose tissue through reduction of *de novo* lipogenesis rather than stimulation of lipolysis. This may explain the lack or loss of *myo*-inositol efficiency in reducing adipose tissue mass in contexts of already well-established obesity (old mice) or reduced *de novo* lipogenesis (high fat diet feeding). Generation of inositol glycan putative insulin second messengers is probably reduced in context of insulin resistance which may explain the reduced effect of *myo*-inositol in both obese mice models. Moreover, *myo*-Inositol did not prevent lipotoxicity and so the associated insulin-resistance in high fat diet fed mice.

In conclusion, *myo*-inositol alone and/or in a context of overnutrition is not a suitable strategy for the prevention or treatment of insulin resistance. Combining it with other insulin sentitizing strategies may however potentiate their action and help reducing insulin-sensitizing drugs use.

Key words : inositol, insulin, diabetes, obesity, skeletal muscle, white adipose tissue, high fat diet, *de novo* lipogenesis.

9

Résumé

**Etude du potentiel insulino-sensibilisant du *myo*-inositol chez la souris :
Evaluation de l'intérêt nutritionnel d'une supplémentation en *myo*-inositol**

Le diabète de type 2 constitue un enjeu majeur de santé publique et la mise au point de stratégies insulino-sensibilisantes est un défi permanent pour les scientifiques.

Cette étude montre qu'une supplémentation en *myo*-inositol améliore la sensibilité à l'insuline et réduit l'accrétion adipeuse chez la souris. L'effet insulino-sensibilisant semble passer, au moins en partie, par un effet direct sur la voie de signalisation insuline (éventuelle implication de médiateurs de type inositol glycanes). La diminution de l'accrétion adipeuse semble, quant à elle, liée à une réduction de l'activité de lipogenèse *de novo* et doit probablement aussi contribuer à l'effet insulino-sensibilisant sur le long terme.

Une supplémentation en *myo*-inositol a également amélioré la sensibilité à l'insuline et réduit l'accrétion adipeuse chez la souris soumise à un régime hypercalorique hyperlipidique, mais n'a pu prévenir le dévelopement d'une obésité et d'une insulino-résistance associée à une lipotoxicité. Par ailleurs, chez des souris âgées obèses et au contrôle glycémique altéré, la supplémentation en *myo*-inositol fut inefficace. Cette réduction ou perte d'effet insulino-sensibilisant dans ces deux modèles murins pourrait être liée à la perte d'efficacité du *myo*-inositol sur la réduction de la masse adipeuse dans un contexte d'obésité déjà installée (souris âgées) et d'activité de lipogenèse *de novo* réduite (régime gras). De plus, la génération de messagers secondaires putatifs de l'insuline de type inositol glycanes est probablement réduite en cas d'insulino-résistance et pourrait aussi expliquer la perte d'efficacité du *myo*-inositol dans ces deux cas.

Finalement, le *myo*-inositol seul et/ou utilisé dans le contexte d'une suralimentation chronique n'est pas une stratégie viable de prévention ou de traitement de la résistance à l'insuline. Par contre, son association avec d'autres stratégies insulino-sensibilisantes pourrait potentialiser son/leurs action(s) et éventuellement aider à réduire l'utilisation de stratégies médicamenteuses.

Mots clés : inositol, insuline, diabète, obésité, muscle, tissus adipeux, régime gras, lipogenèse *de novo*.

Abbreviations

AC: Adenylyl Cyclase
ACC: Acetyl Coenzyme A Carboxylase
AGEs: Advanced Glycation End products
ALBP: Adipocyte Lipid Binding Protein
AMPK: 5'-Adenosine Monophosphate-Activated Protein Kinase
ANOVA: ANalysis Of VAriance
AOA : AntiOxydant Activity
aPKC: atypical Protein Kinase C
AS160: Akt Substrate 160 (a Rab GTPase-activating protein)
ATF-6: Activating Transcription Factor 6
ATGL: Adipose Triglyceride Lipase
ATP-CL: ATP-Citrate Lyase
AUC: Area Under the Curve
AX: Alloxan
BMI: Body Mass Index
BSA: Bovine Serum Albumin
BW: Body Weight
CD36: Cluster of Differentiation 36 (fatty acid translocase)
CDP-DAG: Cytidin DiPhosphate-DiAcylGlycerol
CGI-58: Comparative Gene Identification 58 (ATGL co-activator)
CHOP: C/EBP Homologous Protein
CMP: Cytidin MonoPhosphate
CPT-1: Carnitine Palmitoyl Transferase-1
CRP: C-Reactive Protein
DAG: DiAcylGlycerol
DCI: D-*Chiro*-Inositol
DMA: DiMethylAcetal
DPP-4: Dipeptidyl Peptidase-4
DGAT: Diglyceride acyltransferase
DGK: DiacylGlycerol Kinase
DMEM: Dulbecco's Modified Eagle Medium
DTT: DiThioThreitol
ECM: ExtraCellular Matrix
EDTA: EthyleneDiamineTetraacetic Acid
eIF-4A, eIF-2α: eukaryotic Initiation Factor-4A, -2α
ERK: Extracellular signal-Regulated Kinase
F1,6BPase: Fructose-1,6-BiPhosphatase
FA: Fatty Acid
FAME: Fatty Acid Methyl Ester
FATP: Fatty Acid Transport Protein
FAS: Fatty Acid Synthase
FBS: Fetal Bovine Serum
FFA: Free Fatty Acid
Fox: Forkhead (protein family)
FSH: Follicule Stimulating Hormone
G0S2: G0/G1 Switch gene 2

G3PAT: Glycerol-3-Phosphate Acyl-Transferase
G6Pase: Glucose-6-Phosphatase
GC-FID: Gas Chromatograph equipped with a Flame Ionization Detector
GDM: Gestational Diabetes Mellitus
GFR: Glomerular Filtration Rate
GIP: Glucose-dependent Insulinotropic Peptide
GK: Goto Kakizaki (rat)
GLUT: Glucose Transporter
GLP-1: Glucagon-Like Peptide-1
GPI: Glycosyl-Phosphatidyl-Inositol
GPX: Glutathion Peroxydase
GR: Gluthation Reductase
Grb2: Growth factor receptor-bound protein 2
GS: Glycogen Synthase
GSK3: Glycogen Synthase Kinase 3
GTT : Glucose Tolerance Test
HBP: Hexosamine Biosynthetic Pathway
HDL: High Density Lipoprotein
HFD: High Fat Diet
HK: Hexokinase
HMIT: H^+/*Myo*-Inositol Transporter
HNF: Hepatic Nuclear Factor
HOMA-IR: HOmeostatic Model Assessment - Insulin Resistance (index)
HS: Horse Serum
HSL: Hormone Sensitive Lipase
IBMX: 3-IsoButyl-1-MethylXanthine
ICAM: InterCellular Adhesion Molecule
IDE: Insulin Degrading Enzyme
IKK (IκB Kinase): Inhibitor of nuclear factor kappa-B Kinase (enzyme complex composed of three subunit: IKK-α, IKK-β and IKK-γ)
IL (IL-1β, IL-6, IL-8, IL10): Interleukin-1β, -6 , -8, -10
IMPase: Inositol MonoPhosphatase
INF-γ: Interferon γ
INS-2: Insulin second messenger with a 4-O-(2-amino-2-deoxy-beta-D-galactopyranosyl)-3-O-methyl-D-*chiro*-inositol structure
IPs: inositol phosphates (including in particular: Ins-P, inositol monophosphate ; IP_3, inositol triphosphates ; IP_6 , inositol hexakisphosphates or phytic acid)
IPG: Inositol PhosphoGlycan
IR: Insulin Receptor
Ire1-α: Inositol-requiring protein 1
IRS: Insulin Receptor Substrate
ITT: Insulin Tolerance Test
JNK: c-Jun N-terminal Kinase
K_{ITT}: glucose disappearance rate constant (during an ITT)
KK: Kuo Kondo (mouse)
KRB: Krebs Ringer Bicarbonate (buffer)
LD50: median Lethal Dose
LDL: Low Density Lipoprotein
LH: Luteinizing Hormone
LPS: Lipopolysaccharide
LysoPI: LysoPhosphatidylInositol
MafA: Mammalian homologue of avian MafA/l-Maf

MAPK: Mitogen-Activated Protein Kinase
MCP-1: Monocyte Chemoattractant Protein 1
MEM: Minimum Essential Medium
MetS: Metabolic Syndrome
MG: MonoGlyceride
MGL: MonoGlyceride Lipase
MI: *Myo*-Inositol
MIOX: *Myo*-Inositol OXygenase
MIPS: 1-D-*Myo*-Inositol-Phosphate Synthase
MNCV: Motor Nerve Conduction Velocity
mTOR: mammalian Target Of Rapamycin
MTT: 3-(4,5-dimethylthiazol-2-yl)-2,5-diphenyltetrazolium bromide
NEFA: Non-Esterified Fatty Acid
NFkB: Nuclear Factor kappa B
NOS: Nitric Oxide Synthase
NSY: Nagoya-Shibata-Yasuda (mouse)
NZO: New Zealand Obese (mouse)
OGTT: Oral Glucose Tolerance Test
P70s6K: p70 ribosomal s6 Kinase
PA: Phosphatidic Acid
PCOS: Polycystic Ovary Syndrome
PDE-3B: PhosphoDiEsterase-3B
PDH: Pyruvate DeHydrogenase
PDHP: Pyruvate DeHydrogenase Phosphatase
PDI: Protein Disulfide Isomerase
PDK1: Phosphoinositide-Dependent Kinase 1
Pdx-1: Pancreatic and duodenal homeobox
PEPCK: PhosphoEnolPyruvate CarboxyKinase
PEDF: Pigment Epithelium Derived Factor
PERK: double-strand RNA-activated Protein kinase-like ER Kinase
PFK: PhosphoFructoKinase
PGC1: PPARγ co-activator 1
PI: Phosphatidyl-Inositol
PI3K: Phosphatidyl-Inositol-3-Kinase
PIP_2: Phosphatidyl-Inositol-(4,5)-biphosphate
PIP_3: Phosphatidyl-Inositol-(3,4,5)-triphosphate
PIPs: Phosphatidyl-Inositol Phosphate lipids
PK: Pyruvate Kinase
PKA: cyclic AMP-dependent Protein Kinase
PKB, PKC: Protein Kinase B, or C
PKR: double-strand RNA-dependant Protein Kinase
PLC, PLD: PhosphoLipase C and D
PLIN: Perilipin
PP1, PP2A: Protein Phosphatase 1, or 2A
PPAR: Peroxisome Proliferation-Activated Receptor
PP2Cα: Protein Phosphatase 2C alpha
PP-InsPs: PyroPhosphate forms of Inositol Phosphates
PRX: Peroxiredoxin
PTEN: Phosphatase and TENsin homologue on chromosome 10
PTP-1B: Protein Tyrosine Phosphatase-1B
RCT: Randomized Controlled Trial
RER: Rough Endoplasmic Reticulum

13

ROS: Reactive Oxygen Species
RRP: Readily Releasable Pool
S6K: ribosomal S6 protein Kinase
SDS: Sodium Dodecyl Sulfate
SDT: Spontaneously Diabetic Torii (rat)
SGLT: Sodium-Glucose Linked Transporter
SHBG: Sex Hormone Binding Globulin
SHC: Src Homology and Collagen protein
SHR: Spontaneously Hypertensive Rat
SHIP: Src Homology 2 domain containing Inositol 5'-Phosphatase
SKIP: Skeletal muscle and Kidney enriched Inositol Phosphatase
SMIT: Sodium/*Myo*-Inositol co-Transporter
SOCS: Suppressor Of Cytokine Signaling
SOD: Super Oxide Dismutase
SOS: Son-Of Sevenless
SREBP: Sterol Regulatory Element Binding Protein
STZ: Streptozotocin
TAG: TriAcylGlycerol
TBARS: Thiobarbituric Acid Reactive Substances
TBST: Tris-Buffered Saline Tween
TCA (cycle): TriCarboxylic Acid (cycle)
T1D(M): Type 1 Diabetes (Mellitus)
T2D(M): Type 2 Diabetes (Mellitus)
TG: TriGlyceride
TLC: Thin Layer Chromatography
TLR-4: Toll-Like Receptor 4
TNF-α: Tumor Necrosis Factor α
UPR: Unfolded Protein Response
VLDL: Very Low Density Lipoprotein
WAT: White Adipose Tissue (including epidydymal WAT (eWAT), parametrial WAT (pWAT), retroperitoneal WAT (rWAT) and sub-cutaneous WAT (scWAT))
XBP-1: X-Box Protein 1
ZDF: Zucker Diabetic Fatty (rat)

Table of figures

List of Tables

Chapter 1 – Introduction

1.1 Glycemic Control

1.1.1 Overview

Glycemic control (i.e. blood glucose level maintenance between 0.8 and 1.0 g.L^{-1}) involves hormonal, nervous and metabolic systems that govern the entry or release of glucose from cells to ensure continuous and sufficient energy supply to all organs (and in particular to the central nervous system and red blood cells that are totally glucose-dependent). In this aim, blood glucose can either be downregulated by the action of insulin (the sole hypoglycemic hormone of the body) on its target tissues (muscle, liver, white adipose tissue (WAT)) or upregulated by the action of glucagon, adrenalin, cortisol and/or growth hormone according to the circumstances (e.g. short or lasting fasting period, physical activity, strong emotional stress). Production and secretion of hypoglycemic or hyperglycemic hormones depends on the nature of the stimuli (e.g. hypoglycemia, hyperglycemia, stress).

For example, in post-prandial condition (i.e. after a meal), the amount of glucose absorbed from the intestinal tract is greater than the amount of glucose released by the liver and than that entering into cells so that blood glucose level rises above its "normal" level (i.e. 1g.L^{-1}). This hyperglycemia is detected by the beta-cells of the pancreas that respond to this stimulation by secreting insulin. Insulin then binds to its receptor on target tissues to: 1) stimulate glucose entry into muscle and white adipose cells ; 2) stimulate glucose use for energy production or storage under the form of glycogen or triglycerides ; 3) inhibit glucose production and release by the liver. All these insulin actions result in the reduction of blood glucose level and its return to baseline value (See **Fig. 1**).

In fasting or hypoglycemic conditions, pancreas alpha-cells secrete glucagon and blood glucose is then mainly maintained by the liver which releases glucose from glycogen stores (a process called "glycogenolysis") and then produces extra glucose from other substrates such as some amino acids (a process called "neoglucogenesis") in response to glucagon stimulation. In that condition, adipose tissue and muscle cells uptake and use only few amounts of glucose.
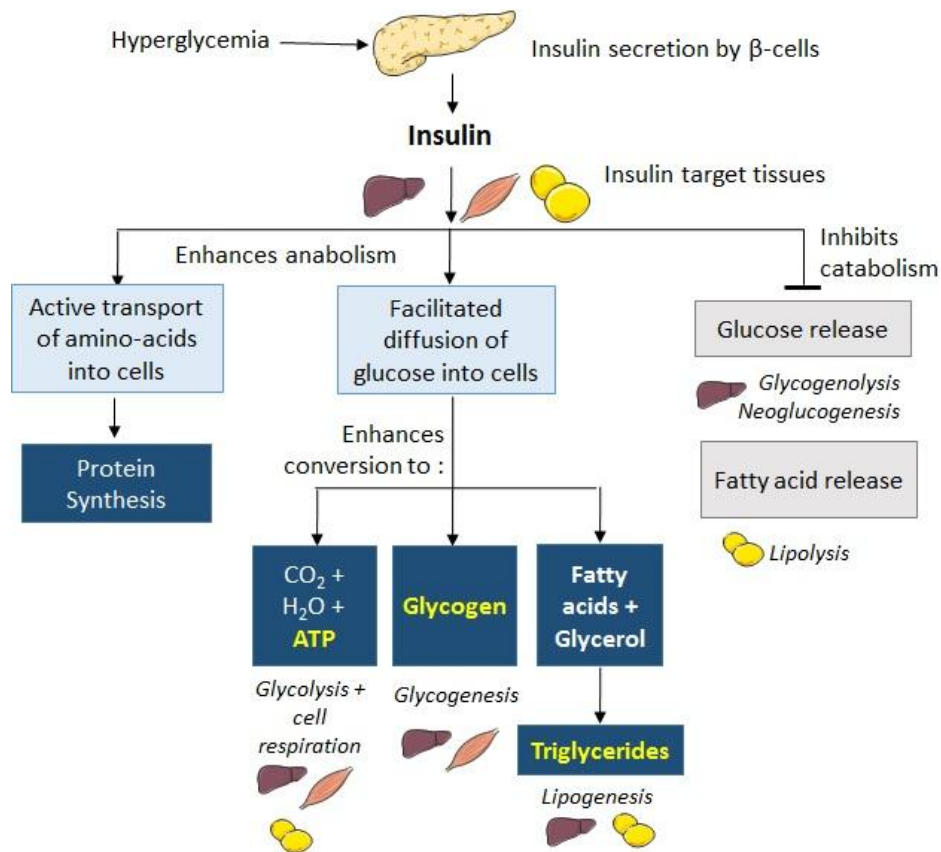
Figure 1 – Overview of the glycemic control and of the anabolic effects of insulin in post-prandial condition.

1.1.2 Insulin

1.1.2.1 Synthesis and secretion by pancreatic beta cells

Insulin structure

Insulin is a peptide hormone produced and stored in vesicles of pancreatic beta cells as a zinc-coordinated hexamer (formed by the association of three insulin dimers). Upon extracellular release, hexamers dissociate into dimers and monomers that are the circulating and biologically active forms of insulin. Monomeric insulin is a small polypeptide of 5.8 kDa composed of two chains (named A and B, and consisting in most species of 21 and 30 amino acids respectively) cross-linked by two disulfide bonds (Wilcox 2005). As would be expected by the biological importance of this molecule, its amino acid sequence is highly conserved among vertebrates (Muglia & Locker 1984) and insulin from one mammal is usually biologically active in another one.

20

Insulin biosynthesis

Insulin is synthesized in significant amounts only by beta-cells of the endocrine pancreas[1] (ie. Islets of Langerhans). Islets of Langerhans are micro-organs scattered among pancreas acini and composed of at least five types of endocrine cells: α-, β-, δ-, ε- and pancreatic polypeptide (PP)-cells. The α- and β-cells are the most abundant (α- and β-cells constituting 15-20% and 65-80% of rat islet cells, respectively) and also the most important in that they secrete two crucial hormones for glucose homeostasis: insulin (β-cells) and glucagon (α-cells). It is considered that endocrine cells disposition into Langerhans islet is not random and that this organisation has a physiological relevance. Many also agree that the human islets endocrine cell architecture is quite different from that of rodent islets. In most rodents, islets are composed of a core region of β-cells surrounded by a mantle region of non–β-cells (i.e. α-, δ-, ε- and PP-cells). It seems that a core-mantle segregation of islet cells is useful in favoring homologous contacts between β-cells, which in turn improves insulin secretion (while heterologous contacts have no effect on insulin secretion) (Bosco et al. 1989). The characteristic islet organisation may also serve to facilitate interactions among the different islet hormones via interstitial or vascular routes (Samols & Stagner 1990; Samols & Stagner 1988). Human islets organization was poorly described and controversial but according to the study of Bosco et al. (Bosco et al. 2010) they have a unique architecture allowing all endocrine cells to be adjacent to blood vessels and favoring heterologous contacts between β- and α-cells, while permitting homologous contacts between β-cells.

Insulin gene is located on the short arm of chromosome 11 (Wilcox 2005) and the insulin mRNA is translated as a single chain precursor called preproinsulin. During insertion into the rough endoplasmic reticulum (RER), preproinsulin is converted to proinsulin by removal of its N-terminal signal peptide by signal peptidases. Proinsulin consists of three domains: an amino-terminal B chain, a carboxy-terminal A chain and a connecting peptide in the middle known as the C peptide. Secretory vesicles then transfer proinsulin from the RER to the Golgi apparatus, whose aqueous zinc and calcium rich environment favors formation of soluble zinc-containing proinsulin hexamers (Wilcox 2005). As immature storage vesicles form from the Golgi, proinsulin is exposed to several specific endopeptidases which excise the C peptide, thereby generating the mature form of insulin. Contrary to zinc-containing proinsulin hexamers, zinc-coordinated insulin hexamers are insoluble. Insulin and an equimolar ratio of free C peptide are packaged in the Golgi into secretory granules which accumulate in the cytoplasm.

---

[1] Endocrine pancreas (i.e. Islets of Langherans) only account for 2-3% of the total mass of the pancreas.

The biphasic insulin secretion

Upon stimulation (e.g. by nutrients like glucose, amino-acids or fatty acids, or by non-nutrient secretagogues), β-cells secrete insulin and C-peptide by exocytosis and insulin diffuses into islet capillary blood and reaches the liver through the pancreatico-duodenal and portal veins. C-peptide has no known biological activity but it is secreted in an equimolar ratio with insulin and contrary to insulin, it does not undergo hepatic degradation. Hence, C-peptide peripheral plasma concentration directly reflects insulin release by pancreatic islets and allows a better determination of β-cell secretion activity than peripheral (post-hepatic) insulin plasma level.

In vivo, glucose-induced insulin secretion is biphasic with a first phase (triggering phase) characterized by a spike in insulin secretion and occurring within the first 5 to 10 minutes, and a second phase (amplifying phase) during which insulin secretion reaches a plateau very quickly, as seen in mice, or shows a progressively slow increase and reaches a plateau in 2-3 hours, as seen in rats and humans (Gerich 2002) (**See Fig. 2**).
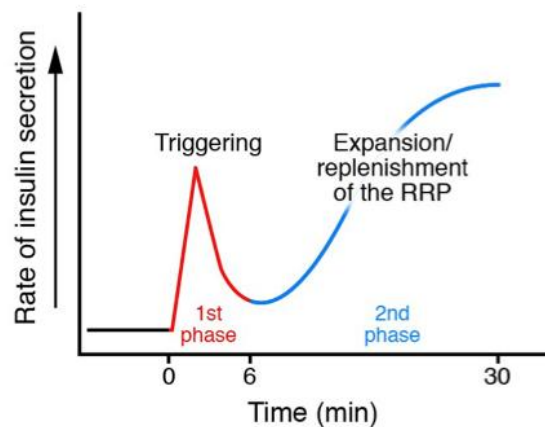
Figure 2 - The biphasic insulin secretion profile. Figure from http://www.proprofs.com. Abbreviation: RRP, readily releasable pool.

The glucose-induced biphasic insulin secretion was first reported in the 1960's (Curry et al. 1968). However, despite subsequent decades of research, the molecular mechanism underlying the biphasic response of the β-cell remains unresolved. The currently accepted theory is the 'storage-limited model' (Henquin, Boitard, et al. 2002; Henquin, Ishiyama, et al. 2002). In this model, it is proposed that biphasic secretion corresponds to the release of geographically or functionally distinct pools of insulin-containing granules. The first phase would result from the rapid fusion of granules that are pre-docked at the plasma membrane (referred to as the 'readily releasable pool' (RRP)). The second phase would come from "deeper" granules (referred to as the 'storage-granule pool') that are mobilized to traffic to the cell periphery to replenish the RRP at the cell surface. Of note, although KCl and other non-nutrient secretagogues can trigger first-phase release, only fuel secretagogues such as glucose can produce a substantial and sustained second-phase insulin release.

22

Loss of first-phase secretion and reduced second-phase secretion are characteristic features of type 2 diabetes (T2D); it is well known that alteration in the first phase of glucose-induced insulin secretion may be the earliest detectable defect in individuals with impaired glucose tolerance and destined to develop type 2 diabetes (Gerich 2002).

Molecular mechanisms of glucose-stimulated insulin secretion (GSIS)

The usual scheme for GSIS molecular mechanisms can be depicted as follow (See **Fig. 3.**) (Seino et al. 2011): extracellular glucose enters the β-cell through the non-saturable transporter GLUT-1/2 so that intracellular glucose directly reflects blood glucose level. Glucose is then metabolized through glycolysis and Krebs cycle increasing the ATP/ADP ratio, which triggers the closure of ATP-sensitive potassium channels (K_{ATP} channels) on the plasma membrane, leading to membrane depolarization and opening of voltage-dependent Ca^{2+} channels (VDCC). Ca^{2+} ions entry into cell increases the intracellular Ca^{2+} level which stimulates the fusion of insulin granules with the plasma membrane and the release of insulin outside the cell by exocytosis (**See Fig. 3).**
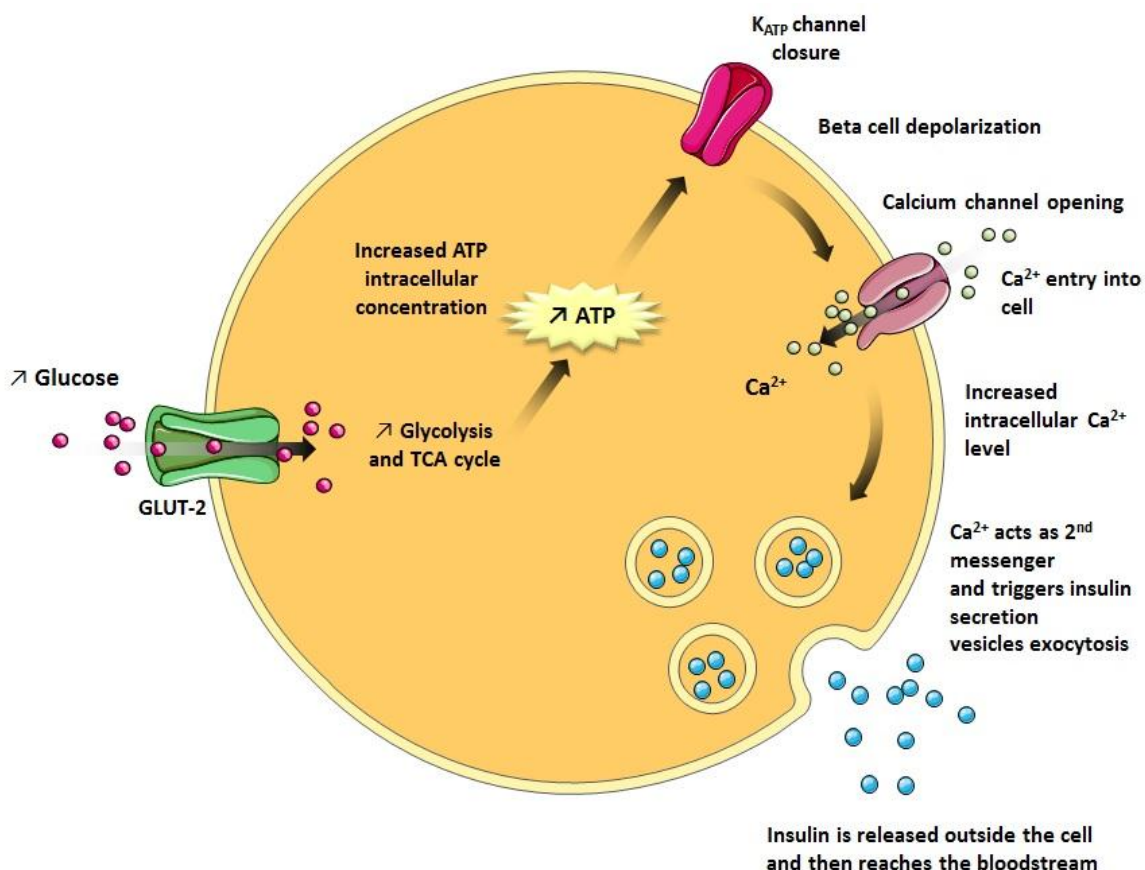
Figure 3 - The stimulus-secretion coupling pathway of glucose-stimulated insulin secretion (GSIS). Figure adapted from N. Pillon PhD thesis (Lyon, 2010). Abbreviation: GLUT-2, Glucose transporter 2.

23

The steps described above and schematized in **Fig. 3** control both first and second phase of insulin release, with additional steps of insulin biosynthesis, packaging into granules and transport to the plasma membrane for the second phase (Henquin, Ishiyama, et al. 2002; Henquin, Boitard, et al. 2002; Barg et al. 2002).

Of note, in post-prandial condition, insulin secretion is not continuous, but oscillates with a period of 3–6 minutes, changing from generating a blood insulin concentration above 800 pmol.L^{-1} or below 100 pmol.L^{-1} (typical fasting blood insulin level being about 57–79 pmol.L^{-1})). These oscillations would help to avoid downregulation of insulin receptors in target cells, and assist the liver in extracting insulin from the blood. These high frequency oscillations are also present in the fasting state but with a reduced amplitude and a little reduced frequency. In addition to the rapid insulin pulses that recur every 5–10 min, slow and large ultradian oscillations of insulin secretion with a period range of 50–120 min have also been described in both humans and animals (Simon & Brandenberger 2002) but their mechanism remains incompletely defined, even if it seems to be a feedback response to nutrients/glucose level oscillations.

1.1.2.2 Insulin actions on muscle, liver and adipose tissue

Insulin is the sole hypoglycemic hormone of the body and it plays a crucial role in the cellular uptake, use and storage of carbohydrates and lipids. Insulin acts primarily on skeletal muscles, white adipose tissue and liver by enhancing their glucose uptake (muscle, white adipose tissue), stimulating glucose use for energy production (glycolysis) or stimulating its storage under the form of glycogen (liver and muscles) or triglycerides (white adipose tissue). Insulin simultaneously inhibits glucagon secretion from pancreatic α-cells, thus signaling the liver to stop glucose production via glycogenolysis and gluconeogenesis.

In addition to its short-term effects on glycemic control, insulin also has trophic effects on the long term through regulation of gene expression. In particular, insulin promotes cell growth, differentiation and protein synthesis in every cell types. Insulin is therefore regarded as a major anabolic hormone.

Insulin enhances glucose uptake (muscle and adipose tissue)

The main mechanism by which cells can uptake glucose is by facilitated diffusion through transporters of the hexose family (13 transporters of the GLUT/SLC2 family, see **Table 1** for GLUT1-5 tissue distribution and characteristics).

24

Table 1
Main glucose transporters

SGLT	Active	Intestinal mucosa, renal tubules (in basolateral membrane).	Co-transport of glucose (or galactose) with 2 sodium ions. Role in **intestinal absorption of glucose** from food and **reabsorption from urine** in kidneys.
GLUT-1	Facilitated	Nervous tissue, red blood cells, endothelial cells, fetal tissues.	High affinity transporter (Km=1,2mM). Ubiquitous. **Baseline uptake of glucose.**
GLUT-2	Facilitated	Liver, pancreas beta-cells, intestinal epithelia, kidneys.	Low affinity transporter (Km=17mM). **Plays a role in glucose sensing.**
GLUT-3	Facilitated	Nervous tissue, placenta, testicules.	High affinity transporter (Km<1mM). Main neuronal transporter.
GLUT-4	Facilitated	Skeletal and cardiac muscles, adipose tissue.	High affinity transporter (Km=5mM). **Recruited by insulin.**
GLUT-5	Facilitated	Small intestine, adipose tissue, kidneys, muscle, brain.	Fructose transporter, high affinity (Km=1,2mM).

Abbreviations : SGLT, Sodium-Glucose linked transporter ; GLUT, Glucose transporter

In striated muscles and adipose tissues, baseline glucose uptake required to sustain cell respiration in all cells is mediated by facilitated diffusion through GLUT-1 (glucose transporter 1). However, the major transporter used for glucose uptake in these tissues is glucose transporter 4 (GLUT-4) and it is made available at the cell surface in a process stimulated by insulin. In fasting/baseline conditions (i.e. with low insulin blood level), GLUT-4 are mainly sequestered in cytoplasmic vesicles so that only few amounts of glucose can enter the cells by facilitated diffusion through GLUT-1. When insulin binds to its receptor at the cell surface, this triggers the IRS/PI3K/Akt cascade of protein activation that leads to the translocation of GLUT-4 vesicles from the cytoplasm to the plasma membrane. Fusion of those vesicles with the plasma membrane allows insertion of those additional glucose transporters, thereby enhancing the cell capacity to take up glucose. When blood levels of insulin decrease and insulin receptors are no longer occupied, the glucose transporters are recycled back into the cytoplasm. See paragraph "molecular mechanisms of insulin action" (page 30) for further details on the IRS/PI3K/Akt signaling pathway.

Insulin enhances glucose use and storage under the form of glycogen (liver, muscle) or triglycerides (WAT, liver)

Glucose oxidative use (glycolysis, tricarboxylic acid cycle (TCA)) - Insulin promotes glucose oxidative use by 1) up-regulating the transcription of the three key regulatory enzymes of glycolysis (i.e. glucokinase (**GK**), phosphofructokinase (**PFK**), and pyruvate kinase (**PK**)) via the transcriptional factor sterol regulatory element binding protein-1 (**SBREP-1**) and 2) stimulating Pyruvate Dehydrogenase (**PDH**) activity and so pyruvate conversion to acetyl-CoA that may then be used in the TCA cycle for ATP production and cellular respiration (or serve as precursor for fatty acid synthesis) (See **Fig. 4**). The transcriptional regulation of glycolysis takes place over a period of hours to days and generally reflect if the person is well-fed or starving.

Glucose non oxidative use (glycogenogenesis, lipogenesis) - Insulin promotes glucose storage under the form of glycogen in liver and muscle cells by indirectly stimulating glycogen synthase (**GS**) activity. Indeed the control of GS is a key step in regulating glycogenesis. Glycogen synthase activity is inhibited by phosphorylations on serine residues by glycogen synthase kinase 3 (**GSK-3**) (on Ser 641, 645, 649 and 653), AMPK (Ser 7) and protein kinase A (PKA). Insulin activates PKB/Akt which inhibits GSK-3 and so activates GS. Glycogen synthase is also activated allosterically by glucose-6-phosphate. Since insulin enhances glucose uptake through GLUT-4 in muscle cells, it also indirectly regulates GS by increasing glucose-6-phosphate formation in these cells.

Insulin also enhances *de novo* lipogenesis in white adipocytes and hepatocytes. *De novo* lipogenesis is the process by which cytosolic acetyl-CoA is converted to fatty acids by the consecutive actions of AcetylCoA Carboxylase (ACC) and Fatty Acid Synthase (FAS) enzymes. Acetyl-CoA produced in the mitochondria by PDH activity is converted to Citrate in the TCA cycle and a part of it can be transferred from mitochondria to cytosol via the tricarboxylate transport system. Cytosolic citrate can be converted back to Acetyl-CoA and oxaloacetate by the action of ATP-Citrate Lyase (**ATP-CL**) and Acetyl-CoA can be used as substrate for *de novo* fatty acid synthesis in the cytosol. Insulin activates lipogenesis by 1) enhancing **PDH, ATP-CL** and **ACC** activities, and 2) enhancing glycolytic (**GK**, **PFK** and **PK**) and lipogenic (**ACC**, **FAS**) enzymes expression through the transcription factor Sterol Regulatory Element Binding Protein-1 (SREBP-1). Finally, insulin promotes fatty acid (coming from diet or *de novo* lipogenesis from glucose) storage under the form of triglycerides by enhancing Glycerol-3-Phosphate Acyl-transferase (**G3PAT**) expression always through SREBP-1 (See **Fig. 4**).
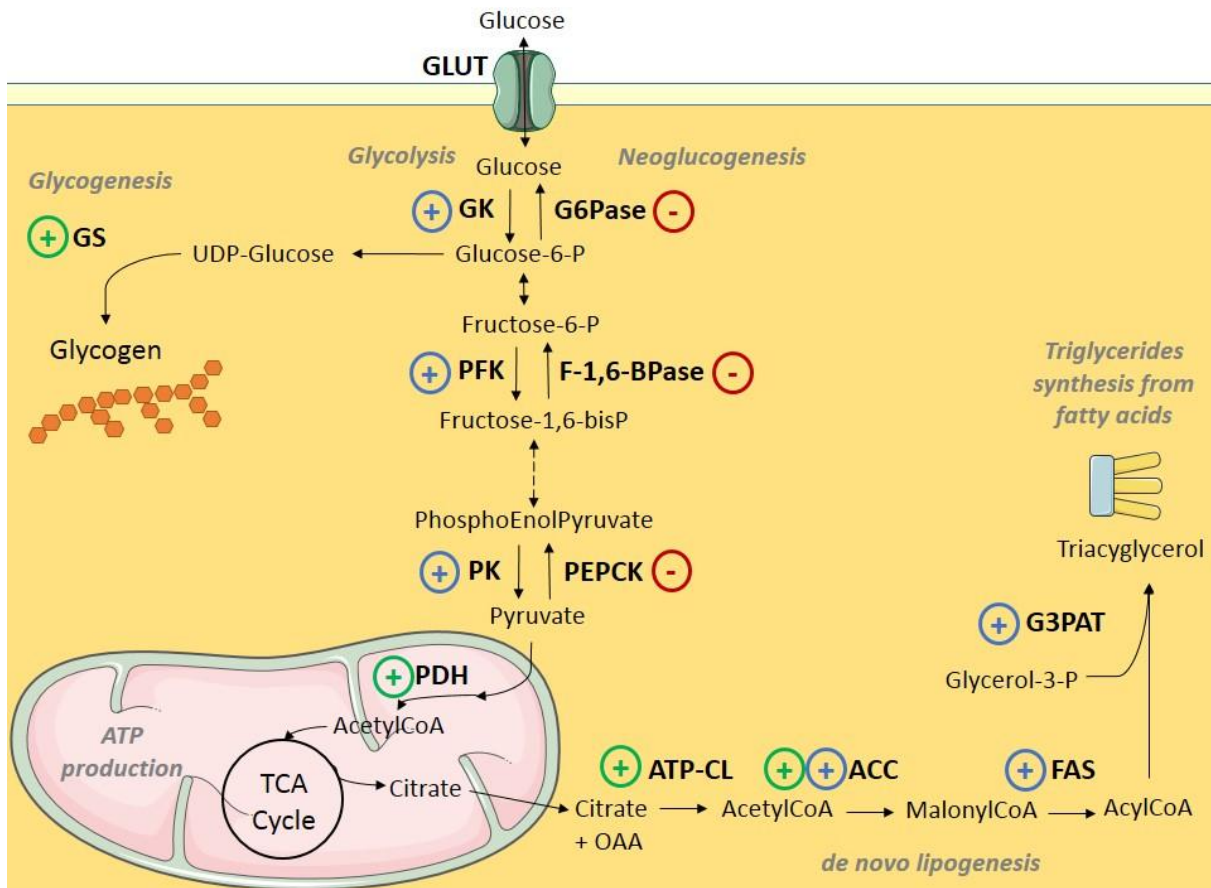
Figure 4 - Glycolysis, glycogenogenesis and lipogenesis regulation by insulin in hepatocyte.
Abbreviations : ACC, AcetylCoA Carboxylase ; ATP-CL, ATP-Citrate Lyase ; FAS, Fatty Acid Synthase ; Fox, forkhead protein family ; F-1,6-BPase, Fructose-1,6-bisphosphatase ; GK, Glucokinase/hexokinase ; GLUT, Glucose transporter ; G3PAT, Glycerol-3-Phosphate Acyl Transferase ; G6Pase, Glucose-6-phosphatase ; GS, Glycogen Synthase ; HNF, Hepatic Nuclear Factor ; PDH, Pyruvate dehydrogenase ; PEPCK, Phosphoenolpyruvate Carboxy Kinase ; PFK, Phosphofructokinase ; PGC1, PPARγ co-activator 1 ; PK, Pyruvate Kinase ; SREBP, Sterol Regulatory Element Binding Protein ; TCA cycle, TriCarboxylic Acid cycle.

Insulin inhibits glucagon secretion by α-cells and thus liver glucose release

Glucagon binding to its receptor on hepatocytes leads to PKA activation which triggers 1) phosphorylation of glycogen phosphorylase and so glucose release from glycogen hydrolysis (glycogenolysis) ; 2) glucose *de novo* production from pyruvate and lactate (neoglucogenesis) through activation of fructose-2,6-bisphosphatase. Insulin inhibits glucagon secretion and so inhibits glucose liver production induced by glucagon. Moreover insulin inhibits the three neoglucogenic enzymes (i.e.

27

glucose-6-phosphatase (G6Pase), fructose-1,6-bisphosphatase (F1,6BPase) and phosphoenolpyruvate carboxy kinase (PEPCK)) genes transcription through the hepatic nuclear factor (HNF)-4, the forkhead protein family (Fox) and the PPARγ co-activator 1 (PGC1) (Puigserver et al. 2003; Saltiel & Kahn 2001). PGC-1 binds and co-activates FoxO1 in a manner inhibited by Akt-mediated phosphorylation.

Insulin inhibits fatty acid release from WAT (lipolysis)

Lipolysis is the process by which triglycerides (TG) are hydrolyzed into non esterified fatty acids (NEFA) and glycerol. Intracellular lipolysis (*versus* gastrointestinal or vascular lipolysis) of TGs involves neutral (pH-optimum around pH 7) lipases including adipose triglyceride lipase (ATGL) and hormone-sensitive lipase (HSL), and acid lipases present in lysosomes (pH optimum between pH 4–5), lysosomal acid lipase (LAL) being the most important acid lipase. In white adipocytes, 90% of TGs hydrolysis is due to neutral hydrolysis (Schweiger et al. 2006; Zechner et al. 2012) and involves the successive actions of three lipases: Adipose TriGlycerides Lipase (ATGL), Hormone-Sensitive Lipase (HSL) and finally monoacylglycerol lipase (MGL) (See **Fig. 5**).

Adipocyte lipolysis regulation is a relatively complex phenomenon in which HSL activity regulation seems to be the main control point. In fasting conditions, adrenalin and glucagon stimulates Adenylyl Cyclase (AC) in adipocytes through binding to their respective G-protein coupled receptors (adrenergic β-1/2/3-receptors and glucagon receptor). Activation of AC raises intracellular cyclic AMP level, thereby activating protein kinase A, which phosphorylates and activates HSL and the lipid droplet protein perilipin-1 (PLIN-1). Phosphorylated PLIN-1 releases ATGL co-activator CGI-58, allowing ATGL full activity for hydrolysis of TG to DG (Zechner et al. 2012). Of note, several other lipid droplet proteins also regulate ATGL and lipolysis in adipocyte and/or hepatocyte (e.g. pigment epithelium-derived factor (PEDF) is secreted by adipocytes and is another positive regulator of ATGL in hepatocyte (Chung et al. 2008; Borg et al. 2011) and G0/G1 switch gene 2 (G0S2) (Yang et al. 2010; Schweiger et al. 2012) negatively regulates ATGL in adipose tissue and liver). Phosphorylated hormone-sensitive lipase (HSL) translocate from the cytosol to the surface of the lipid droplet where it binds to phosphorylated PLIN-1 and activates diglycerides (DG) hydrolysis to monoglycerides (MG) (Zechner et al. 2012). MG are finally hydrolysed to glycerol and fatty acids (FA) by MGL. Docking of adipocyte lipid binding protein (ALBP) to HSL favors the evacuation of FA released by the hydrolysis of TG. (See **Fig. 5**).
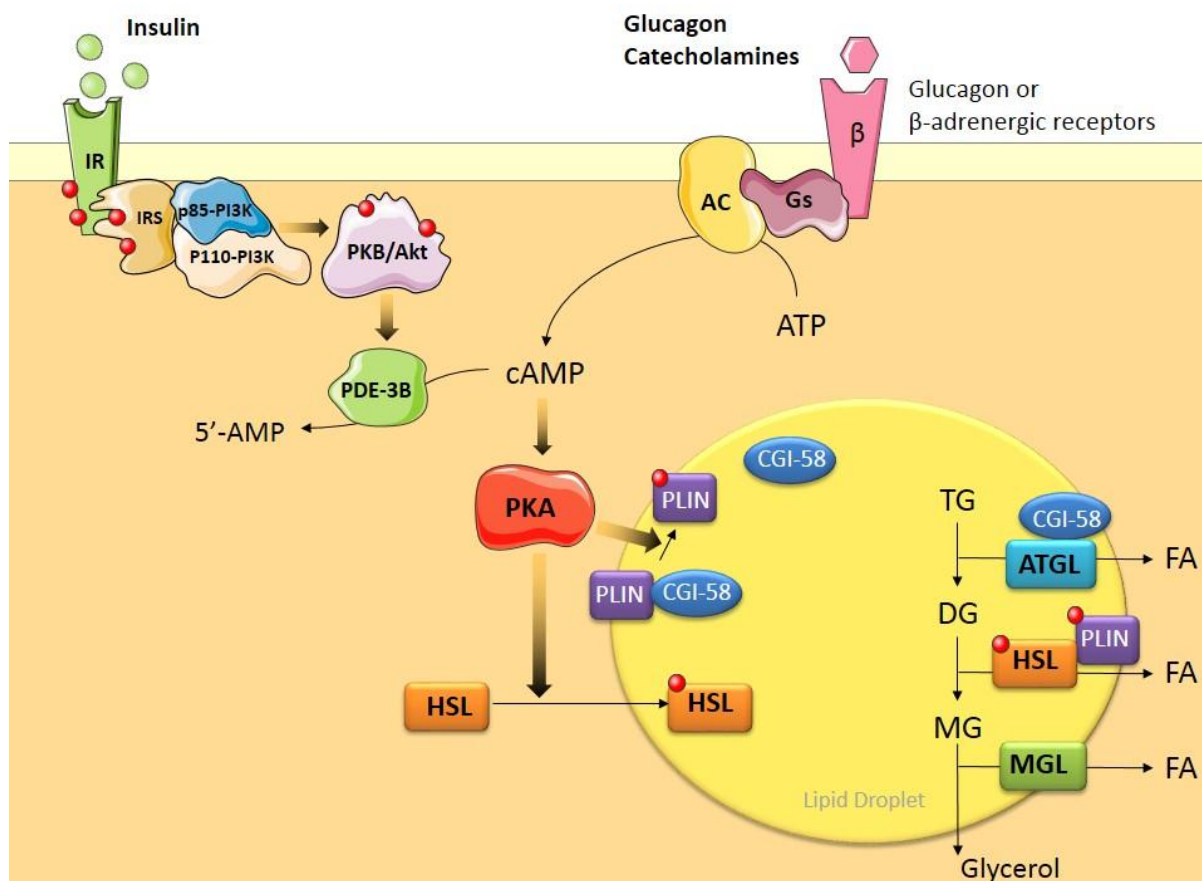
Figure 5 – Molecular mechanisms of adipocyte lipolysis regulation by insulin and glucagon. _Abbreviations_ : AC, Adenylyl Cyclase ; ATGL, Adipose Triglyceride Lipase ; CGI-58, Comparative Gene Identification 58 (ATGL co-activator) ; DG, Diglyceride ; HSL, Hormone Sensitive Lipase ; IR, Insulin Receptor ; IRS, Insulin Receptor Substrate ; MG, Monoglyceride ; MGL, Monoglyceride Lipase ; PDE-3B, Phosphodiesterase-3B ; PI3K, Phosphatidyl-Inositol-3-Kinase; PLIN, Perilipin ; PKA, Protein Kinase A ; PKB/Akt, Protein Kinase B/Akt ; TG, Triglyceride.

Insulin exerts an anti-lipolytic activity and this action is mediated through the IRS/PI3K/Akt pathway that leads to the activation of phosphodiesterase 3B (**PDE-3B**). Activated PDE-3B catalyzes the hydrolysis of cyclic AMP to 5'AMP, thereby decreasing the AMP/ATP ratio and so reducing PKA and HSL activities and lipolysis (**Fig. 5**).

Insulin promotes protein synthesis, cell growth and differentiation

**Protein Synthesis -** Insulin stimulates amino-acid uptake by cells, inhibits protein degradation (through an unknown mechanism) and promotes protein synthesis (Saltiel & Kahn 2001). Under baseline conditions (i.e. low insulin level), the constitutive activity of GSK-3 leads to the phosphorylation and inhibition of eIF2B, a guanine nucleotide exchange factor which regulates the initiation of protein translation. Therefore, upon insulin stimulation, PKB/Akt inactivates GSK-3 which leads to the dephosphorylation of eIF2B and so promotes protein synthesis and amino acids storage (Lizcano &

29

Alessi 2002). PKB/Akt also activates mammalian target of rapamycin (mTOR), which promotes protein synthesis through p70 ribosomal S6 kinase (p70s6k) and eIF4A.

Cell growth and differentiation (Mitogenic responses) - Other signal transduction proteins than PI3K can interact with IRS and these include Grb2 which in turn associates with the guanine nucleotide exchange factor son-of sevenless (SOS) and elicits activation of the Mitogen Activated Protein Kinase (MAPK) cascade (Ras/Raf/MEK/ERK) leading to mitogenic responses (Ogawa et al. 1998). SHC (src homology and collagen protein) is another substrate for the insulin receptor. Upon phosphorylation SHC associates with Grb2 and can therefore activates the MAPK pathway independently of IRS.

Molecular mechanisms of insulin actions – The IRS/PI3K/Akt insulin signaling pathways (Chang et al. 2004). (See **Fig. 6**)

Insulin binding to the α-subunit of its receptor (IR) activates the β-subunit receptor's tyrosine kinase activity, resulting in insulin receptor autophosphorylation and activation. In turn, the activated receptor recruits and phosphorylates a panel of substrate molecules, including insulin receptor substrate family (IRS-1 - 4), Shc isoforms, Gab-1, Cbl, APS and Signal Regulatory Protein (SIRP) family members. Tyrosine phosphorylated IRS (especially IRS-1/2) and Shc can bind Src homology-2 (SH2) domain-containing intermediates such as phosphatidylinositol 3-kinase (PI 3-kinase) and Growth factor-receptor-bound protein 2 (Grb-2), which, in turn, propagate insulin signaling downstream through PI3K-PKB/Akt and MAPK pathways.

When tyrosine phosphorylated IRS-1/2 recruit the heterodimeric p85/p110 PI3K at the plasma membrane, PI3K converts phosphatidylinositol-(4,5)-biphosphate (PIP_2) to the lipid second messenger phosphatidylinositol-(3,4,5)-triphosphate (PIP_3). PIP_3 then recruits 3-phosphoinositide-dependent kinase 1 (PDK1), the serine/threonine protein kinase B (PKB)/Akt, and the atypical protein kinases C ζ and λ isoforms at the plasma membrane by binding their PH-domains. Thereon, PDK1 phosphorylates PKB/Akt and aPKCs on threonine residues of their catalytic domains, causing their activation. Of note, PKB activation occurs through phosphorylation of Thr 308 and Ser 473, mediated by PDK1 and the rictor–mTor complex (mTORC2 or PDK2) respectively. Major targets of activated PKB/Akt are GSK-3 and AS160. PKB/Akt inactivates GSK-3 through phosphorylation of its Ser 9 residue. This inactivation, in parallel to protein phosphatase-1 (PP1) activation, relieves the inhibitory phosphorylation of GS, and so promotes glycogen synthesis. The Rab-GTPase activating protein (Rab-GAP) AS160 contains multiple Akt phosphorylation sites and is phosphorylated by PKB/Akt upon insulin stimulation. Inhibitory phosphorylation of the RabGTPase activating protein AS160 favors the GTP-loaded state of Rab and relieves an inhibitory effect towards GLUT-4 translocation from intracellular compartments to the plasma membrane. In addition to the role of PKB in controlling GLUT-4 translocation, aPKCs act in parallel to – or can even be substitutive for – PKB.

30

Activation of IRS/PI3K/Akt pathway is not sufficient to reproduce the increase in GLUT-4 translocation to the plasma membrane obtained in response to insulin. Another parallel pathway (not depicted in **Fig. 6**) involving a separate pool of insulin receptors and APS, Cbl, CAP, CrkII, C3G and TC10 proteins would also be necessary in the mediation of insulin effect on glucose uptake.

On a third parallel pathway, activated IRS-1/2 and/or Shc recruit Grb2, which associates to the Ras guanine nucleotide exchange factor Son-Of-Sevenless (SOS) and activates the Erk1/2 MAPK pathway. The p38 and JNK stress-activated kinases – whose activation is mainly dependent on stress signals and inflammatory cytokines – have also been shown to be phosphorylated/activated in response to insulin; although the pathway leading to their activation has not yet been fully elucidated.
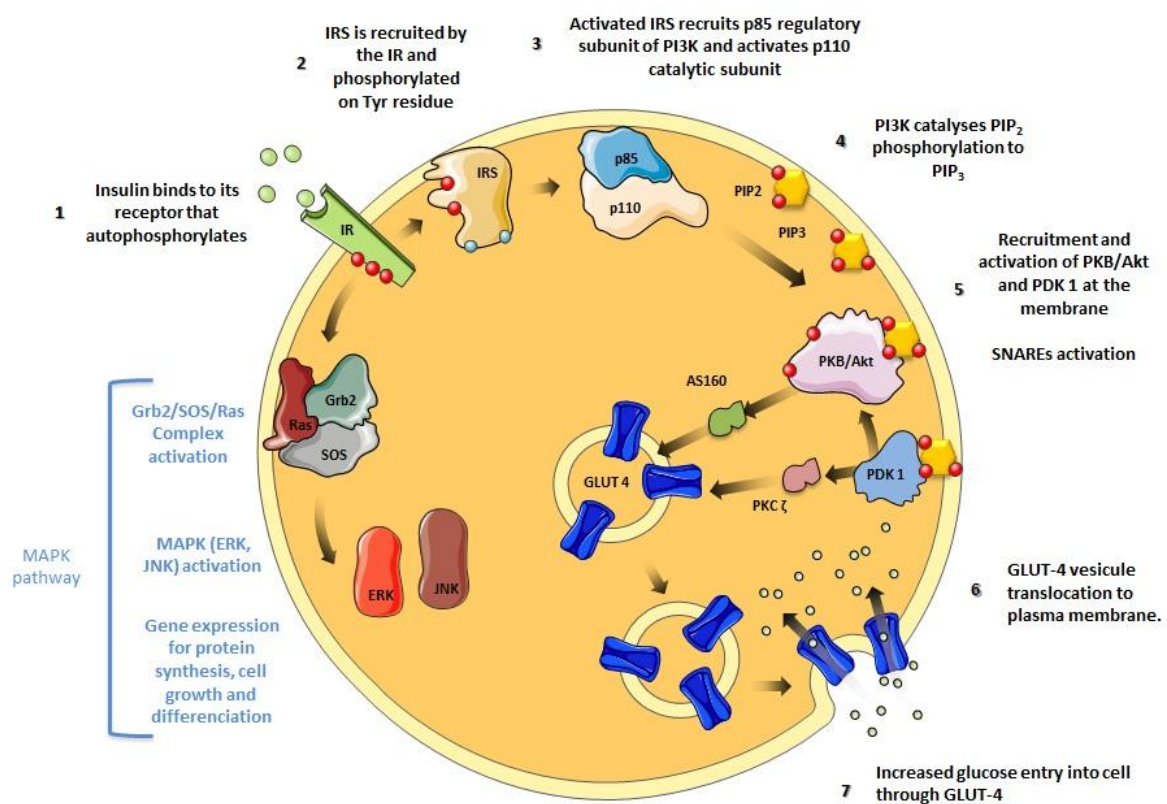
Figure 6 – Molecular mechanisms of insulin signal transduction in muscle and white adipose cells. Figure adapted from N.J. Pillon (Lyon, 2010) & L. Koppe (Lyon, 2013) PhD Thesis. Abbreviations : AS160, Akt Substrate 160 ; ERK, Extracellular-signal-regulated kinase(s) ; GLUT-4, glucose transporter 4 ; Grb2, Growth factor receptor bound protein 2 ; IR, Insulin Receptor ; IRS, Insulin Receptor Substrate(s) ; JNK, C-jun N-terminal Kinase(s) ; MAPK, Mitogen-Activated Protein Kinase(s) ; PDK, Phosphoinositide-dependent Kinase 1 ; PI3K, Phosphoinositide-3-Kinase ; PIP_2, Phosphatidylinositol-(4,5)-biphosphate ; PIP_3, Phosphatidylinositol-(3,4,5)-triphosphate ; SOS, Son-Of-Sevenless (guanine nucleotide exchange factor).

Finally, most of the metabolic actions of insulin are mediated through the IRS/PI3K/Akt pathway but Akt activation leads to different effects according to the cell type (e.g. PDE-3B activation, AS160 and

31

GLUT-4 translocation activation and/or GSK3 inhibition) (See **Fig. 7**) thereby regulating glucose uptake, glycolysis, glycogenesis and/or lipogenesis according to the cell functions. Insulin long term effects on metabolic pathways are mainly mediated by the transcriptional factor SREBP-1 that stimulates expression of anabolic enzymes and represses expression of catabolic enzymes. Activation of MAPK pathway mediates the trophic effects of insulin, enhancing cell proliferation, growth and differentiation.
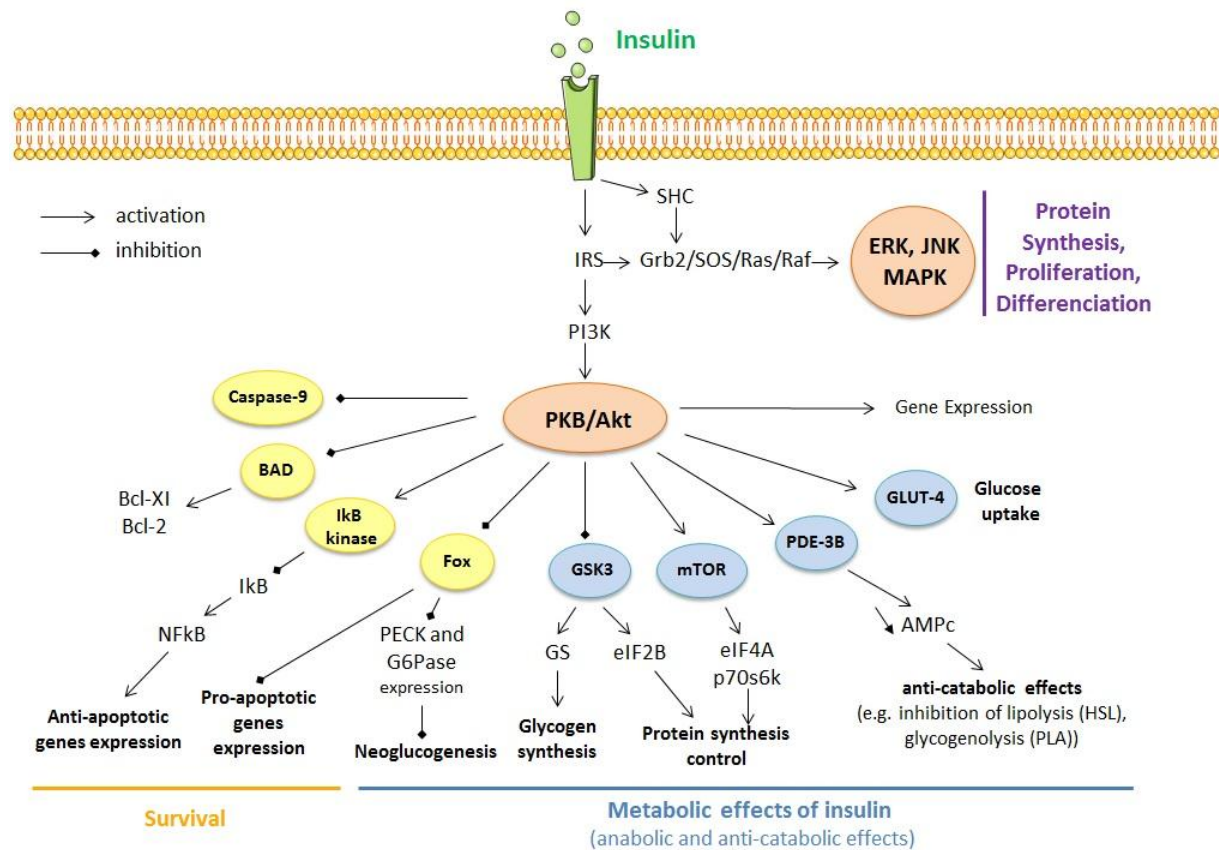
Figure 7 – The pleiotropic actions of insulin mediated by IRS/PI3K/Akt and MAPK pathways. Abbreviations : cAMP, cyclic Adenosine MonoPhosphate ; BAD, Bcl-2-Associated Death promoter protein (proapoptotic factor) ; eIF-2B/4A, eukaryotic Initiation Factor 2B/4A ; ERK, Extracellular-signal Regulated Kinase(s) ; GLUT-4, Glucose transporter 4 ; G6Pase, Glucose-6-phosphatase ; Grb2, Growth factor receptor bound protein 2 ; GS, Glycogen Synthase ; GSK3, Glycogen Synthase Kinase 3 ; HSL, Hormone Sensitive Lipase ; IκB, Inhibitor NFκB ; IR, Insulin Receptor ; IRS, Insulin Receptor Substrate(s) ; JNK, c-Jun N-terminal Kinase ; MAPK, Mitogen-Activated Protein Kinase(s) ; NFκB, nucleor factor kappa B ; PDE-3B, Phosphodiesterase-3B ; PEPCK, PhosphoEnolPyruvate Carboxy Kinase ; PI3K, Phosphosphatidyl-inositol-3-kinase ; p70s6K, p70 ribosomal s6 Kinase ; SHC, src homology and collagen protein ; SOS, Son-Of-Sevenless ; mTOR, mammalian Target Of Rapamycin.

1.1.2.3 Termination of insulin signal and insulin degradation

Physiological negative regulators of insulin signaling (See **Fig. 8**)

Enzymes that are important in the attenuation of PIP$_3$ (Phosphatidylinositol-(3,4,5)-triphosphate) signaling are phosphatases that hydrolyse PI(3,4,5)P$_3$ to PI(4,5)P$_2$ or PI(3,4)P$_2$: the phosphatase and tensin homologue on chromosome 10 (PTEN, a 3'-phosphatase) and the family of SRC homology 2 containing inositol 5'-phosphatase (SHIP, a 5'-phosphatase) proteins, respectively.

Protein Tyrosine Phosphatase 1B (PTP-1B) is another important enzyme in insulin signaling attenuation since it dephosphorylates IR and IRS on their tyrosine residues and so allow their return to their basal state.

Another physiological way of terminating insulin signaling is phosphorylation of IRS proteins on serine residues. Indeed, serine phosphorylations on IRS can impede further "activating phosphorylations" on nearby tyrosine residues by the IR and so prevent p85-PI3K recruitment by IRS. These serine phosphorylations can be performed by many serine/threonine kinases such as the mitogen-activated protein kinases ERK and JNK. Since the MAPK pathway is activated by insulin stimulation, serine phosphorylation on IRS by ERK is a part of the negative feedback loop aiming at ending insulin action.

Finally, termination of insulin signaling is also achieved by internalization of the insulin-insulin receptor complex into endosomes and by insulin degradation (see section "insulin degradation" below).
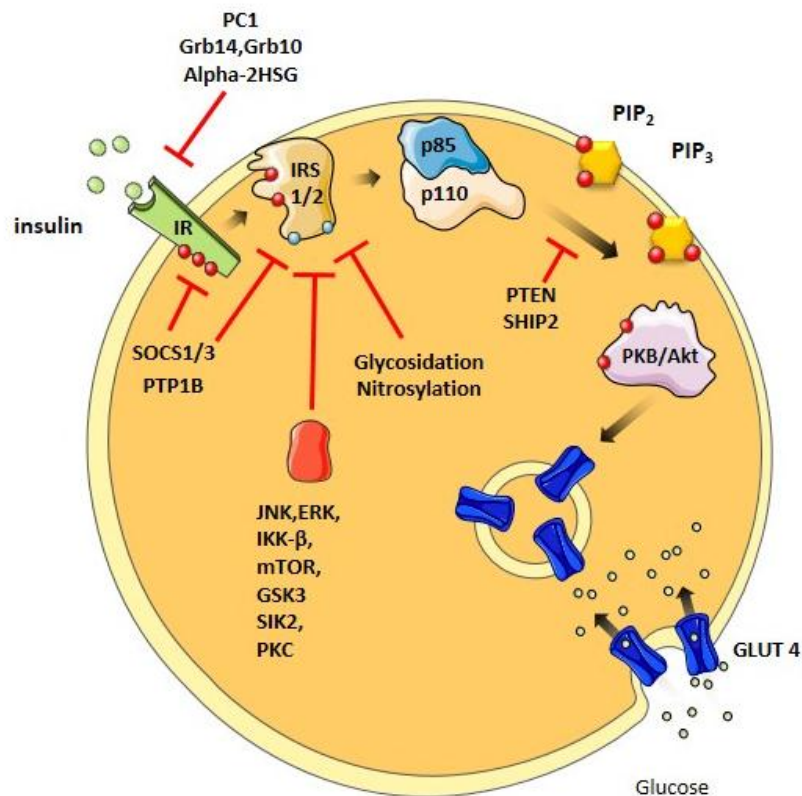
Figure 8 – Molecular mechanisms of termination of insulin signaling. Figure adapted from L. Koppe PhD Thesis, Lyon, 2013. Abbreviations: ERK, Extracellular-signal Regulated Kinase(s) ; GLUT-4, Glucose transporter 4 ; Grb10/14, Growth factor receptor bound protein 10/14 ; GSK3, Glycogen Synthase Kinase 3 ; IκKB, Inhibitor of nucleor factor kappa B kinase ; IR, Insulin Receptor ; IRS, Insulin Receptor Substrate(s) ; JNK, c-Jun N-terminal Kinase ; MAPK, Mitogen-Activated Protein Kinase(s) ; PC1, Plasma Cell membrane glycoprotein 1 (inhibitor of IR tyrosine kinase activity) ; PI3K, Phosphosphatidyl-inositol-3-kinase ; PKC, Protein Kinase C ; p70s6K, p70 ribosomal s6 Kinase ; PTEN, Phosphatase and Tensin homologue on chromosome 10 ; PTP-1B, Protein Tyrosine Phosphatase 1B ; SHC, src homology and collagen protein ; SHIP, Src Homology 2 containing Inositol 5'-Phosphatase ; SIK2, Salt-inducible Kinase 2 ; SOCS, Suppressor Of Cytokine Signaling ; mTOR, mammalian Target Of Rapamycin.

Insulin degradation (Duckworth et al. 1998)

As required to quickly respond to changes in blood glucose level, insulin has a short plasma half-life (4–6 min) (Duckworth et al. 1998). Insulin is first degraded in the liver which removes approximately 50% of portal insulin during first-pass transit, but with wide percentage variations depending on physiological (nutrient intake) or pathological (obesity, diabetes) conditions. Kidneys are the major site of insulin clearance from the systemic circulation, removing approximately 50% of peripheral insulin. Insulin not cleared by liver and kidney is ultimately removed by other tissues and mainly by muscles.

All cells that contain insulin receptors and internalization mechanisms can degrade insulin. The mechanism involves insulin binding to its receptor, internalization, and endosomal and lysosomal partial or complete degradation by insulinases (insulin degrading enzyme (IDE), protein disulfide isomerase

34

(PDI) and acidic proteinases). All internalized insulin is not degraded and part of the intact or partially degraded insulin is either delivered to other sub-cellular sites (cytosol, nucleus, Golgi or other sites) or released by diacytocis or retroendocytosis when insulin receptors are recycled to the plasma membrane. Some insulin is also degraded or partially degraded extracellularly (possibly by extracellular IDE) when bound to its receptor on the cell surface.

1.1.3 Glucagon and other hyperglycemic hormones

1.1.3.1 Glucagon

Glucagon is synthesised and secreted by the pancreatic alpha cells in response to hypoglycemia, sympathetic stimulation (via β2-, α2- and α1-adrenergic receptors), elevation in amino acids (arginine and alanine), cholecystokinin and/or secretin. Glucagon binding to its G-coupled receptors on liver cells, triggers a cascade of protein activation involving adenylyl cyclase (AC), protein kinase A (PKA) and Glycogen Phosphorylase activation (phosphorylase a = active form of glycogen phosphorylase ; phosphorylase b = inactive form). The net result is the release of glucose-1-phosphate from glycogen stores and the subsequent release of glucose into the bloodstream, in a process known as glycogenolysis. As these glucose stores become depleted, glucagon then stimulates glucose *de novo* synthesis (neoglucogenesis) from non-carbohydrate carbon substrates such as pyruvate, lactate, glycerol, glucogenic amino acids (alanine, glutamine) and odd-chain fatty acid in liver and kidney cells. If fasting lasts, the liver produces alternative fuel to glucose (ketone bodies) from fat. Insulin, incretins (GLP-1, GIP and amylin), somatostatin (i.e. Growth Hormone Inhibitory Hormone) and parasympathetic activity are negative regulators of glucagon secretion.

1.1.3.2 Catecholamines, cortisol and growth hormone

In parallel of this "metabolic" regulation of blood glucose by insulin and glucagon, other hormones related to the nervous system can participate to this regulation: adrenaline, cortisol or growth hormone. Adrenaline is produced by the adrenal medulla in response to stress or physical activity ("fight or flight" response) and causes increases in heart rate, blood pressure and blood glucose level (through direct stimulation of liver glycogenolysis) which allows a rapid energy supply to muscles in order to be ready to run or fight immediately. Cortisol is produced in cases of stress or prolonged fasting

period and stimulates liver neoglucogenic enzymes. In case of extended fasting, cortisol also promotes fat release from WAT (via lipolysis) and fat use by the liver to form ketone bodies (ketogenesis). Growth hormone is released by the somatotropic cells of the pituitary gland in response to fasting or vigorous physical exercise and is also hyperglycemic. Of note, high levels of cortisol (naturally produced or drug-induced) or growth hormone cause muscle and adipose tissue insulin resistance.

1.1.3.3 Incretins (GLP-1, GIP) and amylin

Amylin, or Islet Amyloid Polypeptide (IAPP), is a 37 kDa peptide co-secreted with insulin in a ratio of approximately 100:1 by the pancreatic β-cells. Amylin plays a role in glycemic control by slowing gastric emptying and promoting satiety, thereby preventing post-prandial spikes in blood glucose levels.

Incretins are insulinotropic gut-derived hormones: they are secreted in response to food intake by endocrine cells of the small intestine and they promote insulin secretion by pancreatic β-cells after eating, even before blood glucose levels become elevated. Rise in nutrients, and especially glucose, concentration in the intestinal lumen is the trigger for their secretion. Incretins also reduce the rate of nutrients absorption into the bloodstream by slowing gastric emptying and may directly reduce food intake. As described ealier, they also inhibit glucagon secretion by pancreatic α-cells. Glucose-dependent insulinotropic peptide (GIP), also known as gastric inhibitory peptide and glucagon-like peptide-1 (GLP-1) are the two main incretin hormones in human. Both GLP-1 and GIP are rapidly inactivated by the enzyme dipeptidyl peptidase-4 (DPP-4). The mechanism of incretin action is schematized in **Fig. 9**.
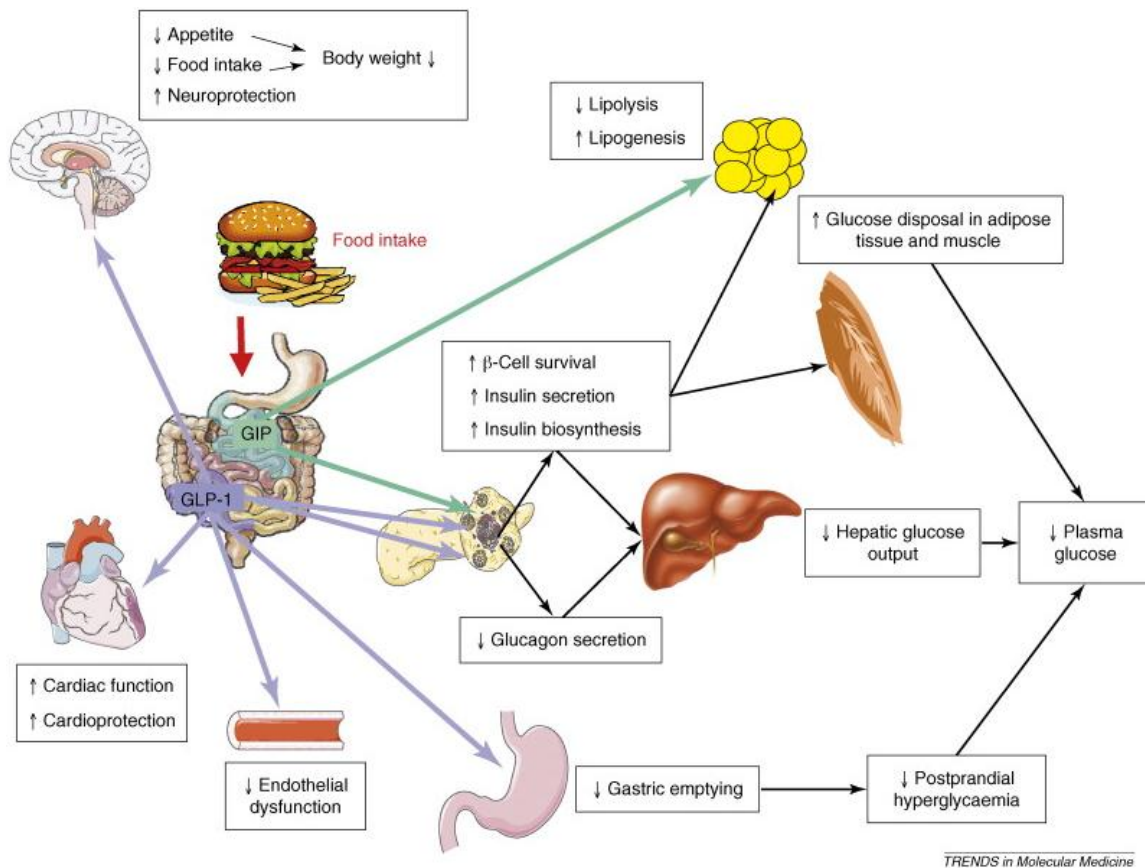
Figure 9 – Incretins GIP and GLP-1 role in glycemic control. Figure from JJ Holst et al, Trends in Molecular Medicine, 2008. Abbreviations: GIP, Glucose-dependent insulinotropic peptide ; GLP-1, Glucagon-like peptide 1.

In recent years, new incretin-based drugs have been developed and approved for the treatment of Type 2 Diabetes. These drugs are meant to be used in complement of other anti-diabetic drugs for type 2 diabetes patients who have difficulties in maintaining an adequate glycemic control. Exenatide (Byetta®) is a peptide GLP-1 receptor agonist. Since it is resistant to degradation by DPP-4, it is more stable and so more effective than native GLP-1. Another GLP-1 agonist drug, Liraglutide (Victoza®), is even more stable and presents the advantage of once-daily dosing. Specific inhibitors of DPP-4 are a new class of drugs that prolong the action of the native incretins by preventing their degradation. These drugs have the suffix "-gliptin" in their name and sitagliptin (Januvia®), saxagliptin (Onglyza®), and linagliptin (Tradjenta®) have gained FDA approval. A considerable advantage of DPP-4 inhibitors is that they can be taken orally, unlike the GLP-1 agonists, which are peptides and must be injected.

1.2 Insulin resistance and Type 2 Diabetes

1.2.1 Definition and classification of Diabetes

Diabetes is a group of metabolic diseases characterized by a state of chronic hyperglycemia (i.e. fasting glycemia > 126 mg.dL^{-1} (7.0 mM) and/or random glycemia or a 2h-post 75g glucose intake glycemia > 200mg.dL^{-1} (11.0mM) attested by twice independent measurements) with disturbances in carbohydrate, fat and protein metabolism resulting from defects in insulin secretion, insulin action, or both (WHO definition). Diabetes affects 347 million people worldwide (WHO data updated in march 2013) and it is expected to rise and be the 7th leading cause of death worldwide by 2030 due to population growth, aging, urbanization, and increasing prevalence of obesity and physical inactivity. Symptoms of marked hyperglycemia and so diabetes include polyuria (frequent urination), polydipsia (increased thirst), weight loss, sometimes with polyphagia (increased hunger), and blurred vision. Impairment of growth and susceptibility to certain infections may also accompany chronic hyperglycemia. Chronic hyperglycemia of diabetes is associated with long-term complications including retinopathy with potential loss of vision; nephropathy leading to renal failure; peripheral neuropathy with risk of foot ulcers, amputations, and Charcot joints; and autonomic neuropathy causing gastrointestinal, genito-urinary, cardiovascular symptoms and sexual dysfunction. Patients with diabetes have an increased incidence of atherosclerotic cardiovascular, peripheral arterial, and cerebrovascular diseases. Indeed, hypertension and abnormalities of lipoprotein metabolism are often found in people with diabetes. (Anon 2010)

The vast majority of diabetes cases fall into two broad etiopathogenetic categories: type 1 and type 2 diabetes.

Type 1 Diabetes - Type 1 Diabetes (T1D) (previously called "insulin-dependent diabetes mellitus" or "juvenile diabetes" because it is usually diagnosed in children or young adults) represents 10% of diabetes cases (WHO, 2013) and results from a deficiency in insulin secretion due to auto-immune destruction of insulin-producing β-cells. T1D occurs in individuals with a genetic predisposition to the disease, predominantly from a human leukocyte antigen (HLA)-related immunogenotype that accounts for approximately 60% of the genetic influence (Skyler JS 2013). In these genetically predisposed individuals, an environmental trigger is thought to initiate an immune response targeting the insulin-secreting pancreatic β cells. The initial immune response may also engender secondary and tertiary immune responses that contribute to the impairment of β-cell function and destruction of β-cells. T1D is

38

generally treated throughout life by exogenous insulin administrations via manual injections or insulin pumps (pancreatic transplants being still experimental).

Type 2 Diabetes - Type 2 diabetes (T2D) (formerly known as "non-insulin-dependent diabetes mellitus" or "adult-onset diabetes") represents most of diabetes cases (90%, WHO, 2013 and 85% in France, 2007-2010 ENTRED study) and is associated to insulin resistance with relative insulin deficiency. Insulin resistance (i.e. decreased response of insulin target tissues to "normal/physiological" insulin stimulation) is the first committed step in the development of T2D. In the early stages of insulin resistance, the pancreas compensates by increasing insulin secretion in an attempt to overcome defects in peripheral insulin action. In response to this increased demand for insulin production, the β-cells hypertrophy. In fasting periods, basal compensation is sufficient to maintain blood glucose in the normal range (people are then normoglycemic but hyperinsulinemic). However, in post-prandial condition, glucose is rapidly absorbed from the gut and a relative lack of insulin, due to inadequate compensation, is detected as the blood glucose level rise over time is exaggerated. This inability to adequately extract and dispose of blood glucose following a meal or a glucose challenge is known as **glucose intolerance** (or impaired glucose tolerance, IGT). This stage of "pre-diabetes" can last several years (depending on genetic predispositions and some environmental factors) until pancreas beta cell start to fail and/or die, reducing the functional beta cell mass. From then on, pancreas can no longer secrete enough insulin to compensate insulin resistance so that chronic hyperglycaemia arises and type 2 diabetes is diagnosed (See **Fig. 10** below).
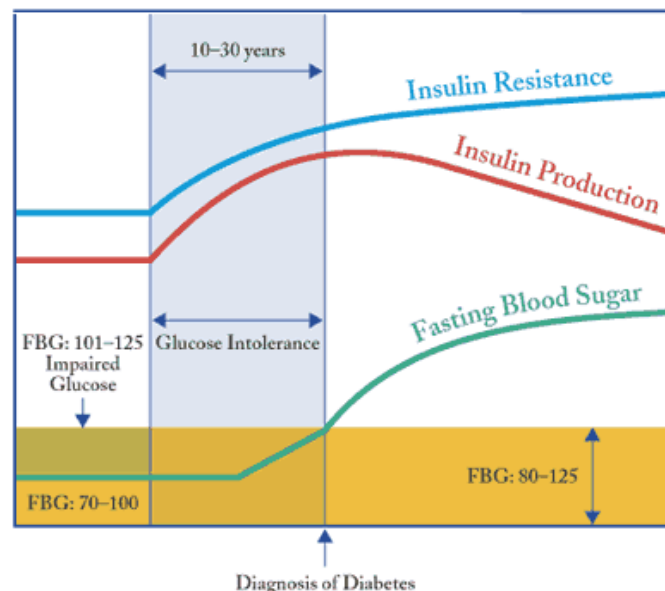
Figure 10 – Progression from pre-diabetes (glucose intolerance) to diabetes. Figure from http://www.med.umich.edu/diabetes/education/type2.htm and adapted from Type 2 Diabetes BASICS 2000, International Diabetes Center, Mineapolis, MN. Abbreviation: FBG, Fasting Blood Glucose (level).

Finally, both T1D and T2D result from beta-cell dysfunction and/or beta cell mass loss, but the triggering factors are quite different between these two forms of diabetes (auto-immunity *versus* excess nutrients toxicity) (see section 1.2.3 for further details on molecular mechanisms of insulin secretion deficiency).

Other but less common forms of Diabetes - Monogenic forms of diabetes (MODY diabetes), pancreatic or hormonal diseases, some genetic syndromes (e.g. Prader-willi) or drug-induced diabetes are other but rare forms of diabetes and will not be further addressed in this manuscript.

Gestational Diabetes - Gestational Diabetes Mellitus (GMD) is the condition defined as any degree of glucose intolerance with onset or first recognition during pregnancy (Anon 2003). About 7% of all pregnancies are complicated by gestational diabetes and it is considered that women with GDM are at increased risk of developing type 2 diabetes after pregnancy. Offspring of these women are also at increased risk of obesity, glucose intolerance, and diabetes in late adolescence and young adulthood. Human pregnancy is characterized by a series of metabolic changes that promote adipose tissue accretion in early gestation, followed by insulin resistance and facilitated lipolysis in late pregnancy (Barbour et al. 2007). If insulin resistance already exists before pregnancy, it worsens during gestation and causes gestational diabetes. Thus, chronic insulin resistance is a central component of gestational diabetes pathophysiology (Barbour et al. 2007).

1.2.2 Insulin resistance

1.2.2.1 Molecular defects and mechanisms underlying insulin resistance

Insulin resistance is a condition in which insulin target cells (e.g. hepatocyte, adipocyte, muscle cell) do not respond properly to a "normal" insulin stimulation and this condition is related to disruptions of the insulin signal transduction. It is worth noting that genetic mutations or defects in proteins of the insulin-signaling cascade rarely underlie the insulin resistance and T2D (Roberts et al. 2013). Insulin resistance and T2D are often associated to obesity or overweight and it is now well supported that environmental factors such as nutrients (especially lipids) oversupply and alterations in substrate metabolism due to physical inactivity are central underpinnings of chronic tissue **inflammation** and **lipotoxicity** phenomenon, and contribute to the manifestation of peripheral insulin resistance. In addition to inflammation and lipotoxicity that are probably the main pathologic phenomenon relating obesity and insulin resistance, **oxidative stress, reticulum endoplasmic stress, mitochondrial dysfunction** and **alterations of gut microbiota composition** are other factors that can

contribute to the development or progression of insulin resistance. All those processes are however somewhat related because they are induced by common factors (e.g. fatty acid overload induces formation of bioactive lipid metabolites (lipotoxicity) and triggers inflammation pathways through binding to toll-like receptors) and because they nearly all lead to the activation of cellular stress-response pathways (e.g. MAPK and NFkB-IKKβ pathways), causing alterations in insulin signal transduction.

Molecular defects of partners of the insulin signaling pathways associated to insulin resistance

Post-receptor defects are thought to account for much, if not all, of the impairment in muscle insulin action observed in T2D (Roberts et al. 2013). Those post-receptor defects include:

(1) **increased serine phosphorylation of IRS** proteins, resulting in decreased tyrosine phosphorylation of IRS and increased proteasome targeting,

(2) **reduced IRS** proteins number, due to reduced expression and/or increased proteasomal degradation,

(3) **increased activity of phosphatases** including src homology 2 domain containing inositol 5'-phosphatase 2 (SHIP2), skeletal muscle and kidney enriched inositol phosphatase (SKIP) , phosphatase tensin homolog deleted on chromosome ten (PTEN), and phosphotyrosine phosphatase 1B (PTP-1B);

(4) **decreased activation of** insulin receptor downstream signaling molecules including **PKB/Akt and atypical PKC.**

Processes leading to serine phosphorylations on IRS

Many agree that impaired insulin action occurs primarily at the level of IRS-1 and as a result of stress serine/threonine kinase activation (e.g. JNK, ERK, IKK, PKC, mTOR, S6K) **that catalyzes inhibitory serine phosphorylation of IRS-1** (Aguirre et al. 2000; Aguirre et al. 2002; Rui et al. 2001; Gual et al. 2005; Roberts et al. 2013). Phosphorylation of IRS proteins at particular serine residues (e.g. Ser 307) impedes IRS interaction with the IR. This leads to reduction in tyrosine phosphorylation of IRS. Reduced IRS phosphorylation on critical tyrosine residues prevents PI3K p85 subunit binding to IRS and so downstream signal transduction. Furthermore, alteration in phosphorylation status, specifically multiple serine phosphorylations, is shown to target IRS-1 for proteasomal degradation (Pederson et al. 2001) and this could explain the reduced IRS-1 protein contents of glucoregulatory tissues harvested from obese and/or diabetic rodents (Wang et al. 2009; Roberts et al. 2013). Several factors can lead to the activation of stress kinases and in particular Reactive Oxygen Species (ROS), inflammatory cytokines (e.g.

TNF-α, IL-1β and IL-6), microbial (LPS) or viral molecules, excessive free fatty acids and/or excessive misfolded proteins load on the ER (ER stress).

Increased ROS production and/or decreased detoxification (**oxidative stress**) can result from many processes including glucotoxicity, mitochondrial dysfunction, ER stress, hypoxia in adipose cells due to WAT hypertrophy, inflammation or reduction in antioxydant defenses. The detailed mechanisms for serine kinases activation mediated by ROS is not clearly understood but a reduced ROS production obtained with antioxidant treatments improves insulin sensitivity. ROS stimulates pro-inflammatory signaling by activation of IKKβ and so also contribute to insulin resistance through this way.

Pro-inflammatory cytokines (TNF-α, IL-6, IL-1β) binding to their cell surface receptors (TNFR, IL-6R and IL-1R respectively) induces pro-inflammatory signaling that leads to the activation of IKKβ and JNK (and also ERK, mTOR and GSK-3). Activation of NFkB-IKKβ and JNK pathways leads to phosphorylation of both IR and IRS-1 proteins on serine residues causing insulin resistance, and to activation of a protein network that enhances transcription of cytokine genes, further exacerbating **inflammation**. Free Fatty Acids and microbial (e.g. LypoPolySaccharide, LPS) or viral components can also trigger inflammation pathways through binding to the toll-like receptors (TLR-4 in particular for FFAs) and thus contribute to the inflammation induced insulin resistance. Inhibition of IKKβ and JNK with anti-inflammatory drugs (salicylates) or gene knock out (IKKβ) improves insulin sensitivity contemporaneously with reductions in serine phosphorylations (Yuan et al. 2001; Kim et al. 2001).

Accumulation of misfolded or modified proteins in the ER (**ER Stress**) triggers the Unfolded Protein Response (UPR). UPR signaling activates JNK pathways through IRE1-α (and possibly PKR; (Rutkowski & Hegde 2010; Nakamura et al. 2010)) and so reduces insulin signal transduction and can contribute to insulin resistance in the context of overfeeding. Chemical chaperones including 4-phenyl butyric acid and taurine-conjugated ursodeoxycholic acids (TUDCA) significantly reduce ER stress thereby improving insulin sensitivity (Özcan et al. 2006).

Another important mechanism that induces insulin resistance by inhibitory phosphorylation on IRS serine residues is the activation of novel PKC isoforms (epsilon (ε) in liver and theta (θ) in muscle) by bioactive lipid metabolites such as DiacylGlycerols (DAGs) (**lipotoxicity**). Intracellular accumulation of DAGs can occur when the rate of its synthesis by lipogenesis and/or its release from triacylglycerols (TAGs) exceeds the rate of its incorporation into triglycerides or phosphatidic acid (PA) (Samuel & Shulman 2012). Mice overexpressing skeletal muscle DGAT1 (the enzyme that catalyzes DAGs acylation into TAGs) accumulate muscle TAGs but have lower DAGs and are protected from lipid-induced muscle resistance (Liu et al. 2007). In contrast, mice with reduced expression of Diacylglycerol kinase δ (DGK$\delta^{+/-}$ mice), the enzyme that converts DAGs into PAs, display increased muscle content in DAGs, but not in TAGs, and exhibit muscle insulin resistance (Samuel & Shulman 2012). Taken together these studies

suggest a potent toxic role for DAGs but disculp intracellular TAGs as pathogenic lipid species for insulin resistance.

Other Processes leading to reduction of IRS activity: IRS degradation, O-glycosylation and role of SOCS

Intracellular IRS-1 protein levels are regulated by the Cullin7 E3 ubiquitin ligase, which targets IRS-1 for ubiquitin-mediated degradation by the proteasome, in a process dependent on mammalian target of rapamycin (mTOR) and the p70 S6 kinase activities (Xu et al. 2008). Indeed, prolonged cells exposure to insulin (e.g. in the case of insulin resistance compensatory hyperinsulinemia), or specific activation of the mTORC1/ribosomal S6 protein kinase (S6K1) branch of the insulin signaling cascade, induces feedback serine/threonine phosphorylation of IRS by mTORC1 and/or S6K1. In cultured cells, multi-site serine/threonine phosphorylation of IRS correlates with their subcellular re-localisation and/or proteasome-mediated degradation (Copps & White 2012).

In addition to multi-site serine/threonine phosphorylations on IRS, nitrosylation of IRS proteins also contribute to the reduction in IRS proteins. Protein S-nitrosylation is a reversible covalent attachment of a NO moiety to thiol sulfhydryls. It could result from increased iNOS expression associated to obesity in insulin-target tissues (Kaneki et al. 2007). *S*-Nitrosylation of the β subunit of insulin receptor or of PKB/Akt in muscle attenuates their kinase activities, and *S*-nitrosylation of IRS-1 reduces its tissue level via proteasome-mediated degradation (Sugita et al. 2005).

Excess glucose influx into the hexosamine biosynthetic pathway (HBP) might increase O-linked beta-N-acetylglucosamine (O-GlcNAc) modifications of various proteins, including proteins of the insulin signaling pathway, possibly modifying their activity. In rat primary adipocytes, O-glycosylation of IRS-1 and Akt-2 has been shown to inhibit their phosphorylation on tyrosine residues, subsequently leading to insulin resistance (Park et al. 2005).

Finally, it has also been shown that some suppressor of cytokine signaling members (i.e. SOCS-1 and SOCS-3) are able to inhibit the insulin signaling pathway by three different mechanisms: (1) inhibition of tyrosine phosphorylation of IRS proteins because of competition at the docking site on the insulin receptor (IR), (2) induction of the proteasomal degradation of IRS and (3) inhibition of the IR kinase. SOCS proteins expression is virtually absent in basal conditions, but it is rapidly and robustly induced in response to several stimuli such as hormones, cytokines and growth factors. A significant correlation between SOCS-3 expression and insulin resistance has been demonstrated *in vivo*. Interestingly, the expression level of SOCS-3 is strikingly increased in insulin-target tissues from both patients and animal models with type 2 diabetes and insulin resistance. While it remains to be established whether the increased expression of SOCS is a cause or a consequence of insulin resistance, a large body of observations supports a role for SOCS proteins in the disease process found in states with insulin resistance. (Lebrun & Van Obberghen 2008)

Processes leading to phosphatases activation

As discussed in section 1.1, the protein tyrosine phosphatase **PTP-1B**, the inositol polyphosphate 3-phosphatase **PTEN** and the polyphosphate 5-phosphatases **SKIP and SHIP2** are physiological negative regulators of insulin signaling. Therefore, it can be expected that enhanced activation of one or several of these phosphatases leads to insulin resistance. Several studies on obese and/or insulin resistant human subjects or rodent models have indeed reported an increased expression and/or activity of PTP-1B and of SHIP2 in some insulin target tissues (Choi & Kim 2010; Roberts et al. 2013). For example, PTP-1B activity displayed a 3-fold increase in muscle and a 2-fold (obese *versus* lean) to 5.5 fold (obese diabetic *versus* lean) increase in fat of obese and insulin-resistant human subjects or rodent models (Ahmad et al. 1995; Ahmad & Goldstein 1995; Ahmad et al. 1997; Cheung et al. 1999). SHIP2 expression levels are elevated in skeletal muscle and adipose tissue from obese and diabetic db/db mice (Hori et al. 2002). PTEN, SHIP2 or SKIP overexpression also inhibit insulin action in cultured cells (Roberts et al. 2013) or induce insulin resistance and glucose intolerance in transgenic mice (Kagawa et al. 2008). However, the exact mechanisms underlying those phosphatases activities and/or expressions enhancement in insulin resistance and obesity are still unclear.

Processes leading to direct PKB/Akt inhibition

In liver and skeletal muscle, insulin-induced protein kinase B/Akt activation can be altered by toxic lipid metabolites (ceramides), possibly through the action of PP2A that dephosphorylates Akt on its Ser 473 residue and through the action of PKCζ (see further details in section 1.2.2.2). Ceramides and DAGs toxicities mediated by different PKCs on insulin signaling are part of the lipotoxicity phenomenon.

S-Nitrosylation of Cys 224 or Cys 296 of PKB/Akt also results in impaired activity, the latter because it prevents the formation of an essential disulfide bridge with Cys 310 (Bashan et al. 2009).

1.2.2.2 Putative etiological pathways leading to insulin resistance development

Insulin resistance is a complex metabolic disorder that defies explanation by a single etiological pathway and what first triggers insulin resistance is difficult to define and is probably different according to the context. However, this pathological condition is strongly associated to obesity and chronic overnutrition. Noteworthy, insulin resistance is often found in people with deep (*versus* superficial) subcutaneous abdominal fat (i.e fat between the skin and the muscle wall) and/or visceral adiposity (i.e., a high degree of fatty tissue underneath the abdominal muscle wall and surrounding visceral organs) and several lines of evidence suggest two strong links. First, visceral adipose tissue is characterized by

44

higher secretion of pro-inflammatory cytokines such as TNF-α and IL-6, and lower secretion of adiponectin, the anti-inflammatory adipokine, as compared with subcutaneous adipose tissue (van Greevenbroek et al. 2013). Second, adipocytes from visceral fat depot show substantially higher fatty acid fluxes than subcutaneous abdominal adipocytes (van Greevenbroek et al. 2013). This excessive release of free fatty acids into the bloodstream (through the portal vein) is related to an accumulation of fat in ectopic depots (i.e. liver, muscle, pancreas and heart) contributing to insulin resistance and β-cell failure development and/or progression.

Finally, two main phenomenons are implicated in insulin-resistance associated to obesity or visceral adiposity: **chronic low-grade tissue inflammation** (especially in WAT and liver) and **ectopic intracellular lipid accumulation**, otherwise termed lipotoxic stress or lipotoxicity. Other processes such as ER stress, mitochondrial dysfunction, gut microbiota alteration and oxidative stress also contribute to insulin resistance but these are nearly all inter-related and linked to inflammation and lipid overload.

Initiation and exacerbation of inflammation in obesity – Model proposed by (de Luca & Olefsky 2008)

The precise physiological events initiating the inflammatory response in obesity remain incompletely understood. Among the proposed theories, one suggests that the expansion of adipose tissue leads to adipocyte hypertrophy and hyperplasia and that large adipocytes outstrip the local oxygen supply causing adipocyte hypoxia with activation of cellular stress pathways (de Luca & Olefsky 2008). Activation of cellular stress pathways then triggers adipose cell autonomous inflammation and the release of cytokines and other pro-inflammatory signals (e.g. IL-6, TNF-α, MCP-1, ICAM) by the hypertrophied adipocytes. Furthermore, as adipocytes enlarge, increased levels of free fatty acids (FFAs) are released by adipocytes which can stimulate the production and release of tumour necrosis factor-α (TNF-α) by macrophages already present in WAT (resident macrophages). Indeed, saturated FFAs bind to the toll-like receptor-4 (TLR-4) at the macrophages cell surface which results in NF-kB activation and TNF-α release. In turn, macrophage-derived TNF-α further activates inflammatory pathways in adipocytes, thereby enhancing the expression of various pro-inflammatory genes (intercellular adhesion molecule-1 (ICAM-1), interleukin-6 (IL-6) and monocyte chemoattractant protein-1 (MCP-1)) through NFkB and reducing adiponectin secretion through PPARγ. As part of the chronic inflammatory process, locally secreted chemokine MCP-1 and ICAM attract monocytes, favor their diapedesis from blood and their infiltration in adipose tissue. In addition, the inflammatory environment favors the conversion of resident and/or newly recruited macrophages from M2 (anti-inflammatory macrophages) to M1 (pro-inflammatory macrophages). This macrophage polarity switch in favor of pro-inflammatory macrophages further exacerbates adipose tissue inflammation (de Luca & Olefsky 2008). Infiltrated macrophages form crown-like structures that surround large dead or dying adipocytes. These tissue macrophages then release cytokines (e.g. TNF-α) that further activate the inflammatory program and

cause insulin resistance in neighboring adipocytes. Insulin-resistant adipocytes release more FFAs due to the loss of anti-lipolytic activity of insulin, which further stimulate inflammatory pathways in infiltrated macrophages (through FFAs binding to TLR-4). Finally, when adipose tissue hypertrophy, an inflammation amplification loop is created between hypertrophied adipocytes and infiltrated or resident macrophages that both secrete pro-inflammatory signals (See **Fig. 11**).
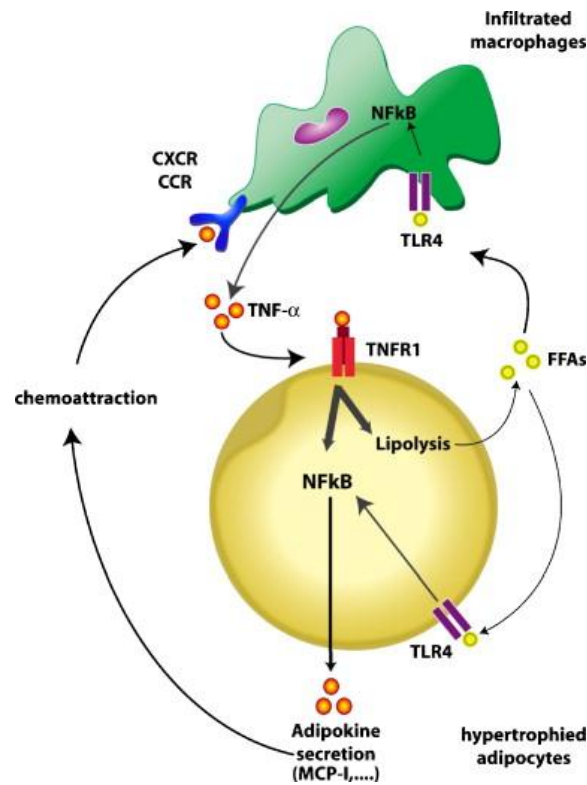
Figure 11 – Inflammation amplification loop in hypertrophied white adipose tissue. Figure from Maury et Brichard, Mol. Cell. Endocrinol, 2010. Abbreviations: CCR/CXCR, chemokine receptors ; FFAs, Free Fatty Acids, MCP-1, Monocyte Chemoattractant Protein 1 ; NFκB, Nucleor Factor kappa B ; TLR-4, Toll-like Receptor 4, TNF-α, Tumor Necrosis Factor alpha ; TNFR1, TNF-α Receptor 1.

This leads to adipocyte dysfunction and adipocyte insulin resistance. Such adipocytes secrete less adiponectin (an insulin-sensitizing adipokine), more pro-inflammatory cytokines and release more FFAs which contribute to insulin-resistance, inflammation and ectopic lipid redistribution to other tissues (e.g. liver, muscle, heart, pancreas).

In addition to inflammation and insulin resistance within adipose tissue, a similar process probably occurs in the liver as liver contains a large pool of tissue-resident macrophages (i.e. Kupffer cells) that can also become activated and release pro-inflammatory cytokines. Kupffer-cells derived cytokines may trigger hepatocyte inflammation signaling pathways and hepatocyte inflammation. In liver, inflammation could also result from increased intracellular lipid content (lipotoxicity) and steatosis that accompany overnutrition and obesity-related adipocytes dysfunction and insulin-resistance.

Besides causing hepatic insulin resistance, this local inflammation of the liver would also contribute to systemic inflammation and secondary insulin resistance in other tissues such as skeletal muscle.

Overnutrition and obesity are often accompanied by elevations in tissue and circulating FFA concentrations, and saturated FFAs can directly activate pro-inflammatory responses in vascular endothelial cells, adipocytes and myeloid-derived cells. These obesity-induced physiological events result in the development of systemic inflammation. Although skeletal muscle insulin resistance can be caused by chronic inflammation, the precise sequence of events connecting inflammation and decreased insulin signaling in myocytes remains poorly elucidated. It is possible that increased circulating FFAs or altered cytokine/adipokine secretion profiles cause secondary insulin resistance in muscle. Extramyocellular adipocytes could also contribute to this process through paracrine signaling. Finally, increased macrophage content has been reported in insulin resistant muscle, raising the possibility of macrophage-mediated tissue autonomous insulin resistance, as in liver and fat. Of course, all these hypothesis are not mutually exclusive.

Finally, it is now clear that **chronic low-grade tissue inflammation is an important contributor to the etiology of obesity and high fat diet-induced insulin resistance**. Macrophages infiltration and polarity switch are important contributors in this process, as well as FFAs release and ectopic lipid redistribution to other organs. Endoplasmic Reticulum overload due to overnutrition also plays a role in tissue inflammation and insulin resistance.
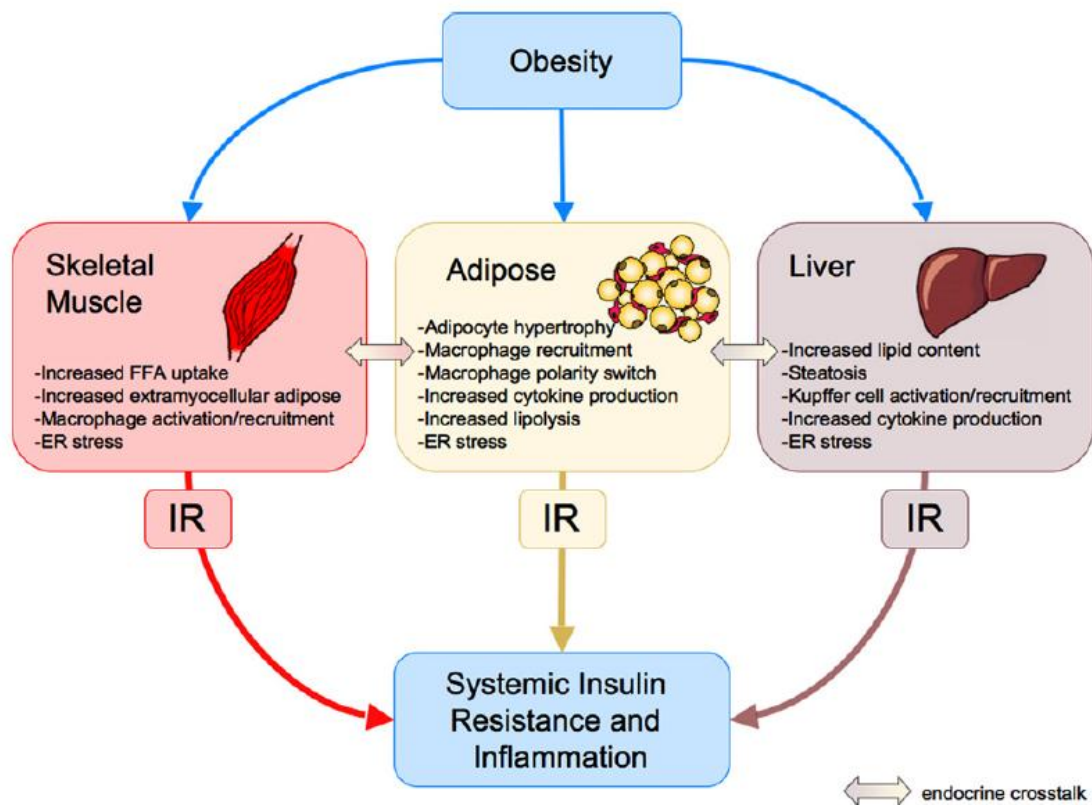
Figure 12 – Obesity is associated to chronic low-grade tissue inflammation, ectopic lipid deposition, ER stress and insulin resistance. Figure from C. de Luca et JM Olefsky, FEBS Letters, 2008 (de Luca & Olefsky 2008). Abbreviations : ER, Endoplasmic Reticulum ; FFA, Free Fatty Acids.

Inflammation-induced insulin resistance

As discussed in section "insulin resistance underlying molecular mechanisms" and as shown in **Fig. 13**, insulin resistance can be mediated by the activation of stress and inflammatory pathways by pro-inflammatory cytokines (TNF-α, IL-6, IL-8 and IL-1β), free fatty acids and also possibly microbial components. Induction of inflammatory pathways leads to inhibition of insulin signal transduction **through** (1) **increased inhibitory serine phosphorylations on IRS** by the activated serine/threonine kinases IKKβ, JNK and SOCS, and (2) increased IRS proteasomal degradation due to increased IRS ubiquitinylation by SOCS, s-nitrosylation by NO (due to increased iNOS expression), and multiple site phosphorylations by serine/threonine kinases, (3) reduced Akt and PI3K activities by s-nitrosylations.
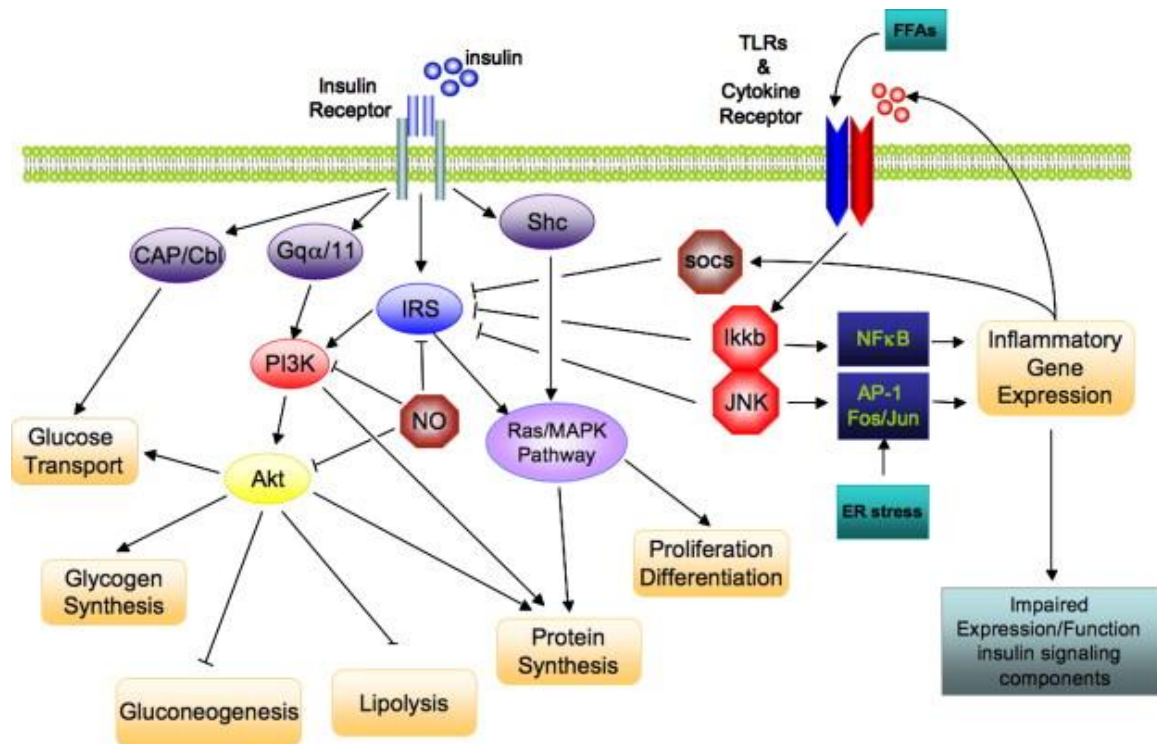
Figure 13 - Interactions between insulin and inflammatory pathways. From Carl de Luca et Jerrold M. Olefsky, 2008. Abbreviations: AP-1, ; Activator Protein 1 ; CAP, Cbl-Associated Protein ; FFAs, Free Fatty Acids ; GLUT-4, Glucose transporter 4 ; IkkB, Inhibitor NFκB Kinase ; IRS, Insulin Receptor Substrate(s) ; JNK, c-Jun N-terminal Kinase ; MAPK, Mitogen-Activated Protein Kinase(s) ; NFκB, nucleor factor kappa B ; NO, Nitric Oxide ; PI3K, Phosphosphatidyl-inositol-3-kinase ; Shc, src homology and collagen protein ; SOCS, Suppressor Of Cytokine Signaling ; TLRs, Toll-Like Receptors ; mTOR, mammalian Target Of Rapamycin.

Ectopic lipid depots (lipotoxicity) plays an important role in obesity-related insulin resistance

When energy intake overpasses energy expenditure (e.g. chronic overnutrition, sedentarity, and/or consumption of energy-rich food) the energy excess is stored under the form of triglycerides in adipose tissue. However, when adipose tissue storage capacity is overwhelmed, the exceeding energy is redistributed under the form of free fatty acids to other organs (e.g. liver, skeletal muscle, heart, pancreas and/or kidney) where it forms ectopic lipid depots, a phenomenon called lipotoxicity. Adipose tissue storage capacity can be insufficient because of an inability of white adipose tissue to further expand (e.g. because of mechanical stress induced by extracellular matrix or by the presence of other tissues or bones ; or because of a blunted triglyceride synthesis and uncontrolled lipolysis associated to adipose tissue dysfunction) while plasma free fatty acids exceeds due to nutrient oversupply or uncontrolled release by adipose tissue (lipolysis) and/or liver (*de novo* lipogenesis).

Upon cellular entry through the fatty acid translocase CD36 or a Fatty Acid Transport Protein (FATP1/2/5), FFAs are rapidly esterified to fatty-acyl-CoenzymeAs (FA-CoAs). FA-CoAs are then successively transferred to a glycerol backbone to form MAGs, DAGs and TAGs, or esterified with

49

sphingosine to form ceramides. In a context of energy excess, the increased FFAs influx stimulates lipogenesis and so DAG, TAG and ceramides intracellular contents increase. Of note, mitochondrial dysfunction often observed in insulin-resistant tissues can also contribute to the accumulation of DAGs and ceramides as a result of reduced or incomplete β-oxidation, in particular due to a decreased PDH activity. Despite some of these lipid metabolites (DAGs and ceramides) are known to act as second messengers in key signaling pathways, their accumulation in liver and skeletal has been associated to insulin resistance development (Samuel & Shulman 2012).

Indeed, DAGs are signal mediators that can activate conventional (PKC-α, -β, -γ) but also novel members of the protein kinase C family (nPKC-θ in skeletal muscle and nPKC-ε in liver). In the liver, DAGs-activated PKC-ε inactivates Insulin Receptor (IR) by phosphorylating it on serine residues. In the skeletal muscle, DAG-activated PKC-θ phosphorylates IRS on serine residues (in particular on Ser 307 and Ser 1101 (Li et al. 2004) residues) which prevents further tyrosine phosphorylations of IRS and impedes PI3K recruitment, thereby reducing insulin signal transduction. Recently, studies in mice overexpressing DGAT2 have suggested an important role of the intracellular localization of DAGs for DAGs-induced PKCs activation (Jornayvaz et al. 2011). This enzyme (DGAT) is localized to the Endoplasmic Reticulum but upon lipid accumulation, it is highly expressed in membranes of lipid droplets. Mice overexpressing DGAT2 develop hepatic steatosis associated with hepatic, but not peripheral insulin resistance. While total DAG content is modestly increased in the DGAT2 transgenic mice (specifically the "lower-overexpressing" strain), the DAG content in the lipid droplets-containing cytosolic fraction is increased by nearly 10-fold and associated with activation of PKC-ε, impairement of insulin signaling, and hepatic insulin resistance.

Several lines of evidence also support a role for ceramides in the pathogenesis of insulin resistance. For example, in mice fed a high fat diet, a treatment with myriocin (a potent serine palmitoyltransferase inhibitor) specifically attenuates the increase in muscle ceramides content, without affecting muscle long-chain acyl-CoA, DAG or TAG contents and improves glucose tolerance. However, myriocin prevents acute skeletal muscle insulin resistance following infusion of palmitate, but not oleate (Holland et al. 2007) suggesting that ceramides role in the pathogenesis of insulin resistance may be limited to saturated fats. Accumulation of ceramides has been associated with impaired Akt2 activity. This appears to be related to a direct effect on Akt2 activation, rather than defects in upstream signaling events. Several mechanisms have been proposed to explain ceramides-mediated Akt2 inhibition. First, ceramides may lead to the activation of Protein Phosphatase 2A (PP2A) (Teruel et al. 2001) which can dephosphorylate Akt2, effectively attenuating insulin signaling. In addition, ceramides may impair insulin action via the atypical PKC isoform PKC-ζ (Powell et al. 2003). PKC-ζ and Akt2 interact intracellularly but dissociate upon insulin stimulation; ceramides impair this disassociation, and furthermore, via PKC-ζ phosphorylation of Akt2, prevent Akt2 activation. Ceramides may accumulate in

calveolin-enriched microdomains and recruit PKC-ζ, which in turn could sequester Akt2 and prevent it from participating in insulin signaling.

Other factors associated with inflammation, ectopic lipids and insulin resistance in obesity

Another potential cause of inflammation and insulin resistance in obesity is **Endoplasmic Reticulum stress** (de Luca & Olefsky 2008). Overnutrition causes mechanical stress, excess lipid accumulation, protein synthesis and abnormal energy metabolism, all of which leading to an overloaded ER. This increased synthetic state in the ER disrupts the normal folding of proteins and accumulation of misfolded proteins activates the unfolded protein response (UPR) that is known to induce stress response pathways. In particular, Özcan et al. (Ozcan et al. 2004) have shown that induction of ER stress in cultured hepatocytes induces insulin resistance via JNK-mediated serine phosphorylation of IRS1, and that this (ER-stress and insulin resistance) can be reversed by a treatment with chemical chaperones (Özcan et al. 2006).

Mitochondrial dysfunction has also been associated with insulin resistance. Indeed, High glucose or FFAs fluxes into cells overwhelms the mitochondrial electron transport system which overproduces anion superoxide (O_2^-) so that it cannot be detoxified properly by the mitochondrial antioxidant enzymes (MnSOD, PRX, GPX and GR). This mitochondrial oxidative stress damages mitochondrial lipids, enzymes and DNA (that is particularly susceptible to oxidative damage since it is not physically protected by histones contrary to nuclear DNA) and leads to mitochondrial dysfunction (Pieczenik & Neustadt 2007). Of note, inflammatory mediators (e.g. TNF-α) have also been associated *in vitro* to increased ROS production and mitochondrial function decay (Moe et al. 2004). Mitochondrial dysfunction is associated to a decreased β-oxidation capacity and so contribute to the accumulation of toxic lipid metabolites (DAGs and ceramides) and ultimately to the lipotoxicity phenomenon. Mitochondrial dysfunction leads to further damages in the cell and contribute to the **oxidative stress** that also induces insulin resistance through activation of stress kinases.

Another possible trigger for the chronic low-grade inflammation and for the obesity and insulin resistance development under a high fat feeding is **metabolic endotoxemia**. The bacterial lipopolysaccharide (LPS) is a major component of the outer membrane in Gram-negative bacteria. Pr. Burcellin research team found that a 4-weeks high-fat diet feeding chronically increased plasma LPS concentration two to three times, a threshold that they have defined as metabolic endotoxemia (Cani et al. 2007), and that this was related to earlier changes in intestinal permeability and microbiota, where the Gram negative (LPS containing bacteria)–to–Gram positive ratio increased during high-fat feeding (Cani et al. 2007). They had previously demonstrated that metabolic endotoxemia induced by LPS subcutaneous low-rate infusion reproduces most of the features of HFD-induced metabolic disease (impaired glucose tolerance, fasted and fed hyperinsulinemia, liver insulin resistance, increased

expression of inflammation factors, macrophages infiltration in WAT and WAT mass /body weight gain) and that on the opposite, LPS receptor CD14 KO mice resisted the occurrence of the diseases (diabetes and obesity). They then hypothesized that HFD feeding causes microflora changes, increasing LPS containing bacteria, and leading to increased intestinal permeability. Alteration in intestinal barrier function results in increased bacterial antigens transfer towards blood and metabolically active tissues, and could there stimulate innate immune response (through macrophages TLR4 and CD14 receptors), resulting in a chronic inflammatory state and consequently impaired metabolic functions such as insulin resistance, hepatic fat deposition and excessive adipose tissue development.

Conclusion

Insulin resistance is a complex metabolic defect that most likely has several etiologies dependent on both genetic predisposition and environmental factors. However, although numerous genetic and physiological factors interact to produce and aggravate insulin resistance, disruption of insulin signal transduction by inhibitory phosphorylations of IRS by serine/threonine kinases seems to be a common underlying mechanism. Chronic low-grade inflammation and ectopic lipid deposition seem to be the common factors that lead to the activation of the stress kinases (See **Fig. 14**) and may be the earliest triggers of insulin resistance in the context of obesity and overfeeding. In all cases, insulin resistance seems to be a response to or a result of a cellular stress/injury.
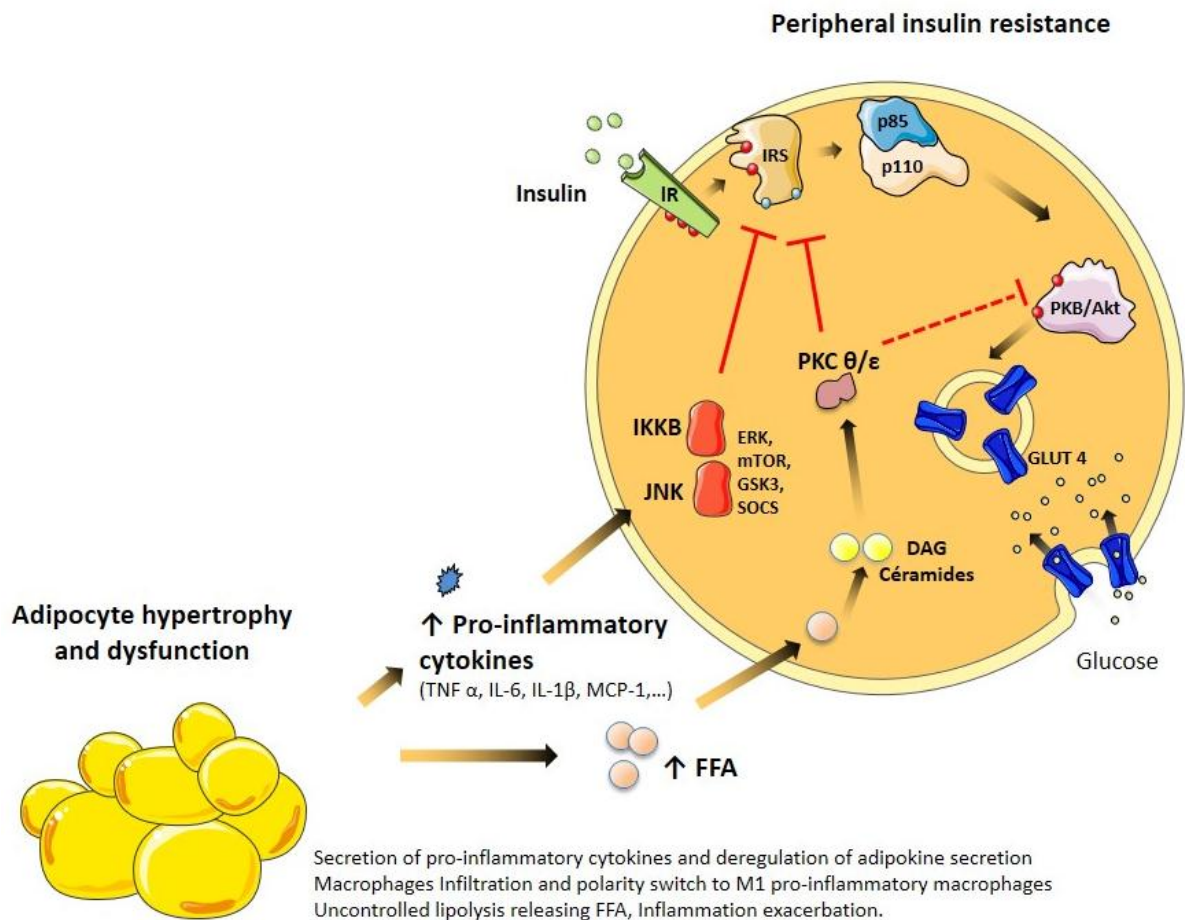
Figure 14 – Chronic low-grade inflammation and ectopic lipid redistribution associated to white adipose tissue dysfunction lead to activation of stress kinases and are major mediators of insulin resistance in the context of obesity. Adapted from L. Koppe PhD thesis, Lyon 2013. Abbreviations : DAG, diacyglycerol, ERK, extracellular signal-regulated kinase, FFA, free fatty acids, GSK3, glycogen synthase kinase 3 , IKKB, Inhibitor of nucleor factor kappa B Kinase, IR, insulin receptor, IRS, insulin receptor substrate, JNK, c-jun N-terminal kinase, IL, interleukine, MCP-1, Monocyte chemoattractant protein 1, PKB, Protein kinase B, PI3K, phosphoinositide-dependent-3-kinase PKC, Protein kinase C, SOCS, Suppressor Of Cytokine Signaling, TNF-α, tumor necrosis factor α.

1.2.2.3 Short-term and long-term consequences of insulin resistance

Insulin resistance is the pathophysiological condition in which normal amounts of insulin are insufficient to produce a normal insulin response from adipose tissue, muscle and liver cells. Hence, loss of insulin sensitivity leads in short-term to:

in muscle :

- **decreased glucose uptake** due to decreased GLUT-4 translocation to plasma membrane (and not due to decreased GLUT-4 expression). This decrease is of about 50% in T2D subjects in comparison with healthy subjects.
- **decreased glucose sequestration into cell** due to decreased phosphorylation to glucose-6-phosphate by hexokinase 2, and so **decreased use** for energy production or storage.
- **decreased glucose storage** under the form of glycogen because of decreased glycogen synthase activity.

in white adipose tissue :

- **decreased glucose uptake** due to both decreased GLUT-4 expression and translocation to plasma membrane.
- **increased release of free fatty acids** due to loss of anti-lipolytic activity of insulin (loss of inhibitory effect on HSL activity).

in liver :

- **increased liver glucose release** through GLUT-2 because of increased glucose production by glycogenolysis and mainly because of increased *de novo* synthesis. Indeed, enhancement in neoglucogenesis is related to 1) increased FFA flux and so increased beta oxidation producing NADH, ATP and Acteyl-CoA that are necessary to neoglucogenesis ; 2) increased glycerol input coming from adipocyte lipolysis and so increased amount of substrate for neoglucogenesis ; 3) chronically increased glucagon secretion that enhances G6Pase and PEPCK gene expression (through cAMP that stimulates the HNF-6 transcription factor and through the cAMP response element binding protein CREB that stimulates expression of PGC-1α that then binds to Foxo1 and HNF-4 transcription factors).
- **reduced glycogen synthesis** due to decreased glycogen synthase activity.
- **altered lipid metabolism** with hypertriglyceridemia, reduced HDL-cholesterol and increased sdLDL-cholesterol.

Finally, insulin resistance leads to **hyperglycemia** and **dyslipidemia** and so to glucotoxic and lipotoxic phenomenon when insulin resistance is not adequately compensated by an increased secretion of insulin by β-cells. Chronic hyperglycemia (Glucotoxicity) can contribute to **β-cell dysfunction and**

apoptosis, insulin resistance progression, and to the pathogenesis of **microvascular** (due to damage to small blood vessels and including neuropathy, retinopathy and nephropathy) **and macrovascular** (due to damage to larger blood vessels, including heart attacks, strokes and insufficiency in blood flow to legs) **long-term complications of diabetes**. Lipotoxicity can affect liver, skeletal muscle, pancreas, heart and kidney functions. Indeed, lipotoxicity can worsen glucotoxicity effect on β-cell function and β-cell mass, contribute to the pathogenesis of liver and muscle insulin resistance, lead to kidney tubulo-interstitial inflammation and fibrosis or even to renal failure, and trigger cardiomyocytes apoptosis and systolic ventricular dysfunction.

β-cell dysfunction and β-cell mass reduction

Given the existence of insulin resistance and a predisposing genetic background to β-cell dysfunction, incapacity of β-cell to adequately compensate insulin resistance results in hyperglycemia and dyslipidemia. Long-term exposure of pancreatic β-cells to high glucose and FFAs levels (i.e. Gluco-lipotoxicity) may both contribute to the progression and acceleration of β-cell failure via ER stress, mitochondrial dysfunction, oxidative stress, inflammation and amyloid deposition. (Popa & Mot 2013) See further details in section "1.2.3 – Insulin deficiency".

1.2.3 Insulin deficiency

Pancreatic β-cells possess the potential to greatly expand their function and mass in both physiologic and pathologic states of nutrient excess and increased insulin demand (Chang-Chen et al. 2008). β-cell response to nutrient excess occurs by several mechanisms, including hypertrophy and proliferation of existing β-cells, increased insulin synthesis and secretion, and formation of new β-cells from progenitor cells (Bonner-Weir et al. 1989; Brüning et al. 1997). In most subjects with obesity-induced insulin resistance, the developmement of compensatory mechanisms such as increased insulin secretion, insulin gene expression and β-cell mass, can succeed to maintain glucose homeostasis and avoid type 2 diabetes development (Kahn 2003; Popa & Mot 2013). In this context (obesity-induced insulin resistance), progression from β-cell compensation to β-cell failure occurs in a subset of genetically predisposed individuals whose pancreas fail to adequately compensate for the increased insulin demand, leading to hyperglycemia and dyslipidemia and so glucolipotoxicity phenomenon (See **Fig. 15**). Glucolipotoxicity then accelerates β-cell function decline (18% per year compared to 2% per year in the initial steps), leads to β-cell apoptosis that does not seems to be adequately compensated by regenerative processes and so results in decreased functional β-cell mass. At type 2 diabetes diagnosis, the β-cell function is already reduced by 50-60% and it seems that the decline has begun about 10-12

years before appearance of chronic hyperglycemia. Typical alterations in β-cell function are characterized by a decreased glucose-induced insulin secretion (increased triggering threshold), alteration of oscillatory patterns of insulin secretion with impairment of both high frequency and ultradian oscillations, reduced or absent first phase insulin secretion, prolonged second phase insulin secretion and gradual, time-dependent irreversible damage to cellular components of insulin production (Popa & Mot 2013).
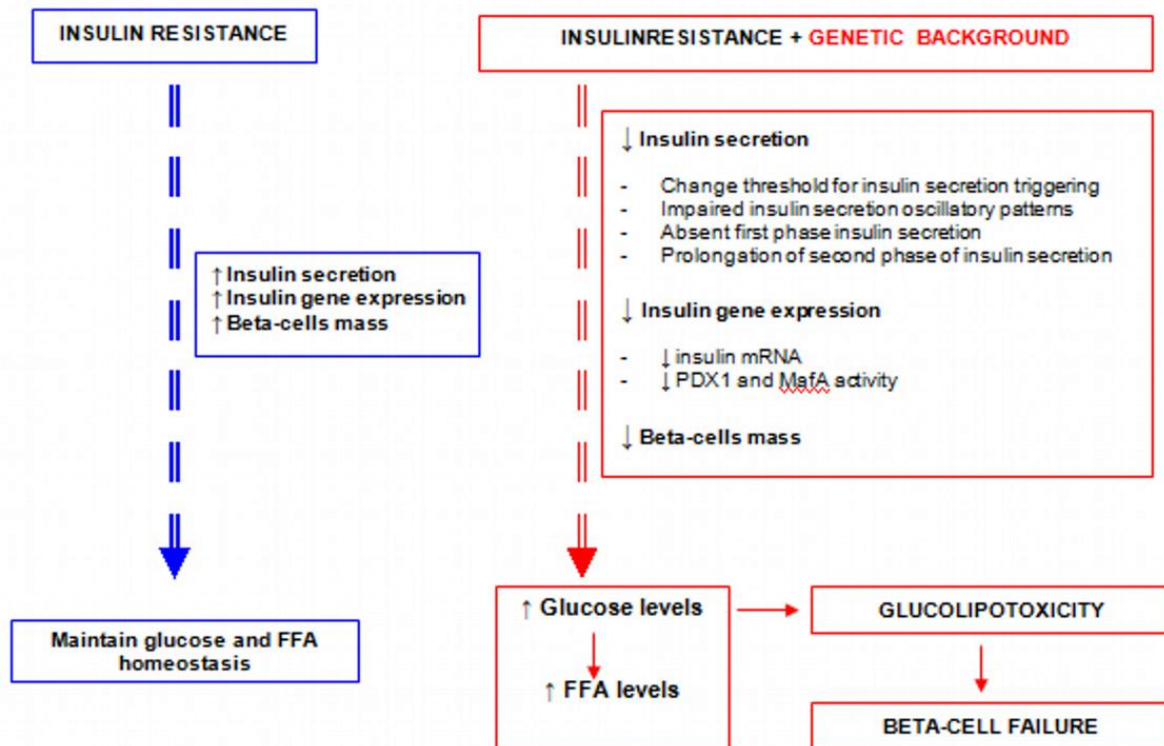
Figure 15 – Place of β-cell dysfunction in natural history of T2D. Figure from Popa et Mota, 2013, chapter 2 InTech. Abbreviations: FFA, Free Fatty Acids ; MafA, mammalian homologue of avian MafA/l-Maf (an insulin transcription factor) ; Pdx-1, Pancreatic and duodenal homeobox 1 (an insulin transcription factor).

Given the existence of insulin resistance and a predisposing genetic background, the mechanisms underlying β-cell dysfunction enhancement and β-cell apoptosis are complex, not completely understood and involve the interplay of numerous factors and conditions. These factors are triggered in the β-cell by the gluco-lipotoxic environment and include mitochondrial dysfunction, ER stress, oxidative stress, islet inflammation and amyloid polypeptide accumulation. All those processes are significantly interconnected and create a vicious cycle that eventually leads to β-cell failure (See **Fig. 16**).

56
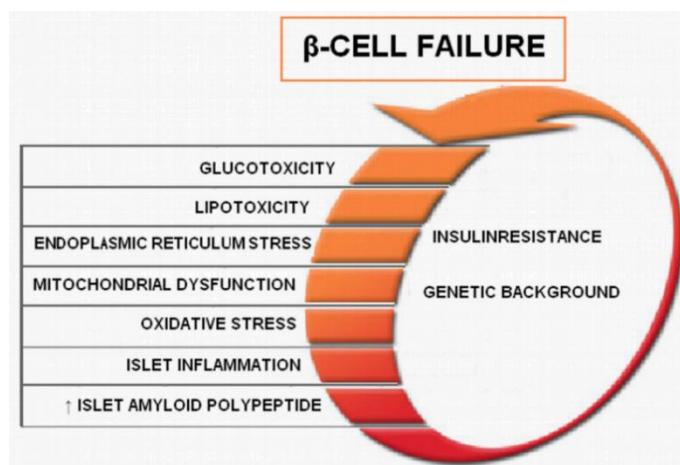
Figure 16 - Potential processes contributing to β-cell failure. Figure from Popa et Mota, 2013.

Under normoglycemic conditions, glucose metabolites are primarily used for energy production through oxidative phosphorylation in the mitochondria. However, under hyperglycemic conditions, excess glucose is available and excessive glucose can be directed to alternative pathways that can lead to ROS production. Among these pathways are glyceraldehyde auto-oxidation to methylglyoxal and glycation (AGEs production), enediol and α-ketoaldehyde formation, dihydroxyacetone and DAG formation with PKC activation, glucosamine and hexosamine metabolism and sorbitol metabolism. Since β-cells contain very little antioxydant enzymes to scavenge ROS, they are highly sensitive to their deleterious effects and mitochondrial dysfunction rapidly arises due to DNA fragmentation, and protein and lipid alterations by ROS. Mitochondrial dysfunction then further increases ROS production, decreases ATP production and favors ceramide formation and lipid partitioning, thereby contributing to β-cell failure. Oxidative stress is one of the mechanisms through which glucotoxicity progressively decreases insulin secretion, insulin gene expression and insulin promoter activity (decreased activities of the insulin transcription factors Pancreatic and duodenal homeobox 1 (PDX-1) and Mammalian homologue of avian (MafA)). The oxidative stress-induced reductions in PDX-1 and MafA activities were linked to reduction in their protein levels. Reduction of PDX-1 protein level was associated to a post-transcriptional loss of PDX-1 mRNA, while reduction of MafA protein level resulted from a post-translational loss of MafA protein. Chronic exposure of β-cells to high glucose ambience can also induce β-cell apoptosis by increasing pro-apoptotic genes expression (Bad, Bid, Bik) while Bcl-xl antiapoptotic gene expression is reduced and that of Bcl-2 remains unaffected (Federici et al. 2001; Poitout & Robertson 2008; Popa & Mot 2013).

There is a strong relationship between glutoxicity and lipotoxicity. Indeed, hyperglycemia increases Malonyl-CoA levels, leading to inhibition of carnitine palmitoyl transferase-1 (CPT-1) and subsequently to decreased β-oxidation and accumulation of long-chain Acyl-CoA esters, generation of ceramides and lipid partitioning. Ceramides *de novo* synthesis has been shown to be implicated in both

57

FFA-induced β-cell death and FFA-induced inhibition of insulin gene expression (i.e. lipotoxicity). Glucose also stimulates lipogenesis through inhibition of AMPK and increased expression of LXR, both resulting in activation of SREBP-1c. Of note, if chronic hyperglycemia is toxic for β-cell function independently of hyperlipidemia, chronic hyperlipidemia is detrimental only when hyperglycemia is present, further supporting the notion that lipotoxicity is nearly a mechanism of glucotoxicity.

In a context of high glucose, high fatty acids levels also alter insulin secretion and expression and can cause β-cell apoptosis but through different/additional mechanisms than glucotoxicity alone. Indeed, saturated fatty acids (i.e. palmitate) were also shown to inhibit insulin gene transcription through decreased PDX-1 and MafA binding activities. However, in this case, this was associated to a decreased ability of PDX-1 to translocate from the cytosol to the nucleus (*vs*. a post-transcriptional loss of PDX-1 mRNA with glucotoxicity alone) and to a reduction in MafA expression level (*vs*. a post-translational loss of MafA protein with glucotoxicity alone). This additional effect of gluco-lipotoxicity *versus* glucotoxicity alone, could be mediated by the action of **ceramides** on JNK and PKB/Akt. Indeed, as in numerous cell types, palmitate increases ceramide production which could activate JNK ; and JNK activation in β-cells has been shown to repress insulin gene transcription through both c-jun-dependent inhibition of E1-insulin promoter box-mediated transcription and c-jun independent inhibition of PDX-1 binding (Poitout & Robertson 2008). Alternatively, ceramides might alter insulin signaling in β-cell by impeding PKB/Akt activation (probably through a PKC) thereby allowing the translocation of the transcription factor Fox01 into the nucleus. In β-cells, PDX-1 and Fox01 exhibit mutually exclusive pattern of nuclear localization, and it is therefore conceivable that increased translocation of Fox01 to the nucleus in response to palmitate results in nuclear exclusion of PDX-1 (Poitout et al. 2006). Gluco-lipotoxicity can also contribute to β-cell failure through **ER stress**. Indeed, High Glucose and saturated fatty acids triggers UPR response (which is mediated by three different signaling pathways : ATF6, IRE1/XBP-1, and PERK/eIF2-α) and leads to 1) down-regulation of PDX-1 and MafA insulin gene promoter activity through ATF-6 (Seo et al. 2008), 2) β-cell apoptosis through CHOP (Eizirik et al. 2008) and 3) suppression of insulin mRNA expression and increased insulin mRNA degradation through IRE-1/XBP-1 (Lipson et al. 2006; Kim et al. 2012). Of note, **inflammatory cytokines** (e.g. IL-1β, IFN-γ) can also trigger UPR. Several studies showed that prolonged exposure of pancreatic islet to chronic high glucose ambience, high saturated fatty acids levels and increased ROS, may activate NF-kB and trigger the production of inflammatory cytokines such as IL-1β, IFN-γ, TNF-α leading to beta-cells inflammation, dysfunction and apoptosis. **Accumulation of cholesterol** inside the β-cell would also mediate (gluco)-lipotoxicity effect on insulin secretion by altering insulin secretory vesicles exocytosis (Poitout & Robertson 2008). Finally, glucolipotoxicity causes increased insulin requirement which leads to increased production of both insulin and amylin. High **amyloid** levels are toxic to β-cells and have been implicated in β-cell dysfunction and apoptosis (Ritzel et al. 2007).

58

Finally, the precise and detailed molecular events occurring in the context of glucolipotoxicity and leading to reduced insulin expression (linked to MafA and PDX-1 reduced activity), secretion and β-cell apoptosis, are not completely unraveled. However, one interesting finding is that insulin resistance in peripheral tissues and β-cell dysfunction share common triggering mechanisms (i.e. bioactive lipid generation and toxicity, oxidative stress, ER stress, mitochondrial dysfunction, inflammation) and are also both related, at least in part, to the activation of stress kinases, among which JNK and PKCs seems to play a particular role.

1.2.4 Animal models of T2D or Metabolic Syndrome

Actually there are numerous animal models available for the study of T2D, especially rodents, although none of these perfectly mimics the human disease due to the large heterogeneity in the latter. Obviously, no single rodent model can represent the onset and development of human T2D in all details. However, taken together the existing rodent models provide a rich array of opportunities for investigators to study the complex pathogenesis and pathophysiological process of T2D. There is no fully unified classification criteria for rodent models of T2D, but here they will be divided into monogenic models, polygenic models (coming for example from selective inbreeding), diet-induced and chemically-induced models. Environmental factors and especially diet and physical activity, more than genetic factors, seem to play a crucial role in most human type 2 diabetes development. Hence, diet-induced rodent models of type 2 diabetes probably better mimic human disease development than genetic models. For this reason, this section will focus more particularly on diet-induced rodent models rather than other models (monogenic, polygenic and chemically-induced models).

1.2.4.1 Monogenic models of spontaneous T2D or MetS

The ob/ob mouse, db/db mouse and Zucker fa/fa rat are the most common examples of T2D models with monogenic background. These diabetic models develop obesity due to mutations in leptin gene (ob/ob) or leptin receptor gene (db/db and fa/fa), which finally lead to hyperphagia, obesity development and emergence of diabetes. For further details on monogenic rodent models see **Table 2** thereafter.

Table 2

Monogenic rodent models of type 2 diabetes and/or Metabolic syndrome

Model	genetic background (strain)	mutated gene	Obesity, over-weight	IGT	Dys-lipidemia	Hyper-tension	CVD	Fatty Liver	Kidney dysfunction	Refs
ob/ob mice	C56BL/6J	leptin, chr 6, (autosomal recessive)	4 wk	12 wk	×	×	24 wk	12 wk	u.d.	[1-8]
db/db mice	C56BL/KsJ	leptin receptor, chr 4, (autosomal recessive)	6 wk	12-13 wk	12-13 wk	12 wk	12-13 wk	20 wk	u.d.	[1], [9]
ZDF rats (fa/fa)	Zucker rat	leptin receptor, (autosomal recessive)	Over-weight 9 wk, obesity 12-15 wk	male fully diabetic at 12 wk, female only develop diabetes on diabetogenic diet	12-15wk	12-15wk	12-15wk	20 wk	31-47 wk	[1], [10], [11]
SDT fatty rats (fa/fa)	SDT rat (Sprague Dawley)	leptin receptor, (autosomal recessive)	Over-weight 6 wk, obesity 14 wk	diabetes from 5 wk (male) or 8 wk (female) with 100% incidence at 16 wk for male	TG and CST elevated from 4 wk and for a long time afterwards	8 wk	u.d.	u.d.	renal tubules lesions and dilatation from 8 wk (male) or 16wk (female), glomerulo-sclerosis from 16 wk (male) or 32wk (female)	[12-13]

Abbreviations : chr, chromosome, CST, cholesterol, CVD, Cardiovascular dysfunction, IGT, Impaired Glucose Tolerance, Refs, References, SDT, Spontaneously Diabetic Torii, TG, Triglycerides, u.d., unaivailable data, ZDF, Zucker diabetic fatty.

References : [1], (Panchal & Brown 2010) *;* [2-8], (Dubuc 1976; Mark et al. 1999; Van den Bergh et al. 2008; Dobrzyn et al. 2010; Zaman et al. 2004; Park et al. 2011; Bigorgne et al. 2008) ; [9], (Goncalves et al. 2009) ; [10], (Wang et al. 2013) ; [11], (Leonard et al. 2005) ; [12-13] (Matsui et al. 2008; Kemmochi et al. 2013).

1.2.4.2 Polygenic models of spontaneous T2D or MetS

Kuo Kondo (KK) mouse, New Zealand Obese (NZO) mouse, Nagoya-Shibata-Yasuda (NSY) mouse and Otsuka Long-Evans Tokushima Fatty (OLETF) rats are the major heralds of the category of obesity-induced diabetes models with polygenic background. Polygenetic non-obese models of diabetes include the Goto Kakizaki (GK) rat and recently the Spontaneously Diabetic Torii (SDT) rat. Characteristics of some of these models are summarized in **Table 3.**

Table 3 - Some polygenic rodent models of type 2 diabetes and/or Metabolic syndrome

Model	Genetic Background	Obesity, overweight	IGT, Diabetes	Dyslipidemia	HT	CVD	Fatty Liver	Kidney dysfunction	Refs
KK(Ay) mice	cross between **KK** and **C57BL/6** strains + transfer of A^y gene	8 weeks, moderate obesity due to hyperphagia	IGT around 10 wks	Hypertriglyceridemia and hypercholesterolemia	higher SBP at 21 wks and possibly earlier	microangiopathy and myopathy	15-17 wks and possibly before	early membrane basement thickening (12-16 wks) and aggravation (23 wks)	[14-20]
NZO mice	selective inbreeding for heavy weight from New Zealand mouse	8 wks, obesity associated to leptin resistance and hyperphagia	impaired hepatic and peripheral insulin sensitivity and first phase insulin secretion from 4-5 wks	hypercholesterolemia	higher SBP at 6 wks	develop cardiac hypertrophy and atherosclerosis	enhanced liver lipogenesis	Glomerular proliferation, mesangial deposits, mild basement membrane thickening, and glomerulosclerosis	[15-23]
NYS mice	selective inbreeding for IGT from **Jc1:ICR** mouse	8 wks, mild obesity, abdominal and visceral fat accretion	IGT 12-15wks ; 98% diabetes incidence in male and 31 % in female at 48 wks	12-15 wks	u.d.	12-15 wks	Spontaneous development in an age-dependent manner	u.d.	[10], [24-26]
GK rats	selective inbreeding for glucose intolerance from **Wistar** rat	non-obese model of T2D	IGT 4 wks, males develop T2D at 14-16 wks	8 wks	No change in blood pressure after 14 months	20 wks cardiac hypertrophy, decreased systolic function	8 wks	60 wks	[1], [27]
male OLETF rats	selective breeding from a colony of **Long-Evans** rats	8 wks overweight, 20 wks mild obesity	100% diabetes incidence in males at 25 wks	8 wks hypertriglyceridemia	14 wks	60-66 wks, cardiac hypertrophy, LV systolic and diastolic dysfunction	34 wks	40 wks diffuse glomerulosclerosis	[1], [28-29]
male SDT rats	spontaneously diabetic strain of Sprague-Dawley rat	non-obese model of T2D	IGT from 12-16 wks due to hypo-insulinemia, diabetes at 20 wks, 100% incidence at 40 wks	hypertriglyceridemia by 35 wks	u.d.	u.d.	u.d.	renal lesions appearance at 24 wks and aggravation with aging	[30-33]

Abbreviations : A^y *gene, yellow obese gene (agouti), CVD, Cardiovascular dysfunction; GK, Goto-Kizaki ; HT, hypertension, IGT, Impaired Glucose Tolerance ; KK, Kuo Kondo ; LV, Left Ventricular ; NYS, Nagoya-Shibata-Yasuda ; NZO, New Zealand Obese ; OLETF, Otsuka Long-Evans Tokushima Fatty ; SBP, Systolic Blood Pressure ; SDT, Spontaneously Diabetic Torii ; u.d., unaivailable data*

References : [14-20], (Diani et al. 1987; Ohashi et al. 2006; Ma et al. 2007; Chen et al. 2002; Chen et al. 2009; Wei et al. 2011; Moroki et al. 2013) [15-23], (Melez et al. 1980; Andrews et al. 1980; Igel et al. 1997; Veroni et al. 1991; Ortlepp et al. 2000; Ortlepp et al. 2002; Becker et al. 2004; Kluge et al. 2012; Vogel et al. 2013) ; [24-26], (Ueda et al. 1995; Ueda et al. 2000; Hamada et al. 2001) ; [27], (Goto & Kakizaki 1981) ; [28-29], (Kawano et al. 1994; Moran & Bi 2006) ; [30-33], (Shinohara et al. 2000; Sasase et al. 2007; Ohta et al. 2011; Sasase et al. 2013).

1.2.4.3 Diet-induced models of T2D or MetS

The modern diet, especially the Western diet, is richer in saturated fats and carbohydrates such as fructose and sucrose. This increase in calorie intake has been associated with many diet-induced complications including metabolic syndrome (MetS), cardiovascular diseases and nonalcoholic fatty liver disease (Massiera et al. 2010; Lim et al. 2010). Carbohydrates and/or fat-enriched diets have been extensively used in rodents to mimic these signs and symptoms of human metabolic diseases. (Panchal & Brown 2010)

High Fat Diet (adapted from (Panchal & Brown 2010))

High-fat diets have been used for many decades to induce obesity, dyslipidaemia and insulin resistance in rodents. Those diet-induced rodent models of metabolic syndrome develop complications that resemble the human ones and these complications may extend to cardiac hypertrophy, cardiac fibrosis, myocardial necrosis, hepatic steatosis and diabetic nephropathy (Woods et al. 2003; Aguila & Mandarim-de-Lacerda 2003; Buettner et al. 2006; Deji et al. 2009; Kobayasi et al. 2010). C57BL/6 mouse is the most commonly used mouse strain with this diet because it was shown to better respond to it than other strains. Different types of high-fat diets can be used with variations in fat content (ranging between 20% and 60% energy as fat) and/or fat source (animal fat sources, such as lard or beef tallow, or vegetal fat sources such as olive or coconut oils) (Buettner et al. 2006). Long-term feeding of rats (60% of energy) or mice (35% fat wt/wt) with high-fat diet increased body weight, as early as after 2 weeks of diet, compared to standard diet-fed rodents (Lei et al. 2007; Sutherland et al. 2008). However, at least 4 weeks of high-fat diet feeding were necessary to obtain an apparent phenotype (Sutherland et al. 2008). Soon or later, long term feeding of rodents with high fat diet of both animal and plant-derived fat sources finally led to moderate hyperglycaemia and impaired glucose tolerance in most rat and mouse strains (Kim et al. 2010; Sweazea et al. 2010). Increased body weight, deposition of liver triglycerides and plasma concentrations of triglycerides, free fatty acids and insulin, and decreased plasma adiponectin concentration were observed with high fat diets (42% calories from fat) based on lard, olive or coconut oil fat sources (Buettner et al. 2006). Such diets also induced hepatic steatosis but with no signs of inflammation and fibrosis (Buettner et al. 2006). Of note, unlike lard and olive oil-derived high fat diets, coconut oil-derived diet did not alter insulin sensitivity (Buettner et al. 2006). Beef tallow-derived high fat diets (40% of energy) increased plasma lipids, insulin and leptin concentrations and also caused hepatic steatosis (Hsu et al. 2009). Although high-fat diet induces most of the symptoms

62

of human metabolic syndrome in rodents, it does not really resemble the diet causing metabolic syndrome and associated complications as the human diet is more complex than a high-fat diet.

High Fructose Diet (adapted from (Panchal & Brown 2010))

Since the 1970s, the commercial use of fructose as sweetener has dramatically increased in the United States and so fructose became an important and pervasive ingredient in Western diets (Tappy et al. 2010), in particular under the form of high-fructose corn syrup (sucrose from beet or cane, fruits and honey being the other main dietary sources of fructose). Unlike glucose fed rodents, fructose fed rodents displayed symptoms of metabolic syndrome including high blood pressure, insulin resistance, impaired glucose tolerance and dyslipidemia (high plasma triglycerides but without changes in plasma cholesterol concentrations (Miatello et al. 2005; Nakagawa et al. 2005)) (Tran et al. 2009; Tappy et al. 2010). Fructose feeding also induced ventricular dysfunction (Patel et al. 2009), renal injury (Nakayama et al. 2010) and hepatic steatosis (Kawasaki et al. 2009) (due to its ability to activate *de novo* lipogenesis in the liver (Basciano et al. 2005), See **Fig. 17**). Indeed, during metabolism, fructose bypasses the rate-limiting step of glycolysis (i.e. the reaction catalyzed by phosphofructokinase) which leads to an uncontrolled supply of carbon substrates for lipogenesis in liver in cases of high fructose intake (Rutledge & Adeli 2007). In addition, unlike glucose, fructose did not trigger insulin secretion by pancreatic β-cells, possibly because of the absence of the fructose transporter (GLUT5) on β-cells (Bray et al. 2004). Concerning its capacity to induce obesity, discrepancies still exist with some authors reporting a positive effect (Bocarsly et al. 2010) and others that did not confirmed it (Patel et al. 2009).
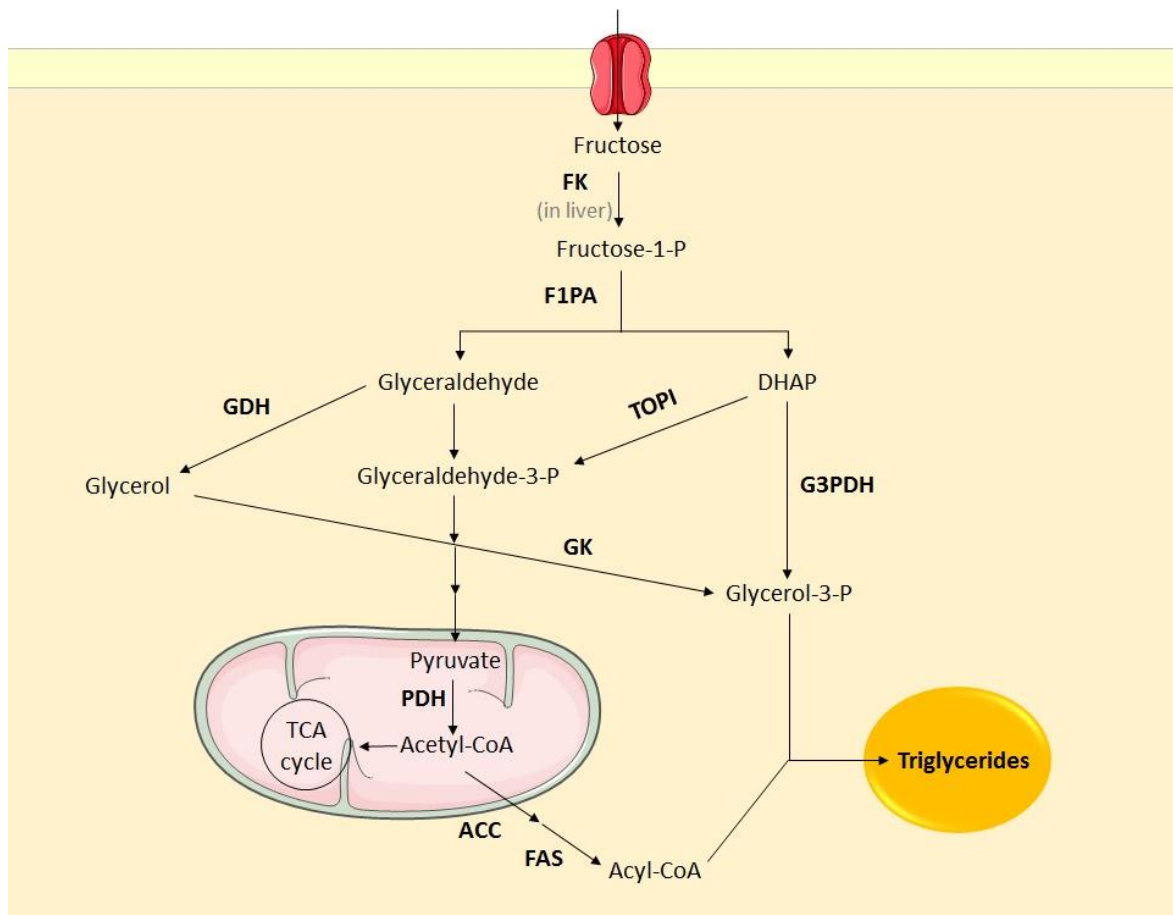
Figure 17 – Hepatic fructose metabolism: a highly lipogenic pathway. Figure inspired from SK Panchal and L. Brown, Journal of Biomedicine and Biotechnology, 2011 (Panchal & Brown 2010) . Fructose is readily absorbed from the diet and rapidly metabolized principally in the liver. Fructose can provide carbon atoms for both the glycerol and the acyl portions of triglyceride. Fructose is thus a highly efficient inducer of *de novo* lipogenesis. High concentrations of fructose can serve as a relatively unregulated source of acetyl CoA. In contrast to glucose, dietary fructose does not stimulate insulin or leptin secretion (which are both important regulators of energy intake and body adiposity). Stimulated triglyceride synthesis is likely to lead to hepatic accumulation of triglyceride, which has been shown to reduce hepatic insulin sensitivity (Basciano et al. 2005). Abbreviations : ACC, Acetyl-Coenzyme A Carboxylase ; DHAP, Dihydroxyacetone phosphate ; FAS, Fatty Acid Synthase ; FK, FructoKinase ; F1PA, Fructose-1-phosphate aldolase ; GDH, Glycerol Dehydrogenase ; GK, GlyceroKinase ; G3PDH, Glycerol-3-Phosphate Dehydrogenase ; PDH, Pyruvate Dehydrogenase ; TOPI, Triose Phosphate Isomerase.

High sucrose Diet (adapted from (Panchal & Brown 2010))

As a dietary source of fructose, sucrose has also been used to mimic human metabolic syndrome in animal models. However, regarding obesity induction, results of sucrose feeding were variables as those obtained with high fructose diet (Kanarek et al. 1987; Santuré et al. 2002). Sucrose, like fructose, induced lipogenesis in rats along with increased plasma concentrations of insulin, leptin, triglycerides, glucose and free fatty acids, and impaired glucose tolerance (Lombardo et al. 1996; Coelho et al. 2010). Sucrose feeding in rats led to an insulin resistant state with no change in fasting plasma insulin and glucose concentrations, but higher postprandial plasma concentrations of insulin and glucose (Santuré

et al. 2002). Sucrose feeding also induced hepatic steatosis (Huang et al. 2010) and increased systolic blood pressure and left ventricular mass in rats (Sharma et al. 2008). No changes were found however in kidneys of high sucrose-diet fed rats (Andrews et al. 1992).

High Carbohydrate/High Fat Diet (adapted from (Panchal & Brown 2010))

A combined high carbohydrates/high fat diet with fat derived from either animal or plant sources, better mimics the human diet than only high fat or carbohydrates diets. This combined diet should induce metabolic syndrome (i.e. insulin resistance, impaired glucose tolerance, dyslipidemia, obesity and hypertension) in rodents. Different sources and amounts of carbohydrates (fructose or sucrose mainly) and fats (different sources) have been used in different studies (Panchal & Brown 2010; Lomba et al. 2010; Kohli et al. 2010; Chun et al. 2010).

Among the high sucrose/high fat diet tested on rodents, sucrose content ranged between 10% and 30%, whereas fat content varied between 20% and 40% (Parekh et al. 1998; Murase et al. 2001; Sato et al. 2010; Alzoubi et al. 2013). In rodents, high-sucrose/high-fat diet feeding had increased body weight, abdominal fat accretion, hyperinsulinemia, hyperglycemia and hyperleptinemia (Parekh et al. 1998; Murase et al. 2001). Sucrose/fat combination also induced hepatic steatosis and increased hepatic lipogenic enzymes (Sato et al. 2010).

Fructose/fat combinations were also used to induce metabolic syndrome. In those cases, the fructose content ranged from 10% to 60%, either in the diet, drinking water or both, whereas the fat content varied between 20% and 60% (Panchal et al. 2011; Wada et al. 2010; Axelsen et al. 2010; Couturier et al. 2010; Ménard et al. 2010). High fructose/high fat feeding increased body weight and triglycerides, cholesterol, free fatty acids and leptin plasma concentrations (Wada et al. 2010; Panchal et al. 2011). Such combined diet also caused hyperinsulinemia, insulin resistance, glucose intolerance, increased abdominal fat accretion, hepatic steatosis and inflammation (Wada et al. 2010; Panchal et al. 2011). The rats fed with the high fructose/high fat diet showed cardiac hypertrophy, increased ventricular stiffness, ventricular dilatation, cardiac inflammation and fibrosis, hypertension, decreased cardiac function and endothelial dysfunction along with mild renal damage and increased pancreatic islet mass (Panchal et al. 2011).

Since rodents fed a high carbohydrates/high fat diet develop all the complications of human metabolic syndrome and as this combined diet reproduces more closely the human modern diet (sometimes called a "cafeteria diet") than the other high calorie diets, this model is probably the best to study the human metabolic syndrome or to test anti-diabetic treatments.

Israeli sand rats and Nile Grasse rats under lab diet (adapted from (Panchal & Brown 2010))

Feeding wild rodents with laboratory diet has also been tested for the development of diabetes and obesity. Among the wild rodents used, the Nile rat (African grass rat; *Arvicanthis niloticus*) and sand rat (*Psammomys obesus*) are two examples. In the wild, these rats do not develop diabetes but diabetes arised when they were kept upon laboratory conditions on chow diet (Chaabo et al. 2010). After one year age under laboratory standard diet, these rats displayed hyperglycemia, hyperinsulinemia and dyslipidemia (Noda et al. 2010). They also developed liver steatosis, abdominal fat deposition, and hypertension (Chaabo et al. 2010; Noda et al. 2010). These rats may be promising models for metabolic syndrome research, even though the disease signs develop upon normal diet rather than the high-carbohydrate, high-fat diet in humans.

1.2.4.4 Chemically-induced models of T2D or MetS

Streptozotocin (STZ) and alloxan (AX) are structural analogues of glucose that enter pancreatic β-cells through GLUT2 (Schnedl et al. 1994; Lenzen 2008). STZ or AX accumulation within pancreatic β-cells induces cells death through ROS and free radicals mechanisms. Due to its alkylating properties, STZ causes alkylation and thus fragmentation of DNA, modifies biological macromolecules and finally destroys β-cells, causing insulin-dependent like diabetes. Single injections of AX or STZ induce selective necrosis of pancreatic β-cells in rats and mice (180 mg/kg (Arora et al. 2009)) thereby producing rodent models of type 1 diabetes. However, although STZ and AX type 1 diabetes models result in hyperglycemia and insulinopenia, they do not bear strong autoimmune features. (Chatzigeorgiou et al. 2009).

Multiple low-doses of STZ (40 mg/kg, i.p.) to mice for five consecutive days have been shown to produce Type 2 Diabetes and to be a suitable model for the study of long term diabetes complications (Arora et al. 2009).

Low-dose STZ or AX given neonatally or immediately after birth in rats (following different dose and time protocol for each agent) also produces Type 2 Diabetes in rat adulthood (Portha et al. 1974; Weir et al. 1981; Chatzigeorgiou et al. 2009). However, the development of diabetes in these animals is accompanied by a decrease in β-cell mass and thus in insulin secretion. Therefore, the combination of STZ administration with a high fat or high fructose diet or its use in a rodent strain genetically predisposed for insulin resistance, produces models that develop overt hyperglycemia in the presence of normal blood insulin and, hence, are regarded as more appropriate for T2D studies (Srinivasan & Ramarao 2007; Chatzigeorgiou et al. 2009).

66

1.3   Inositol

Inositol is a cyclitol naturally present in animal and plant cells, either in its free form or as a bound-component of phospholipids or inositol phosphates derivatives. It plays an important role in various cellular processes, as the structural basis for secondary messengers in eukaryotic cells, and in particular as inositol triphosphates (IP_3), phosphatidyl inositol phosphate lipids (PIP_2/PIP_3) and possibly inositol glycans. For this reason, inositol, mainly in the isomeric form *myo*-inositol, is essential or important for the smooth running of a wide range of cell functions, including cell growth and survival (Eagle et al. 1956), development and function of peripheral nerves (Chau et al. 2005), osteogenesis (Dai et al. 2011) and reproduction (Carlomagno et al. 2011; Condorelli et al. 2012; Ciotta et al. 2011; Unfer et al. 2011; Condorelli et al. 2011; Beemster et al. 2002) (See **Fig. 18**).
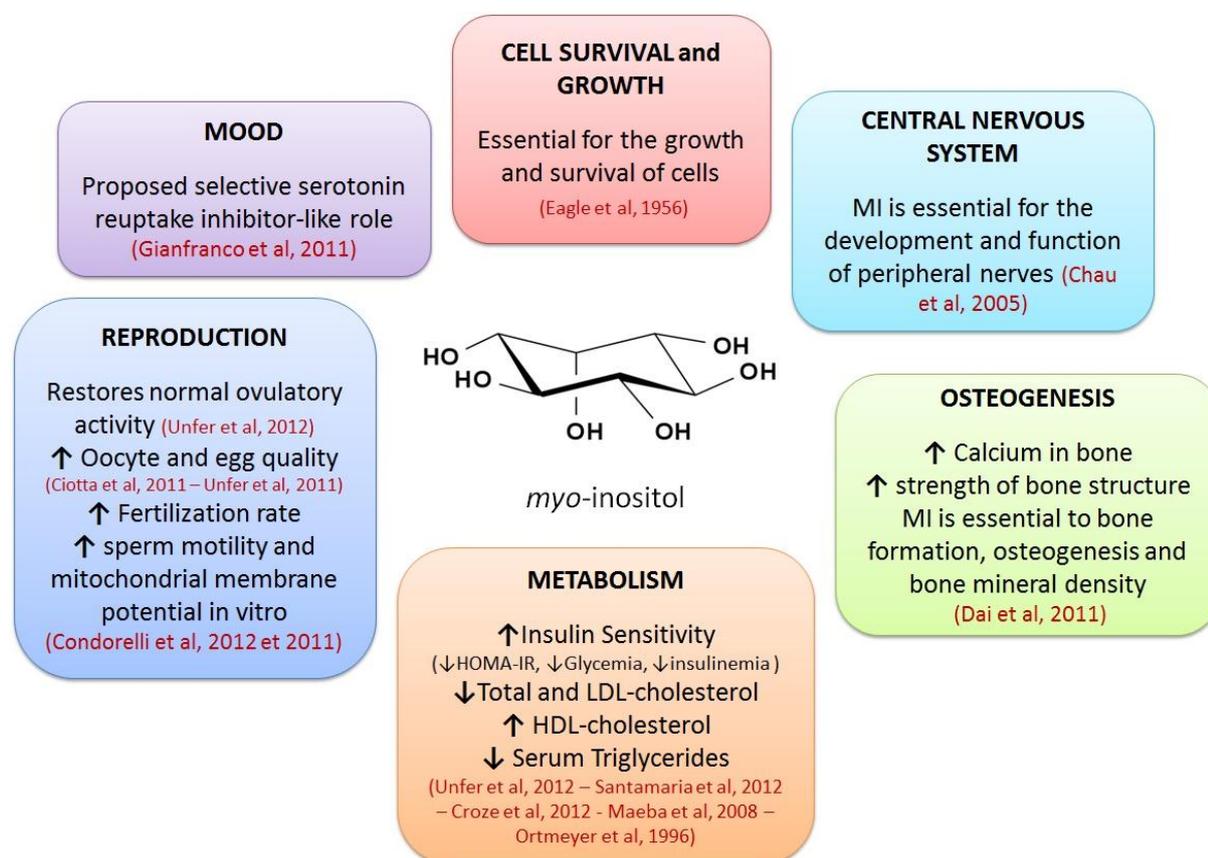
Figure 18 – Essential role of *myo*-inositol for some cellular functions and benefits of a dietary supplement.

In addition to various biological functions for the treatment of diseases such as depression, panic disorder or polycystic ovary syndrome (Benjamin, Agam, et al. 1995; Benjamin, Levine, et al. 1995;

67

Nestler et al. 1999; Iuorno et al. 2002; McLaurin et al. 2000), some inositol derivatives exhibit insulin-mimetic activity and were shown to be efficient in lowering blood glucose level (Bates et al. 2000; Shen et al. 2012; H. K. Ortmeyer et al. 1993; Ortmeyer et al. 1995; Ortmeyer 1996). Dietary supplementation with inositol isomers or derivatives could then constitute nutritional strategies to fight or prevent diabetes.

1.3.1 Biological forms and dietary sources

Inositol or cyclohexane-1,2,3,4,5,6-hexol is a polyol existing under nine stereoisomeric forms depending on the spatial orientation of its six hydroxyl groups (**Fig. 19**). **Myo-inositol**, or *cis*-1,2,3,5-*trans*-4,6-cyclohexanehexol, **is the predominant isomeric form of inositol found present in nature and in our food.**

(1) *myo*-inositol (2) *scyllo*-inositol (3) *muco*-inositol

(4) *D-chiro*-inositol (5) *L-chiro*-inositol (6) *neo*-inositol

(7) *allo*-inositol (8) *epi*-inositol (9) *cis*-inositol
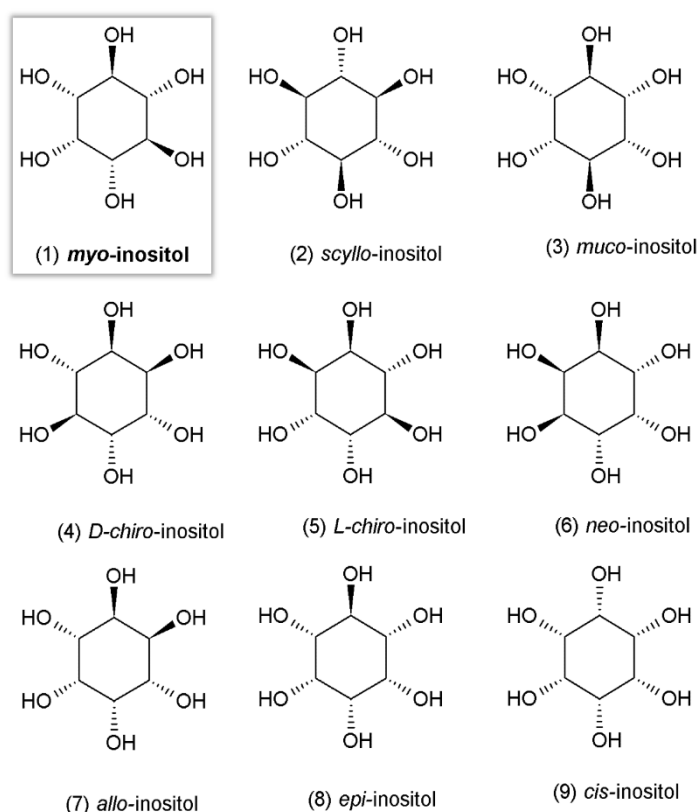
Figure 19 – Structures of the nine isomers of inositol. Inositol exists under 9 stereoisomeric forms through epimerization of its hydroxyl groups. *myo*-Inositol (framed) is the most common isomer of inositol in foodstuffs and animal tissues.

myo-Inositol was once considered to belong to the vitamin B family, however, because it is produced in sufficient amount by the human body from D-glucose, it is no more regarded as an essential nutrient. Human diet from animal and plant sources can contain *myo*-inositol in its free form, as inositol-containing phospholipid (phosphoinositides) or as phytic acid (inositol hexaphosphate or IP_6) (Holub 1986). Indeed, all living cells (animal, plant, bacteria, fungi) contain inositol phospholipids in their membranes, and phytic acid is the principal storage form of phosphorus in many plant tissues, especially bran and seed. Hence, the greatest amounts of *myo*-inositol in common foods are found in fresh fruits and vegetables, and in all foods containing seeds (beans, grains and nuts). Especially high phytic acid contents are found in almonds, walnuts and Brazil nuts (9.4, 6.7 and 6.3% of dry weight, respectively) (Schlemmer et al. 2009) and oats and bran contain more *myo*-inositol than cereals derived from other grains. Among the vegetables, the highest contents are observed in the beans and peas, leafy vegetables being the poorest vegetable sources. Among the fruits, cantaloupe and citrus fruits (with the exception of lemons) have extraordinarily high contents of *myo*-inositol : for example, a portion of grapefruit juice (120g) contains about 470 mg of *myo*-inositol (Clements & Darnell 1980). **The amount of *myo*-inositol present in the 2500 kcal American diet is approximately 900 mg, of which 56% is lipid-bound (i.e. in the form of phospholipids)**. However, the *myo*-inositol intake provided by common foods can range from 225 to 1500 mg/day per 1800 kcal depending on the composition of the diet (Clements & Darnell 1980).

1.3.2 Dietary *myo*-inositol uptake and metabolism

1.3.2.1 Digestion and Absorption

myo-Inositol from phytic acid can be released in the gut of monogastric animals by the enzymes phytases, which occurs in the intestinal mucosa. Phytases (*myo*-inositol hexaphosphate phosphohydrolases, EC 3.1.3.8 and EC 3.1.3.26) are found in plants, microorganisms and in animal tissues (Schlemmer et al. 2009). These enzymes are capable of releasing free inositol, orthophosphate, and intermediary products including the mono-, di-, tri-, tetra- and penta-phosphate forms of inositol. Much of the ingested inositol hexaphosphate is hydrolyzed to inositol. A considerable fraction of the ingested *myo*-inositol is consumed in the form of phosphatidylinositol (PI) that may be hydrolyzed by a pancreatic phospholipase A in the intestinal lumen. The resulting lyso-phosphatidylinositol (lysoPI) may be then reacylated via acyltransferase activity upon entering the intestinal cell or further hydrolyzed with the release of glycerylphosphorylinositol (Holub 1986).

Virtually all of the free *myo*-inositol ingested (99.8%) is absorbed from the human gastrointestinal tract, through an active transport system involving a Na^+/K^+-ATPase (Holub 1986). In normal and healthy subjects, the circulating fasting plasma *myo*-inositol concentration has been found to be approximately 30 µM and it turns over with a half-life of 22 min (Holub 1986; Clements & Darnell 1980). *myo*-Inositol is also present in small but significant amounts in phospholipids in association with the circulating serum lipoproteins, and as phytic acid at a level of about 0.1 to 0.4 µM.

1.3.2.2 Organ and Tissue Incorporation

Lewin et al. (Lewin et al. 1976) followed the distribution of radiolabelled *myo*-inositol after intraperitoneal injection in male rats. Radiolabelled *myo*-inositol accumulated rapidly (within 1 hour) and in large amounts in the thyroid, coagulating gland and seminal vesicles. Other tissues, such as the pituitary, prostate gland, liver and spleen, also concentrated *myo*-inositol quite actively. Of note, all the organs of the male reproductive tract (the vas deferens, epididymis, coagulating gland, seminal vesicle and prostate) except testis had radioactivity levels that were approximately 10 to 30 fold those of blood serum. The muscle tissues studied (diaphragm and heart) concentrated little inositol and adipose tissue (epididymal fat pad) was apparently unable of concentrating it from the blood, as well as the brain and testis which are, however, organs with high levels of endogenous inositol. Most of the radioactivity was found in the aqueous trichloroacetic acid extract, largely as free *myo*-inositol in most organs, with the exception of the liver where the lipid fraction contained most (approximatively 60%) of the radio-labelled *myo*-inositol accumulated.

Lewin et al also reported that in bilaterally nephrectomized rats, *myo*-inositol catabolism did not occur since the sole pathway of inositol catabolism in the rat takes place in the kidney. As expected, nephrectomized rats were essentially unable to convert inositol into CO_2, whereas the sham-operated rats catabolized about 16% of the injected inositol to CO_2. The nephrectomized rats accumulated more radioactivity in most of the organs tested, presumably because significant amounts of the administered inositol are normally metabolized or excreted by the kidney. An interesting exception to the rule was the brain, which accumulated more radioactivity in sham-operated than in nephrectomized animals. This may be due to the presence of metabolites of inositol, produced by the kidney, which are more prone to cross the blood/brain barrier than is inositol (Holub 1986).

1.3.2.3 Cellular Uptake

Cells normally derive inositol from three sources: (1) *de novo* biosynthesis from glucose-6-phosphate by 1-D-*myo*-inositol-phosphate synthase (MIPS) and inositol monophosphatase (IMPase), (2) dephosphorylation of inositol phosphates derived from breakdown of inositol-containing membrane phospholipids ; or (3) uptake from the extracellular fluid via specialized *myo*-inositol transporters (Deranieh & Greenberg 2009).

Inositol can be transported from extracellular fluid via three specialized *myo*-inositol transporters: sodium-dependent *myo*-inositol transporters 1 and 2 (SMIT1/2), and H^+-*myo*-inositol transporter HMIT, that co-transports *myo*-inositol with H^+ (Fu et al. 2012). SMIT1 and SMIT2, co-transport two sodium ions along the concentration gradient, to generate enough energy to actively transport *myo*-inositol. SMIT1 and SMIT2 are both expressed in the brain and may be responsible for regulating brain *myo*-inositol level that is about 100-fold greater than those found in the periphery. Active *myo*-inositol transport through SMIT2 also mediates *myo*-inositol uptake in apical membrane of rat small intestine (although SMIT1 is present) and is responsible for *myo*-inositol reabsorption in rabbit kidney (Molitoris et al. 1980; Lin et al. 2009). This active transport is inhibited by D-glucose and phlorizin and accounts for the inosituria occurring in diabetes mellitus. Of note, SMIT2 (but not SMIT1) also transports *D-chiro*-inositol.

1.3.2.4 Metabolism

MI *de novo* biosynthesis. *myo*-Inositol can be synthesized endogenously from D-glucose in rat testis, brain, kidney and liver (Eisenberg Jr. & Bolden 1963; Hauser & Finelli 1963) in three steps : first glucose is phosphorylated by hexokinase, second, glucose-6-phosphate is converted to *myo*-inositol-1-phosphate by MIPS, and finally, *myo*-inositol-1-phosphate is dephosphorylated by IMPase to produce free MI (See **Fig. 20**). The second step is the rate limiting step of MI biosynthesis in most organisms (Meng et al. 2009). In human, this endogenous biosynthesis of inositol is rather important in the kidney since it produces about 2g/day so the endogenous daily production is about 4g in the binephric human, which is significantly above the daily dietary intake (about 1g/day). Extrarenal tissues can also contribute to the endogenous production of inositol in human and animals. Indeed, one half of the free inositol content of the rabbit brain comes from endogenous production *in situ,* the other half being transported from the blood.

71
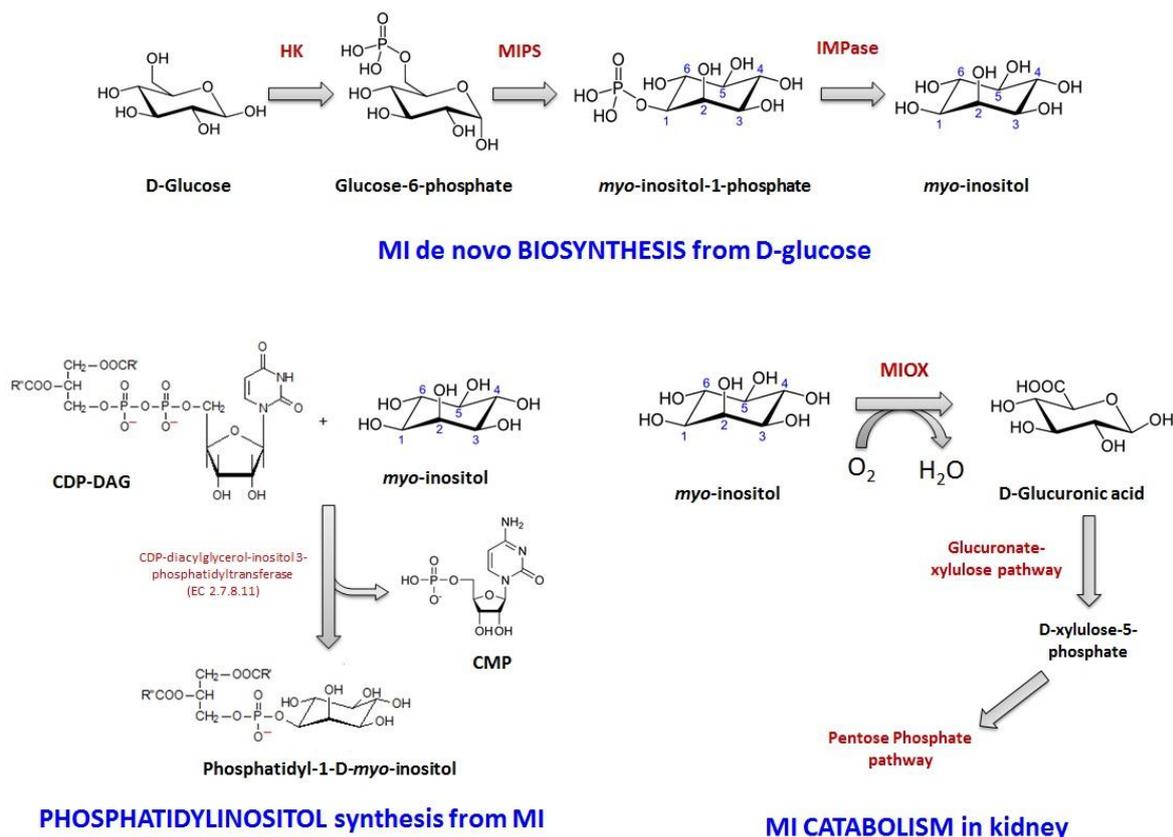
Figure 20 - *myo*-inositol de novo biosynthesis, incorporation into phospholipids and catabolism. Abbreviations : HK, hexokinase ; MIPS, 1-D-*myo*-inositol-phosphate synthase ; IMPase, inositol monophosphatase ; CDP-DAG, Cytidin diphosphate-diacylglycerol ; CMP, Cytidin MonoPhosphate ; MIOX, *myo*-inositol oxygenase.

MI conversion to isomers and derivatives or incorporation into phospholipids. *myo*-Inositol can lead to numerous derivatives through either epimerization, phosphorylation or methylation of one or several of its hydroxyl groups. Nonetheless, several of these derivatives cannot be obtained from *myo*-inositol in animal cells. For example, the inositol isomers *L-chiro-, allo-, cis-,* and *epi-* are synthetically prepared compounds. Methylated inositol derivatives such as D-pinitol, sequoyitol or quebrachitol can be found in some plant species but these compounds are unlikely produced from *myo*-inositol in human body. In cells, *myo*-inositol exists under many phosphorylated forms from monophosphorylated forms (Ins-1-P, Ins-3-P or Ins-4-P) to the hexaphosphorylated form (IP_6 or phytic acid) and even to pyro-phosphate forms ($PP\text{-}InsP_4$, $PP\text{-}InsP_5$, $[PP]_2\text{-}InsP_3$ or $[PP]_2\text{-}InsP_4$). Even so, the mono-, di- and tri-phosphorylated forms cannot come directly from the phosphorylation of *myo*-inositol by kinases, since such enzymes do not exist in human cells, but they can come from the dephosphorylation of more phosphorylated forms by specific phosphatases, and/or from phosphoinositides hydrolysis (i.e. inositol-1,4,5-triphosphate comes from the hydrolysis of phosphatidyl-inositol-(4,5)-biphosphate by Phospholipase C) (see **Fig. 21**).
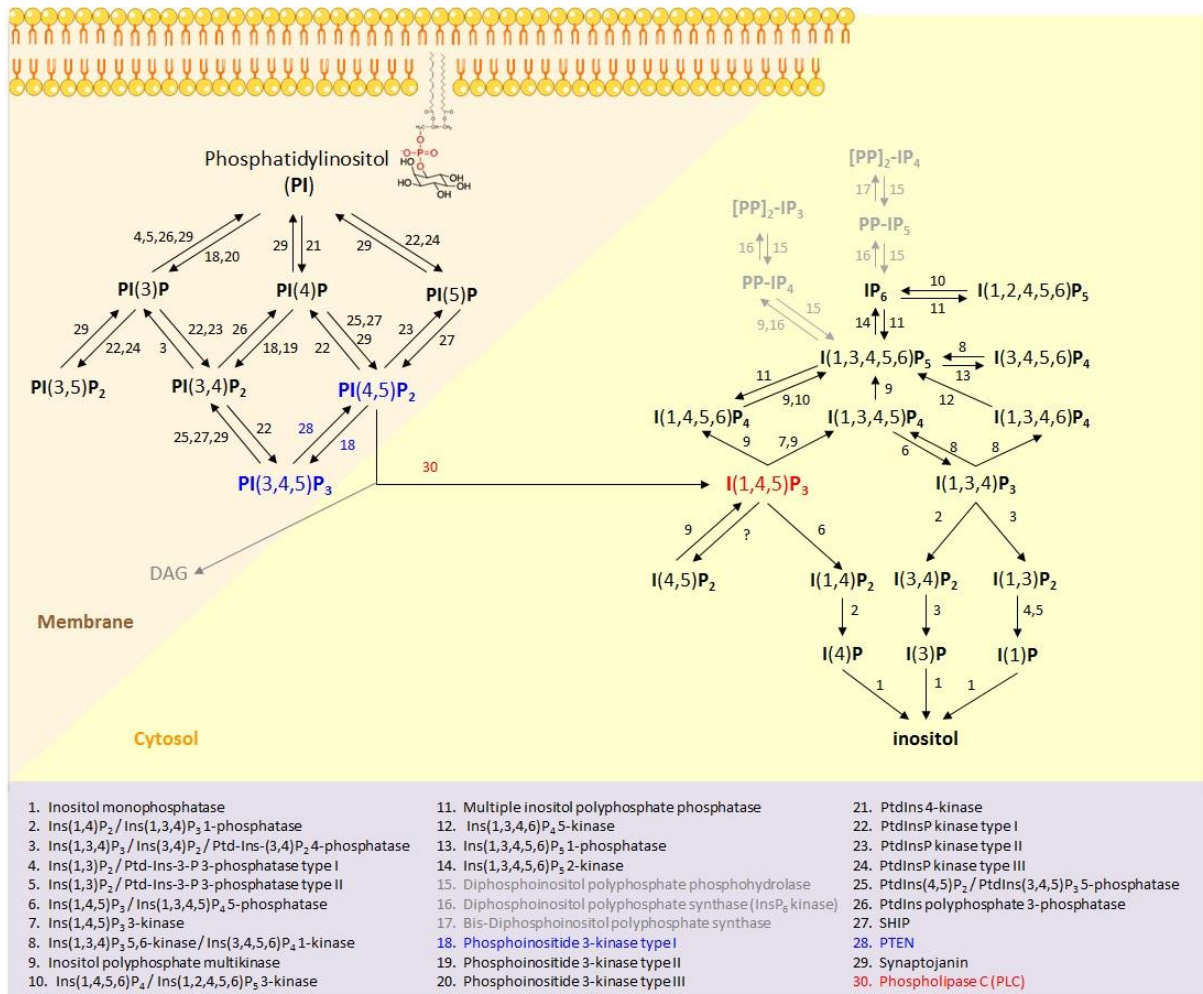
Figure 21 - Phosphoinositides metabolim in eukaryotic cells. Figure adapted from Abel K et al., J Cell Sci 2001.

The naturally occurring inositol isomers are *myo-, D-chiro-, scyllo-, muco-* and *neo-. In vivo* conversion of *myo*-inositol to *D-chiro*-inositol can occur in tissues expressing the specific epimerase. Pak et al measured a conversion rate of radiolabeled [³H]-*myo*-inositol to [³H]-*D-chiro*-inositol of about 7.6% in rat blood and 8.8% in rat muscle and liver (Pak et al. 1992). An epimerase interconverts *myo*- and *scyllo*-inositol with simultaneous production of *neo*-inositol in bovine brain (Hipps et al. 1977). However, in the study of Pak et al, labeling of inositol isomers other than *D-chiro*, namely *scyllo-, neo-* and *muco*-inositol, was minimal, approximately 0.06% of radiolabelled *myo*-inositol (Pak et al. 1992).

Finally, only a small amount of *myo*-inositol or none is converted to other isomers or methylated derivatives in mammalian tissues and cells and it is primarily found as free *myo*-inositol or bound covalently to phospholipids, as the structural basis for a number of secondary messengers, including inositol triphosphates (IP$_3$), phosphatidylinositol (PI) and polyphosphoinositides (i.e. PI(4)P, PI(4,5)P$_2$ and PI(3,4,5)P$_3$, in much lower concentrations than phosphatidylinositol). Phosphatidylinositols (PI) are

synthesized *in vivo* from *myo*-inositol and cytidine diphosphate-diacylglycerol (CDP-DAG) (**Fig. 20**). This synthesis is catalyzed by phosphatidylinositol synthase with a relatively high K_m (1.5-2.5 mM) (Takenawa & Egawa 1977; Benjamins & Agranoff 1969) for *myo*-inositol making intracellular MI homeostasis potentially important to numerous cell functions. Phosphatidylinositol phosphate lipids (PIPs) are a product of class I, II and III phosphoinositide 3-kinases (PI 3-kinases) acting on phosphatidylinositol. As explained above, many inositol phosphates are produced through the hydrolysis of phosphatidylinositol phosphates by phospholipase C and may also be synthesized or remodeled by many kinases and phosphatases (See **Fig. 21**).

myo-Inositol and *D-chiro*-inositol can also be bound components of glycosylphosphatidylinositol (GPI) anchors and of inositol phosphoglycans (IPGs) that would constitute second messengers of insulin action in the GPI/IPG pathway. See section 4.3 of this review for further details on this putative secondary signaling pathway of insulin.

MI Catabolism. The kidney is the sole organ of importance in the catabolism of *myo*-inositol since $[2-^{14}C]$-inositol was not degraded to $^{14}CO_2$ in nephrectomized rats in contrast with sham operated rats (Howard & Anderson 1967; Lewin et al. 1976). *myo*-Inositol is catabolized to D-glucuronic acid by *myo*-inositol oxygenase (MIOX) exclusively in the kidney. Through subsequent metabolic steps, D-glucuronic acid can lead to D-xylulose-5-phosphate which can enter the pentose phosphate cycle (See **Fig. 19**). In human subjects, urinary excretion accounts for a small fraction of the disposal of inositol by the kidney. Therefore, the kidney appears to be an important regulator of plasma inositol concentration in human subjects.

1.3.3 Tolerance

myo-Inositol supplementation is well tolerated and relatively safe since *myo*-inositol LD50 in mouse is 10 000 mg/kg bodyweight when orally administered (Anon 1996). In human, *myo*-inositol in a daily dose up to 18 g per os for 3 months or 2g/day for 1 year is safe and well tolerated. Side effects, when present, are mild and mainly gastrointestinal in nature (nausea, flatus and diarrhea) (Lam et al. 2006; Carlomagno & Unfer 2011).

1.3.4 Inositol metabolism abnormalities associated to insulin resistance

MI and DCI are involved in an array of cellular functions and abnormalities in their metabolism have been involved in the development of several diseases states (e.g. Bipolar, Panic and Obsessive Compulsive Disorders, Depression, Alzheimer's Disease) and in particular in the development of insulin resistance and diabetic complications. Indeed, in primary sites for the development of diabetic microvascular complications (kidney, sciatic nerve, retina and lens) a concomitant depletion of intracellular *myo*-inositol and accumulation of intracellular sorbitol is commonly observed in diabetic animal models and human subjects (Winegrad 1987; Chang 2011). In addition to this tissue-specific *myo*-inositol depletion, type 2 diabetic human subjects (Kennington et al. 1990) and experimental models (rhesus monkeys (Kennington et al. 1990), Goto Kakizaki (GK) rat (Sun et al. 2002)) excrete excessive amounts of MI and decreased amounts of DCI in urine (a phenomenon called inosituria). This urinary excretion pattern leads to a decrease in DCI to MI urinary ratio. The same inositol abnormal pattern is observed in insulin sensitive tissues (liver, muscle, fat and kidney) of human (Asplin et al. 1993) and animal (Sun et al. 2002) diabetic subjects.

1.3.4.1 Intracellular MI depletion

Putative mechanisms of MI intracellular depletion. MI intracellular concentration is regulated through processes such as extracellular MI uptake, de novo biosynthesis, regeneration (phosphoinositides cycle), efflux and degradation (See **Fig. 22**).
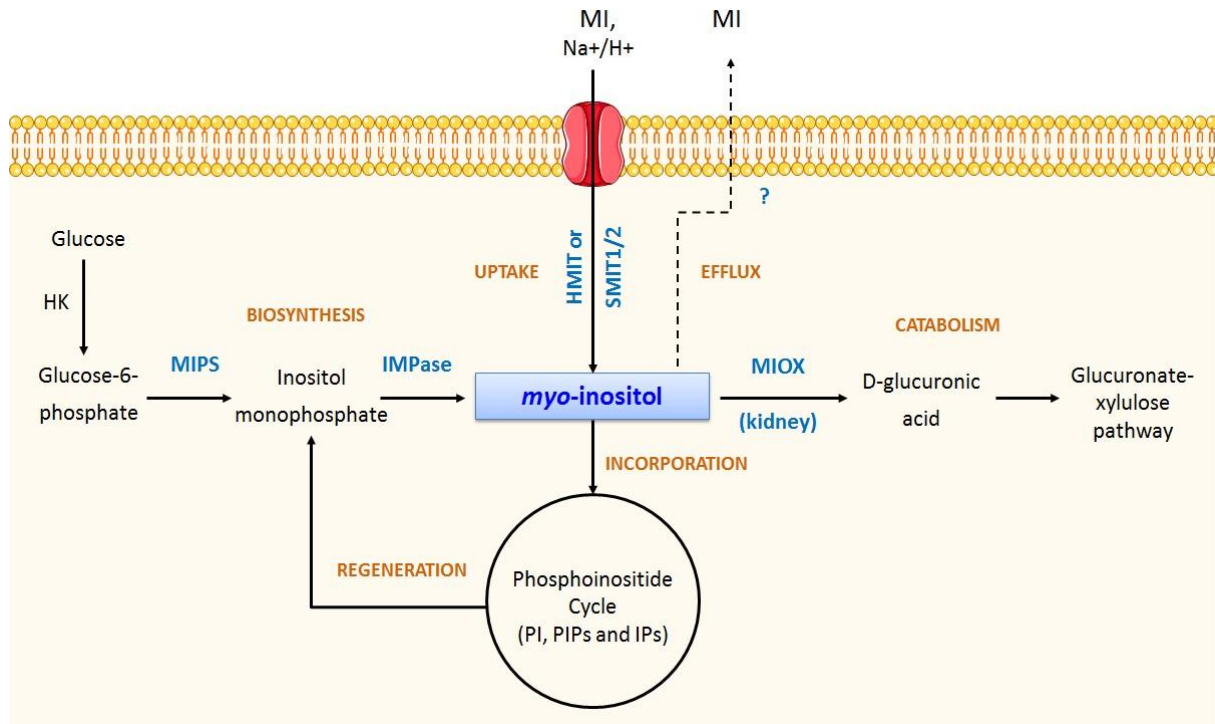
Figure 22 - *myo*-inositol intracellular level regulation. *myo*-inositol intracellular level depends on its extracellular uptake through specific transporters (HMIT/SMIT1/SMIT2), its de novo biosynthesis from glucose (HK, MIPS and IMPase), its regeneration or entry into the phosphoinositides cycle, its efflux and/or its catabolism by MIOX (in kidney). Figure adapted from HHG Chang PhD thesis, 2011. Abbreviations: HK, hexokinase, HMIT, H$^+$/*myo*-inositol transporter, IMPase, inositol monophosphatase, MIOX, *myo*-inositol oxygenase MIPS, 1-D-*myo*-inositol-phosphate synthase, SMIT1/2, Sodium-dependant *myo*-inositol transporter 1/2.

Alteration of one or several of these processes can lead to inositol intracellular abnormalities. In diabetes mellitus, inhibition of cellular MI uptake, altered MI biosynthesis, enhanced MI efflux due to sorbitol intracellular accumulation and increased MI degradation are putative mechanisms of MI intracellular depletion (Chang 2011).

Indeed, a reduction of MI uptake was observed in cells (aorta, nerve cells and brush border vesicles) cultured in medium containing ambient glucose (Greene & Lattimer 1982; Yorek & Dunlap 1989; Olgemöller et al. 1990). This glucose-induced MI uptake inhibition results from a competition between MI and glucose for MI transporters since MI and glucose exhibit structural similarities (Haneda et al. 1990). Therefore, under hyperglycemic conditions, high glucose ambience could impair extracellular MI uptake and so contribute to the MI intra-tissue depletion observed in diabetes. However, hyperglycemia *per se* is not sufficient to explain this intra-tissular MI depletion since the use of aldose reductase inhibitors (which selectively inhibit the conversion of glucose to sorbitol) corrected sorbitol intracellular accumulation and concomitantly inositol intracellular depletion, without affecting hyperglycemia (Chang 2011).

In tissues possessing osmolyte efflux systems such as neuronal tissues, a rapid intracellular sorbitol accumulation can result in an osmotic stress that may favour the net efflux of osmolytes such as MI through the volume-sensitive organic osmolyte anion channels and thus reduce intracellular MI levels (Chang 2011). This sorbitol-induced osmotic stress was important in diabetic lens but may not mediate MI depletion in other tissues (Beyer-Mears et al. 1992; Reddy et al. 1992).

In the testes of diabetic animals, a significant reduction (50%) in the activity of MIPS, the enzyme regulating the first and critical step of MI biosynthesis, was observed (Whiting et al. 1979). However, no changes in MIPS activity were observed in the other organs (kidney, brain, and nerves) and even if the rate of MI biosynthesis is intrinsically greater in testes, the contribution of this MIPS activity reduction in MI intracellular depletion remains unclear (Chang 2011).

Finally, an up-regulation of MIOX, the enzyme that breaks down MI, was observed at both mRNA and protein levels in the kidney of animal models of diabetes (STZ-diabetic rat (Chang 2011), db/db mice (Nayak et al. 2005)), insulin resistance (high fat diet-induced insulin resistant C57BL/6 mice (Chang 2011)) or hypertension (SHR rat). In all cases (normoglycemic hypertensive rat, insulin resistant mice or hyperglycemic STZ-rat), MIOX up-regulation was associated with an intra-renal MI deficiency (Chang 2011). These findings suggest that MI depletion in the kidney is not directly attributable to hyperglycaemia *per se* and may instead reflect in one aspect the up-regulation of the glucuronate-xylulose pathway as indicated by the elevated MIOX expression and activity. In addition, the activation of MIOX and its subsequent glucuronate-xylulose pathway have been implicated in the development of diabetic nephropathy through the activation of fibronectin (Xie et al. 2010).

Consequences of MI depletion: possible role in diabetic microvascular complications. As explained above, inositol is involved in many cell functions, especially as a precursor of phophatidylinositol and phosphoinositides. Since the K_m for the biosynthesis of PI from MI is relatively high (i.e. in the millimolar range), a depletion of intracellular *myo*-inositol could have a negative impact on the synthesis and availability of PI and PIPs in cells. Indeed, altered PI metabolism associated to MI deficiency has been observed in the sciatic nerve of streptozotocin-diabetic rat model (Clements & Stockard 1980). Since altered PI turnover is associated with impaired Na^+/K^+-ATPase activity, abnormal Na^+/K^+-ATPase activity may be a direct consequence of intracellular MI deficiency and a possible mechanism of diabetic microvascular complications. Indeed, in neuronal cells, Na^+ and K^+ ions are essential for the maintenance of membrane potential for neurotransmitter-induced excitement and altered Na^+/K^+-ATPase activity has been associated to impaired nerve conductivity (Sima, Dunlap, et al. 1997; Sima, Thomas, et al. 1997) and could be linked to the pathological changes observed in diabetic neuropathy (axonal degeneration and demyelination) (Llewelyn 2003) through a possible inhibition of cell growth, transformation and differentiation (Oishi et al. 1990).

The hyperglycemia-induced MI depletion is also associated with the hemodynamic disturbances in the diabetic kidney, which are believed to be directly responsible for the development of glomerulosclerosis and its attendant proteinuria (Chang 2011). On the other hand, the depletion of MI may also affect the normal physiological function of renal tubular epithelial cells, resulting in increased accumulation of extracellular matrix (ECM), which may lead to renal tubulointerstitial fibrosis. Therefore, the depletion of MI plays an important role in the development and progression of diabetic nephropathy (Kanwar et al. 2008; Xie et al. 2010).

Despite a lack of well-defined aetiological mechanisms, the MI depletion observed under hyperglycemic conditions in insulin insensitive tissues seems to contribute to the development of diabetic microvascular complications, together with the four major and more recognized pathways, namely : increased Advanced Glycation End products (AGEs) formation, activation of protein kinase C (PKC), increased hexosamine and sorbitol pathways (Chang 2011).

1.3.4.2 Inosituria and decreased DCI to MI ratios in insulin target tissues

Putative mechanisms of inosituria and altered inositol profiles. Larner and colleagues described a decreased urinary excretion of DCI and an increased urinary excretion of MI in human subjects and rhesus monkey with Type 2 Diabetes (10 folds higher than in healthy subjects) (Kennington et al. 1990). A similar urinary excretion profile was observed in studies of the Goto Kakizaki rat (Suzuki et al. 1991). Although this fact was known since 1859 (Neukomm et al, 1859 quoted by (Needham 1924)), the cumbersome analytic procedures for inositol prevented a thorough study of the mechanism of this abnormality at this time. In 1954, the increased inositol clearance observed in diabetes mellitus was related to glycosuria rather than polyuria (Daughaday et al. 1954; Daughaday & Larner 1954) . In monkeys the inositol excretion pattern became more marked with the progression of the disease from normal to obese non-diabetic to diabetic (H K Ortmeyer et al. 1993) and additional studies on humans and monkeys demonstrated that this altered inositol profile in urine was more directly related to the underlying insulin resistance rather than to the type 2 diabetes *per se* (with a correlation between the decrease in urinary DCI and the severity of insulin resistance measured by five distinct parameters (H. K. Ortmeyer et al. 1993)). Altered ratios of increased *myo*-inositol to decreased *chiro*-inositol in urine have even been proposed as an index of insulin resistance in human subjects (Larner & Craig 1996).

An altered DCI to MI ratio was also found in autopsy and biopsy muscles of type II diabetic subjects. In autopsy muscle, urine and hemodialysate samples, chiro-inositol was decreased about 50% compared to control subjects (Asplin et al. 1993). In the muscle biopsy specimens, no DCI was detected in the type II diabetic samples either before or after insulin administration. MI, in contrast, was present

78

in the type II diabetic samples in increased amounts over controls and was further increased with insulin administration (Kennington et al. 1990). To explain this inositol imbalance associated with insulin resistance, a defect in MI to DCI epimerization activity was postulated. To test this hypothesis, the existence of such a MI to DCI conversion was demonstrated *in vivo* in rats (Pak et al. 1992) and *in vitro* in fibroblasts (Pak et al. 1993) in a process stimulated by insulin. It was then shown that this epimerase activity is dependent on time, pH, tissue (liver and kidney being more active enzymes sources) and co-factors availability, full activity being obtained with the co-factors NADH and NADPH (Sun et al. 2002). In keeping with this hypothesis, a strikingly decreased conversion of [^{3}H]-MI to [^{3}H]-DCI was observed in muscle, liver and fat cytosolic extracts of Goto Kakizaki type 2 diabetic rats compared to Wistar control rats (conversions of 20-25% in controls were reduced to basal levels of 5% or less in GK rat) (Sun et al. 2002). This 2-3 fold decreased epimerase activity in insulin target tissues of GK rat is consistent with the decrease in DCI content (and so in DCI to MI ratio) observed in the same tissues and also seen in human muscle autopsy of type 2 diabetics (Asplin et al. 1993). Finally, the decreased MI to DCI epimerase activity observed in GK rat insulin target tissue extracts may play a role in explaining the decreased urine and tissue DCI content (and decreased DCI to MI ratios) related to insulin resistance.

Consequence of inosituria and altered tissues DCI to MI ratios in diabetes. Excessive urinary MI excretion could reduce MI plasma level and consequently emphasize MI intracellular depletion, particularly in tissues heavily dependent on extracellular MI import. Decreased production of DCI from MI reduces the availability of intracellular DCI for its incorporation into IPGs, putative downstream second messengers of insulin. Indeed, type 2 diabetes mellitus patients display decreased IPG levels in muscle biopsies as compared to healthy controls (Kennington et al. 1990). Therefore, the decreased DCI content in insulin target tissues could reduce insulin signal transduction involving IPGs and so further enhance or contribute to the insulin resistance in those tissues. Depleted plasma levels of DCI observed in PCOS (a syndrome characterized by insulin resistance and hyperinsulinemia, see section 4.1) patients further emphasize the correlation between impaired plasma DCI and insulin resistance.

To sum up this section, insulin resistance and diabetes are associated with 1) abnormally low levels of DCI in urine, plasma and insulin target tissues (liver, muscle, fat) ; 2) excessive MI urinary excretion and 3) intracellular MI deficiency in insulin insensitive tissues (kidney, sciatic nerve, lens and retina). DCI deficiency could emphasize insulin resistance in liver, muscle and fat while MI depletion in specific tissues could play a role in the development or aggravation of diabetic microvascular complications (neuropathy, nephropathy and retinopathy). Therefore, it seems reasonable to speculate on a possible beneficial effect of MI and/or DCI supplementation in diabetes to restore depleted MI and/or DCI intra-tissue levels.

1.3.5 Insulin-mimetic properties of some inositol isomers

1.3.5.1 DCI, D-pinitol and other inositol derivatives with insulin mimetic properties

Lessons from animal studies. The effectiveness of certain inositol isomers or derivatives, especially DCI and D-pinitol, in lowering post-prandial blood glucose level had been reported in normal rats (H. K. Ortmeyer et al. 1993) and in several animal models of insulin-resistance with or without diabetes mellitus : hypoinsulinaemic STZ-diabetic mice (Bates et al. 2000) or rat (Kawa, Taylor, et al. 2003), low-dose STZ Type 2 diabetic rat (H. K. Ortmeyer et al. 1993; Fonteles et al. 2000), KK-Ay mice (Yao et al. 2008), or insulin resistant rhesus monkey (Ortmeyer et al. 1995). The magnitude of the acute blood glucose lowering effect was generally about 15-20 % with D-pinitol (10-20 mg.kg^{-1}) (Fonteles et al. 2000; Kawa, Taylor, et al. 2003) or DCI 15 mg.kg^{-1} (Fonteles et al. 2000) at 120 min after administration, and was enhanced to about 45-50 % when DCI or pinitol was co-administered with manganese. Of note, acute D-pinitol treatment (100 mg.kg^{-1}) was inefficient in lowering baseline glucose or insulin blood levels, or in improving glucose tolerance in severely insulin-resistant ob/ob mice and normal non-diabetic mice (Bates et al. 2000). Studies on DCI and D-pinitol showed that this blood glucose lowering effect was obtained with either oral administration or injections, and it was apparently related to an insulin sensitizing activity rather than an insulin secretion stimulating activity. The exact underlying molecular mechanisms are still unclear but it probably passes through an interaction with the insulin signaling pathway, resulting in an increased GLUT-4 translocation to the plasma membrane (Yap et al. 2007; Dang et al. 2010; Yamashita et al. 2013) and/or an increased glycogen synthesis and glucose oxidative use through increased Glycogen synthase and PDH activity (Larner et al. 2010). Those two latter actions would be mediated by the production/release of inositol glycans, putative insulin second messengers (see section 1.3.5.2 for further details). In addition to show blood-glucose lowering effects, treatments with DCI or D-pinitol also improved the complications associated to insulin-resistance and diabetes like dyslipidemia (Geethan & Prince 2008; Choi et al. 2009; Nascimento et al. 2006; Yao et al. 2008), endothelial dysfunction (Nascimento et al. 2006), hepatic enzymes activity alterations (Sivakumar & Sorimuthu P Subramanian 2009) and protection of pancreatic, kidney and hepatic tissues from ROS-injury induced by STZ (Sivakumar & Sorimuthu Pillai Subramanian 2009; Sivakumar et al. 2010a; Sivakumar et al. 2010b). Indeed, the activities of the hepatic enzymes such as hexokinase, pyruvate kinase, glucose-6-phosphate dehydrogenase, glycogen synthase and hepatic glycogen content were significantly ($p<0.05$) increased whereas the activities of glucose-6-phosphatase, fructose-1,6-

80

bisphosphatase, lactate dehydrogenase and glycogen phosphorylase were significantly ($p < 0.05$) decreased in STZ-diabetic rats treated with oral administrations of D-pinitol 50 mg.kg^{-1} for 30 days (Sivakumar & Sorimuthu P Subramanian 2009). Positive effects of D-pinitol or DCI on diabetes complications were associated to the reduction in blood glucose levels and were also often associated to an attenuation of oxidative stress and inflammation in STZ-induced diabetes models. For example, oral administration of D-pinitol (50 mg.kg^{-1} body weight (BW), 30 days.) resulted in significant ($p < 0.05$) attenuation in blood glucose, AGEs, glycosylated hemoglobin and pro-inflammatory markers such as TNF-α, IL-1β, IL-6, NF-κB p65 unit and NO and significant ($p < 0.05$) elevation in the plasma insulin level. In addition, D-pinitol instigated a significant escalation in the levels of hepatic tissue non-enzymatic antioxidants and in the activities of enzymatic antioxidants of diabetic rats, with significant decrease in lipid peroxides and hydroperoxides formation ($p < 0.05$) (Sivakumar et al. 2010a) and in protein carbonyls.

myo-Inositol also reduced post-prandial blood glucose level when given acutely and in high dosages (1.5 g.kg^{-1}) to some obese insulin-resistant rhesus monkeys (Ortmeyer 1996). However, in contrast to DCI or D-pinitol, it only enhanced GLUT-4 density at the plasma membrane in skeletal muscle of mice when administered *in vivo* (Dang et al. 2010), but not *in vitro* on isolated muscles or L6 myotubes (Yap et al. 2007). Recently, the herbal constituent sequoyitol, the 5-O-methyl form of *myo*-inositol, was also shown to exert anti-diabetic effects in mice when administered chronically. Indeed, both subcutaneous and oral administrations of sequoyitol (80 mg.kg^{-1} per day) for 8-10 weeks improved hyperglycemia, glucose intolerance and enhanced insulin signaling in liver of ob/ob insulin resistant mice (Shen et al. 2012).

Lessons from clinical studies. Results from clinical studies were contrasted and different according to the type of subjects enrolled and to the inositol derivative used.

D-pinitol. In a study of Davis et al. (Davis et al. 2000) on obese insulin resistant or mildly diabetic subjects, four weeks of D-pinitol treatment (20 mg.kg^{-1}) did not alter baseline glucose production, insulin-mediated glucose disposal, or rates of appearance of free fatty acids and glycerol in plasma despite that plasma levels of both D-pinitol and D-*chiro*-inositol were responsive to pinitol ingestion. A study on non-diabetic older people also failed to show a beneficial effect of pinitol treatment (1 g in a non-nutritive beverage twice a day for 7 weeks) on glucose tolerance (Campbell et al. 2004). In contrast, in a double-blind and randomized controlled trial (RCT) on Korean patients with type II diabetes mellitus (Kim et al. 2005), soybean derived-pinitol (600mg twice daily, 13 weeks) significantly decreased mean fasting plasma glucose, insulin, fructosamine, HbA1c, and the homeostatic model assessment insulin resistance index (HOMA-IR, $P < 0.001$). D-pinitol also significantly decreased total cholesterol, LDL-cholesterol, the LDL/HDL-cholesterol ratio, and systolic and diastolic blood pressure and increased HDL-

cholesterol (P<0.05) and thereby reduced the cardiovascular risk associated to diabetes in these subjects. The acute effect of 1.2 g of D-pinitol (purified from soybean) on post-prandial blood glucose control was also confirmed on type II diabetic Korean subjects by the same research team (Kang et al. 2006). They also evaluated the effect of pinitol therapy (20 mg.kg^{-1} BW, 12 week) in type 2 diabetic patients who were poorly controlled with hypoglycemic drugs, such as sulfonylurea, metformin and/or insulin (Kim et al. 2007). After D-pinitol treatment, fasting glucose, post-prandial glucose levels, and HbA1c were significantly decreased (p<0.05) while fasting serum adiponectin, leptin, free fatty acid, and CRP levels did not change.

D-chiro-inositol. DCI treatment was only tested on women with Polycystic Ovary Syndrome (PCOS), an endocrine disorder characterized by an hyperandrogenism and associated to ovulatory dysfunction, insulin resistance and hyperinsulinemia. Nestler et al. (Nestler et al. 1999) first evaluated the potential beneficial effect of DCI administration in order to improve insulin sensitivity in women with PCOS. Women were given 1.2 g of DCI once daily for 6 to 8 weeks which improved the area under the curve of insulinemia during an OGTT but did not changed glucose tolerance, decreased serum free testosterone and triglycerides levels and blood pressure. Similar results were found by the same group on lean PCOS women (Iuorno et al. 2002). However, it seems that *myo*-inositol rather than DCI, is most suitable for the restoration of the ovulatory function in PCOS women because increasing DCI dosage progressively worsened oocyte quality and ovarian response in the study of Isabella and Raffone (Isabella & Raffone 2012) while *myo*-inositol has been shown to restore ovulatory function in PCOS (Papaleo et al. 2007; Gerli et al. 2007; Venturella et al. 2012) (reviewed in (Unfer et al. 2012)) and improve oocyte quality (Unfer et al. 2011; Carlomagno et al. 2011; Galletta et al. 2011).

myo-Inositol. *myo*-inositol had first been tested in humans in the context of PCOS, for the improvement in metabolic and endocrine parameters and for restoration of ovulation and showed positive results: significant reduction in serum levels of insulin, free testosterone, LH, triglycerides, total cholesterol and LH/FSH ratio, restoration of ovulatory cycle and improvement in glucose tolerance (Gerli et al. 2003; Papaleo et al. 2007; Gerli et al. 2007; Genazzani et al. 2008; Costantino et al. 2009; Raffone et al. 2010; Artini et al. 2013). It was even concluded with a level **Ia** of evidence that *myo*-inositol supplementation (1 to 4 g/day) is a safe and efficient strategy to improve several of the hormonal and metabolic disturbances of PCOS (restoration of ovulation and improvement of oocyte quality, reduction in clinical and biochemical hyperandrogenism, reduction in dyslipidemia) probably because it reduces hyperinsulemia (Unfer et al. 2012). More recently, *myo*-inositol supplementation also showed beneficial effects for the prevention or treatment of gestational diabetes (Corrado et al. 2011; Matarrelli et al. 2013; D'Anna et al. 2013) or metabolic syndrome in post-menopausal women (Giordano et al. 2011; Santamaria et al. 2012) (See for review (Croze & Soulage 2013) in supplements of this manuscript).

However larger studies are necessary to conclude on the efficiency of *myo*-inositol for this two latter contexts.

Finally, neither *myo*-inositol nor DCI dietary supplementation were tested in clinical trials for the prevention or treatment of insulin-resistance or type 2 diabetes not related to PCOS, gestation or post-menopause period. Moreover, the few clinical trials with D-pinitol led to conflicting results so further studies are still necessary to conclude on the potential interest of inositol derivatives for the prevention or treatment of diabetes.

1.3.5.2 Inositol phosphoglycans – putative second messengers of insulin

The exact mechanisms of action of some inositol isomers (DCI) or derivatives (e.g. D-pinitol, sequoyitol) with insulin-mimetic activities are still unclear. A putative mechanism of action implies inositol phosphoglycans (IPGs) containing MI or DCI as insulin mediators.

The discovery of IPGs has emerged from the observation that the canonical model of insulin signaling invoking phosphorylation of insulin receptor substrates (IRS), phosphoinositides 3 kinase (PI3K) and protein kinase B/Akt (PKB/Akt) accounts for most, but not all, intracellular actions of insulin. Non-oxidative and oxidative glucose disposal by activation of glycogen synthase (GS) and mitochondrial pyruvate dehydrogenase (PDH) remain indeed incompletely explained by such model. Moreover, insulin stimulates both cellular glucose uptake and glycogen synthesis but these actions sometimes occur in a disconnected manner suggesting the possible existence of not only one but two parallel signaling pathways connecting the insulin receptor to the activation of glucose uptake and its metabolic intracellular disposal. Consequent research on second messengers of insulin action led to the discovery of two IPGs as putative insulin mediators, extracted from rat liver and released in response to insulin. Their chemical nature was revealed later: the first glycan termed IPG-P (Inositol Phosphoglycan-Phosphatase stimulator) contained methylated DCI (i.e. D-pinitol) and galactosamine and activated PDH phosphatase ; the other one termed IPG-A (Inositol Phosphoglycan-AMP kinase inhibitor) contained MI and glucosamine and inhibited cAMP-dependent protein kinase (PKA) and adenylate cyclase (AC) (Larner et al. 1988). Both types of IPG have been shown to additionally contain neutral sugars and phosphate residues. IPG-A and IPG-P were both insulin mimetic when administered *in vivo* in normal or diabetic rats: they reduced hyperglycemia dose-dependently by intravenous injection in low-dose STZ type 2 diabetic rat and stimulated glucose incorporation into glycogen in rat diaphragm muscles by intraperitoneal injection (Huang et al. 1993). The origin of their insulin-stimulated production was first brought to light in 1986 by the discovery that inositol glycans release from hepatic plasma membranes in response to insulin was reproduced by addition of a phosphatidylinositol-specific phospholipase C

83

(Saltiel & Cuatrecasas 1986). Numerous reports then confirmed that insulin, other growth factors and classical hormones, stimulated the hydrolysis of glycosyl-phosphatidylinositol (GPI) generating water-soluble inositol phosphoglycan (IPG) second messenger. The origin of IPG-A is thought to be *myo*-inositol-containing GPI, as both PLC and PLD mediated hydrolysis of GPI yield biologically active IPG molecules (reviewed in (Jones & Varela-Nieto 1999)). Point-mutated and kinase-deficient insulin receptors fail to couple the generation of IPG-A through GPI hydrolysis, implying in some way that IPG-A release from GPI is controlled by insulin-stimulated tyrosine phosphorylation events. For DCI glycans (IPG type P like), Larner and colleagues propose that they are hydrolyzed from membrane phospholipids and/or GPI linked proteins such as alkaline phosphatase (Larner et al. 2010). Indeed, bovine liver has four GPI lipid species with 1:1 molar ratios of chiro-inositol and galactosamine like IPGs of P type.

Further evidence for a possible role of IPGs as insulin second messengers comes from studies on isolated rat adipocytes, in which IPGs released from GPI extracted from rat liver or purified from hemodialysate (Actovegin®) mimicked the anti-lipolytic and lipogenic effects of insulin (Machicao et al. 1990; Kelly et al. 1987). The anti-lipolytic effect of such IPGs was associated with a reduction in the cAMP production stimulated by isoproterenol (Machicao et al. 1990). This effect is probably related to an inhibitory effect of these IPGs on adenylate cyclase and/or cAMP kinase, likely to IPG-A type. The stimulation of lipogenesis from glucose might be explained by PDH activation, similarly to IPG-P type; PDH and ACC are indeed two important control points for *de novo* lipogenesis from glucose. In addition, a purified *chiro*-inositol-containing IPG mediator (IPG-P type) from beef liver directly activated G3PAT in cell-free preparations of BC3H1 myocytes and Wistar rat adipocytes and is probably a mediator of this insulin action (Farese et al. 1994).

Further efforts allowed the identification of a novel putative mediator of insulin purified from beef livers and termed INS-2 (Larner et al. 2003). Its exact chemical structure was determined and further confirmed by its chemical synthesis: it was a 4-O-(2-amino-2-deoxy-beta-D-galactopyranosyl)-3-O-methyl-D-*chiro*-inositol. This unique pinitol β-1,4-galactosamine structure is contrasted with the more common *myo*-inositol α-1,6-galactosamine structure determined in other *myo*-inositol glycans. The bioactivity of this galactosamine *chiro*-inositol pseudo-disaccharide Mn^{2+} chelate was studied. This allowed the proposition of a new model of insulin signaling depicting the production of INS-2 in response to insulin and its role as second messenger of insulin action.

This new model proposed by Larner and colleagues (**Fig. 23**) (Reviewed in (Larner et al. 2010)) incorporates how insulin activates GS and PDH via a *chiro*-inositol glycan second messenger like INS-2 and how insulin activates GLUT-4 translocation to the plasma membrane. As depicted in **Fig. 23**, binding of insulin activates insulin receptor (IR) tyrosine kinase that autophosphorylates, recruits IRS proteins and phosphorylates them on Tyr residues to serve as scaffolds. A principal IR/IRS target is PI3K that generates PIP_3 to activate the phosphorylation of PKB/Akt by the PDK. After several steps, Akt activation

84

leads to the translocation of GLUT-4 vesicles to the plasma membrane to increase glucose transport into the cells. In parallel of this IRS/PI3K/Akt pathway, IR activation would be also coupled to the heterotrimeric G protein Gq itself coupled to a GPI-phospholipase (possibly GPI phospholipase D, PLD) (See the review of Larner et al, 1999 (Larner & Huang 1999) for further details). Activation of the phospholipase would release an inositol glycan second messenger INS-2 from a GPI lipid precursor in the inner and/or outer leaflets of the plasma membrane. INS-2 could be released either directly into the cytosol or outside the cell and then transported back into a neighboring cell or into the original cell via an ATP-dependant inositol glycan transporter (anti-inositol glycan antibodies inhibition studies (Romero et al. 1990), cultured cell dilution experiments (Romero et al. 1993) and impermeant fluorescent tag experiments (Varela et al. 1990) all supporting the extracellular generation/release of IPGs hypothesis). Inside the cell, INS-2 would bind and allosterically activates two members of the Mg^{2+}-dependent protein phosphatase family: cytosolic PP2Cα and mitochondrial PDHP. In the cytosol, activated PP2Cα stimulates glycogen synthase directly and indirectly via PI3K/PDK/Akt/GSK3 pathway. Indeed, it has been reported that PP2Cα dephosphorylates the Ser-608 residue of PI3Kα p85 regulatory subunit, resulting in activation of PI3Kα p100 catalytic subunit. The consecutive activation of PKB/Akt leads to the inactivation of glycogen synthase kinase 3 (by phosphorylation on its Ser-9 residue) resulting in activation of glycogen synthase. Other signaling events occur downstream of activated Akt and lead in particular to the activation of mTOR kinase and GLUT-4 translocation to the plasma membrane. Not depicted in **Fig. 23** but possibly important, it has been observed that PP2Cα also inactivates AMPK by dephosphorylation of its Thr-172 in hepatocytes, heart and hypothalamus. In the mitochondria, allosteric activation of PDHP by INS-2 as a manganese chelate dephosphorylates Pyruvate dehydrogenase (PDH) thereby enhancing the oxidative glucose disposal.

The model depicted in **Fig. 23** and the studies on IPGs provide a possible explanation for the observed effect of insulin on GS and mitochondrial PDH activation that were not fully explained by the conventional model. It also proposes a conceptual framework for the origin, production and actions of *chiro*-inositol-containing glycans as second messengers working in a complementary and synergistic manner with the better-accepted pathways of insulin signaling.

However, this model does not explain the putative role and actions of *myo*-inositol containing glycans and some questions remains to be elucidated. In particular:

- Why a GLUT-4 translocation and a glucose uptake enhancement were observed in response to several inositol isomers without insulin stimulation in some animal and in vitro studies (Yap et al. 2007; Dang et al. 2010)? Is there a baseline production of IPGs independently of insulin stimulation?

85

- What is the phospholipase releasing inositol glycans and from which precursor lipids and proteins? Are inositol glycans released extracellularly and/or intracellularly?
- If existing, what is/are the inositol glycan transporter(s) in plasma and mitochondrial membranes?
- Does a MI, sequoyitol, DCI or pinitol supplementation increase IPGs production and how?
- How many inositol glycan second messenger of insulin exist? Are they different depending on the species, tissue or cell type? Is the structure of plasma IPGs different from that of tissular IPGs?
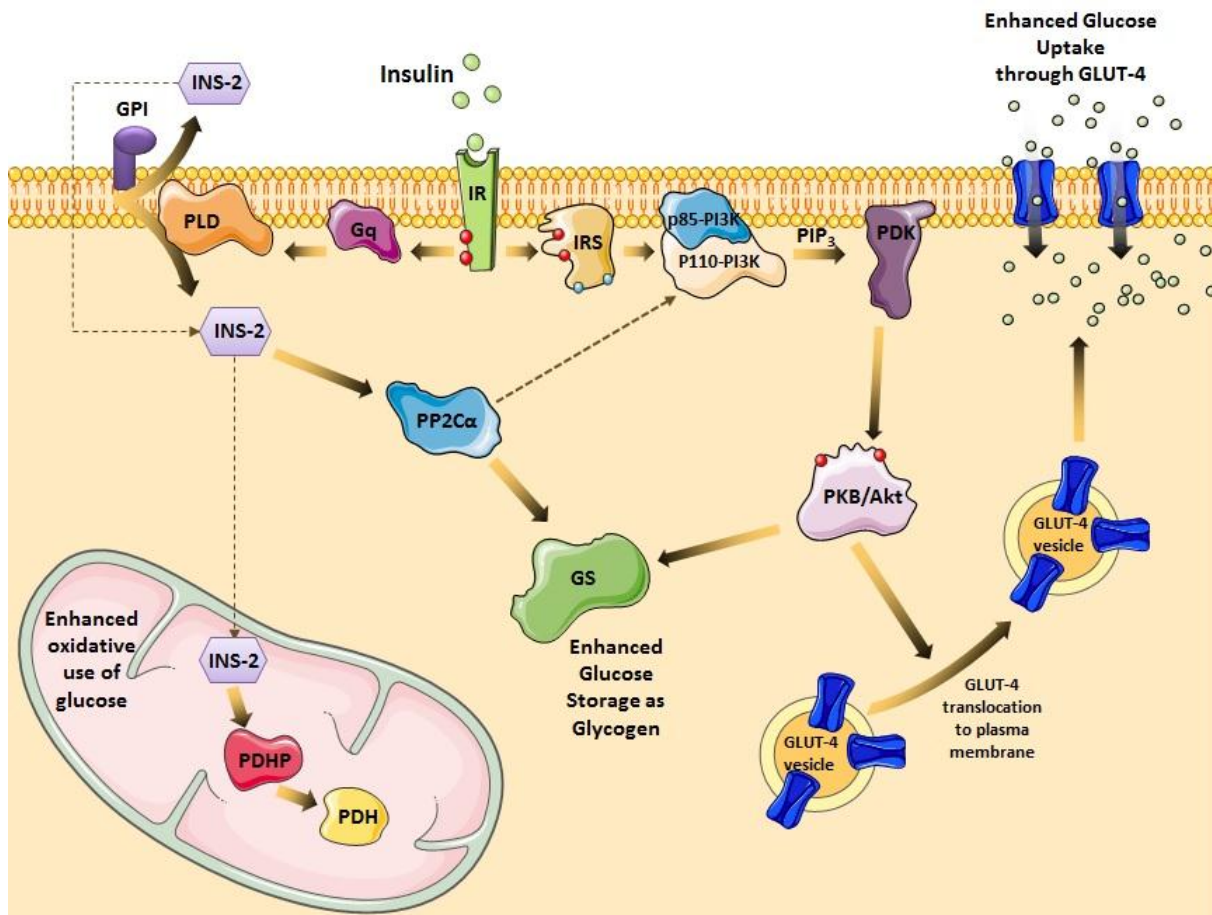
Figure 23 – New model of insulin-signaling proposed by Larner and co-workers - Inositol glycans as putative second messengers (INS-2) of insulin. Adapted from the review of (Larner et al. 2010)). In this model, insulin binding to its receptor (IR) leads to autoactivation of the receptor and the activated IR can transduce the signal through two parallel signaling pathways. The first and well-accepted pathway of insulin implies the recruitment and activation of substrates of insulin receptor (IRS) by the activated IR. Subsequent protein activations (PI3K, PDK-1) finally leads to PKB/Akt recruitment and activation at the plasma membrane. Activated PKB/Akt induces GLUT-4 translocation to the plasma membrane and so enhances glucose entry into the cell. In the second putative pathway, the IR is coupled to a G protein itself coupled to a phospholipase (possibly PLD or PLC) that catalyzes the hydrolysis of a GPI. The insulin-induced hydrolysis of the GPI releases an inositol phosphoglycan containing D-*chiro*-inositol which acts as a putative second messenger of insulin (INS-2) mediating insulin effects on glucose oxidative and non-oxidative disposal. INS-2 binds and allosterically activates two Mg^{2+}-dependent protein phosphatases : PP2Cα in the cytosol and PDHP in the mitochondria. Activated PP2Cα stimulates Glycogen Synthase directly and also indirectly through possible activation of PI3K, Akt and subsequent inhibition of GSK3. In the mitochondria, activated PDHP stimulates PDH and so Glucose oxidative use. Those two pathways acts together to mediate insulin action in a complementary and synergistic manner. Abbreviations: IR, Insulin receptor, GLUT-4 Glucose transporter 4, GPI, glycosyl phosphatidylinositol, GS, Glycogen Synthase, GSK3, Glycogen synthase kinase 3, INS-2, insulin second messenger, PDH, pyruvate dehydrogenase, PDHP, pyruvate dehydrogenase phosphatase, PDK-1, phosphoinositide-dependent kinase 1, PI3K, phosphoinositide 3 kinase, PKB/Akt, protein kinase B/Akt, PLC, phospholipase C, PLD, phospholipase D, PP2Cα, phosphoprotein Phosphatase 2C alpha.

Chapter 2 – Rationale and Objectives

The increase in the prevalence of metabolic syndrom and/or type 2 diabetes urged scientists to find natural or synthetic compounds able to help in regulating blood glucose levels. Since Insulin resistance is the first comminted step in the development of type 2 diabetes, and preceeds pancreatic β-cells failure and the subsequent insulin deficency, we aimed to find a strategy of prevention or treatment of insulin resistance. As preventive strategies are designed to people that are not yet unhealthy (diabetes in this case), we though that a "nutritional" strategy would probably better suits than a "pharmacological" strategy to improve insulin sensitivity in pre-diabetic subjects, since nutrient supplements cause generally fewer side effects than drugs.

Inositol, which was formerly referred to as vitamin B7, is a cyclitol naturally occurring in nature and foodstuffs and several inositol isomers (e.g. D-*chiro*-, *myo*-inositol) and derivatives (e.g. D-pinitol, sequoyitol) have been shown to possess insulin mimetic properties. In particular, acute administration of D-*chiro*-inositol (DCI) or D-pinitol or *myo*-inositol (MI) lowered post-prandial blood glucose level in different animal models of diabetes or insulin-resistance (Bates et al. 2000; H. K. Ortmeyer et al. 1993; Ortmeyer et al. 1995; Ortmeyer 1996) through an improvement of insulin-sensitivity (DCI, pinitol). *myo*-Inositol is by far the most abundant isomeric form of inositol in living cells and in foodstuffs making this isomer as one of the best candidate for a inositol-based nutritional strategy.

The aims of this thesis were then to :

1) Test the potency of a chronic *myo*-inositol supplement to improve blood glucose control in mice.
2) Determine if the blood glucose lowering effect of *myo*-inositol results from an insulin-sensitizing effect and/or from an insulin-secretion stimulating effect.
3) Unravel the molecular mechanism of action of *myo*-inositol and inositol isomers/derivatives
4) Test the potency of a dietary *myo*-inositol supplement to prevent or restrain insulin resistance development induced by a high calorie diet in mice.

Chapter 3 - Material and Methods

3.1 Chemicals and antibodies

myo-Inositol, was purchased from Sigma Aldrich, (Saint Quentin Fallavier, France), recombinant Human insulin (100 UI/ml, Actrapid®) was from Novo Nordisk, (La Défense, France). Anti-Phospho-Akt 1/2/3 rabbit IgG (7985R) and anti-Akt 1/2/3 rabbit IgG (8312) antibodies were purchased from Santa Cruz Biotechnology (Santa Cruz, Heidelberg, Germany), anti-tubulin mouse IgG antibody was from Sigma Aldrich, anti-mouse IgG and anti-rabbit IgG antibodies were from BioRad (Marnes-la-Coquette, France). Super Signal® West Pico Chemiluminescent Substrate and Restore™ Western Blot Stripping Buffer were obtained from Thermo Scientific (Perbio, Brebières, France). Other chemicals were obtained from Sigma Aldrich when no other origin is specified.

3.2 Animal experiments: Ethics

All experiments were carried out according to the guidelines laid down by the French Ministère de l'Agriculture (n° 87-848) and the E.U. Council Directive for the Care and Use of Laboratory Animals of November 24th, 1986 (86/609/EEC). Animal experiments were performed under the authorization n°69-266-0501 (INSA-Lyon, DDPP-SV, Direction Départementale de la Protection des Populations - Services Vétérinaires du Rhône), according to the guidelines laid down by the French Ministère de l'Agriculture (n° 87-848) and the E.U. Council Directive for the Care and Use of Laboratory Animals of November 24th, 1986 (86/609/EEC). Marine Croze (n°692661241) and Christophe Soulage (n°69266257) hold special licenses to experiment on living vertebrates issued by the french Ministry of Agriculture and Veterinary Service Department.

3.3 Chronic MI supplementation of healthy mice

Animals

Female CD-1 Swiss mice (30-35g) were purchased from Janvier SA (Le Genest-Saint-Isle, France) and housed in an air-conditioned room with a controlled environment of 21 ± 0.5°C and 60-70% humidity, under a 12h light/dark cycle (light on from 07:00h to 19:00h) with free access to food (13,4 kJ/g, 65% carbohydrates, 11% fat, 24% proteins (w/w), AO3, SAFE, Augy, France) and water.

myo-Inositol treatment

Sixty mice were randomly assigned to receive daily intraperitoneal injection of either a saline solution (NaCl 0.9%, w/v) or *myo*-inositol (1.2 mg.g^{-1} BW) for 15 days. Food intake and body weight were measured twice weekly. Food consumption was calculated as the difference between the amount given and that removed from the cage. A second set of mice (n=20) was given *myo*-inositol in drinking water (6 g.L^{-1}) for 15 days. Water consumption was measured to assess daily *myo*-inositol intake.

Metabolic challenges

Glucose tolerance test (GTT): After an overnight fast, animals were injected intraperitoneally with 1 g.kg^{-1} body weight of D-glucose in sterile water. Blood glucose was measured before and 15, 30, 60 and 90 min after injection. On an independent group of animals (n=5), 200 μL of blood were collected by retro-orbital sinus puncture from each mouse into a heparinized microcentrifuge tube, 30 min after glucose load in order to measure plasma insulin level at the hyperglycaemic phase of the test. Blood was centrifuged 2 min at 3500 g (4°C) to prepare plasma. Plasma samples were snap frozen in liquid nitrogen and stored at -20°C until insulin assay.

Insulin tolerance test (ITT): After an overnight fast, animals were injected intraperitoneally with 0.30 UI.kg^{-1} BW of recombinant human insulin. Blood glucose was measured before and 15, 30, 60 and 120 min after insulin injection. The glucose disappearance rate for ITT (K_{ITT}; %.min^{-1}) was calculated using the formula given by Lundbeak (1962) (Lundbaek 1962): $K_{ITT} = 0.693 \times 100 / t_{1/2}$ where $t_{1/2}$ was calculated from the slope of the plasma glucose concentration, considering an exponential decrement of glucose concentration during the 40 min after insulin administration (González-Ortiz et al. 2006).

Insulin secretion test: L-arginine induced insulin secretion. After an overnight fast, mice were injected intraperitoneally with 1 g.kg^{-1} BW of L-arginine in saline and blood was withdrawn at 0, 2 and 5 min after injection in heparinized microtubes. Blood was centrifuged 2 min at 3500 g (4°C) to prepare plasma. Plasma samples were snap frozen in liquid nitrogen and stored at -20°C until insulin assay.

Blood sampling for plasmalogens quantitation in red blood cells

After 10 days of treatment with or without *myo*-inositol, 300 µL of blood were collected on heparin by retro-orbital sinus puncture using a Pasteur pipette. Blood was centrifuged 1 min at 3500 g and plasma was collected and snap frozen into liquid nitrogen. Red blood cells pellet was rinsed with saline solution and snap frozen into liquid nitrogen and then stored at -80°C until plasmalogen quantitation by Gas Chromatography (GC).

Sacrifice and tissue dissection

The body weight and body length were measured and Lee index (an index of adiposity in rodents) was calculated as the cubic root of BW divided by naso-anal length (Lee 1929; Bernardis & Patterson 1968). Mice were then sacrificed by cervical dislocation. Blood (750 µL) was collected by heart puncture on heparinized tube, centrifuged 2 min at 3500 g to prepare plasma. Plasma samples were snap frozen in liquid nitrogen and stored at -80°C until analysis. Liver, heart, kidneys, tibialis and gastrocnemius muscles, parametrial, retroperitoneal and subcutaneous inguinal white adipose tissue (WAT) were dissected out according to anatomical landmarks, weighed to the nearest milligram, snap frozen in liquid nitrogen and stored at -20°C.

Cellularity study: Measurement of adipocyte size and number

Cell size - Preparation of adipose tissue for determination of cell size was performed essentially as described by Etherton, Thompson & Allen (1977) (Etherton et al. 1977). Briefly, 30-40 mg of parametrial WAT were immediately fixed in osmium tetroxide and incubated at room temperature for 96h and then adipose cell size was determined by a Beckman Coulter Multisizer IV with a 400 µm aperture. The range of cell sizes that can effectively be measured using this aperture is 20–240 µm. The instrument was set to count 1,000 particles, and the fixed-cell suspension was diluted so that coincident counting was <10%. Cell-size distributions were drawn from measurement of at least 12,000 cell diameters per animal.

Cell number - DNA content in parametrial WAT was measured, after delipidation of the samples, by a standard fluorimetric method using bisbenzimide and calf thymus DNA as standard (Labarca & Paigen 1980). Briefly, 100 mg of WAT were homogenized into 1mL of fluorescence buffer 1x (10 mM Tris HCl, 1 mM EDTA and 0.2 M NaCl, pH 7.4). Delipidation of the lysates was performed by extraction of neutral lipid by 4 mL of hexane. 200-500 µL of delipidated aqueous fraction were kept at -20°C for DNA quantitation. 10-30 µL of aqueous fraction or 10 µL of calf thymus DNA standard solution were added to 3 mL of bisbenzimide 1 $\mu g.mL^{-1}$ in fluorescence buffer 1x. After 10 min of incubation at room temperature and in the dark, intensity of the fluorescence developed was measured with a fluorometer with an excitation wavelength of 360 nm and an emission wavelength of 460 nm. Fluorescences of samples and of standard solutions are corrected by fluorescence of the standard solution without DNA.
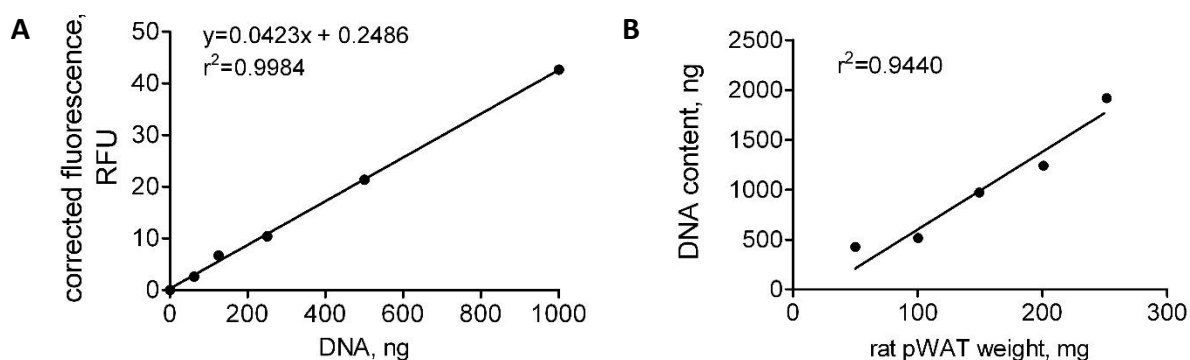
Figure 24 – White Adipose tissue DNA assay method validation for adipocyte number estimation. Fluorescence of 10 µL of standard solution or 10-30 µL of white adipose tissue sample in 3 mL bisbenzimide solution is measured, after 10 min of incubation in the dark, with a fluorometer at an excitation wavelength of 360 nm and an emission wavelength of 460 nm. Fluorescence is corrected by fluorescence of the standard solution without DNA. **A) DNA standard curve.** DNA from calf thymus was solubilized into 8 mM NaOH and 6.25, 12.5, 25.0, 50 and 100 ng.µL^{-1} solutions were obtained by successive dilutions. Concentration of the 50 ng.µL^{-1} solution was checked by measurement of the absorbance at 260 nm considering that 50ng.µL^{-1} of double strand DNA has an absorbance of 1.0 at this wavelength. **B) DNA content of a weight range (50, 100, 150, 200 and 250 mg) of a same adipose tissue sample** (pWAT from a Wistar rat) was estimated and linearity was tested. A linear correlation was found between the DNA content and the weight of a same white adipose tissue sample, with a greater correlation for sample of at least 100 mg of adipose tissue (r^2=0.9705).

Cell number in samples is then calculated from DNA quantitation considering that a mice diploid cell contains 6.47 pg of DNA. Finally, results are corrected to take into account the loss of DNA in the organic phase during the process of delipidation that has been estimated at 15 %.

Isolation of adipocytes

Five mice of each group were killed by cervical dislocation, parametrial and retroperitoneal fat pads were dissected out, pooled and adipocytes were isolated. Adipose tissue was weighed, minced and digested in 7 ml of Krebs Ringer Bicarbonate (KRB, pH 7.40) buffer containing 6 mM glucose, 1% (w/v) fatty acid-free bovine serum albumin (BSA) and 1.5 mg.ml^{-1} collagenase (type II, C6885, Sigma Aldrich). The vial was shaken (40 cycles.min^{-1}) at 37°C for 60 min. The resulting cell suspension was filtered through a nylon membrane (250 µm) and washed three times with KRB buffer containing 4% fatty acid-free BSA. Then adipocytes were resuspended in KRB buffer containing 4% fatty acid-free BSA and counted in a hemacytometer.

Lipogenesis assay

Lipogenesis was measured in mouse isolated adipocytes as the incorporation of [14C]-acetate into neutral lipids as previously described (Zarrouki et al. 2010). Briefly, aliquots (100 µl) of cell suspension were incubated in MEM medium containing 1 % fatty acid-free BSA and 1 µCi of [14C]-acetate for 4h at

92

37°C with gentle shaking (40 cycles.min^{-1}). Neutral lipids were extracted using Dole's extraction fluid (isopropanol/heptane/H_2SO_4 1N, 40/10/1, v/v/v) and [^{14}C] was detected by liquid scintillation counting. Counting results were then normalized to lipid content.

Lipolysis

Aliquots of the cell suspension (100 µl) were distributed in 2 ml-polystyrene vials containing KRB buffer 4 % BSA with or without isoproterenol hydrochloride (5 µM). Adipocytes were incubated at 37°C with gentle shaking (40 cycles.min^{-1}) for one hour. The reaction was stopped by placing vials on melting ice. The floating adipocytes were discarded by aspiration and lipolysis was quantified by measuring the release of extracellular glycerol using a kit (Glycerol assay, R-Biopharm, Saint Didier aux Monts d'Or, France).

Biochemical measurements

Fasting and non-fasting blood glucose levels were measured with a glucometer (Accu Check Performa, Roche diagnostic, Meylan, France). The plasma insulin level was determined with mouse insulin EIA kit (SpiBio, Montigny-le-Bretonneux, France) according to the manufacturer's instructions. The homeostasis model assessment of insulin resistance (HOMA-IR) was calculated using glucose and insulin concentrations obtained after 16 h of food withdrawal, using the following formula: fasting blood glucose (mg.dl^{-1}) × fasting insulin (µU.ml^{-1})/405. Plasma total cholesterol, triacylglycerols and non-esterified fatty acid (NEFA) levels were measured with the following commercial kits, Cholesterol RTU (bioMérieux, Marcy-l'Etoile, France), Triglyceride PAP (bioMérieux) and NEFA-C (WAKO, Sobioda, Montbonnot, France) according to manufacturer's recommendations. Plasma adiponectin and leptin concentrations were determined with enzymo immuno assays (Cayman Chemicals, distributed by SpiBio) according to the manufacturer's guidelines. All assays were performed at least in duplicates. The muscle and hepatic lipids were extracted using the modified procedure developed by Folch (Folch et al. 1957) using chloroform-ethanol (2:1, v/v) and total lipid extract was estimated gravimetrically.

Resistance to oxidative stress induced by paraquat

Mice were given or not *myo*-inositol in drinking water (6 g.L^{-1}) (n=10). Water consumption was measured daily to assess *myo*-inositol intake. Mice were intraperitoneally injected daily at 10:00 am, for the duration of the experiment, with 15 mg.kg^{-1} BW of paraquat (Sigma Aldrich) prepared as a 7 mM solution in sterile saline. Their health status was observed and recorded twice daily for 10 days. Survival curves (Kaplan Meier curve) were plotted using GraphPad Prism and data were analysed using Gompertz software as previously described (Doubal & Klemera 1997; Klemera & Doubal 2000).

93

Plasma total antioxidant activity

The total plasma antioxidant activity was measured as described by (Koracevic et al. 2001). Briefly, the assay measured the capacity of 10 µl of plasma to inhibit the production of thiobarbituric acid reactive substances (TBARS) produced from sodium benzoate under the influence of the free oxygen radicals derived from Fenton's reaction. A solution of 1 mM uric acid was used as standard and results were expressed as mM equivalent uric acid.

Antioxidant activity (AOA) of myo-inositol aqueous solutions concentration range

Protocol for measurement of plasma antioxidant activity (see section "plasma total antioxydant activity") was adapted here to a series of *myo*-inositol concentrations (0.1, 0.5, 1.0, 2.5, 5.0, 10.0, 25.0, 50.0 and 100.0 $g.L^{-1}$) in PBS. The only change in the protocol for plasma AOA was that the 10µL of plasma were replaced by 10 µL of *myo*-inositol solution.

In vivo and ex vivo insulin stimulation

In vivo insulin stimulation - To further explore insulin signaling in skeletal muscle, control and *myo*-inositol mice received their last intraperitoneal *myo*-inositol or saline injection 60 min prior to sacrifice. In each group, mice were then randomly assigned to receive either saline or insulin (0.75 $UI.kg^{-1}$ BW, i.p.) 30 min before sacrifice. Mice were killed by cervical dislocation, gastrocnemius muscle was rapidly dissected out, blotted dry and snap frozen in liquid nitrogen.

Ex vivo insulin stimulation - To decipher whether *myo*-inositol was able to directly act on muscle, we performed an *in vitro* incubation of skeletal muscle with *myo*-inositol and *in vitro* insulin stimulation. Mice were killed by cervical dislocation, gastrocnemius were rapidly dissected out bilaterally and chopped into small pieces with a scalpel. Muscle pieces were incubated in 3 ml of MEM medium containing 100 nM insulin and 1 mM *myo*-inositol, 1 mM *D-chiro*-inositol or 1 mM mannitol as an osmotic control. Muscles were incubated for 15 min at 37°C, blotted dry and snap frozen in liquid nitrogen.

Immunoblotting – insulin induced phosphorylation of PKB/Akt in skeletal muscle

Gastrocnemius was homogenised in standard lysis buffer (20 mM Tris-HCl, 138 mM NaCl, 2.7 mM KCl, 1 mM $MgCl_2$, 5% Glycerol and 1 % Nonidet P40) supplemented with protease and phosphatase inhibitors (5 mM EDTA, 1 mM Na_3VO_4, 20 mM NaF, 1 mM DTT, Protein inhibitor cocktail, Sigma Aldrich). Lysates were centrifuged 15min at 13 000g to discard insoluble materials. Supernatant protein content was quantified by Bradford assay. 60 µg of proteins of tissue lysate soluble fraction were boiled 5 min in Laemmli buffer and separated by 10 % sodium dodecyl sulfate – polyacrylamide gel electrophoresis (SDS-PAGE). After transfer to a nitrocellulose membrane, and aspecific sites blockage with Bovine Serum

94

Albumin (BSA) 5 % in TBST (10 mM Tris-HCl at pH 8.0, 150 mM NaCl and 0.05 % Tween-20), PKB/Akt activating phosphorylation on serine was detected using primary anti-phospho(Ser 473)-Akt(1/2/3) antibody (1/1000[e] in TBST 3% BSA – Overnight, 4°C) and then secondary antibody (anti-rabbit, 1/10 000[e] TBST – 1h, room temperature) conjugated with horseradish peroxidase. Of note, three nitrocellulose membrane lavages of the 10 min with TBST were performed between each step to remove unbounded or weakly (aspecifically) bounded material. Membranes were processed for chemiluminescence and proteins were quantitated by densitometry using Quantity One software (BioRad). In order to normalise for equal protein loading, membranes were stripped and re-blotted with anti-total Akt(1/2/3) antibody and then anti-α-tubulin antibody.

Gas Chromatography : Fatty acid analysis

Red blood cells were homogenized by sonication in PBS. 10 μg of intern standard 1,2-diheptadecanoyl-*sn*-glycero-3-phosphoethanolamine (PE di 17:0) were added precisely to the cell lysate using a Hamilton syringe. Total lipids were extracted by the modified procedure developed by Folch (Folch et al. 1957) using chloroform-ethanol (2:1, v/v). Briefly, 6 mL CHCl$_3$ and 3 mL EtOH were added per milliliter of cell lysate, and organic lower phase was collected after vortex and 10 min centrifugation at 700 g. Aqueous phase was extracted twice by chloroform-ethanol (2:1, v/v) and first and second extraction organic phases were pooled. Organic phase solvents were evaporated under a nitrogen flux. Lipid residue was dissolved in 50 μL of chloroform-ethanol (2:1, v/v) and then applied with a capillary onto a silica gel plate (20 cm x 20 cm, previously rinsed with methanol) for thin layer chromatography. Extern standard (about 30 μg) of phospholipid ethanolamine (PE) from bovine brain was also applied on the TLC plate in a parallel depot. A first migration in 100 mL diisopropylether for 1h30 separated neutral lipids and phospholipids. Phospholipids sub-classes were then separated by a second migration using a more polar eluent (CHCl$_3$/methanol/methylamine (61:19:5, v/v/v)) for about 2 hours. TLC plates were sprayed with dichlorofluorescein (20 mg into ethanol 95% (v/v)) and lipid spots were detected under UV. Silica of the phospholipid ethanolamine spot was scraped, collected into a glass tube and resuspended into 500 μL of toluene/methanol (2:3, v/v). Transesterification of phospholipids was performed by addition of 500 μL of trifluorobromide (BF$_3$) 14% (w/v) in methanol and warming at 100°C for 1h30 under a nitrogen atmosphere. Reaction was stopped on ice and 1.5 mL of 10 % (w/v) K$_2$CO$_3$ and fatty acid methyl esters (FAME), deriving from diacylglycerophospholipids, and dimethylacetals (DMA), deriving from plasmalogens, were extracted with 2 mL pestipur. After 10 min centrifugation at 500 g, organic upper phase was collected and evaporated under nitrogen. Lipid residue was solubilized into 100 μL of pestipur isooctane and FAME and DMA were analysed by Gas Chromatography (Gas chromatograph equipped with a Flame Ionization Detector (GC-FID) (Agilent technologies, Marnes-la-Coquette, France).

3.4 Dietary MI supplementation of mice fed a diabetogenic and obesogenic diet

Animals

Male C57Bl/6JRj mice (15-20 g) were purchased from Janvier SA (Le Genest-Saint-Isle, France) and housed in an air-conditioned room with a controlled environment of 21 ± 0.5°C and 40-70% humidity, under a 12h light/dark cycle (light on from 07:00h to 19:00h) with free access to food (Chow diet : 13,4 kJ.g^{-1}, 65% carbohydrates, 11% fat, 24% proteins (w/w), AO3, SAFE, Augy, France) and water.

Diet and myo-inositol supplementation

Thirty mice were randomly assigned to be either under standard diet (Control group with Chow diet – C) or high fat diet with (HF-MI) or without (HF) *myo*-inositol supplementation (0.58 mg.g^{-1} BW) in drinking water (n=10 mice per group) for 4 months. In the HF and HF-MI groups, the chow diet (2016C, Harlan) see **Table 4** for diet composition) was replaced by the high fat diet (TD.06414, Research diets, Harlan Laboratories Inc, Indianapolis, USA, see **Table 4**) when mice were about 25 g (i.e. 3 weeks after randomisation). At the same time, *myo*-inositol was added to drinking water (6 g.L^{-1}) in the HF-MI group. High fat diet and *myo*-inositol supplement were given for 4 months. Food intake and body weight were measured twice and once weekly, respectively. Food consumption was calculated as the difference between the amount given and that removed from the cage. Water consumption was measured to calculate daily *myo*-inositol intake.

Table 4
Diet composition

	Standard diet	High fat diet
Reference	2016C	TD.06414
Nutrient composition (g/100g)		
Carbohydrates*	48.5	27.3
Proteins	16.4	23.5
Lipids	4.0	34.3
Energy density (kJ/g)§	12.6	21.3
From (%)		
Carbohydrates	66.0	21.3
Proteins	22.0	18.4
Lipids	12.0	60.3

*Mean composition of the standard and high fat diets from HARLAN Laboratories Inc. Data were obtained from HARLAN Laboratories Inc (Indianapolis, USA). *Available carbohydrates only. §Note that energy density is calculated from ingredient analysis or manufacturer data.*

Insulin tolerance test

Insulin tolerance test was performed after nearly 3 months (80 days) of high fat diet with or without *myo*-inositol supplementation. After an overnight fast, animals were injected intraperitoneally with 0.5 UI.kg^{-1} BW of recombinant human insulin. Blood glucose was measured before and 15, 30 and 60 min after insulin injection. The glucose disappearance rate for ITT (K_{ITT}; %.min^{-1}) was calculated as described in section 3.3.

Urine collection

24h-diuresis was collected in polycarbonate metabolic cages (Charles River Laboratory, L'Arbresle, France) after 1 month of chow or high fat diet. During urine collection, animals were given free access to food and water. The volume of each 24-hr urine sample was measured gravimetrically. Urine were centrifuged 10 min at 9000 rpm to discard cells and insoluble materials, and aliquots of supernatant were removed and stored at −80°C until analyzed.

Sacrifice and tissue dissection

Animals were deeply anesthetized with pentobarbital (60 mg.kg^{-1}). The body weight and length were measured. Terminal cardiac blood (750 µL) punctures were realized on heparinized tube and blood was centrifuged 2 min at 3500 g to prepare plasma. Plasma samples were aliquoted, snap frozen in liquid nitrogen and stored at -80°C until analysis. Liver, heart, kidneys, gastrocnemius muscles,

epididymal, retroperitoneal and subcutaneous inguinal white adipose tissues (WAT) were dissected out according to anatomical landmarks, weighed to the nearest milligram, snap frozen in liquid nitrogen and stored at -80°C. Pieces of liver were fixed into buffered paraformaldehyde (10% w/v) pH 7.4 for histological sections and 30-40 milligrams of rWAT were fixed in osmium tetroxide for measurement of cell size as described above.

Liver histopathological study

Liver slices were fixed in 10% formalin solution for at least 24h. Fixed tissues were then embedded in paraffin and 5-6 μm sections were realised with a microtome and stained with haematoxylin and eosin (H&E). Nonalcoholic Steatohepatitis (NASH) was assessed under a light microscope (Zeiss).

Cellularity study: Measurement of adipocyte sizes and numbers

The cellularity of rWAT (i.e. number and size of adipose cells) was performed as described above (section 3.3)

Fatty Acid Synthase (FAS) assay

Epidydimal white adipose tissue (30-50 mg) was homogenized in 1 mL of ice-cold sucrose buffer (0.25 M sucrose, 1 mM DTT, 1 mM EDTA, and a mixture of protease inhibitors) pH 7.4. Homogenates were centrifuged at 105,000 g (0°C) for 60 min, fat cake was discarded and the clear infranatant was freezed at –20°C for determination of FAS activity. FAS activity was measured spectrophotometrically by monitoring oxidation of NADPH at 340 nm as described by Bazin & Ferré (Bazin & Ferré 2001). Briefly, 100 μl of infranatant were mixed with 700 μL of 100 mM potassium phosphate buffer (pH 6.5) containing 200 μM NADPH and 100 μM acetyl-CoA. Absorbance at 340 nm was monitored in a heated chamber spectrophotometer at 37°C for 3 min to measure baseline NADPH oxidation. The reaction was started with 100 μL of 100 mM potassium phosphate buffer (pH 6.5) containing 600 μM malonyl-CoA and reaction was assayed for 5 min at 37°C to determine FAS-dependent oxidation of NADPH (molar extinction coefficient of NADPH at 340 nm: $\varepsilon = 6220$ M.cm^{-1}). Results are expressed in nmol of NADPH oxidized per min per mg of tissue.

MIOX assay

Kidneys were homogenized in a lysis buffer (1 mg/10μL) containing 20 mM sodium acetate, 1 mM FeSO$_4$, 2 mM l-cysteine, 1 mM glutathione and 1x inhibitor cocktail, pH 6.0 followed by a brief sonication. Lysates were then centrifuged 30 min at 13000 g, 4°C. 100 μL of supernatant were added to 900 μL of MIOX reaction buffer (50 mM sodium acetate, 2 mM cysteine, 1 mM FeSO$_4$, 60 mM *myo-*

98

inositol, pH 6.0) and MIOX assays were then performed at 30°C for 30 min. MIOX reaction was terminated by incubating samples 5 min in boiling water. Samples were then centrifuged 10 min at 12 000 g, 4°C to remove precipitates. The D-glucuronate formed from MI by MIOX reaction was then determined in the supernatant by the orcinol assay. Briefly, a double volume of freshly prepared orcinol reagent (28 mM orcinol and 3 mM $FeCl_3$ dissolved in HCl 12 N) was added to both the supernatant and the standard solutions of D-glucuronic acid, and incubated in boiling water for 30 min. Reaction was stopped on ice (5 min). Colorimetric readings were made at 670 nm for the D-glucuronic acid standards and for the kidney samples. For each kidney sample, a negative control was prepared following the same procedure but negative samples were boiled directly 5 min prior to MIOX reaction (i.e. just after addition of the lysate supernatant to the MIOX reaction buffer and so prior to reaction at 30°C). MIOX activity of the sample was then expressed as the quantity of D-glucuronic acid formed during the 30 min of reaction (calculated from the difference of A_{670nm} between the sample and its negative control) per mg of kidney.
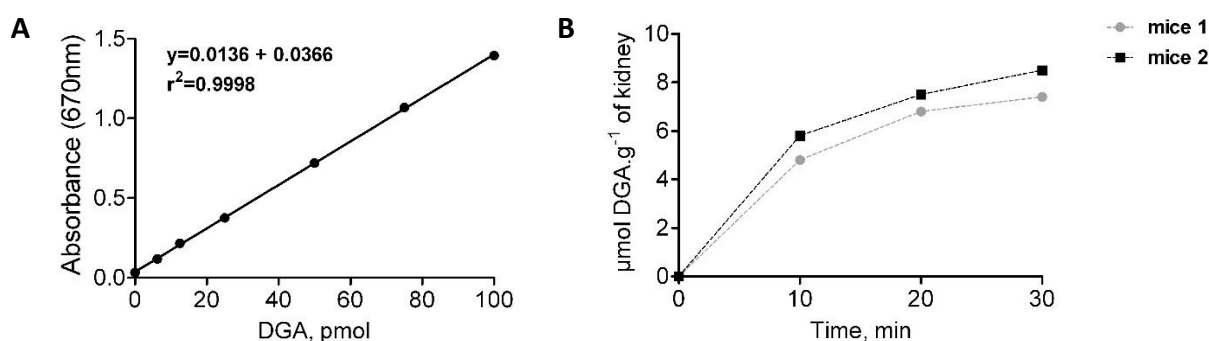
Figure 25 - MIOX assay procedure validation. A) D-glucuronic acid (DGA) standard curve for orcinol assay measured at 270 nm after 30 min of reaction in boiling water. **B) Kinetic of DGA production** (0, 10, 20 and 30 min of reaction in MIOX buffer at 30°C) by kidney MIOX activity of two CD-1 mice taken randomly in a control group of another experiment to test and validate the procedure. DGA standard curve is linear (R^2=0.9998), kidney samples absorbances at 670nm are within the range of standard curve linearity and the shape of the curve of DGA production by kidney samples along time resembles that of an enzymatic kinetic.

myo-Inositol measurement in urine and tissues.

myo-Inositol was determined by the gas chromatography method described by Kawa et al (Kawa, Przybylski, et al. 2003). Briefly, one volume of ethanol was added to an equal volume of urine. Samples were vortexed and evaporated to dryness under nitrogen at 40°C. For the determination of free *myo-*inositol, tissues were deproteinized with an equal amount of 0.3 N $Ba(OH)_2$ and 0.3 N $ZnSO_4$ and centrifuged and the supernatant was evaporated to dryness. Dried samples were sonicated for 5 min with 1 ml of trimethylsilylmidazole: pyridine (1:1, v/v) containing 200 µg of phenyl-α-D -glucoside as an internal standard, and were derivatized for 1 hr at 80°C. Two microliters of derivatized samples or

standards were injected into a gas chromatograph (Shimadzu) equipped with a flame ionization detector and split injector. Inositols were separated on a silica capillary SP-2380 column (60 m × 0.22 mm). Column temperature was programmed from 150° to 200°C at the rate of 3°C.min^{-1}, and then to 325°C at the rate of 7°C.min^{-1}. Initial and final temperatures were held for 5 and 20 min, respectively. The injector and detector temperatures were held at 270° and 350°C, respectively. The carrier gas was hydrogen at 1.5 ml.min^{-1}, and the split ratio used was 1:40.

Biochemical measurements

Plasma glucose, insulin, triglycerides and cholesterol levels were determined following the same experiment procedures as described in section 3.3 for Swiss CD-1 mice study.

3.5 Ancillary experiments

Effect of chronic *myo*-inositol supplementation on old CD-1 Swiss mice

Sixteen CD-1 female mice of about 12 months-old were randomly assigned to be supplemented (n=8 *myo*-inositol mice) or not (n=8 control mice) with 1.0 mg.g^{-1} BW *myo*-inositol added in their drinking water for one month. Mice were sacrificed after one month of supplementation and dissected out for organs collection and weighting, as described in section 3.3, "sacrifice and tissue dissection".

On a similar but independent group of ten old mice (BW (mean ± SEM) were of 53.8 ± 1.9 g for control and 50.8 ± 2.7 g for *myo*-inositol mice, n=5, no significant difference at the p<0.05 level), an insulin tolerance test was performed after one week of *myo*-inositol supplementation (mean daily *myo*-inositol intake : 0.64 ± 0.5 mg.g^{-1} BW) on fasting mice, as described earlier (see section 3.3, paragraph "Metabolic challenges – Insulin tolerance test ")

Effect of acute oral administration of *myo*-inositol on insulin signaling in liver and gastrocnemius muscle of CD-1 swiss mice

Twenty four old and obese CD-1 Swiss mice (BW (mean ± SEM) : 45.3 ± 1.0 g for control and 46.6 ± 1.3 g for *myo*-inositol mice, n=12, no significant difference at the p<0.05 level) were fasted overnight and randomly assigned to receive either water or *myo*-inositol (1.2 mg.g^{-1} BW) aqueous solution by oral gavage 60 min prior to sacrifice. Half of the mice in each group (control and *myo*-inositol) were also randomly assigned to receive or not an intraperitoneal injection of insulin (0.5 UI.kg^{-1} BW) 30 min after oral gavage and so 30 min prior to sacrifice. Mice were sacrificed by cervical dislocation and gastrocnemius muscles and liver were rapidly dissected out and snap frozen into liquid nitrogen. Organs

100

were stored at -20°C until protein were extracted for western blotting of PKB/Akt. See section 3.3 for immunoblotting procedure.

Cell Culture

C2C12 myoblasts (Mus musculus, reference CRL-1772) and 3T3-L1 (Mus musculus, reference CL-173) were purchased from ATCC (LGC Standard, Molsheim, France). Both C2C12 myoblasts and 3T3-L1 fibroblasts cell lines were maintained at 37°C in an incubator with a 5% (v/v) CO_2 atmosphere and were cultured in high glucose (4.5 $g.L^{-1}$, i.e. 25 mM) Dulbecco's Modified Eagle Medium (DMEM) supplemented with 10% (v/v) heat-deactivated (30 min, 56°C) Fetal Bovine Serum (FBS) (South Africa origin, BioWest, Nuaillé, France), 100 $UI.mL^{-1}$ penicillin, 100 $\mu g.mL^{-1}$ streptomycin and 3 mM L-glutamine.

3T3-L1 adipocytes differentiation. Murine 3T3-L1 fibroblasts were cultured in complete medium in 12-well plates, seeded with about 50 000 cells per well. When fibroblasts reached total confluence (j_{-2} of differentiation), the proliferation medium was replaced by the first differentiation medium, i.e. complete medium (10% FBS) supplemented with insulin (Actrapid®, 5µg/mL), isobutylmetyhylxanthine (IBMX, 0.5 mM), dexamethasone (25 nM) and rosiglitazone (10 µM) for 48 hours. At j_0 of differentiation, the first medium of differentiation was replaced by the second medium of differentiation, i.e. complete medium (10% FBS) supplemented with only insulin (Actrapid®, 5 µg/mL) and rosiglitazone (10 µM) for additional 48 hours (i.e. until j_{+2} of differentiation). At j_{+2} of differentiation, the medium was replaced by complete medium (10% FBS) until the end of the fibroblasts differentiation into adipocytes (j_{+10}-j_{+12}). The degree and quality of differentiation was followed by checking the apparition and growing of intracellular lipid droplets under a light microscope. Adipocytes were used at 10-12 days of differentiation.

C2C12 myotubes differentiation. Myoblast cell line C2C12 was cultured in 12 or 96 well (MTT test) plates seeded with about 25 000 - 30 000 cells per square centimeter. When cells reached about 80-90% confluence (before being at complete confluence), the complete 10% FBS medium was replaced by the differentiation medium (i.e. complete medium with 2% (v/v) Horse serum (South Africa origin, BioWest, Nuaillé, France) instead of 10 % (v/v) FBS). From then, myoblasts start to merge and form tubular structures that can be observed under a light microscope. After about 4-5 days in 2% Horse Serum medium, cells are nearly all differentiated into myotubes and can be used for treatments and experiments.

101

MTT viability test

MTT test principle - MTT test (Cell Proliferation Kit I, Roche) measures cell proliferation, viability and metabolic activity. It is based on the cleavage of MTT (3-[4-5-dimethylthiazol-2-yl]-2,5-diphenyl tetrazolium bromide) salt (yellow), into formazan (purple) by a mitochondrial enzyme. Formazan crystals are insoluble and precipitate inside cells. Crystals are dissolved into a lysis buffer and the purple color intensity can be measured spectrophotometrically and reflects the number of metabolically active (and so living) cells.

MTT test protocol - Cells cultured in 96-well plates were treated overnight in 100 µL of treatment medium without serum (serum starvation) or pretreated 72h in complete medium with or without *myo*-inositol and then serum-starved for 4 hours in 100 µL of medium without serum. 10 µL of MTT were then added to the 100 µL of medium without serum in all cell-seeded wells (plus one or two wells without cell for control of non-survival) and cells were incubated at 37°C for 45 min to 1 hours for myotubes and for 4 hours for myoblasts in proliferation (differentiated and confluent cells are more metabolically active than proliferative undifferentiated cells). Formazan crystals formation in positive control wells (untreated cells) was checked under a light microscope. MTT crystals were then dissolved by addition of 100 µL per well of Lysis buffer and overnight incubation at 37°C. Absorbances of the lysates were read at 550 and 690 nm (reference). Absorbance in each well ($DO_{550} - DO_{690}$) was corrected by the absorbance ($DO_{550} - DO_{690}$) of the negative control well without cells, and viabilities were then expressed in % of viability as compared to the untreated cells.

Treatment tested – a) 72h treatment of C2C12 differentiated into myotubes with or without 0.1, 0.25, 0.5, 0.75 or 1.0 mM *myo*-inositol; b) overnight treatment of C2C12 proliferating myoblasts 24 hours after seeding (8500 – 10000 cells per well) with or without 0.25, 0.5, 1.0, 2.5, 5.0, 7.5 and 10.0 mM *myo*-inositol ; c) 3h30 pre-treatment of C2C12 proliferating myoblasts 24 hours after seeding (8500 – 10000 cells per well) with or without *myo*-inositol 1 mM and then overnight treatment of cells with 0.1, 0.25, 0.50, 0.75, 1.0, 2.5 and 5.0 µM H_2O_2 in serum free medium with or without 1 mM *myo*-inositol.

Immunoblotting – insulin induced phosphorylation of PKB/Akt in C2C12 myotubes

Cell treatments - C2C12 myotubes were pre-treated 72h in 2% Horse Serum medium (high glucose) supplemented or not with *myo*-inositol 1 mM. Cells were then serum starved for 4 hours in serum free medium with or without *myo*-inositol 1 mM and finally stimulated 20 min in serum free medium with or without insulin 100 nM. Reaction was then stopped by replacement of the treatment medium by cold PBS buffer. PBS buffer was then rapidly removed and cells were stored at -20°C until protein were extracted for western blotting.

Protein extraction - Proteins of C2C12 myotubes cultured in 12-well plates were extracted by scraping the cell layer in 150 µL of standard lysis buffer (20 mM Tris-HCl, 138 mM NaCl, 2.7 mM KCl, 1 mM MgCl$_2$, 5% Glycerol and 1% Nonidet P40) supplemented with protease and phosphatase inhibitors (5 mM EDTA, 1 mM Na$_3$VO$_4$, 20 mM NaF, 1 mM DTT, Protein inhibitor cocktail, Sigma Aldrich). Lysates were centrifuged 15 min at 13,000 g, 4°C to discard insoluble material. Lysates protein concentrations were determined with Bradford protein assay.

SDS-PAGE and western blot – 30 µg of tissue lysate soluble fraction proteins were boiled 5 min in Laemmli buffer and separated by 10% sodium dodecyl sulfate – polyacrylamide gel electrophoresis (SDS-PAGE). After transfer to a nitrocellulose membrane, and aspecific sites blockage with Bovine Serum Albumin (BSA) 5% in TBST (10 mM Tris-HCl at pH 8.0, 150 mM NaCl and 0.05 % Tween-20), Akt activating phosphorylation on serine was detected using primary anti-phospho(Ser 473)-Akt(1/2/3) antibody (1/1000^e in TBST 3% BSA – Overnight, 4°C) and then secondary antibody (anti-rabbit, 1/10000^e TBST – 1h, room temperature) conjugated with horseradish peroxidase. Membranes were processed for chemiluminescence and proteins were quantitated by densitometry using Quantity One software (BioRad). In order to normalise for equal protein loading, membranes were stripped and re-blotted with anti-total Akt(1/2/3) antibody and then anti-α-tubulin antibody.

Effect of MI on adipocyte differentiation and/or lipogenic activity

Oil red O staining of lipid droplets. 3T3-L1 pre-adipocytes were incubated from day 2 (j$_{+2}$) to day 10 (j$_{+10}$) of differentiation in 10 % FBS complete medium alone (control, C), or supplemented with 1mM mannitol (osmotic control, Man) or *myo*-inositol (MI), and the mediums were renewed every 2 days. After 10 days of differentiation, cells were washed twice with phosphate buffered saline (PBS) and fixed in 10 % (v/v) formalin for 1 hour at room temperature. Fixed cells were washed three times with deionized water, stained with Oil Red O (60 % (v/v) of Oil Red O dye at 0.6 % (w/v) in isopropanol, 40% (v/v) water) for 20 min at room temperature, washed again three times with deionized water and stained lipid droplets were observed under a light microscope. In order to quantify the lipid droplets, supernatant (water) was removed and the Oil red O staining the lipid droplets was dissolved into isopropanol (1 mL per well). Intensity of the red staining of isopropanol was then measured by spectrophotometry at 520 nm.

Lipogenesis from acetate. After 9 days of differentiation, 3T3-L1 adipocytes were treated 72h with or without *myo*-inositol 1 mM in complete medium. At j$_{+12}$ of differentiation, adipocytes were incubated with 1 µCi of [^{14}C]-acetate for 3h at 37°C. Neutral lipids were extracted using Dole's extraction fluid (isopropanol/heptane/H$_2$SO$_4$ 1N, 40/10/1, v/v/v) and [^{14}C] was detected by liquid scintillation counting. Results were normalized to protein concentration quantified by Bradford assay.

3.6 Statistical analysis

Data are expressed as means ± SD (n<4) or means ± SEM (n≥4). Data were analyzed using GraphPad Prism v5.0 software (GraphPad software, La Jolla, USA) and Statview 4.5 (Abacus concept, Berkeley, USA). Multiple comparisons were performed using ANOVA followed when appropriate by posthoc Fisher PLSD tests. Results of GTT, ITT and arginine tests were compared by two-way analysis of variance (time, treatment). Simple comparisons were performed using Student's *t*-test. When appropriate, Welch's correction for inequality of variances was applied. Regression analyses were performed using linear regression. Adipocyte volume distribution curves were compared with the Kolmogorov-Smirnov two-sample test using "R" software (www.R-project.org). Differences were considered significant at the p<0.05 level. Survival curves (Kaplan Meier curve) were analysed using Gompertz software as previously described (Doubal & Klemera 1997; Klemera & Doubal 2000).

Chapter 4 - Results

4.1 Chronic *myo*-inositol treatment improves insulin sensitivity and reduces fat accretion in mice

Chronic treatment with myo-inositol reduced white adipose tissue accretion

To evaluate its *in vivo* activity, mice received daily injections of *myo*-inositol (1.2 mg.g^{-1} per day) or saline for 15 days. Biometric data for each group are shown in **Table 5**.

Table 5
Biometric data and tissue weights in control and *myo*-inositol mice (1.2 mg.g^{-1} per day, intraperitonal injection).

	control	*myo*-inositol	change	p-value
Biometric data				
BW, g	31.7 ± 0.7	31.8 ± 1.0	0%	0.963
Body length, cm	10 ± 0.1	10.3 ± 0.1	+3%	0.362
Lee index	316 ± 3	308 ± 2	-3%	0.023*
Organ weights				
Liver, mg/10 g BW	394 ± 24	403 ± 14	+2%	0.749
Heart, mg/10 g BW	49 ± 2	46 ± 1	-6%	0.416
Kidneys, mg/10 g BW	114 ± 4	120 ± 2	+5%	0.193
Gastrocnemius, mg/10 g BW	43 ± 3	45 ± 2	+5%	0.589
Tibialis, mg/10 g BW	18 ± 1	19 ± 1	+5%	0.605
White Adipose tissue weights				
pWAT, mg/10g BW	259 ± 19	160 ± 23	-38%	0.003***
rWAT, mg/10g BW	37 ± 4	23 ± 5	-38%	0.02*
scWAT, mg/10g BW	95 ± 14	77 ± 7	-19%	0.269
total WAT, mg/10g BW	391 ± 15	260 ± 37	-33%	0.003***

Data are mean ± SEM for n=14 in each group. Data were compared using Student t test and when appropriated Welch correction for variance inhomogeneity. Differences were considered significant at the p<0.05 level. Abbreviations: BW, body weight ; WAT, white adipose tissue ; pWAT, parametrial WAT ; rWAT, retroperitoneal WAT ; scWAT, subcutaneous WAT.

Body weights of *myo*-inositol-treated animals were not significantly altered compared with saline-treated animals. Neither food intake nor water intake were different between saline- and *myo*-inositol-

treated animals. The mean daily food intake was 48.1 ± 0.9 and 50.5 ± 3.8 kJ.24h^{-1} for mice treated with saline and *myo*-inositol, respectively (n=14, p=0.573). Organs (liver, heart, kidneys and muscles) weights, taken as representative of lean mass, were not different between the two groups but *myo*-inositol treatment significantly reduced adiposity as evidenced by a lower adiposity index (Lee index n=14, p<0.05) and a significantly reduced fat mass accretion (-33%, n=14, p<0.005). *myo*-Inositol treatment significantly reduced accretion of intra-abdominal fat pad, that is, retroperitoneal and parametrial fat pads while no effect was noticed on sub-cutaneous fat pad, that is, inguinal fat pad (**Table 5**). Indeed, parametrial and retroperitoneal WAT masses were reduced by 38% in *myo*-inositol treated animals, while subcutaneous WAT mass remained unaltered. Of note, the fat mass loss was not associated with ectopic redistribution of lipids in liver or skeletal muscles as evidenced by the measurement of tissues lipid contents (**Table 6**).

Table 6
Tissue lipid content in control and *myo*-inositol mice.

	control	*myo*-inositol	change	p-value
Liver lipids, mg/g	47.8 ± 3.0	46.9 ± 3.5	-2%	0.852
Muscle lipids, mg/g	9.3 ± 2.4	9.0 ± 1.9	-3%	0.935

Data are mean ± SEM for n=10-12 in each group. Data were compared using Student t test and when appropriated Welch correction for variance inhomogeneity. No Difference was significant at the p<0.05 level.

Effect of chronic treatment with myo-inositol on plasma metabolites

The plasma metabolites levels for each group are shown in **Table 7**. The plasma levels of triacylglycerols or total cholesterol were not affected by *myo*-inositol treatment. However, plasma level of non-esterified fatty acids was sharply reduced in *myo*-inositol mice (-37%, n=14-16, p<0.001). Fasting blood glucose level was not significantly different between the two groups (n=14, p=0.41) while fed plasma glucose level of *myo*-inositol mice was significantly lower than that of control mice (-10%, n=14, p<0.05). The homeostasis model assessment of insulin resistance (HOMA-IR) was calculated as a clinical parameter for the insulin resistance, from the values of blood glucose and insulin plasma levels. The HOMA-IR index for *myo*-inositol group was similar to that of control group (n=6, p=0.89). In good agreement with the reduction of fat accretion observed in *myo*-inositol mice, we noticed a significant decrease in plasma leptin concentration (-63%, n=9–10, p<0.05). Plasma leptin concentration was negatively correlated with total white adipose tissue mass (n=19, r^2=0.741, p<0.0001, **see Fig. 26**). In contrast, no difference in plasma adiponectin level was noticed between the two groups (**Table 7**).

Table 7

Plasma and tissue analysis in control and *myo*-inositol mice.

	control	*myo*-inositol	change	p-value
Plasma glucose				
Fed glucose, mM	7.34 ± 0.26	6.61 ± 0.2	-10%	0.031*
Fasted glucose, mM	4.33 ± 0.28	4.61 ± 0.18	+6%	0.713
Fasted insulin, pM	257.7 ± 22.15	227.8 ± 23.2	-11%	0.996
HOMA-IR	1.70 ± 0.15	1.74 ± 0.19	+2%	0.895
Plasma adipokins				
Leptin, ng/ml	13.7 ± 3.1	5.1 ± 1.4	-63%	0.02*
Adiponectin, µg/ml	24.5 ± 1.0	25.9 ± 1.6	+6%	0.457
Plasma lipids				
Triacylglycerols, mM	1.31 ± 0.17	1.19 ± 0.15	-10%	0.349
NEFA, mM	0.54 ± 0.02	0.34 ± 0.01	-37%	<0.001***
Total cholesterol, mM	3.81 ± 0.34	3.26 ± 0.27	-16%	0.293

Data are mean ± SEM for n=10-12 in each group. Data were compared using Student t test and when appropriated Welch correction for variance inhomogeneity Differences were considered significant at the p<0.05 level. Abbreviations: HOMA-IR, homeostasis model assessment of insulin-resistance, NEFA, non-esterified fatty acids.
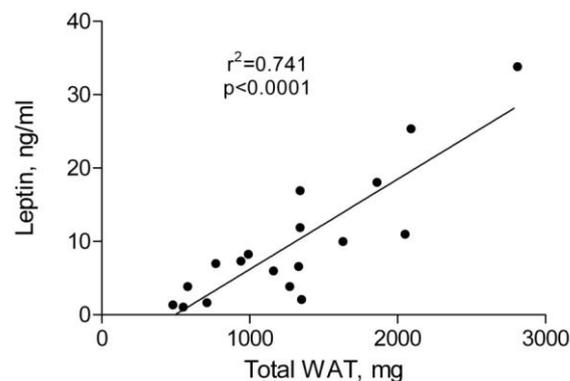
Figure 26 - Plasma leptin concentration is correlated with white adipose tissue (WAT) mass in control and *myo*-inositol treated mice (n= 19).

Chronic treatment with myo-inositol improved glucose tolerance and insulin sensitivity

To get an insight into glucose homeostasis, glucose, insulin and arginine challenges were performed in *myo*-inositol and saline-treated mice. Glucose tolerance test showed that the glucose load induced a marked and transient rise in blood glucose level with a complete normalisation 90 min after injection (**Fig. 27A**). Under the same conditions, *myo*-inositol mice exhibited a lower blood glucose level than control mice at 15 and 30 min after glucose injection (n=10, p<0.05 and p<0.001, respectively), suggesting a better glucose tolerance. Consequently, the area under the curve of glycaemia was significantly lower in the *myo*-inositol mice (11660 ± 329 mg.dl^{-1}.min^{-1}) compared to control mice (14420 ± 873 mg.dl^{-1}.min^{-1}) indicating a faster glucose disposal (n=10, p<0.05). The better glucose tolerance may be attributed to either increased peripheral insulin sensitivity, an improved glucose-stimulated insulin secretion or both.To determine whether the observed glucose tolerance was the result of greater insulin secretion, insulin was assayed during the glucose tolerance test. Baseline plasma insulin levels were not different, but insulin secretion in response to hyperglycaemia (i.e. 30 min after glucose injection) was significantly lower for the *myo*-inositol group (**Fig. 27B**, n=5, p<0.005) suggesting a better insulin
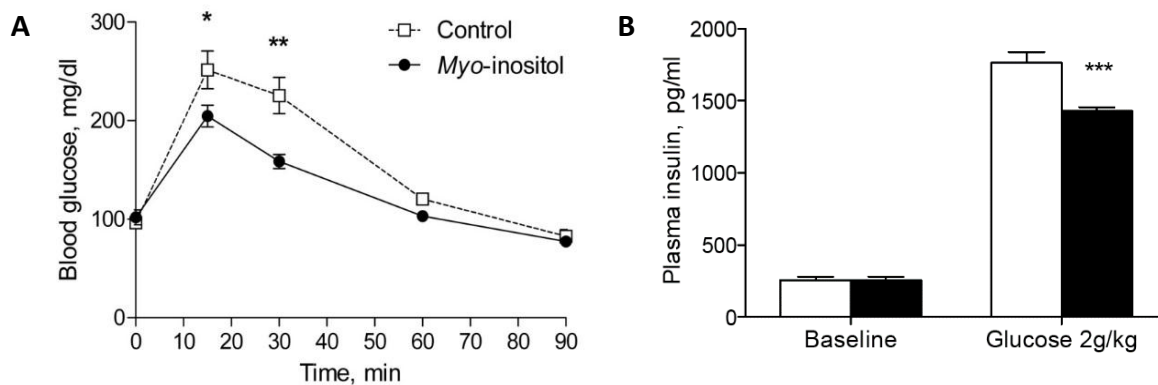
sensitivity rather than a greater insulin secretion.

Figure 27 – *myo*-inositol improves mice glucose tolerance. Glucose tolerance was explored using glucose tolerance test (GTT). **A** – Blood glucose level evolution after intraperitoneal administration of glucose (1g.kg^{-1} i.p) to fasting mice (n=10). **B**. Insulin plasma level at the hyperglycaemic phase (30 min after i.p. glucose injection) of the ipGTT (n=5).

To further measure the *in vivo* insulin response of *myo*-inositol treated mice, we performed administration of the non-glucose secretagogue arginine. The acute insulin response (2 min after arginine injection) was similar in the two groups (**Fig. 28**) excluding difference in insulin secretion capacity.
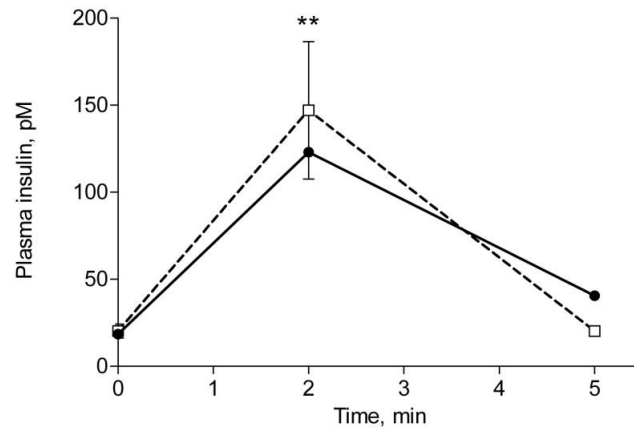
Figure 28 – *myo*-inositol does not influence insulin secretion. Plasma insulin concentration was measured after intraperitoneal administration of a non-glucose insulin secretagogue (Arginine, 1 g.kg^{-1}) (n=5). **, p<0.005, difference from baseline level. Note that no difference was found to be significant between the 2 groups at p<0.05 level.

The results of the insulin tolerance test (ITT) are shown in **Fig. 29**. Insulin administration (0.3 UI.kg^{-1}) triggered a significantly (p<0.01) larger hypoglycaemic response in *myo*-inositol mice (-45% in blood glucose level) compared to control mice (-25%). The glucose disappearance rate (K$_{ITT}$) was two-fold higher in *myo*-inositol than in control mice (10.3 ± 1.2 *versus* 5.8 ± 1.6 %.min^{-1}, n=7-9, p<0.05). Taken together, the results of the metabolic challenges indicated a better glucose tolerance due to a better insulin sensitivity of *myo*-inositol treated mice.
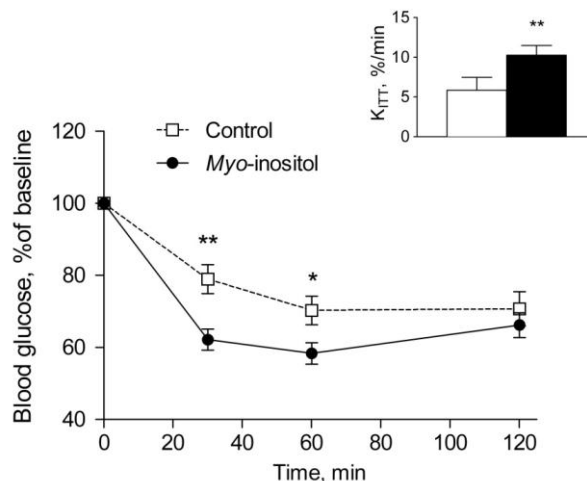
Figure 29 – *myo*-inositol improves insulin sensitivity. Insulin sensitivity was explored using insulin tolerance test. Blood glucose level was measured after intraperitoneal injection of insulin (0.3 UI.kg^{-1}) to fasting mice. **Insert** – Plasmatic Glucose disappearance rate (K$_{ITT}$) during the insulin tolerance test. Results are expressed as mean ± SEM for n=7-9 mice in each group. *p<0.05, **p<0.01, significant difference between saline and *myo*-inositol treated mice.

109

Interestingly, the glucose disappearance rate (K_{ITT}) that reflects insulin sensitivity, was negatively correlated with central fat mass (**Fig. 30**, r=-0.718, p<0.002). Hence, the reduction in fat mass accretion could be a major determinant of the long-term insulin-sensitizing effect of *myo*-inositol treatment.

Figure 30 – Insulin sensitivity is negatively correlated with central white adipose tissue mass. n=16. Central WAT was calculated as the sum of the intra-abdominal WAT pad weights, namely retroperitoneal and parametrial fat pads.

Chronic treatment with myo-inositol potentiated insulin signaling in skeletal muscle

To get an insight into the molecular mechanisms underlying MI insulin-sensitizing effect, phosphorylation of PKB/Akt (a key protein in insulin signal transduction) was explored in skeletal muscle after *in vivo* insulin stimulation. Results from immunoblotting (**Fig. 31A**) showed a twofold increase in phosphorylation level of PKB/Akt in the gastrocnemius muscle of control mice in response to insulin (+66%, p<0.05). *myo*-Inositol treatment increased PKB/Akt phosphorylation under baseline conditions (+66% from unstimulated control, p<0.05) as well as in response to insulin (+166% from unstimulated control, p<0.05) suggesting an additive effect of insulin and *myo*-inositol. Some authors (Larner et al. 2010; Dang et al. 2010) suggested that *in vivo*, *myo*-inositol is metabolically converted into other inositol isomers (especially *D-chiro*-inositol) which could mediate its effects on glucose metabolism. To challenge this view, mouse isolated gastrocnemius were incubated in presence of 1 mM of *myo*-inositol, *D-chiro*-inositol or mannitol (as an osmotic control) with or without insulin (100 nM). *myo*-Inositol but not *D-chiro*-inositol potentiated insulin induced PKB/Akt phosphorylation on Serine 473 in baseline as well as insulin-stimulated conditions (**Fig. 31B**) suggesting a direct action of *myo*-inositol on muscle or its conversion *in situ* to an active metabolite.

110

A

B

Figure 31 – *myo*-Inositol potentiated insulin signaling in skeletal muscle. A- Immunoblotting study of *in vivo* insulin induced phosphorylation of PKB/Akt in gatrocnemius muscle of mice daily treated with *myo*-inositol or saline. **B-** *myo*-Inositol potentiated insulin signaling in skeletal muscle *ex vivo*. Immunoblotting study of *ex vivo* insulin induced phosphorylation of PKB/Akt in gatrocnemius muscle. Mouse gastrocnemius muscle were incubated for 15 min with 1 mM *myo*-inositol, *D-chiro*–inositol or mannitol as a control and stimulated with insulin (100 nM, 15 min). Note that *myo*-inositol but not *D-chiro*-inositol potentiated insulin induced serine- phosphorylation of PKB/Akt. Results are expressed as mean ± SD for n=3-5 mice in each group. Different letters indicate a significant difference at the p<0.05 level.

myo-Inositol is active when orally administered

To test whether *myo*-inositol was active when given *per os (p.o.)*, mice were given *myo*-inositol in drinking water rather than through intraperitoneal (*i.p.*) injections. We therefore tested the effect of 15 days of oral administration of *myo*-inositol on fat accretion in mice (**Table 8**). The mean daily intake of *myo*-inositol was **0.90 ± 0.04 mg.g^{-1}** per day. Oral administration of *myo*-inositol decreased fat accretion to the same extent than intraperitoneal administration (-38%, **Table 8**) and in both intra-peritoneal and sub-cutaneous fat depots (See **Fig. 32A**). The 2-way ANOVA indicated a main effect of treatment (p<0.05), a main effect of WAT site (p<0.001), as well as a treatment × WAT site interaction (p<0.05). Indeed, parametrial WAT, retroperitoneal WAT and subcutaneous WAT weights were decreased by 34% (p<0.05), 33% (p<0.05) and 47% (p<0.01), respectively in *myo*-inositol animals while no difference was noticed for muscle or organ weights. Dietary *myo*-inositol supplement (0.9 mg.g^{-1} per day) significantly reduced fat accretion in mice showing that *myo*-inositol was active after oral administration (**Fig. 32A**). *myo*-Inositol treated mice (*p.o.* or *i.p*. administration) exhibited a lower white adipose tissue accretion relative to their body mass than control mice (**Fig. 32B**). Indeed, the slope of the linear regression of fat accretion in control mice was (226.2 ± 36.6 mg WAT/g BW, r^2=0.65) while it was (128.6 ± 30.5 mg

WAT/g BW, r^2=0.45) in *myo*-inositol treated mice (significant difference between the slopes, p=0.04, n=24 in each group).

Table 8
Biometric data and organ weights in mice fed for 15 days with *myo*-inositol (0.9 mg.kg^{-1} per day).

	control	*myo*-inositol	change	p-value
Bometric data				
BW, g	37.6 ± 1.2	34.9 ± 1.4	-7%	0.157
Body length, cm	10.6 ± 0.1	10.4 ± 0.2	-2%	0.279
Lee index	316 ± 3	314 ± 4	-1%	0.646
Organ weights				
Liver, mg/10g BW	422 ± 10	437 ± 13	+4%	0.413
Heart, mg/10g BW	45 ± 2	46 ± 1	+2%	0.496
Kidneys, mg/10g BW	114 ± 3	119 ± 5	+4%	0.373
Gastrocnemius, mg/10g BW	41 ± 2	44 ± 2	+7%	0.440
Tibialis, mg/10g BW	20 ± 1	20 ± 1	0%	0.992
Adipose tissue weights				
Total WAT, mg/10g BW	724 ± 70	447 ± 74	-38%	0.014*

Data are mean ± SEM for n=10 in each group. Data were compared using Student t test and when appropriate Welch correction for variance inhomogeneity. Differences were considered significant at the p<0.05 level. Abbreviations: BW, body weight, WAT white adipose tissue, pWAT, parametrial WAT, rWAT, retroperitoneal WAT, scWAT, subcutaneous WAT.
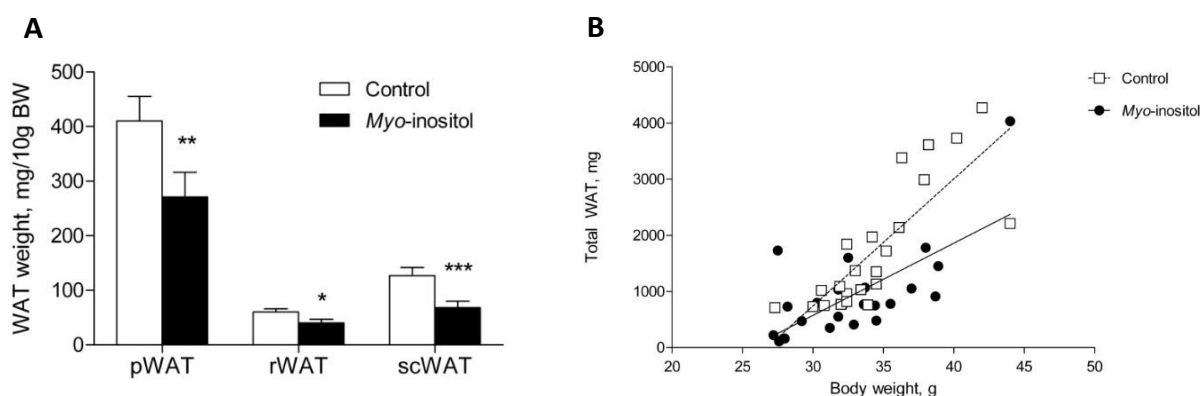
Figure 32 – *myo*-inositol reduces fat accretion when given orally. A- Respective weights of WAT depots for *myo*-inositol and control mice. Results are expressed as mean ± SEM for n=10 mice per group. ** p<0.01 and *** p<0.005. **B-** Total WAT mass relative to the body weight in *myo*-inositol and control mice.

To analyse whether changes in WAT accretion resulted from a reduction in the number of adipocytes, a decreased triglyceride accumulation in adipocytes or both, we performed a cytological analysis of parametrial WAT pad. The distribution frequencies of adipocyte volume for saline or *myo*-inositol treated mice are shown in **Fig. 33A,B**. A significant shift leftward was observed in frequency distribution of adipocyte volumes of mice treated with *myo*-inositol compared with control animals.
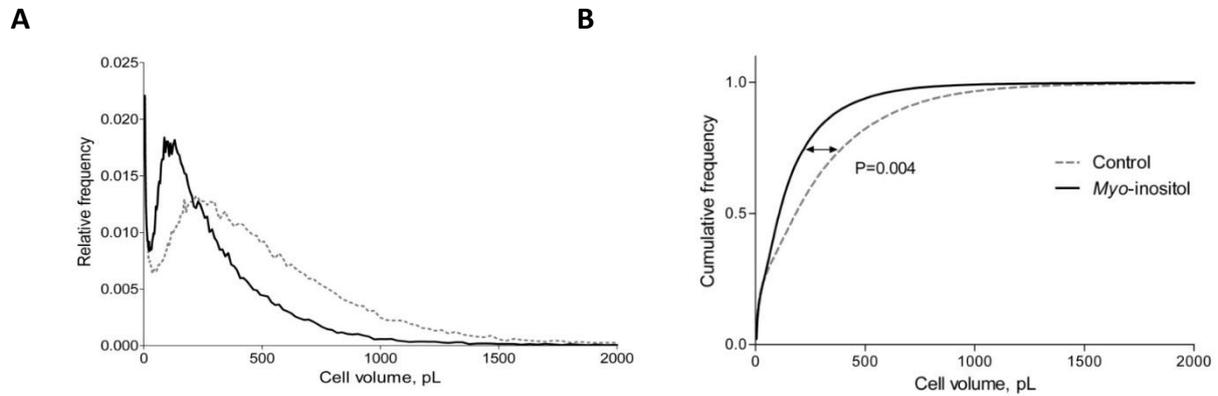
Figure 33 – The reduced fat accretion in *myo*-inositol mice is related to a diminution in adipocyte size. Adipocytes volume frequency distribution (**A**) and cumulative frequency distribution (**B**). Individual measurements were performed on 12-14,000 adipocytes using osmium tetroxide - coulter counter procedure as described in Methods. Frequency distribution of adipocytes volumes for control (dotted line) and *myo*-inositol (solid line) treated animals. Note that distribution of adipocyte volume was shifted leftward (i.e. towards smaller volumes) in *myo*-inositol mice. In each group, adipocytes were pooled from 8-10 mice.

The cellular characteristics of parametrial WAT in control and *myo*-inositol-fed mice are shown in **Table 9**.

Table 9
Cellularity of parametrial white adipose tissue in mice fed with *myo*-inositol (0.9 mg.kg^{-1} per day) for 15 days

	control	*myo*-inositol	change	p-value
pWAT, mg	830 ± 48	549 ± 81	-34%	0.015*
Cell diameter, μm	69.0 ± 2.0	59.8 ± 3.0	-13%	0.02*
Cell weight, ng	176.3 ± 15.6	117.8 ± 19.0	-33%	0.03*
Nb cells, x10^6	5.21 ± 0.62	5.29 ± 1.23	+2%	0.950
DNA content μg/pad	63.0 ± 13.0	53.4 ± 10.1	-15%	0.568

Data are mean ± SEM for n=9-10 in each group. Data were compared using Student t test and when appropriate Welch's correction for variance inhomogeneity. Differences were considered significant at the p<0.05 level. Abbreviation: pWAT parametrial white adipose tissue.

The reduction of WAT accretion resulted from a reduction in the volume of adipocytes (*i.e.* hypotrophia) (see **Fig. 34**) rather than from a decrease in the total number of adipocytes per fat pad (*i.e.* hypoplasia).
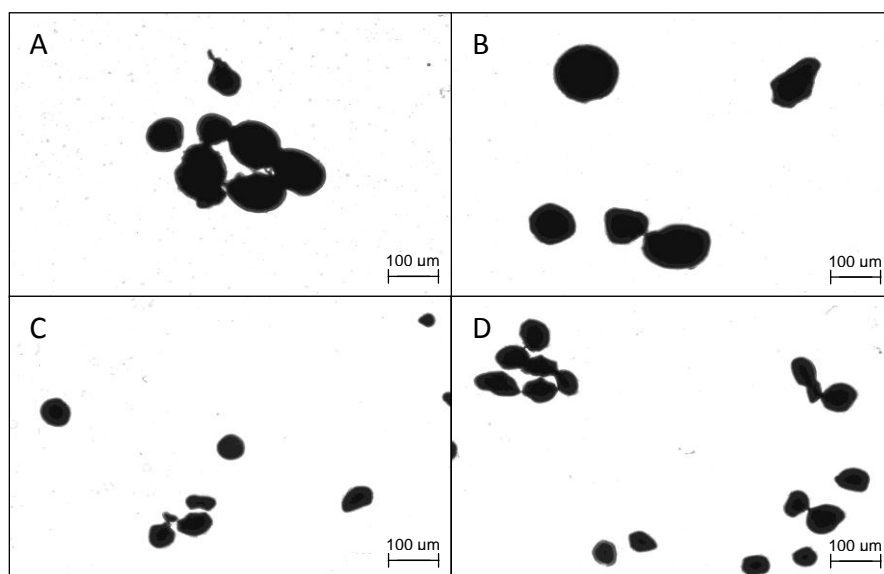
Figure 34 – Typical pictures of osmium tetroxide-fixed adipocytes from saline (A,B) or *myo*-inositol treated mice (C,D). Adipocytes were isolated from epididymal fat pad as described in Methods. (× 100). Note that adipocytes from *myo*-inositol mice were smaller than those from control mice.

Indeed, mean adipocyte diameter was reduced by 13% in *myo*-inositol treated mice (n=9–10, p<0.05) resulting in a 33% decrease in adipose cell volume (n=8–10, p<0.01). The total number of adipocytes per parametrial fat pad, calculated from cell weight, failed to show any difference in the total number of adipocytes between *myo*-inositol and control mice. As DNA amount reflects adipose cell number more accurately than any other method, we performed DNA assay in parametrial WAT. No difference was observed in DNA content, excluding a decrease in the total number of adipocytes in pWAT pads.

To get an insight into the mechanisms of *myo*-inositol action on adipose cells, we measured both the lipolytic response to catecholamines and *de novo* lipogenesis. To this end, mice were fed for 15 days with *myo*-inositol in drinking water (6 g.L^{-1}) and lipogenesis and lipolytic activities were measured on adipocytes isolated from parametrial fat pad of control and *myo*-inositol fed mice (**Fig. 35**). No significant difference in baseline or isoproterenol stimulated lipolytic activity was observed between the two groups (**Fig. 35A**). Lipogenesis from ^{14}C-acetate however was significantly reduced in isolated adipocytes from *myo*-inositol supplemented mice compared to control mice (118.5 ± 14.8 CPM.mg^{-1} lipids for *myo*-inositol fed mice *versus* 248.8 ± 35.5 CPM.mg^{-1} lipids for control mice, **p=0.0095) (**Fig. 35B**).
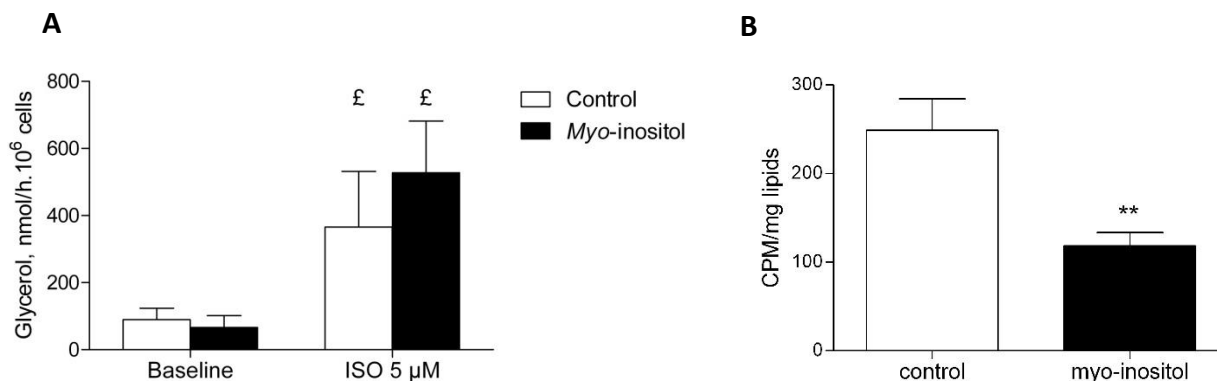
Figure 35 – *myo*-Inositol effect on lipolysis or lipogenesis of isolated adipocytes. A- Lipolysis and **B** - lipogenesis measured on isolated adipocytes from control or *myo*-inositol (0.9 mg.g^{-1}, 15 days) supplemented mice (data are mean ± SEM for n=5). Lipolysis data were analysed with 1-way ANOVA and £ indicate significant difference at the $p<0.05$ level between baseline and isoproterenol stimulated condition. Lipogenesis data were analysed with student t-test, **$p<0.01$. Abbreviation: ISO, isoproterenol.

Mice treated with myo-inositol exhibited a better resistance to oxidative stress

Repeated (chronic) intraperitoneal administrations of low levels of paraquat lead to mortality within few days. The survival time of *myo*-inositol-treated mice was longer than saline treated mice (**Fig. 36A**) as indicated by a median survival time of 2.5 and 4.0 days for saline and *myo*-inositol treated mice, respectively (Log-rank - Mantel-Cox Test, $p<0.05$). The survival curves for both *myo*-inositol and saline animals adhered closely to the Gompertz survival function, with regression coefficients $r^2 = 0.963$ and 0.967 for *myo*-inositol and saline mice, respectively. The Gompertz parameter R_0 ("age-independent" mortality rate) was similar in both groups. However, parameter K ("age-dependent" mortality rate) was higher in saline mice than in *myo*-inositol treated animals. Parameter K can be interpreted as the rate of aging, or a measure of the increase in mortality rate with passing time, in this case, duration of the exposure to paraquat. Thus, the decrease in parameter K in *myo*-inositol mice indicated a better resistance to oxidative damages. In good agreement, the *myo*-inositol treated mice exhibited higher total antioxidant plasma activity than control mice (0.72 ± 0.04 versus 0.49 ± 0.03 mM equivalent of uric acid, +46%, n=9-10, $p<0.005$, **Fig. 36B**).

115
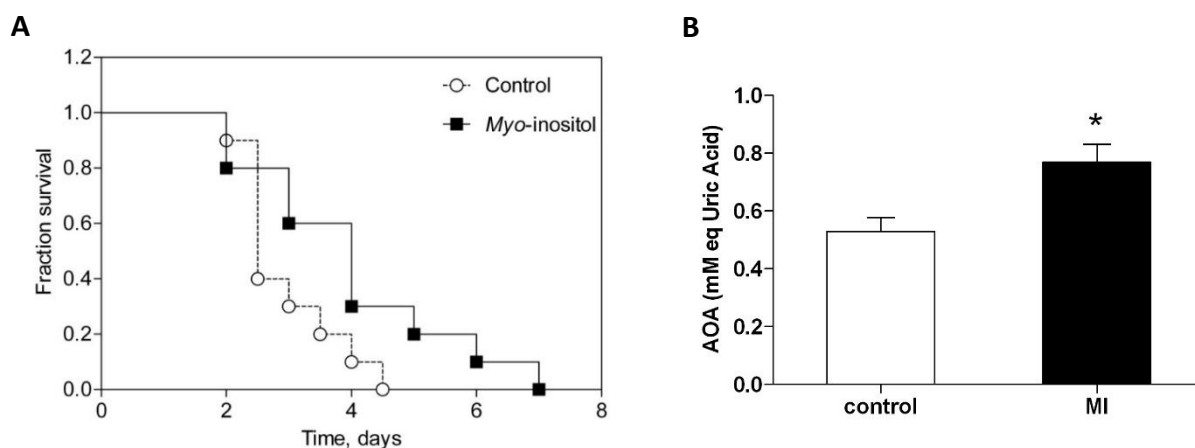
Figure 36 – Chronic treatment with *myo*-inositol (1.2 mg.g^{-1} per day) increased resistance to oxidative stress. A- Survival of mice exposed to paraquat. Control (dashed step curve) and *myo*-inositol (solid step curve) treated mice were injected intraperitoneally with 15 mg paraquat per kg body weight once a day, n=10 mice per group. **B-** Plasma antioxidant activity in saline *myo*-inositol treated mice. Results are expressed as mean ± SEM for n=10 mice per group.

myo-Inositol is not a ROS scavenger/anti-oxydant by itself

In order to test the anti-oxydant/ROS scavenging power of high concentrations of *myo*-inositol, we measured the anti-oxidant activity of a concentration range of *myo*-inositol solutions.
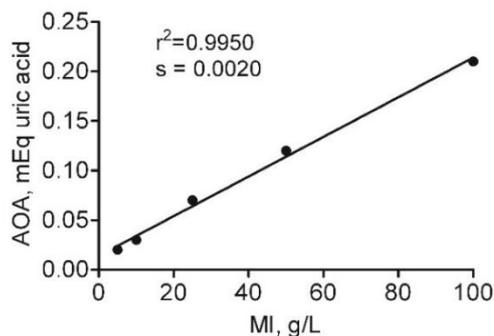
Figure 37 – *myo*-inositol aqueous solution did not have significant anti-oxydant activity compared to a uric acid solution.

AOA of *myo*-inositol aqueous solutions was greatly correlated with *myo*-inositol concentration (r^2=0.9950) and the slope was significantly different from zero (p=0.0001)(**Fig. 37**). However, the slope is very weak and even the highest concentration of *myo*-inositol (100g.L^{-1}, i.e. 0.55 mol.L^{-1}) has a very little AOA compared to uric acid (0.21 mEq uric acid). In conclusion, as expected by its chemical structure, *myo*-inositol molecule is not anti-oxydant and cannot quench ROS by itself, even in very high dosages. Hence, *myo*-inositol protection against paraquat induced ROS damages is more probably related to an induction of anti-oxydant enzymes (e.g. SOD, catalase, GPx, GST) and/or to an elevation in endogenous antioxydant substances.

Plasmalogen content of Red Blood cells

Some studies (Pettegrew et al. 2001; Hoffman-Kuczynski & Reo 2005; Maeba et al. 2008) suggest that a chronic *myo*-inositol treatment would enrich cell membranes in plasmalogens, a phospholipid sub-class that possesses a vinyl-ether linkage in position sn-1 of the glycerol backbone, instead of an ester linkage. The double bound of the vinyl-ether linkage could react with reactive species and quench them, making plasmalogens potent endogenous anti-oxidants. Plasmalogens are essentially present in cell membranes as plasmenylethanolamine. We then quantified plasmalogens content of the phosphatidylethanolamine pool in red blood cells of mice treated 15 days with *myo*-inositol 1.2 mg.g^{-1} (intraperitoneal administration) (**Table 10**) to test whether a plasmalogen membrane enrichment could mediate *myo*-inositol effect on mice survival to paraquat toxicity.

Table 10
Red Blood Cells (RBC) phosphatidyl-ethanolamine composition in FAME and DMA of mice treated or not with *myo*-inositol 1.2 mg.g^{-1} for 15 days.

	FAME and DMA composition of phosphatidyl-ethanolamine pool (molar %),		change	p-value
	control	***myo*-inositol**		
16: 0-DMA	4,68 ± 0,39	4,18 ± 0,28	-10,7%	0,32
16:0	8,21 ± 0,97	6,91 ± 0,43	-15,9%	0,25
16:1 n-7	0,24 ± 0,11	ND		
18:0-DMA	2,39 ± 0,05	2,42 ± 0,19	1,1%	0,90
18:1 n-9-DMA	1,28 ± 0,07	1,21 ± 0,06	-5,3%	0,52
18:0	7,96 ± 0,39	8,07 ± 0,43	1,4%	0,85
18:1 n-9	19,88 ± 0,49	20,17 ± 0,66	1,5%	0,73
18:2 n-6	7,54 ± 0,34	7,08 ± 0,31	-6,1%	0,34
20:1 n-9	0,44 ± 0,03	0,08 ± 0,08	-82,3%	0,02
20:3 n-6	1,48 ± 0,06	1,46 ± 0,09	-1,4%	0,86
20:4 n-6	31,22 ± 0,89	32,72 ± 0,34	4,8%	0,15
24:0	4,93 ± 0,27	5,02 ± 0,17	1,7%	0,80
22:5 n-3	1,01 ± 0,05	1,09 ± 0,03	8,3%	0,17
22:6 n-3	9,17 ± 0,50	9,60 ± 0,26	4,7%	0,46
Total	100,00 ± 0,00	100,00 ± 0,00		
% Plsm-Et	8,35 ± 0,51	7,81 ± 0,54	-15%	0,67
16:0 DMA/16:0	0,59 ± 0,03	0,61 ± 0,02	3,6%	0,59
18:0 DMA/18:0	0,30 ± 0,02	0,31 ± 0,03	0,1%	0,99

Data are expressed as mean ± SEM, n=6 mice per group. Data were analyzed by student t-tests with welch correction when necessary and differences were considered significant at the p<0.05 level. Abbreviations: DMA, dimethylacetal ; FAME, Fatty Acid Methyl Ester ; Plsm-Et, plasmenyl-ethanolamine (plasmalogen with an ethanolamine head group) ; ND, not detected.

However, we found no significant difference between control and *myo*-inositol treated mice concerning the plasmalogen content of their red blood cells, neither for the total percentage of plasmalogens in PE (8.35 ± 0.51 % for saline versus 7.84 ± 0.54 for *myo*-inositol mice, p=0.67), nor for the fraction of DMA among the 16:0 or 18:0 fatty acids (FAME plus DMA).

4.2 Dietary *myo*-inositol supplement did not prevent insulin resistance or obesity development in mice fed a high fat diet, but improved insulin sensitivity and reduced fat deposition

***myo*-Inositol dietary supplementation reduced fat accretion but did not prevent obesity development under HFD.**

To evaluate *myo*-inositol capacity to reduce fat accumulation under obesogenic diet, mice were fed a high fat diet (60% calories from fat) with or without a *myo*-inositol dietary supplement (0.58 ± 0.2 mg.g^{-1} BW per 24h) for four months. Body weight, calorie intake and *myo*-inositol intake were monitored throughout the study (See **Fig. 38**). Note that no difference of body growth, daily or cumulative energy intake were observed between HF and HF-MI groups throughout the study period, but significantly higher values were observed for this parameters in high fat diet groups compared to control group as early as two weeks of diet for BW. Indeed, the mean daily calorie intake was of 53.9 ± 0.8 kJ/day for HF mice, 54.0 ± 0.9 kJ/day for HF-MI mice *versus* 46.0 ± 1.5 kJ/day for chow diet fed mice, n=29-30, p<0.05). After four months of diet with or without supplement, each mice had taken about 5548.7 kJ for HF mice and 5528.0 kJ plus 44 kJ from MI supplement for HF-MI mice, versus 4651.7 kJ for control mice. Finally, the mean body weights of mice after 4 months of diet were of 32.0 ± 0.6, 46.6 ± 0.9 and 45.8 ± 1.2 g for C, HF and HF-MI mice respectively (See **Fig. 38** and **Table 11**).
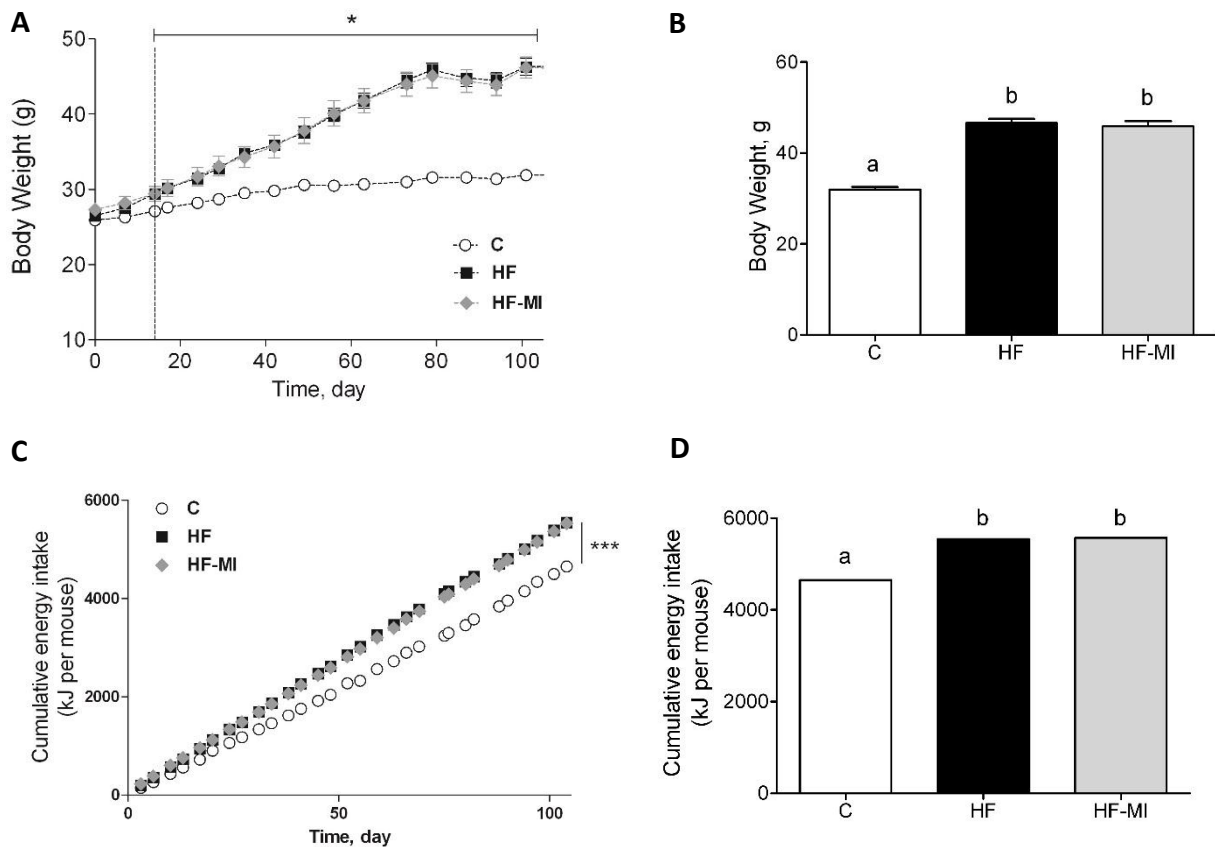
Figure 38 – Body weight and energy intake monitoring throughout the study. A) Body weight evolution, **B)** mean body weights at sacrifice, **C)** cumulative energy intake evolution and **D)** cumulative energy intake mean value at sacrifice of mice fed a chow (C) or high fat diet with (HF-MI) or without (HF) a dietary *myo*-inositol supplement (0.58 mg.g^{-1} BW) for four months. Results are expressed as mean ± SEM for n=10 mice per group.

Biometric data for each group after 4 months of diet are presented in **Table 11**. Body lengths were unaltered between the three groups while body weights, and so the Lee indexes, of high fat fed animals were markedly increased compared with chow diet fed animals (BW of 46.6 ± 0.9 g for HF group and 45.8 ± 1.2 g for HF-MI group *versus* 32.0 ± 0.6 g for control group, p<0.0001). No significant difference was found however between the two high fat groups (HF and HF-MI). Organs (liver, heart, kidneys and muscles) weights, taken as representative of lean mass, were not significantly different between the three groups with exception of kidneys that were bigger in high fat groups (significant difference for HF-MI group). High fat diet sharply increased fat storage (total WAT weight four to five folds higher in HF compared to Control group: 6330 ± 254 versus 1405 ± 138 mg, p<0.0001) and *myo*-inositol supplement significantly restrained this fat accumulation in WAT (5255 ± 331 mg, i.e. a reduction of about 17% in the total WAT weight compared to HF group without MI, p<0.01). This difference between HF and HF-MI groups was statistically significant for the retroperitoneal and subcutaneous fat pads.

119

Table 11
Biometric data and organ weights in C57Bl/6JRj mice fed a high fat (HF) diet and supplemented with *myo*-inositol (0.58 mg.g^{-1} BW).

	C	HF	HF-MI	p-value
Biometric data				
BW, g	32.0 ± 0.6[a]	46.6 ± 0.9[b]	45.8 ± 1.2[b]	<0.0001
Body length, cm	9.7 ± 0.1[a]	10.1 ± 0.1[a]	10.2 ± 0.1[a]	<0.0001
Lee index, x10^3	327 ± 2[a]	355 ± 2[b]	351 ± 3[b]	<0.0001
Organ weights				
Liver, mg	1397 ± 84	1735 ± 145	1641 ± 107	0.122
Heart, mg	147 ± 5	150 ± 5	156 ± 8	0.556
Kidneys, mg	372 ± 14[a]	414 ± 13[a]	460 ± 25[b]	0.006
Gastrocnemius, mg	153 ± 5[a]	165 ± 2[a]	172 ± 5[b]	0.017
Adipose tissue weight				
Total WAT, mg	1405 ± 138[a]	6330 ± 254[b]	5239 ± 323[c]	<0.0001

Data are mean ± SEM for n=10 in each group. Data were compared using 1-way ANOVA and when appropriated PLSD Fischer post hoc tests. Difference where considered significant at the p<0.05 level and different letters indicate significant differences between groups (p<0.01). Abbreviations: BW, body weight, WAT white adipose tissue, eWAT, epididymal WAT, rWAT, retroperitoneal WAT, scWAT, subcutaneous WAT.
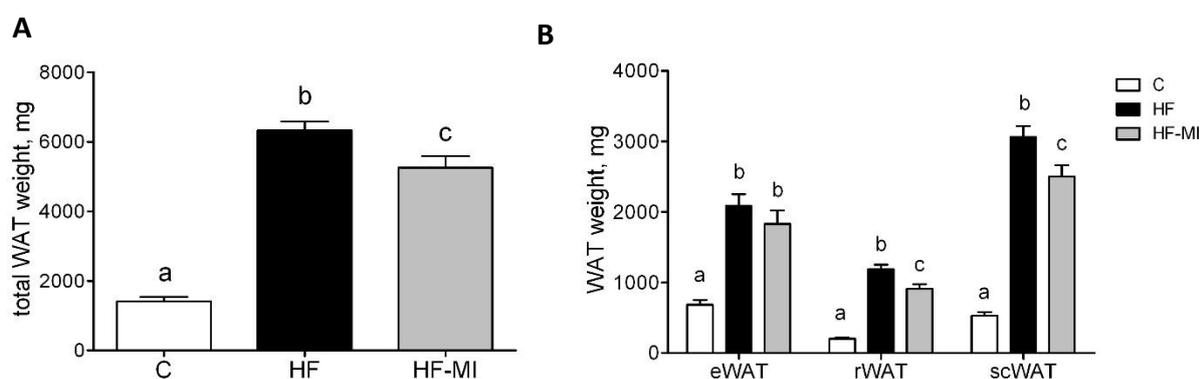
Figure 39 – White adipose tissue weights. A) Total and **B)** epididymal, retroperitoneal and subcutaneous white adipose tissue weights of mice fed a chow (C) or high fat diet with (HF-MI) or without (HF) a dietary *myo*-inositol supplement (0.58 mg.g^{-1} BW) for four months. Data are mean ± SEM for n=10 in each group. Data were compared using 1-way ANOVA and when appropriated PLSD Fischer post hoc tests. Different letters (a, b and c) indicate significant differences between groups (p<0.01). Abbreviations: WAT white adipose tissue, eWAT, epididymal WAT, rWAT, retroperitoneal WAT, scWAT, subcutaneous WAT.

120

High Fat Diet caused hyperglycemia, hyperinsulinemia and dyslipidemia.

The plasma metabolites levels for each group are shown in **Table 12**. High fat diet induced hyperglycemia with compensatory hyperinsulinemia as assessed by the marked increase in HF and HF-MI fasting plasma levels of glucose (11.9 ± 0.9 mM for HF and 10.0 ± 0.9 mM for HF-MI versus 5.2 ± 0.3 mM for C group) and insulin (112.4 ± 11.9 pM for HF ; 118.0 ± 12.0 for HF-MI versus 64.4 ± 11.3 pM for C group). The homeostasis model assessment of insulin resistance (HOMA-IR) was calculated as a clinical parameter for the insulin resistance, from the values of blood glucose and insulin plasma levels. The HOMA-IR indexes for HF and HF-MI groups were similar between them but significantly higher than that of control group, indicating insulin resistance in high fat diet fed mice. High fat fed groups also displayed increased fasting plasma levels of total cholesterol (2.21 ± 0.20 g.L^{-1} for HF; 2.34 ± 0.16 g.L^{-1} for HF-MI *versus* 1.24 ± 0.07 g.L^{-1} for C mice, $p<0.0001$) and decreased fasting plasma levels of triglycerides compared to control group (0.53 ± 0.06 g.L^{-1} for HF; 0.45 ± 0.05 g.L^{-1} for HF-MI *versus* 0.94 ± 0.16 g.L^{-1} for C mice, $p<0.001$).

Table 12
Plasma metabolites in C57Bl/6JRj mice fed a high fat diet (HFD) and supplemented with MI (0.58 mg.g^{-1}) for four months.

	C	HF	HF-MI	p-value
Fasting glucose, mM	5.2 ± 0.3[a]	11.9 ± 0.9[b]	10.0 ± 0.9[b]	<0.0001
Fasting insulin, pM	64.4 ± 11.3[a]	112.4 ± 11.9[b]	118.0 ± 12.0[b]	<0.0001
HOMA-IR	2.4 ± 0.5[a]	8.8 ± 1.5[b]	7.8 ± 1.2[b]	<0.0001
Triacylglycerols, g.L^{-1}	0.94 ± 0.16[a]	0.53 ± 0.06[b]	0.45 ± 0.05[b]	<0.001
Total cholesterol, g.L^{-1}	1.24 ± 0.07[a]	2.21 ± 0.20[b]	2.34 ± 0.16[b]	<0.0001

Data are mean ± SEM for n=10 in each group. Data were compared using 1-way ANOVA and when appropriate PLSD Fischer post hoc tests. Difference where considered significant at the p<0.05 level and different letters (a and b) indicate significant differences. Abbreviations: HOMA-IR, homeostasis model assessment-insulin resistance.

Altered metabolism of inositol in HFD mice: Insulin resistance is associated with intracellular inositol depletion in kidney and liver that was corrected by MI supplementation.

Insulin resistance and hyperglycemia are reported to be associated with increased *myo*-inositol urinary excretion (inosituria) and inositol intra-tissue depletion (Daughaday & Larner 1954; Kennington et al. 1990; H K Ortmeyer et al. 1993; Chang 2011) so we measured urine, kidney and liver inositol contents after 1 (urine) or 4 (tissues) months of normal or diabetogenic (HF) diet. One month high fat diet feeding induced glycosuria (277.4 ± 61.6 *versus* 0.12 ± 0.02 μmol of glucose per 24h for chow diet fed mice, $p=0.0108$) and inosituria (325.8 ± 40.8 versus 97.6 ± 14.1 nmol of *myo*-inositol per 24h for

121

chow diet fed mice, p=0.0061) (See **Table 13**) and the *myo*-inositol urinary excretion was well correlated to the glucose urinary excretion as shown in **Fig. 40.** No significant difference was found concerning the creatinine urine level between chow diet fed mice and high fat diet fed mice at 1 month of diet (9.7 ± 1.4 versus 6.9 ± 0.9 µmol per 24h, n=5, p=0.1376). Finally, urinary *myo*-inositol to creatinine ratio was significantly higher in high fat diet fed mice (54.6 ± 14.1 versus 10.4 ± 1.3, p=0.0143).

Table 13
Urinary glucose, inositol and creatinine content in mice fed a standard (C) or high fat (HF) diet for 1 month.

	C	HF	change	p-value
Glycosuria, µmol.24h^{-1}	0.12 ± 0.02	277.4 ± 61.6	+231067%	0.011*
Inosituria, nmol.24h^{-1}	97.6 ± 14.1	325.8 ± 40.8	+234%	0.006**
Creatininuria, µmol.24h^{-1}	9.7 ± 1.4	6.9 ± 0.9	-29%	0.138
MI/Creatinine ratio	10.4 ± 1.3	54.6 ± 14.1	+425%	0.014*

*Data are mean ± SEM for n=5 in each group. Data were compared using Student t test and when appropriate Welch correction for variance inhomogeneity. Difference was considered significant at the p<0.05 level (*p<0.05 and **p<0.01).*
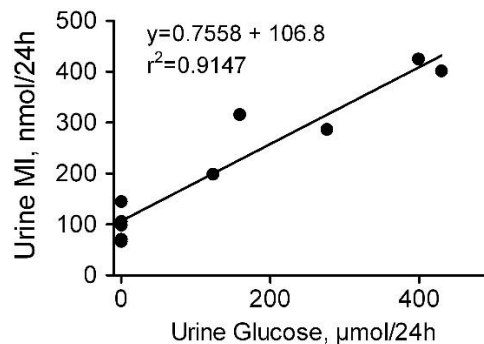
Figure 40 – High fat feeding-induced inosituria is well correlated with glycosuria. After 1 month of chow (n=5) or high fat (n=5) diet feeding, 24h urines were collected and urine *myo*-inositol and glucose levels were determined as described in Material and Methods.

High Fat diet induced a significant reduction in liver (**Fig. 41B** : 0.30 ± 0.03 µmol.g^{-1} in HF mice livers *versus* 0.55 ± 0.04 µmol.g^{-1} in C mice livers, p<0.005) and kidney (**Fig. 41A** : 2.2 ± 0.1 µmol.g^{-1} in HF mice kidneys *versus* 3.4 ± 0.3 µmol.g^{-1} in C mice kidneys, p<0.005) contents in *myo*-inositol. This intracellular *myo*-inositol depletion was completely prevented by *myo*-inositol supplementation in liver (0.66 ± 0.09 µmol.g^{-1}) and partially corrected in kidney (2.9 ± 0.3 µmol.g^{-1}).
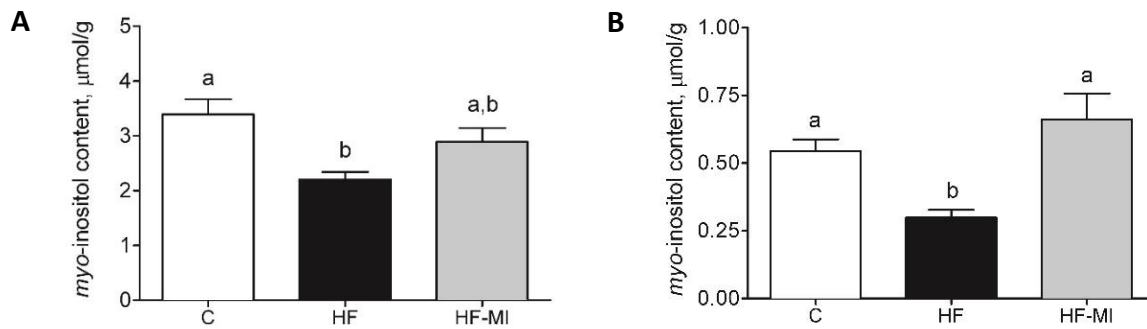
Figure 41 – Intra-tissue free *myo*-inositol content. A) Kidney and **B)** liver *myo*-inositol content of mice fed a chow (C) or high fat diet with (HF-MI) or without (HF) a dietary *myo*-inositol supplement (0.58 mg.g^{-1} BW) for four months. Data are mean ± SEM for n=7-9 in each group. Data were compared using 1-way ANOVA. Different letters indicate significant difference at the p<0.005 between a and b.

Hyperglycaemia can increase *myo*-inositol catabolism is the kidney by enhancing MIOX expression and activity (Nayak et al. 2011). We then measured MIOX activity in the kidneys and found a lower MIOX enzymatic activity in kidneys from high fat diet fed mice (3.2 ± 0.3 for HF and 3.2 ± 0.4 µmol DGA produced in 30 min per g of kidney) compared to kidneys from standard diet fed mice (5.0 ± 0.2 µmol DGA produced in 30 min per g of kidney, p<0.01)(**Fig. 42**).
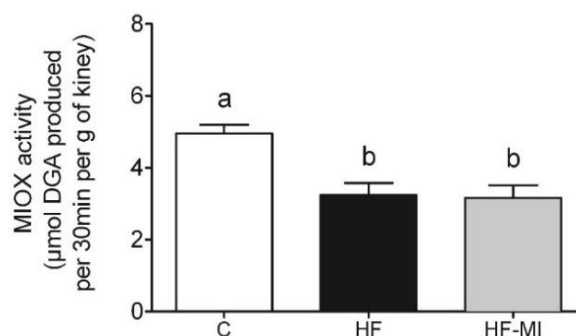
Figure 42 – Kidney *myo*-inositol oxygenase (MIOX) activity. MIOX assay in C57BL/6JRj mice fed a chow (C) or high fat diet with (HF-MI) or without (HF) a dietary *myo*-inositol supplement (0.58 mg.g^{-1} BW) for four months. Data are mean ± SEM for n=5 in each group. Data were compared using 1-way ANOVA. Significant difference between a and b at the p<0.01 level.

myo-Inositol supplementation reduced the HFD-induced insulin resistance.

Insulin sensitivity was evaluated by insulin tolerance tests between three and four months of diet with or without treatment and their results are shown in **Fig. 43**. Insulin administration (0.5 UI.kg^{-1}) triggered a significantly greater hypoglycaemic response in control mice (-37% in blood glucose level at 30 min compared to baseline) compared to high fat diet mice that nearly did not respond to insulin stimulation (-4% for HF and -14% for HF-MI at 30 min versus baseline). However, HF-MI mice hypoglycaemic response to this exogenous insulin stimulation was improved compared to HF mice, as

123

assessed by the significant difference in their glucose disappearance rates (K_{ITT}) : 0.58 ± 0.17 %.min^{-1} versus 0.20 ± 0.07 %.min^{-1}, respectively (p<0.05).
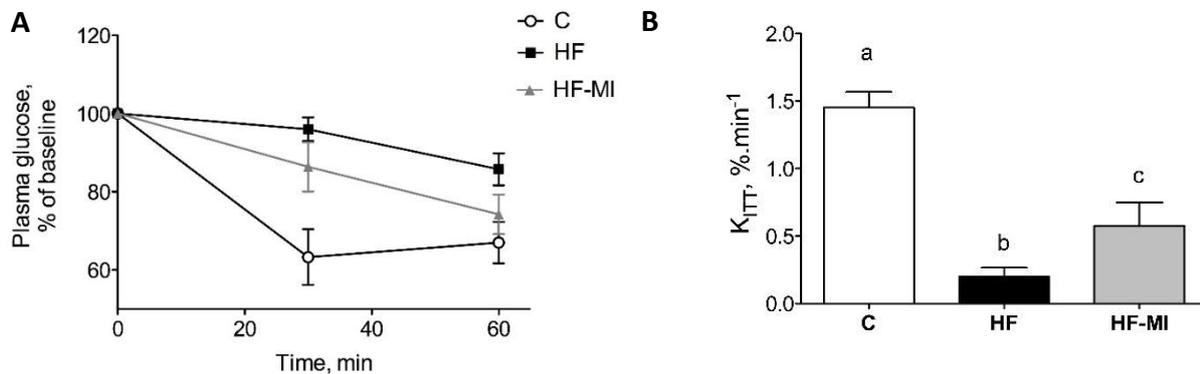
Figure 43 – *myo*-Inositol improved insulin sensitivity in mice fed a high fat diet. Insulin sensitivity was explored using insulin tolerance test after 3 to 4 months of chow or HF diet, with or without MI dietary supplementation (0.58 mg.g^{-1}). **A)** Blood glucose level evolution after intraperitoneal injection of insulin (0,5 UI.kg^{-1}) to fasting mice. **B)** Plasmatic Glucose disappearance rate (K_{ITT}) during the insulin tolerance test. Results are expressed as mean ± SEM for n=6-8 mice in each group. Different letters indicate a significant difference at p<0,05, between b and c, and p<0,01, between a and b, and between a and c.

Noteworthy, the glucose disappearance rate (K_{ITT}) that reflects insulin sensitivity, was negatively correlated with central fat mass (**Fig. 44**, r^2=-0.995, p=0.0027). Hence, the improvement in insulin sensitivity by *myo*-inositol supplementation is probably related to the reduction observed in fat mass accretion in that group compared to the other HF group.
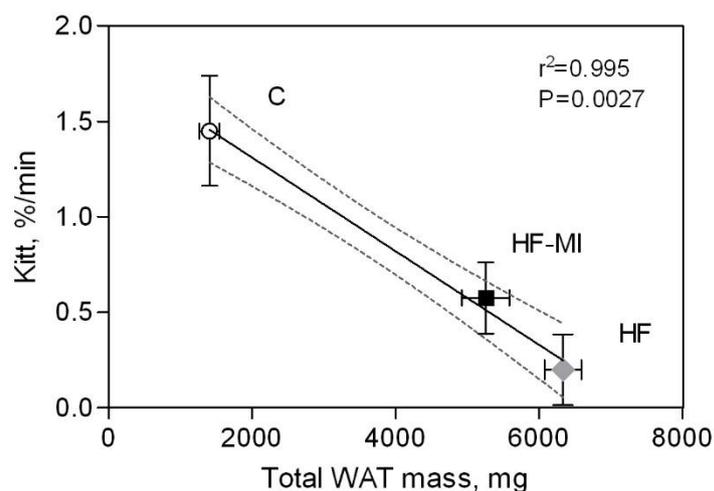
Figure 44 – Insulin sensitivity is negatively correlated with total white adipose tissue mass. n=6-8 mice per group. The dotted lines indicate the 95% confidence interval.

124

myo-Inositol supplementation restrained fat accretion through FAS activity inhibition.

High fat diet caused important fat accumulation in the different white adipose tissue depots (i.e. inguinal, retroperitoneal and epidydimal fat pads) which led to hypertrophia (i.e. increase in cell size) and hyperplasia (i.e. increase in cell number) of these tissues. Indeed, mice from HF group had 4 to 5 times more total white adipose tissue than mice from C group (6330 ± 254 mg versus 1405 ± 138 mg) and this was related to a significant increase in adipocyte cell number (as assessed by DNA quantitation in rWAT, $4.91 \pm 0.54.10^6$ cells for HF *versus* $1.14 \pm 0.16.10^6$ cells for C mice, p<0.0001, n=8-10) and size (see **Table 14**). *myo*-Inositol supplementation significantly reduced this fat accumulation under high fat diet (reduction of about 17% in total WAT mass compared to HF group : 5255 ± 331 mg versus 6330 ± 254 mg) and this result is confirmed by the significantly smaller mean cell volume or weight of HF-MI adipocytes compared to HF adipocytes. Of note, no significant difference was observed in WAT cell number between HF and HF-MI groups.

Table 14

Cellularity of retroperitoneal WAT in C57Bl/6JRj mice fed a high fat diet (HFD) and supplemented with MI (0.58 mg.g^{-1}) for four months.

	C			HF			HF-MI			p-value
rWAT										
pad weight, mg	198	±	67[a]	1185	±	65[c]	927	±	77[b]	<0.0001
Cell diameter, µm	71.8	±	2.7	81.4	±	4.4	77.7	±	5.4	>0.05
Cell weight, ng	674	±	69[a]	1403	±	189[c]	1308	±	236[b]	<0.01
Number of cell, x10^6	1.14	±	0.16[a]	4.91	±	0.54[b]	4.53	±	0.38[b]	<0.0001
DNA, µg/pad	7.4	±	1,0[a]	31.8	±	3.5[b]	29.3	±	2.5[b]	<0.0001

Data are mean ± SEM for n=8-10 in each group. Data were compared using 1-way ANOVA and when appropriate PLSD Fischer post hoc tests. Difference where considered significant at the p<0.05 level and different letters (a and b) indicate significant differences. Abbreviations: WAT white adipose tissue, eWAT, epididymal WAT, rWAT, retroperitoneal WAT.

To get insights into *myo*-inositol mechanism of action in reducing fat storage, we measured the activity of the lipogenic enzyme Fatty Acid Synthase (FAS) (See **Fig. 45**). FAS activity was highly reduced in HF group compared to C group (11.1 ± 0.9 versus 26.33 ± 2.1 mU.mg^{-1} protein respectively, p<0.005, n=9) because of FAS repression by fat overload. Indeed, under HFD, leptin is produced by adipocytes in response to excess fat storage and represses FAS expression. FAS activity was further and significantly reduced in HF-MI group compared to HF group (6.0 ± 0.6 versus 11.1 ± 0.9 mU.mg^{-1} protein respectively, p<0.05, n=9) which could explain MI repressive effect on WAT fat accumulation.
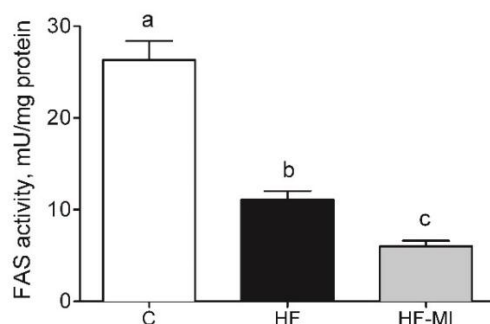
Figure 45 – *myo*-Inositol treatment further reduced FAS activity in mice fed a high fat diet. Fatty Acid Synthase (FAS) activity was measured on epididymal white adipose tissue depots of mice after 4 months of chow or high fat diet feeding with or without a *myo*-inositol supplement (0.58 mg.g^{-1}). Data are mean ± SEM for n=9 in each group. Data were compared using 1-way ANOVA. Different letters indicate significant difference at the $p<0.0001$ between a and b or c and $p<0.05$ between b and c.

High Fat Diet caused lipotoxic lipid redistribution to liver and muscle that could not be prevented by myo-inositol supplementation.

Ectopic lipid redistribution to insulin sensitive tissues other than white adipose tissue (i.e. skeletal muscle and liver) was evaluated by measurement of intra-tissue lipid content (See **Fig. 46A**) and by observation of lipid droplet in histological liver sections (**Fig. 46B**). Livers of both HF and HF-MI groups displayed steatosis as revealed by the presence of numerous lipid droplets in the liver sections of these mice compared to the livers of chow diet fed mice, and by the huge amount of lipid found in their liver compared to control livers (12.6 ± 1.9 % for HF mice; 12.7 ± 1.4 % for HF-MI versus 4.1 ± 0.1 mg.100mg^{-1} of liver for C mice, $p<0.01$). Ectopic lipid redistribution was also observed in gastrocnemius muscles of HF and HF-MI mice that contained nearly as much intracellular lipids as a normal liver (4.7 ± 0.4 and 4.4 ± 0.3 mg.100mg^{-1} of muscle, respectively, compared to 1.6 ± 0.1 mg.100mg^{-1} for control mice muscles, $p<0.0001$). Finally, high fat diet feeding causes important ectopic lipid redistribution to other organs than adipose tissue and *myo*-inositol supplementation could not counteract this lipotoxic phenomenon.
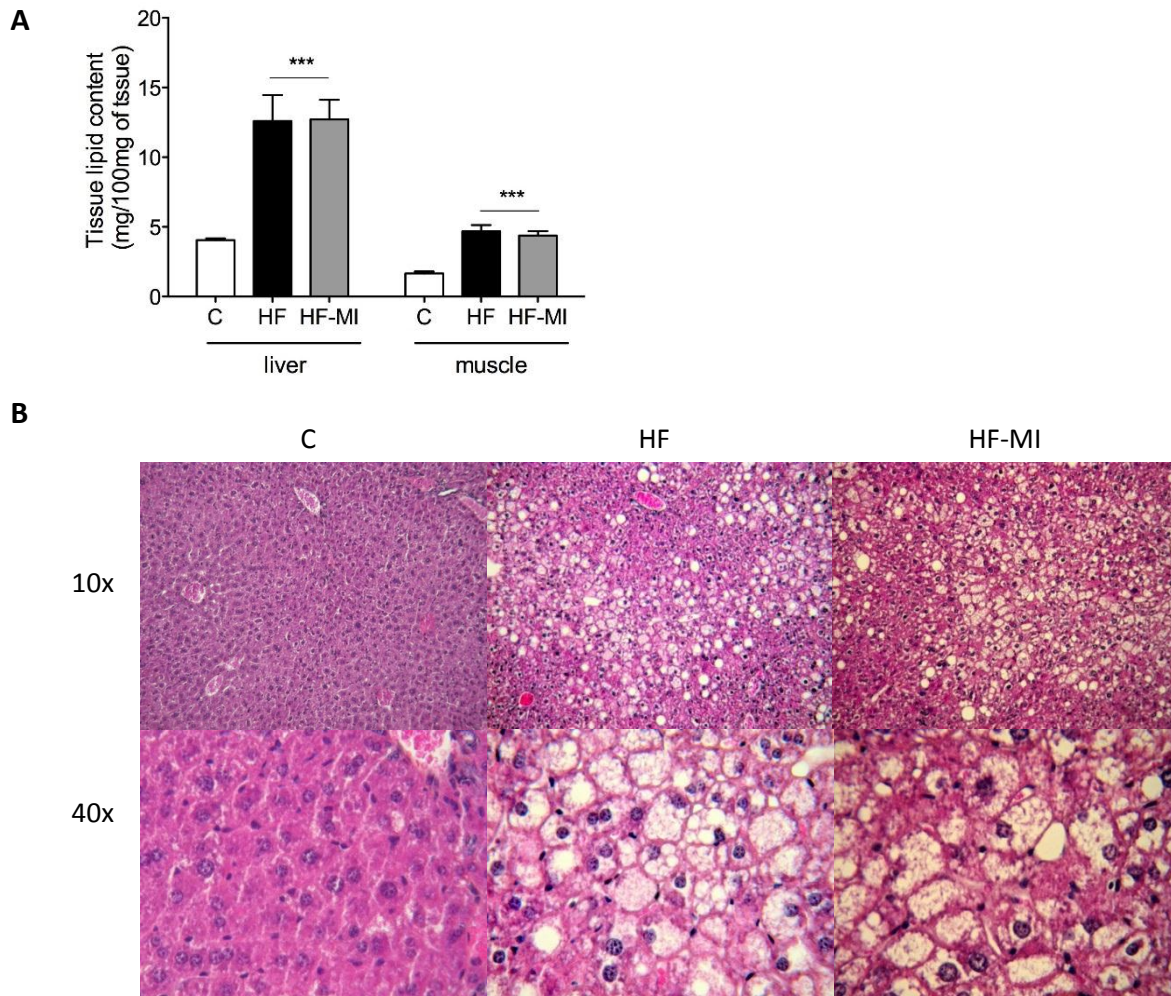
Figure 46 – *myo*-**Inositol could not prevent ectopic lipid redistribution and fatty liver development under high fat feeding. A)** intracelluar lipid content in liver and gastrocnemius muscle (n=10, ***p<0.0001) and **B)** Liver histological sections (optical zoom 10x and 40x) of mice fed a chow (C) or high fat diet with (HF-MI) or without (HF) a dietary *myo*-inositol supplement (0.58 mg.g^{-1} BW) for four months.

4.3   Chronic *myo*-inositol supplementation did not trigger fat loss or improve insulin sensitivity in treatment of spontaneously obese mice of 12 months-old

myo-**Inositol did not induced weight loss in spontaneously obese old CD-1 mice**

We previously showed that chronic *myo*-inositol supplementation could reduce fat accretion in mice fed a normal diet (section 4.1) or an obesogenic diet (section 4.2). In order to further understand

127

myo-inositol effect on fat mass, we then tested *myo*-inositol capacity to reduce fat mass/trigger fat mass loss when an overweight or obesity is already present. 12 months-old CD-1 female mice spontaneously develop an overweight or obesity in standard laboratory conditions. We then supplemented such mice with *myo*-inositol in their drinking water for 1 month to test here *myo*-inositol as a potential "treatment" of obesity rather than as a "preventive strategy". After one month of supplementation, mice were sacrificed and their organs and fat depots were dissected out and weighted. Mice were effectively obese, as revealed by their mean body weight (51 ± 4 g for control mice and 51 ± 5 g for *myo*-inositol treated mice) and by their total white adipose tissue weight (7.70 ± 1.14 g for control mice and 7.56 ± 1.18 g for *myo*-inositol fed mice). No significant difference of lean or fat mass was observed however between the *myo*-inositol treated and the control mice groups. (See **Table 15**).

Table 15
Biometric data and organ weights in 12 months-old mice fed with *myo*-inositol one month.

	control	*myo*-inositol	change	p-value
Biometric data				
BW, g	51 ± 4	51 ± 5	0%	0.904
Body length, cm	11.2 ± 0.2	11.4 ± 0.2	+2%	0.585
Lee index, x10^3	327 ± 5	324 ± 5	-1%	0.611
Organ weights				
Liver, mg/10g BW	405 ± 23	332 ± 20	-22%	0.03*
Heart, mg/10g BW	35 ± 2	33 ± 2	-6%	0.398
Kidneys, mg/10g BW	101 ± 8	76 ± 10	-25%	0.07
Gastrocnemius, mg/10g BW	32 ± 2	33 ± 3	+3%	0.855
Adipose tissue weights				
pWAT, mg/10g BW	936 ± 148	945 ± 167	+1%	0.969
rWAT, mg/10g BW	166 ± 35	182 ± 32	+10%	0.738
scWAT, mg/10g BW	204 ± 28	178 ± 22	-13%	0.488
Total WAT, mg/10g BW	1509 ± 224	1482 ± 232	-1%	0.936

Data are mean ± SEM for n=8 in each group. Data were compared using Student t test and when appropriate Welch correction for variance inhomogeneity. Difference where considered significant at the p<0.05 level. Abbreviations: BW, body wt, WAT white adipose tissue, pWAT, parametrial WAT, rWAT, retroperitoneal WAT, scWAT, subcutaneous WAT.

myo-Inositol did not treat insulin resistance in old and obese CD1 mice

The insulin tolerance test performed on one year-old and obese (body weights of about 50 g) CD-1 mice after one week of *myo*-inositol dietary supplement, showed no beneficial effect of *myo*-inositol on insulin sensitivity (**Fig. 47**). It also showed a weak response to insulin stimulation (0.5 UI.kg^{-1}) in both old mice groups, compared to a younger (1 month-old) mice group, suggesting an insulin resistance in both groups of old mice. Indeed, insulin triggered a reduction of about 70% in blood glucose level for 1 month-old mice *versus* a reduction of about 30 % for 12-months old mice, 60 min after administration.
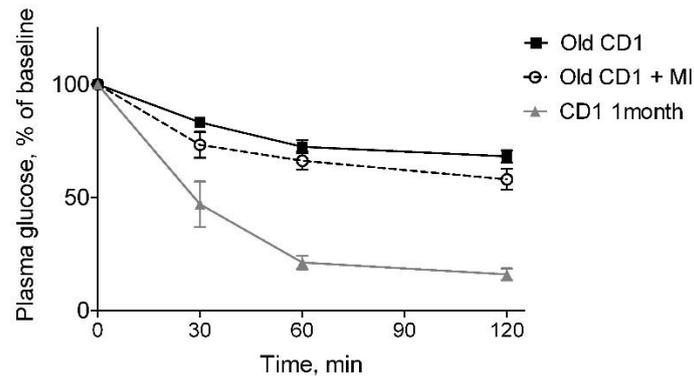
Figure 47 – *myo*-Inositol dietary supplement did not improve insulin sensitivity in old and obese CD-1 mice. Insulin sensitivity was evaluated by an insulin tolerance test after one week of *myo*-inositol oral supplementation (0.64 mg.g^{-1}) on one year old and obese CD-1 mice (For comparison, a group of 4 young (i.e. one month-old) and lean CD-1 mice was added and is represented by the grey solid curve). Blood glucose level evolution was monitored 0, 30, 60 and 120 min after intraperitoneal injection of insulin (0.5 UI.kg^{-1}) to fasting mice. Results are expressed as mean ± SEM for n=4-5 mice in each group. One-way ANOVA analysis indicated no significant difference at the p<0.05 between the curves of control and MI supplemented old mice.

No significant difference was observed between MI-supplemented and control mice concerning their lipid profiles (See **Table 16**). Both mice groups had normal total cholesterol plasma levels, and slightly elevated but physiological levels of plasma triglycerides. Measurement of liver intratissue lipid content showed no difference either between *myo*-inositol and control CD-1 old mice. Liver lipid contents were however slightly elevated and suggest the beginning of a steatosis development. This probably explains the elevated fasting plasma glucose levels since lipotoxicity can cause hepatic insulin resistance.

Table 16

Plasma and liver lipid contents

	control		*myo*-inositol		change	p-value
Triacylglycerols, mM	1.75 ± 0.4		1.14 ± 0.21		-35%	0.2007
Cholesterol, mM	4.52 ± 0.58		3.53 ± 0.27		-22%	0.1590
Liver lipid content, mg.100mg^{-1}	6.7 ± 0.6		7.0 ± 0.7		4%	0.7446

Data are expressed as mean ± SEM for n=8 mice per group. Data were compared using Student t test and when appropriate Welch correction for variance inhomogeneity. No significant difference was found at the p<0,05 level.

Effect of acute oral administration of myo-inositol on PKB/Akt activation level in muscle and liver of old and obese CD-1 mice.

We studied PKB/Akt activation level in two insulin target tissues (gastrocnemius muscle and liver) of old and obese (mean body weights of 45.0 ± 1.0 and 46.6 ± 1.3 g for control and *myo*-inositol mice respectively) CD-1 Swiss mice after acute oral administration of *myo*-inositol 60 min prior to sacrifice and 30 min prior to insulin stimulation (0.5UI.kg^{-1} i.p., 30 min prior to sacrifice) (**Fig. 48 A and B**). In both gastrocnemius muscle and liver, *myo*-inositol acute administration was without effect on PKB/Akt stimulation. In gastrocnemius muscle, insulin stimulation triggered a two-fold increase in the fraction of PKB/Akt activated (2.1 ± 0.2 a.u. for insulin stimulated control versus 1.0 ± 0.1 a.u. for unstimulated control, p=0.0275). However, *myo*-inositol did not further enhance PKB/Akt activation level, neither in absence (1.2 ± 0.3 a.u. for *myo*-inositol mice without insulin versus 1.0 ± 0.1 a.u. for control, n=5-6, no significant difference at the p<0.05 level) nor in presence of insulin stimulation (2.0 ± 0.1 a.u for *myo*-inositol plus insulin versus 2.1 ± 0.2 a.u. for control insulin, n=6, no significant difference at the p<0.05 level). Similar results were found in liver with levels of PKB/Akt phosphorylation on serine 473 residue of 1.0 ± 0.1, 1.0 ± 0.2, 2.7 ± 0.2 and 2.8 ± 0.6 a.u. for control, *myo*-inositol, control plus insulin and *myo*-inositol plus insulin groups, respectively (no significant effect of *myo*-inositol at the p<0.05 level and significant effect of insulin at the p<0.05 level).
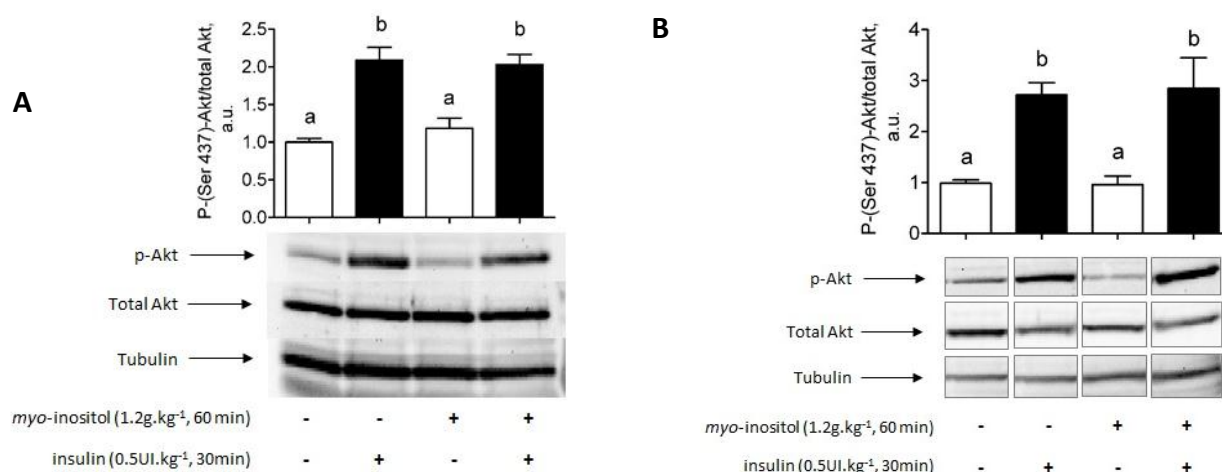
Figure 48 - Single oral administration of *myo*-inositol to old and obese CD-1 mice did not activate PKB/Akt in gastrocnemius and liver neither in baseline nor in insulin stimulated condition. CD-1 Swiss mice received a single dose of *myo*-inositol (1.2 mg.g^{-1}) or drinking water by oral gavage 60 min prior to sacrifice and were stimulated with insulin (0.5 UI.kg^{-1}) or not (physiological serum) by intraperitoneal injection 30 min later. At sacrifice, liver and gastrocnemius muscles were snap frozen and PKB/Akt activation state was studied in those tissues by western blotting (A) Gastrocnemius muscle, n=5-6 ; B) Liver, n=3-4). Data are expressed as mean ± SEM or Sd. Different letters indicate a significant difference at $p<0.05$ level.

4.4 Effect of *myo*-inositol *in vitro* on 3T3-L1 adipocytes or C2C12 muscle cells

***myo*-Inositol treatment effect on PKB-Akt activation state in vitro in C2C12 myotubes**

To get insights into *myo*-inositol insulin sensitizing mechanism of action, we tested *myo*-inositol capability to directly stimulate PKB/Akt in muscle cells (i.e. without previous conversion to another form in a different organ or cell type). In this aim, were pre-treated or not C2C12 myotubes for 72h with MI 1 mM and then stimulated or not the cells with insulin 100 nM for 20 min. PKB/Akt activation state was then evaluated by measurement of the fraction of PKB/Akt that was phosphorylated on serine 473 residue by western blotting (**Fig. 49**). In these conditions, insulin stimulated PKB/Akt phosphorylation on Ser 473 (11.72 ± 1.41 a.u. *versus* 1.0 a.u. for unstimulated control) but *myo*-inositol pre-treatment was without effect, neither alone (1.07 ± 0.24 a.u.) nor with insulin stimulation (11.78 ± 1.424). Of note, the non-toxicity of the 1mM *myo*-inositol pre-treatment for 72h on C2C12 myotubes was previously

checked by a MTT test (viability of MI treated cells was 99.5 ± 1.2 % that of control cells, and was not significantly different of it at the p<0.05 level).
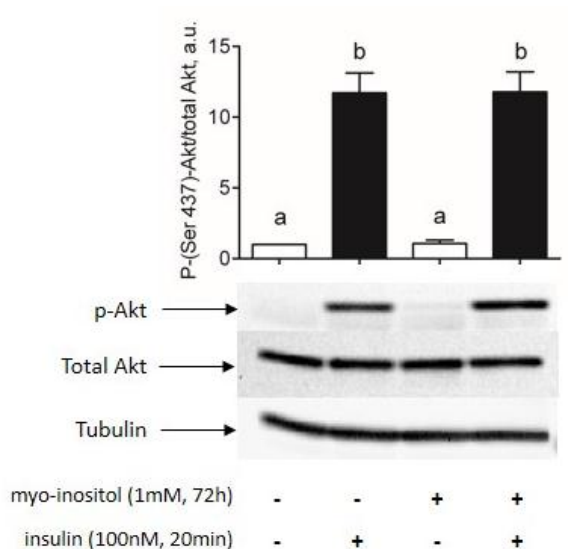
Figure 49 – In vitro, *myo*-inositol pre-treatment of C2C12 myotubes for 72h did not further stimulated PKB-Akt in baseline or insulin stimulated condition. C2C12 myotubes (j+8 of differentiation) were pre-treated 72h with *myo*-inositol 1 mM and then stimulated 20 min with insulin 100 nM. PKB/Akt activation was evaluated by measuring the fraction of PKB/Akt phosphorylated on serine 473 residue by western blotting. n=6, different letters indicate a significant difference at the p<0.001 level.

myo-Inositol effect against ROS-induced cell death

We tried to see if a *myo*-inositol treatment (1 mM for 3h30 alone + overnight in presence of H_2O_2, 1 mM) could protect muscle cells (C2C12 cell line) against oxidative stress-induced cell death. In this way, we first checked that *myo*-inositol overnight treatment, even in concentrations up to 10 mM, did not alter cell viability (See **Fig. 50A**). We then tested if a *myo*-inositol pretreatment of C2C12 myoblats (1 mM) could reduce cell mortality induced dose dependently by a concentration range of the pro-oxidant H_2O_2 (hydrogen peroxide) (See **Fig. 50B**). Survival curves of C2C12 myoblasts against H_2O_2 were dose-dependent but *myo*-inositol treated cells curve and control cells curve were superimposed. Hence, *myo*-inositol pre-treatment did not prevent H_2O_2-induced cell death.
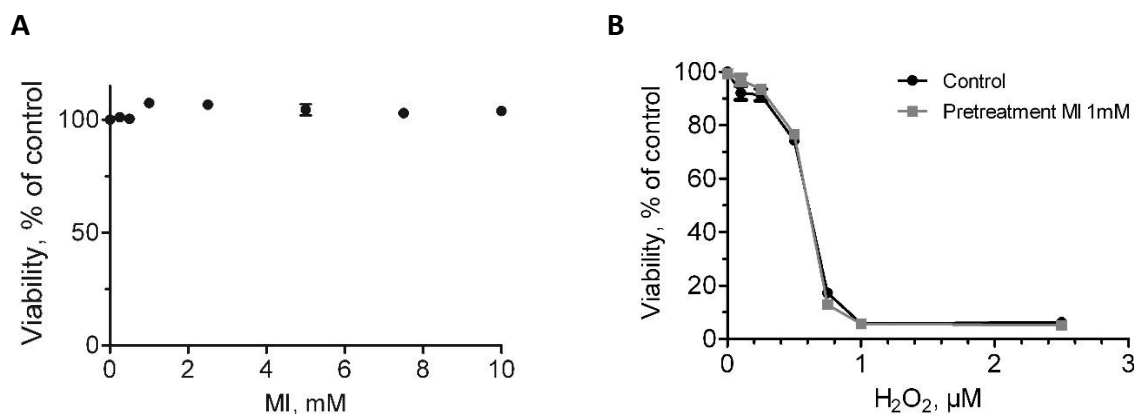
Figure 50 – *myo*-Inositol did not alter cell viability but did not protect C2C12 myoblasts against death-induced by H$_2$O$_2$. MTT viability tests were performed on C2C12 myoblasts in proliferation that were **A**) treated with *myo*-inositol at 0, 0.25, 0.5, 1.0, 2.5, 5.0, 7.5 and 10 mM in serum free medium overnight, or **B**) pre-treated with *myo*-inositol 1 mM for 3h30 and then treated overnight with or without H$_2$O$_2$ at 0.1, 0.25, 0.5, 0.75, 1.0 and 2.5 µM in serum free medium with or without *myo*-inositol 1 mM. n=6, no significant difference at the p<0.05 level between MI treated and control conditions (A) one-way ANOVA, B) two-way ANOVA analysis).

myo-Inositol treatment of 3T3-L1 does not influence adipocyte differentiation or triglyceride accumulation in lipid droplets

myo-Inositol reduced fat accretion in mice, so we tested if *myo*-inositol could directly reduce lipid accumulation in lipid droplets *in vitro* in an adipocyte cell line. However, treatment of 3T3-L1 pre-adipocytes from j$_{+2}$ to j$_{+12}$ of differentiation with *myo*-inositol 1 mM did not alter lipid droplet triglyceride accumulation that occur during the differentiation process of 3T3-L1 fibroblasts to adipocytes, as assessed by the estimation of lipid droplet content by O Red Oil staining (100.0 ± 1.8 % for C, 99.8 ± 1.9 % for Man 1 mM and 102.9 ± 1.3 % for *myo*-inositol, n=4, no significant difference at the p<0.05 level) (**Fig. 51A**).

We also evaluated the lipogenic activity of 3T3-L1 adipocytes more directly, through measurement of the amount of ^{14}C-acetate that was used as substrate for triglyceride synthesis. Adipocyte were treated or not with *myo*-inositol 1 mM in complete medium (10 % SVF, high glucose) for 72 h prior to lipogenesis assay. Results of *de novo* lipogenesis measurement in differentiated adipocytes were consistent with those of O red oil staining since no significant difference was found between control and *myo*-inositol treated cells concerning their capacity to incorporate ^{14}C-acetate into neutral lipids (2394 ± 116 dpm.µg^{-1} of protein for *myo*-inositol treated adipocytes *versus* 2407 ± 154 dpm.µg^{-1} for untreated adipocytes, n=6, p=0.9478) (**Fig. 51B**).
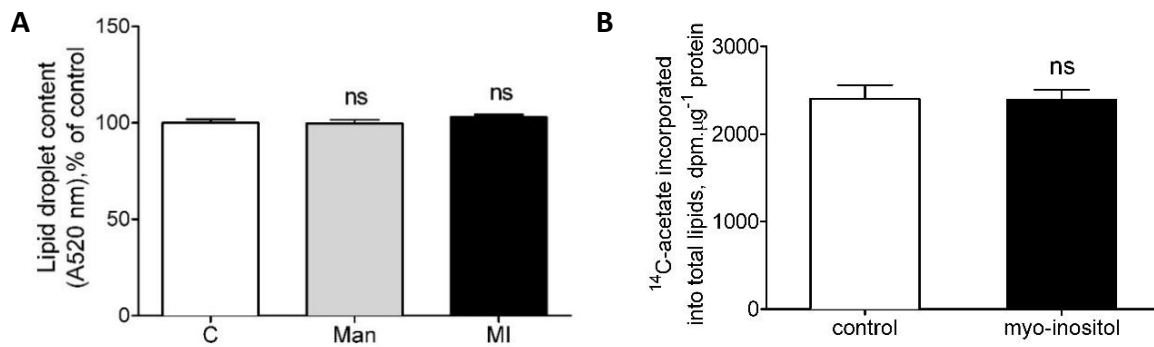
Figure 51 – *myo*-Inositol treatment of 3T3-L1 did not affect adipocyte differentiation and intracellular triglyceride accumulation. A) Lipid content of lipid droplets estimated by O red oil staining of 3T3-L1 adipocytes after 12 days of differentiation with or without (C) mannitol 1mM (Man, osmotic control) or *myo*-inositol 1mM (MI) from j+2 to j+12 of differentiation. n=4, ns, no significant difference at the p<0.05 level. **B)** Lipogenesis from ^{14}C-acetate, n=6.

Chapter 5 – Discussion

5.1 Chronic *myo*-inositol treatment improved insulin sensitivity and reduced fat accretion in mice

Several animal experiments showed that inositol isomers or derivatives like D-*chiro*-inositol, *myo*-inositol or D-pinitol lowered post-prandial blood glucose level when given acutely. In a primary set of experiments, we tested the potency of a chronic *myo*-inositol supplementation to improve glucose control and insulin sensitivity. To this end, female CD1 mice were given daily injection (1.2 mg.g^{-1}) or were fed with *myo*-inositol in drinking water (0.9 mg.g^{-1}) for 10 to 15 days. Our results demonstrated that intraperitoneally as well as orally administered *myo*-inositol significantly improved glucose tolerance and insulin sensitivity, reduced fat accretion and improved mice resistance to oxidative damage.

5.1.1 Chronic MI supplementation improved glucose homeostasis through an improvement in insulin sensitivity

myo-Inositol blood glucose lowering activity was related to an insulin sensitizing effect, rather than an insulin secretion stimulating effect, as evidenced by the results of the different metabolic challenges (improvement in glucose tolerance without higher insulin secretion during the GTT (**Fig. 27**), improvement in insulin sensitivity revealed by the ITT (**Fig. 29**) and no change in insulin secretion in response to stimuli, as evidenced by the arginine challenge (**Fig. 28**). The fact that fed glycaemia but not fasted glycaemia (**Table 7**) was reduced by *myo*-inositol supplementation further demonstrate that *myo*-inositol acts through potentiation of insulin action. These results are consistent with those of Ortmeyer et al. who previously demonstrated that addition of *myo*-inositol to the meal of type 2 diabetic rhesus monkeys lowered urinary and post-prandial blood glucose levels (Ortmeyer 1996), and which gave rise to a patent in 1998 for the treatment of hyperglycaemia (Hansen et al. 1998). In contrast, earlier studies on streptozotocin diabetic rats had failed to show any improvement in hyperglycemia with dietary *myo*-

135

inositol (Greene et al. 1975). In a more recent study (Nascimento et al. 2006), orally administered *myo*-inositol for 4 weeks (20 mg.kg^{-1} per 12 h) reduced plasma glucose by 8.8 ± 1.4 % in alloxan-diabetic rat compared to vehicle diabetic rats but the difference was not significant at the $p<0.05$ level. This could be explained by the fact that MI hypoglycemic effect involves an improvement in insulin sensitivity and so could not counteract hyperglycaemia in animal models of type 1 diabetes wherein insulin is missing. In addition, MI cellular uptake is competitively inhibited by glucose so its action is probably mitigated under severe hyperglycemic conditions and more particularly when MI dosage in not high (20 mg.kg^{-1} per 12h in the study of Nascimiento). In healthy C57BL/6 male mice, Dang et al. reported that acute oral administration of *myo*-inositol lowers plasma glucose after an oral GTT (Dang et al. 2010) and stimulate GLUT-4 translocation to the plasma membrane, which support our results. The herbal constituent sequoyitol, the 5-O-methyl form of *myo*-inositol, was also efficient in improving glucose tolerance in ob/ob mice when chronically administered by either subcutaneous or oral administration (Shen et al. 2012). Sequoyitol was shown to potentiate insulin action on liver (i.e. increased insulin ability to suppress liver glucose production) and adipocytes (i.e. increased adipocytes glucose uptake) by directly stimulating insulin signaling in primary or cell line cultures of hepatocytes and adipocytes.

Human studies are also on the whole consistent with our results, showing improvement in metabolic parameters and in particular reduction in glycemia, insulinemia, HOMA-IR index and/or glucose tolerance in women with gestational diabetes (D'Anna et al. 2013; Matarrelli et al. 2013; Corrado et al. 2011), post-menopausal metabolic syndrome (Santamaria et al. 2012; Giordano et al. 2011) and patients with polycystic ovary syndrome (PCOS) (See for review (Unfer et al. 2012), plus (Minozzi et al. 2013)). In a study on human hyperlipidemic subjects including both men and women (with or without metabolic syndrome), a positive effect of *myo*-inositol supplementation (5-10 g per day, for 2 weeks) on fasting glycaemia was observed but only in the sub-group of hyperlipidemic subjects with metabolic syndrome (Maeba et al. 2008). Accordingly, we found no significant difference in fasted glycemia between non-insulin resistant CD-1 Swiss mice treated or not with *myo*-inositol (See **Table 7**).

If *myo*-inositol blood glucose lowering effect in presence of insulin (*e.g.* post-prandial condition or glucose load, insulin resistance with compensatory hyperinsulinemia) is rather well established, the underlying molecular mechanisms are still unclear and lead to some discrepancies.

5.1.2 Chronic MI supplementation improvement in insulin sensitivity was associated with an activation of insulin signaling pathway

The exact mechanisms of action of MI and other inositol isomers (DCI) or derivatives (e.g. D-pinitol, sequoyitol) with insulin-mimetic activities remain unclear and debatable. A putative mechanism of action implies inositol phosphoglycans (IPGs) containing MI or DCI as insulin mediators released in response to insulin stimulation. DCI-containing IPG would act on a parallel pathway of the conventional IRS/PI3K/Akt pathway (See **Fig. 23**). This secondary pathway would lead to increased PDH and GS activities, independently of PKB/Akt activation, but would also possibly converge on PI3K and so activate GS through PKB/Akt. Some authors proposed that *myo*-inositol may act through conversion to DCI that would be a more active metabolite. This hypothesis is based on several observations : 1) low doses (10µg.g^{-1} BW) of *myo*-inositol were reported to be inefficient for the regulation of plasma glucose level in rat with streptozotocin-induced diabetes contrary to low doses of *D-chiro*-inositol (H. K. Ortmeyer et al. 1993) ; 2) in contrast to some other inositol stereoisomers (including *D-chiro*-inositol), *myo*-inositol failed to stimulate glucose uptake *in vitro* in L6 muscle cells (Yap et al. 2007) but triggered GLUT-4 translocation to the plasma membrane *in vivo* (Dang et al. 2010) in C57BL/6 skeletal muscle ; 3) *myo*-inositol can be converted to DCI in vivo by a specific epimerase, but with a small conversion rate (7.6 and 8.8 % in blood and muscle respectively (Pak et al. 1992)) which could explain why *myo*-inositol is only active in high dosages while DCI is active in lower dosages.

Here, we demonstrated that *myo*-inositol potentiated insulin action *in vivo* as well as *in vitro* (See **Fig. 31 A and B**). Indeed, according to the result of the immunoblotting on PKB-Akt in mice gastrocnemius muscle, it can be presumed that *myo*-inositol treatment improves insulin sensitivity via the induction of the intracellular insulin signaling cascade at the level of this protein (PKB-Akt) and possibly even upstream in the cascade (e.g. PI3K). These results are in good agreement with data from Dang et al (Dang et al. 2010) who demonstrated that orally administered *myo*-inositol increased GLUT-4 translocation to plasma membrane in gastrocnemius muscle at a basal level (i.e. in absence of insulin stimulation) and in response to a glucose load (2 g.kg^{-1} BW) (i.e. in presence of insulin). Moreover, Shen et al. recently showed that both sequoyitol (5-O-methyl-*myo*-inositol) and *myo*-inositol (100 µM, 12h pretreatment) potentiated insulin action (10 nM, 5 min) on IR, IRS and PKB/Akt activating phosphorylations (Ser 473 and Thr 308 for PKB/Akt) in hepatocytes and adipocytes. However, no effect of *myo*-inositol or sequoyitol alone (i.e. in absence of insulin stimulation) was observed in those conditions (acute *in vitro* stimulation, 100 µM, 12h pretreatment). Taken together, these results indicate that the increased glucose uptake and GLUT-4 translocation to plasma membrane observed with *myo*-inositol could be mediated through the canonical PI3K/PKB-Akt pathway. PKB/Akt activation in response

137

to *myo*-inositol could result from enhanced activation of PI3K, which could be related to 1) activation by PP2Cα in response to inositol glycan second messengers (from DCI-containing IPGs) as depicted in **Fig. 23**), or 2) increased availability in PI3K substrate (PIP$_2$) due to phosphoinositide pool enrichment from *myo*-inositol precursor. The first hypothesis implies that *myo*-inositol is metabolically converted to DCI and then integrated into a DCI-containing inositol phosphoglycan (unless *myo*-inositol containing IPGs acts in the same manner as DCI-containing IPGs). The results from Shen et al are however not in full accordance with this first hypothesis because they showed that *myo*-inositol and sequoyitol enhanced insulin signaling at the level of IRS1 and even of the IR, while DCI-IPGs pathway is proposed to converge on IRS/PI3K/Akt pathway only at the level of PI3K and so downstream of IRS-1. Another inconsistency with the DCI-IPGs hypothesis to explain MI (and other inositol derivatives) effect is that several inositol isomers were shown to stimulate glucose uptake and/or GLUT-4 translocation to the plasma membrane in baseline condition (i.e. without insulin stimulation) while DCI containing inositol second messengers are supposed to be released in response to insulin stimulation (See **Fig. 23** and (Pak et al. 1993; Larner et al. 2010)). Moreover, *myo*-inositol conversion to DCI is also supposed to be insulin-dependent (Pak et al. 1998; Sun et al. 2002). Finally, the second hypothesis (enrichment of phosphoinositide pool) is not more satisfactory since IRS1 would not be activated in this case neither (PIP$_2$ to PIP$_3$ conversion plays a role upstream of PKB/Akt but downstream of IRS-1, See **Fig. 6** or **23**). In addition, PI3K activity is unlikely regulated by the availability of its substrate PIP$_2$ in the plasma membrane because this latter is present in excess (30 µM PIP$_2$ for 0.05 µM PIP$_3$, that is to say 600 folds more substrate than product (Dawes 2006)) ; it is more probably regulated by IRS-1 binding and phosphorylation events.

In order to challenge the hypothesis of a metabolic conversion of *myo*-inositol to *D-chiro*-inositol *in vivo*, we tested the effects of *myo*-inositol and *D-chiro*-inositol on Protein Kinase B activation state in mouse isolated gastrocnemius muscles, with or without insulin stimulation (**Fig. 31B**). According to our result however, *myo*-inositol but not *D-chiro*-inositol potentiated insulin induced PKB/Akt phosphorylation on Serine 473. Hence *myo*-inositol effect on PKB/Akt activation *in vivo* (**Fig. 31A**) seems to be independent of its metabolic conversion to *D-chiro*-inositol.

Finally, further studies are still needed to decipher the exact molecular mechanism of action of *myo*-inositol or inositols in insulin target cells. Implication of inositol glycans putative second messengers of insulin as mediators of some inositols insulin-mimetic activities remains unclear, as their molecular mechanism of action (and especially MI-containing IPGs mode of action). Furthermore, recent data showed that over a large collection of synthetic IPGs, none were found to be insulin mimetic (Hecht et al. 2010). Another possible and still unexplored target for inositol action on GLUT-4 translocation to the plasma membrane is the 5'AMP-activated protein kinase (AMPK). However, like other hypothesis, it only explains some results (GLUT-4 translocation to the plasma membrane in a way independent and additive with that of insulin) but not all (potentiation of insulin action on IR, IRS and PKB/Akt activation).

Indeed, AMPK acts on glucose transport downstream of PKB-Akt: AMPK phosphorylates and inhibits the Rab-GTPase–activating proteins termed AS160 and TBC1D1, which leads to an increase in the levels of active (GTP-bound) Rab8A and promotes relocalization of GLUT4 to the plasma membrane.

5.1.3 Chronic MI supplementation reduced fat accretion which may contribute to the improvement in insulin sensitivity

In our first study on "lean" CD-1 Swiss mice, a significant reduction in fat mass (about -33%) was observed in mice supplemented either orally or intraperitoneally with *myo*-inositol. Insulin sensitivity is strongly related to body fat content even within subjects with normal BMI (Bogardus et al. 1985). Since obesity has generally been regarded as an important contributory factor in peripheral insulin resistance, the question arises as to whether the lower adiposity of the *myo*-inositol mice is the primary factor responsible for the reported changes in insulin sensitivity. Indeed, increased visceral fat is associated with decreases in peripheral and hepatic insulin sensitivity (Coon et al. 1992; Carey et al. 1996; Gastaldelli et al. 2002) and in good agreement, surgical extraction of visceral fat has been shown to reverse insulin resistance in young obese and old male rodents (Gabriely et al. 2002). We noticed in the present study a good correlation between insulin sensitivity (estimated through K_{ITT} index) and fat mass suggesting that fat mass loss could be a determining factor of *myo*-inositol insulin-sensitizing action in the long term, in addition to its action on insulin signaling in muscle. Adipose tissue is now recognized as a major secretory tissue (Mohamed-Ali et al. 1998) releasing into blood flow many hormones and cytokines (named adipokines) that affect metabolism. Several adipokines have been involved in insulin resistance (e.g. resistin, TNF-α, IL6) or as insulin sensitizing factor (e.g. adiponectin). However, *myo*-inositol treatment was not associated with an increase in plasma adiponectin level excluding a role for adiponectin in its insulin sensitizing effect. Hypertrophy of white adipose tissue exacerbates the secretion of pro-inflammatory cytokines, such as IL-6, IL-1, IL-8, and TNF-α while regulatory cytokines, such as IL-10, are decreased. Accumulated fat is therefore associated with low-grade inflammation that could contribute to metabolic syndrome and insulin resistance associated with overweight (Wisse 2004; Trayhurn & Wood 2004). We noticed a significant decrease in plasma NEFA levels in *myo*-inositol mice (see **Table 7**). The adverse effects of increased NEFA availability on insulin sensitivity are well known from the works of Randle et al. (Randle et al. 1963) and of (Boden et al. 1994) showing that increased availability of fatty acids decreases glucose utilization in muscle. NEFA are also a potent stimulus to hepatic glucose production (Ferrannini et al. 1983), (Boden et al. 1994). The decrease of plasma NEFA level could therefore underlie the improvement of insulin sensitivity. Furukawa et al (2004) reported

139

that increased oxidative stress in accumulated fat was an important pathogenic mechanism of obesity-associated metabolic syndrome (Furukawa et al. 2004). Fat accumulation correlated with systemic oxidative stress in both humans and mice. Production of ROS was selectively increased in adipose tissue of obese mice, associated with a blunted expression of antioxidative enzymes. The decrease in WAT mass described in the present study could contribute to the improved resistance to oxidative stress and better redox status. This effect can contribute to the improvement of insulin sensitivity as does most antioxidant substances (Velussi et al. 1997; Rudich et al. 1999; Paolisso et al. 1995; Bashan et al. 2009; Ansar et al. 2011).

5.1.4 MI supplementation reduced fat accretion through an anti-lipogenic activity rather than a lipolytic activity.

We reported for the first time an inhibitory effect of MI supplementation on WAT accretion. The exact mechanism involved in *myo*-inositol supplementation effect on fat mass is still incompletely defined. It seems however to be related to an anti-lipogenic action rather than a pro-lipolytic action, as evidenced by the results shown in **Fig. 35 A** and **B**. This effect on lipogenesis could be related to a reduction in ACC and/or FAS activity (and/or gene expression). In accordance with this hypothesis, it was shown that the presence of inositol (11 µM) in culture medium of the yeast *Saccharomyces cerevisiae* repressed FAS genes expression, and so FAS and ACC activities, by two to three fold (Chirala 1992). In contrast, lack of inositol in culture medium de-repressed FAS genes and restored higher FAS and ACC activities. In yeast, these effects are explained by the presence of the UAS_{INO} upstream activation sequence and of a cis element (GCCAA) that act synergistically to regulate FAS genes expression. To test the hypothesis of a reduction in lipogenic enzymes (ACC and/or FAS) activities, we measured FAS activity (because FAS is downstream of ACC) in white adipose tissue of C57BL/6JRj mice after 4 months of diet (chow or high fat diet) with or without *myo*-inositol supplement. As expected, fatty acids of the high fat diet strongly reduced FAS activity, and *myo*-inositol supplementation further reduced it (See **Fig. 45**). Hence, *myo*-inositol effect on white adipose tissue may be related to a reduction in lipogenesis through FAS, and eventually also ACC, activities and/or gene expression.

5.1.5 Chronic MI supplementation enhanced resistance to oxidative injury

myo-Inositol supplementation enhanced mice resistance to oxidative injury as evidenced by their improved survival to paraquat challenge and their higher plasma anti-oxydant activity. As expected by its molecular structure and as confirmed by the measurement of *myo*-inositol solution antioxydant activity (See **Fig. 38**), *myo*-inositol is not anti-oxydant by itself and even in very high dosages, it cannot quench reactive species efficiently. The effect of *myo*-inositol supplementation on redox status is then either mediated through conversion in other forms or derivatives, or through induction of antioxidant defenses. Accordingly, a recent study on Jian carp (Jiang et al. 2011) confirmed the antioxidant potency of chronic *myo*-inositol treatment, showing that *myo*-inositol pre-supplementation prevented copper-induced oxidative damage *in vivo* and *ex vivo* on intestine, presumably through the induction of key antioxidant enzymes, including superoxide dismutase (SOD), catalase (CAT), gluthatione peroxidase (GPx) and Gluthatione-S-transferase (GST). Some studies also suggest that *myo*-inositol chronic supplementation could increase membrane pools of plasmalogens, which are potent endogenous antioxydants. Though, we did not observed such enrichment when we quantified plasmalogens derivates (dimethylacetals) in mice red blood cells (See **Table 10**). This result cannot however definitively exclude a possible enrichment in cell membrane of brain or other tissues. Finally, some studies also reported a direct antioxidant activity of phosphorylated forms of *myo*-inositol (i.e. phytic acid) via iron III chelation (Graf 1990), and of derivatives such as *D-chiro*-inositol and D-pinitol, through the quenching of superoxide anion and hydroxyl radical (Nascimento et al. 2006).

In summary, this first study on healthy mice shows that a chronic treatment with *myo*-inositol 1) improves glucose tolerance in mouse by increasing insulin sensitivity 2) potentiates insulin action on the conventional PI3K/Akt insulin signaling pathway 3) reduces fat mass accretion through reduction in lipogenesis 4) improves antioxidant status and resistance to oxidative damages. Further studies are however needed to precise the mechanisms underlying those effects of *myo*-inositol. *myo*-Inositol only exhibited an extremely low toxicity as its oral LD50 in mouse is 10 000 mg.kg^{-1} (*myo*-inositol Material Safety Data Sheet). In Human, no serious adverse effects were observed in doses up to 18 g.day^{-1} for up to 3 months. Only minor and non-life threatening gastrointestinal adverse events were reported with daily intake of high doses of *myo*-inositol (up to 30 g.day^{-1}) (Lam et al. 2006). *myo*-Inositol could therefore constitute a viable and safe nutritional strategy to delay or prevent insulin-resistance development and/or type 2 diabetes onset. We then tested this nutritional strategy for the prevention of obesity and insulin resistance development in C57BL/6 mice fed a high fat diet, as well as in old (and spontaneously obese) CD1 mice.

5.2 Dietary *myo*-inositol supplement did not prevent insulin resistance or obesity development in mice fed a high fat diet, but improved insulin sensitivity and reduced fat deposition

5.2.1 HFD-feeding induced inosituria and liver and kidney intra-tissue MI depletion

Insulin resistance and hyperglycaemia are often associated with inosituria (i.e. excessive urinary excretion of inositol) and intra-tissue inositol depletion (See section 1.3.4 – inositol metabolism associated to insulin resistance). For the first time, we found back such abnormalities in inositol metabolism in C57BL/6JRj mice fed a high fat diet, with an increased content of inositol in urine after 1 month of HFD feeding and a decreased content of inositol in liver and kidneys at four months (**Table 13** and **Fig. 41 A** and **B**). In HFD-fed mice, inositol intracellular content was fully restored with *myo*-inositol oral supplementation in liver (**Fig. 41B**) and partially restored in kidneys (See **Fig. 41A**). This difference could be explained by the fact that liver is the first organ supplied by dietary *myo*-inositol through the portal vein while kidneys are the primary site of inositol catabolism (especially by MIOX) and excretion. Moreover MIOX activity was reported to be enhanced in mice after 1 month of HFD (45% energy as fat) (Chang 2011) and in conditions of high glucose (Nayak et al. 2005) which could explain a less efficient restoration of intracellular inositol pool in kidney cells compared to hepatocytes. However, after 4 months of HFD (60% energy as fat), we found that MIOX activity was not enhanced but rather significantly reduced. This difference could be explained by the fact that kidney function and structure is probably more profoundly altered in mice after 4 months of high fat diet with 60% of fat than in mice fed a HFD with 45% of fat for 1 month. Deji et al (Deji et al. 2009) studied kidney structure and function of C57BL/6 mice and they showed that after 12 weeks (i.e. 3 months) of high fat diet (60% fat) feeding, mice showed albuminuria, an increase in glomerular tuft area, mesangial expansion, and renal pathophysiological alterations including renal lipid accumulation, an increased accumulation of type IV collagen in glomeruli, an increase in macrophage infiltration in the renal medulla and an impaired sodium handling. In addition, down-regulation of MIOX was observed in acute ischemic renal injury and was only restored when renal function was recovered (Hu et al. 2000). MIOX activity reduction observed

after 4 months of HFD may be then related to structural and functional changes in kidneys of obese and insulin resistant mice (i.e. nephropathy). Enhanced catabolism of *myo*-inositol by MIOX may occur in the first weeks of high fat diet feeding and may contribute at this time to the intra-tissue *myo*-inositol depletion. However, competitive inhibition of inositol uptake by glucose (inhibition of renal tubular reabsorption and cellular uptake by cells) seems to be the major cause of intracellular *myo*-inositol depletion under hyperglycemic conditions. Accordingly, we found a strong correlation between glycosuria and inosituria after 1 month of chow or high fat diet feeding (See **Fig. 40**).

5.2.2 Dietary MI supplement did not prevent obesity development under HFD-feeding, but reduced fat accumulation in white adipose tissue.

myo-Inositol supplementation reduced fat accumulation and white adipose tissue hypertrophy but did not prevent obesity development under high fat feeding. This can be explained by the fact that *myo*-inositol supplementation seems to act through inhibition of lipogenic enzymes activities which are already strongly inhibited by the excess in free fatty acids provided by the high fat diet. *myo*-Inositol positive effect on fat mass is then mitigated under conditions of fatty acid overload ; and the little reduction in white adipose tissue weight of *myo*-inositol supplemented HFD-fed mice is related to the little additional reduction in FAS activity provided by *myo*-inositol compared to non-supplemented HFD-fed mice (**Fig. 45**). Consequently, out of a use in complement of a balanced diet, *myo*-Inositol cannot be an efficient strategy to prevent weight gain and obesity development. Moreover, as nearly all the strategies for weight loss or weight management that prevent fat storage or trigger fat destocking from adipose tissue without enhancing fat oxidation, *myo*-inositol supplementation may favour ectopic lipid redistribution to non-adipose tissue (e.g. liver, muscle, pancreas, heart, kidneys) in a context of dietary lipid overload and poor energy expenditure through physical activity. If existing, this toxic phenomenon could not be evidenced in this study because mice already had a fatty liver due to the high fat diet feeding for four months (**Fig. 46 A and B**) so may be mice supplemented with *myo*-inositol started to present ectopic lipid depots before non-supplemented high fat fed mice but we cannot assert or invalidate it. Hence, for a better efficiency on fat mass and for a safer use, *myo*-inositol supplementation should be used in complement of a rather healthy way of life (not too unbalanced diet and/or physical activity) as many weight management strategies.

5.2.3 Dietary MI supplement did not prevent insulin resistance development under high fat feeding, but improved insulin sensitivity.

High fat diet feeding induced peripheral and liver insulin resistance with compensatory hyperinsulinemia as evidenced by the reduced response to insulin during the ITT (**Fig. 43**), the fasting hyperglycaemia and hyperinsulinemia and so the increased HOMA-IR index (**Table 12**). This insulin resistance is associated with obesity (Fig. 37B, 38 and 43) and ectopic lipid depots in liver and muscles (**Fig. 46**). Lipotoxicity and chronic low-grade inflammation are then probably the major causes of this diet-induced insulin resistance. *myo*-Inositol supplementation did not prevent this insulin resistance and only slightly improved insulin sensitivity in mice fed a high fat diet. The little improvement in insulin sensitivity seemed to be of the same extent as the little reduction in white adipose tissue mass, as shown by the good correlation between the mean K_{ITT} and the mean white adipose tissue weights for each group (**Fig. 44**). However, even if it seems to confirm the results found in the first study on healthy mice (strong correlation between individual K_{ITT} and white adipose tissue weight (**Fig. 30**)), we cannot really conclude on this correlation because we only have the three group mean values for K_{ITT} and WAT weight and not the individual and corresponding values for each mice. Since *myo*-inositol could not prevent ectopic lipid deposition in liver and muscles, it did not prevent the insulin-resistance induced by lipotoxicity. If *myo*-inositol supplementation indeed enhance the production and release of IPGs in response to insulin, this could have slowed down the progression of insulin resistance and be responsible for the little difference observed in insulin sensitivity between the two HF groups. Theoretically, enhancing IPGs production and release could have been a good strategy to counteract stress kinases (e.g. activated by pro-inflammatory cytokines or bioactive lipids) inhibitory effects on insulin signaling since IPGs apparently converge on IRS/PI3K/Akt pathway downstream of IRS, which is the main target of stress kinases. However, in practice, *myo*-inositol effects were mitigated. This could be explained by several things: 1) hyperglycaemia induced by high fat diet (and then maintained by insulin resistance) inhibits inositol uptake by cells and so probably reduces the effect of *myo*-inositol supplementation ; 2) the high fat diet-induced fatty acid overload inhibits *de novo* lipogenesis from acetate and/or glucose and so probably attenuates *myo*-inositol effects on FAS activity and white adipose tissue mass ; and reduction in fat mass seemed to be an important contributory factor to insulin sensitivity improvement with *myo*-inositol ; 3) the high fat diet used (60% fat) was very strong (very diabetogenic and obesogenic) and caricatural, with a rapid insulin resistance development (1 month) and was may be difficult to counteract with a simple nutritional strategy ; 4) if *myo*-inositol to D-*chiro*-inositol conversion is required for efficiency, and since this conversion is reported to be dependent on

144

insulin action, the effect of *myo*-inositol in condition of insulin resistance is mitigated. Moreover, DCI-IPGs release is also dependent on insulin receptor activation by insulin which may also be compromised in a context of lipotoxicity (e.g. putative serine (inhibitory) phosphorylation on insulin receptor by DAGs-activated PKC-ε in liver).

Finally, *myo*-inositol supplementation is not a viable strategy to prevent insulin resistance in sedentary subjects with a chronic high calorie and unbalanced diet. It may probably be more efficient for subjects at genetic risk of developing type 2 diabetes but with a less extreme way of life, or in complement of another treatment and of a balanced diet in insulin resistant subjects.

5.2.4 Dietary MI supplement did not alter plasma lipid profile in HFD-fed mice.

Human studies with *myo*-inositol supplement nearly always showed an improvement in plasma lipid profiles, with a reduction in plasma triglycerides, total and LDL-cholesterol and an increase in HDL-cholesterol, thereby reducing the cardiovascular risk associated to insulin resistance (Gerli et al. 2007; Maeba et al. 2008; Costantino et al. 2009; Giordano et al. 2011; Santamaria et al. 2012). High fat diet fed mice displayed hypercholesterolemia but no significant difference was found between *myo*-inositol supplemented and only high fat fed mice (**Table 12**). This result is not that surprising since rodents are quite different from humans concerning cholesterol metabolism and are then poor models for cholesterol-related human diseases (e.g. atherosclerosis). In particular, rodents do not have cholesterol ester transfer protein (CETP) activity. CETP facilitates the transfer of HDL cholesterol esters from plasma to the liver. As a consequence rodents have HDL as major cholesterol carrying lipoproteins which is quite different from humans. Another difference is that in rodents but not in humans, LXR activation enhances hepatic cholesterol catabolism (partly through increased expression of cytochrome P450 7A1, the rate-limiting enzyme in the classic conversion of cholesterol to bile acids).

Four months 60% high fat feeding was not associated with hypertriglyceridemia but rather to a reduction in plasma triglycerides (**Table 12**). Petit et al. (Petit et al. 2007) also found low plasma triglycerides levels in mice fed a high fat diet and showed that this was attributable to a more efficient chylomicron clearance from blood. ApoC-II and apoC-III are known to be a strong activator and a strong inhibitor, respectively, of Lipoprotein Lipase (LPL), an enzyme responsible for blood chylomicron clearance. A higher apoC-II/apoC-III mRNA levels ratio was found in jejunum (and so chylomicron) of chronically high fat fed mice. The greater plasma triglycerides clearance observed in chronically high fat

145

fed mice is then attributable to an increased LPL activity, as confirmed by the absence of difference in plasma triglycerides of high fat fed mice after a lipid load in presence or absence of the LPL inhibitor tyloxapol (Petit et al. 2007).

5.3 Dietary MI supplement did not improve insulin resistance or obesity spontaneously developed by laboratory mice with aging

5.3.1 MI supplementation did not decrease WAT weight in established obesity

Twelve months-old CD-1 Swiss mice spontaneously developed obesity with aging under a normal laboratory environment. These mice weighted about 51 ± 5 g and presented a greater adiposity than the C57BL/6JRj obese mice after 4 months of high fat feeding (1509 ± 224 mg/10g BW for old-CD1 mice *versus* 1366 ± 67 mg/10g BW for C57BL/6JRj fed a HFD for 4 months, and 391 +/-15 mg/10g BW for the healthy CD1-Swiss mice used in the first study) (**Table 15**) so these mice indeed represented a good model of spontaneous and well-established obesity. In these obese mice, *myo*-inositol supplementation failed to decrease white adipose tissue mass. This result is in accordance with the proposed mechanism of action of *myo*-inositol (i.e. reduction in *de novo* lipogenesis through reduction in FAS activity, and no effect on lipolysis) that prevent fat accretion rather than stimulate fat destocking. In conclusion, *myo*-inositol supplementation is more efficient in prevention of weight gain rather than in treatment of overweight or obesity.

5.3.2 MI supplementation did not improve insulin sensitivity in old and obese mice

According to the insulin tolerance test performed on old CD-1 Swiss mice after one week of oral *myo*-inositol supplementation or not (**Fig. 47**), mice were poorly sensitive to insulin action and *myo*-inositol supplementation did not improve mice response to insulin stimulation. In accordance, we found no additive effect of insulin and acute *in vivo myo*-inositol stimulation on PKB-Akt activation level in liver or gastrocnemius muscle of another group of obese CD-1 mice (**Fig. 48 A** and **B**). As discussed earlier, if *myo*-inositol insulin-sensitizing activity depends on its conversion to DCI and/or integration into IPGs and release as inositol glycan second messenger of insulin, its action may be mitigated in conditions of insulin-resistance or reduced insulin sensitivity because these events are stimulated by insulin. This is confirmed by the observation that DCI-IPG release is uncoupled with insulin stimulation in obese women with PCOS and so insulin-resistance (Baillargeon et al. 2010). Another possible explanation is that *myo*-inositol action on insulin sensitivity in the long term seems to be in good part related to its effect on fat mass. Indeed, in the previous studies performed on mice with chronic *myo*-inositol supplementation, the improvement in insulin sensitivity observed was always well correlated with the fat mass. The fact that no improvement in insulin sensitivity was obtained in obese mice in which fat mass was not either altered by *myo*-inositol supplementation, confirms this hypothesis.

5.4 *In vitro* experiments on cells cultured in high glucose medium failed to show any direct effect of *myo*-inositol

All *in vitro* experiments on C2C12 muscle cells and 3T3-L1 adipocytes (**Fig. 49-51**) were performed in high glucose culture medium (4.5 g.L^{-1} i.e. about 25 mM) and could not have been done in low glucose culture medium because cells cannot survive 24 hours in such conditions. However, as stated earlier, glucose competitively inhibits *myo*-inositol uptake by cells (with a Ki of 21 mM in mouse cerebral microvessel endothelial cells (Yorek et al. 1991)) and so causes a reduction in *myo*-inositol uptake. In such conditions, it is then possible that not enough *myo*-inositol enters into cells to be efficient in improving insulin sensitivity, reducing *de novo* lipogenesis or improving cells anti-oxydant defenses. As consequence, cells cultured in high glucose medium does not seem to be a suitable model to

147

experiment direct effects of *myo*-inositol on a particular tissue or cell type. Accordingly, in studies of other research groups, *myo*-inositol treatment (1 mM, 15 min) of L6 myotubes did not stimulate 2-deoxyglucose uptake (Yap et al. 2007) while an *in vivo* administration (1 g.kg^{-1} BW) enhanced GLUT-4 translocation to the plasma membrane in baseline condition and in response to a glucose load (Dang et al. 2010). *Ex vivo* experiments on isolated organs incubated in 1 g.L^{-1} glucose culture medium are then more suitable for such experiments but only enables acute treatments. Chronic effect can then only be tested *in vivo* and so systemic or direct effects on a special tissue cannot be dissociated.

5.5 Parallel with human studies

5.5.1 Evidences from clinical studies with *myo*-inositol

Human studies with *myo*-inositol were mainly performed in women with Polycytsic Ovary Syndrome, and the six randomized controlled trials are reviewed in (Unfer et al. 2012) and recapitulated in the table from the same review (See **Table 1 in Supplements** of this manuscript). Polycystic ovary syndrome (PCOS) is a common endocrine and metabolic disorder affecting 5-10 % of women in reproductive age and characterized by hyperandrogensim, polycystic ovaries and ovulatory dysfunction. Insulin resistance with compensatory hyperinsulinemia and central obesity are frequent metabolic features associated with PCOS and are key factors in the pathogenesis of anovulation and hyperandrogenism. Indeed, hyperinsulinemia could produce hyperandrogenism in PCOS women via two distinct and independent mechanisms: 1) by stimulating androgen production by the ovary and 2) by directly reducing the liver secretion of testosterone transporter (SHBG for Sex Hormon Binding Globulin) thereby reducing its serum level (Bremer 2010). Hence, improving insulin-sensitivity in these women often reduce hyperinsulinemia, hyperandrogenism, and restores ovulatory function. *myo*-Inositol 2-4 g per day supplement for at least 12 to 16 weeks indeed improved metabolic (reduced HOMA-IR index and/or reduction of the AUC of glucose and insulin during an oral GTT, decrease in systolic and diastolic blood pressure, in plasma triglycerides, LDL and total cholesterol levels and increase in HDL cholesterol level (Gerli et al. 2007; Costantino et al. 2009) and hormonal parameters (decreased LH, FSH, and testosterone circulating levels, and increased SHBG, estrogens and progesterone circulating levels (Papaleo et al. 2007; Genazzani et al. 2008; Gerli et al. 2007; Artini et al. 2013)), and restored spontaneous ovarian activity (ovulation and menstrual cyclicity) and fertility in most women with PCOS.

148

Hence **Unfer et al provided level Ia evidence[2] of *myo*-inositol effectiveness as first line treatment for PCOS** (with a dosage of 2-4 g/day for 12-16 weeks in those studies and no side effects reported in these conditions)**, with an action mainly based on its insulin-sensitizing activity which has a positive effect on the reproductive axis.**

Other human studies were done recently in pregnant women with or at risk of developing a gestational diabetes, and in post-menopausal women with metabolic syndrome. These studies are recapitulated in **supplementary Table 2**. A supplement of MI (2-4 g/day) to a controlled diet for 8 weeks in gestational diabetes (Corrado et al. 2011) and for 6 to 12 months in post-menopausal women with Metabolic Syndrome (Santamaria et al. 2012; Giordano et al. 2011) further improved fasting serum insulin and blood glucose levels, and consequently the HOMA-IR index compared to the diet treatment alone (-75% at 6 and 12 months compared to baseline in post-menopausal women with MI vs. -42% for the placebo group with the diet only ; about -50% at 8 weeks with MI in women with gestational diabetes vs. -29% in the placebo group with diet only). In pregnant women with a family history of Type 2 Diabetes (D'Anna et al. 2013), a 4 g/day MI supplement throughout the pregnancy also significantly reduced the fasting and 1h-glycemia at OGTT, and reduced the incidence of gestational diabetes by 40% (6% cases vs 15.3% in the placebo group). **A reduction of 65% of the risk for gestational diabetes (odd ratios 0.35) with MI was registered in this study.** The improvement in glucose control obtained in the women supplemented with MI resulted in a significant reduction of some hyperglycemia-related pregnancy outcomes, in particular fetal macrosomia and high mean fetal weight. In postmenopausal women, the cardiovascular risk parameters were also further improved with the MI supplement with a reduction in blood pressure, in total and LDL-cholesterol, in serum triglycerides (-34%) and an enhancement of the HDL-cholesterol (+21%). Finally, **after 6 months or one year of supplementation, the MI added to the diet of the post-menopausal women improved significantly almost all the metabolic parameters studied compared to the placebo group and even treated the Metabolic Syndrome of 20% of the women of the study group** (8 on 40) while only one patient on 40 (2.5%) had no longer a metabolic syndrome in the placebo group with the diet alone.

Finally, all the randomized controlled trials performed with *myo*-inositol supplementation (2-4g per day) in complement of a controlled diet showed positive results with mainly an improvement in insulin sensitivity (HOMA-IR reduction, 1h glycaemia after OGTT reduced), in lipid profiles and blood pressure, reducing the risk of type 2 diabetes and cardiovascular events.

---

[2] According to the Centre for Evidence-Based Medicine (CEMB), a level 1a evidence for a therapy effectiveness or inefficiency is provided by systematic reviews (with homogeneity) of Randomized Controlled Trials.

5.5.2 Comparison with our results

Ours results are globally consistent with the humans studies performed with *myo*-inositol dietary supplementation, in that they show an insulin-sensitizing effect in the long term. The one-year clinical trial (Santamaria et al. 2012) on post-menopausal women with metabolic syndrome also showed a reduction in the Body Mass Index (reduction from 31.5 ± 2.4 to 30.2 ± 1.1 kg.m^{-2}) and in the Waist Circumference (from 115 ± 12 to 107 ± 2.8 cm) with *myo*-inositol plus controlled diet (while no effect was obtained with diet alone), confirming the effect we found on white adipose tissue. However, the effect of *myo*-inositol on adipose tissue mass is less important in humans than in mice. This can be explained by the fact that *myo*-inositol apparently acts on white adipose tissue *de novo* lipogenesis and it has been shown that this process is much lower in humans compared with rodents (according to many, the liver is the main site of lipogenesis in the human). Indeed, under comparable dietary conditions, lipogenesis is about 5 times lower in pieces of human adipose tissue versus pieces of rat under comparable dietary conditions (Swierczynski et al. 2000). Rat adipose tissue exhibits higher lipogenic potential than human adipose tissue (Letexier et al. 2003). These differences (both in lipogenic enzyme activities and in the rate of lipogenesis itself) are not surprising, because the rodents are known to be metabolically more active than the human.

An additional explanation is that post-menopausal women were already overweighed (BMI > 30 kg.m^{-2}) before starting the *myo*-inositol supplementation and, as we showed in our study on obese old mice, *myo*-inositol is more efficient in prevention than in treatment of weight gain due to its anti-lipogenic rather than pro-lipolytic activity. In accordance with this view, Gerli et al. (Gerli et al. 2007) noticed an inverse relationship between body mass and treatment efficacy, concerning the metabolic risk factors, and even a lack of response to *myo*-inositol supplementation in the morbidly obese (BMI > 37 kg.m^{-2}, mean BMI = 42.6 kg.m^{-2}) sub-group of women with PCOS. Indeed, it was observed that morbidly obese women showed a similar number of ovulations during 16-wk *myo*-inositol treatment to the leaner women (BMI < 37 kg.m^{-2}, mean BMI = 29.2 kg.m^{-2}), but they showed no indication of changes in either BMI or HDL cholesterol. In contrast a little but significant weight loss (p<0.01) was recorded in the *myo*-inositol group of leaner women, whereas the placebo group actually increased weight (p<0.05). Associated with the weight loss were significant reductions in circulating leptin and increased HDL cholesterol concentrations in the *myo*-inositol-treated group. Noteworthy, in this study on obese or morbidly obese PCOS women, no change in fasting glucose concentrations, fasting insulin, or insulin responses to glucose challenge was recorded after 14 weeks of treatments. This is consistent with the result of our ITT and PKB-Akt western blotting on old and spontaneously obese CD-1 mice.

150

Taken together**, these results support the notion that *myo*-inositol efficiency is inversely related to body mass index and/or insulin resistance**. This supports the hypothesis of Larner and colleagues according to which *myo*-inositol would be converted to DCI *in vivo* and then incorporated into DCI-IPGs. Indeed, since both MI to DCI epimerase activity and inositol-glycan second messenger release from plasma membrane DCI-IPGs would be stimulated by insulin, this could explain why *myo*-inositol is more efficient in healthy (i.e. insulin sensitive) mice or subjects, than in insulin resistant and obese mice or subjects. Combination of *myo*-inositol with other insulin sensitizing agent (e.g. metformin) or with DCI in a physiological ratio would probably potentiate *myo*-inositol supplementation effect. Supporting this view, metformin treatment enhanced the insulin-stimulated release of DCI-IPG mediators in obese women with PCOS. Combining *myo*-inositol with a balanced diet and/or a physical activity probably also improves its efficiency. Noteworthy, all the human studies were performed in complement of a controlled diet and show that, in this context, *myo*-inositol supplementation can prevent gestational diabetes development, reduce the incidence of metabolic syndrome in post-menopausal women and nearly treat PCOS.

Conclusion

myo-Inositol supplementation improves insulin sensitivity, reduces fat storage and seems to enhance anti-oxydant defenses (See **Fig. 52**). Improvement in insulin sensitivity probably results from acute effects of *myo*-inositol on insulin signaling through DCI-IPGs mediators in conditions of insulin stimulation (i.e. postprandial condition, exogenous insulin stimulation), but also from long term effects of *myo*-inositol on white adipose tissue (correlation between BMI or WAT weight and insulin sensitivity). *myo*-Inositol effect on white adipose tissue seems to be related to a reduction in *de novo* lipogenesis enzymes activity (i.e. FAS and possibly also ACC) and maybe expression. This may explain why *myo*-inositol treatment is less efficient in conditions of impaired insulin sensitivity and obesity. Moreover, since *myo*-inositol cellular uptake is competitively inhibited by glucose, its effect may be also mitigated by hyperglycemia and chronic overfeeding. However, *myo*-inositol supplementation could help to counteract the hyperglycemia-induced inositol intracellular depletion in some tissues of diabetes subjects. Since such inositol metabolism abnormalities are sometimes related to cellular dysfunctions (e.g. impairment in nerve conduction velocity), *myo*-inositol supplementation could help restoring intracellular inositol pools and some cellular functions.

Finally, if associated to a controlled and rather balanced diet, *myo*-inositol supplementation could be beneficial in prevention of insulin resistance or weight gain, or as first line treatment for women with PCOS. However, it does not seem to be a good strategy for the treatment of an already established insulin resistance, diabetes and/or obesity. Combining it with other insulin-sensitizing strategies may improve its efficiency and possibly help reducing other insulin-sensitizing drugs dosages. Additional clinical studies should be done in people at genetic risk of developing a type 2 diabetes, or in people with slight insulin resistance (in both men and women, and out of women with PCOS) to conclude on the relevance and therapeutic interest of *myo*-inositol supplementation in such conditions.
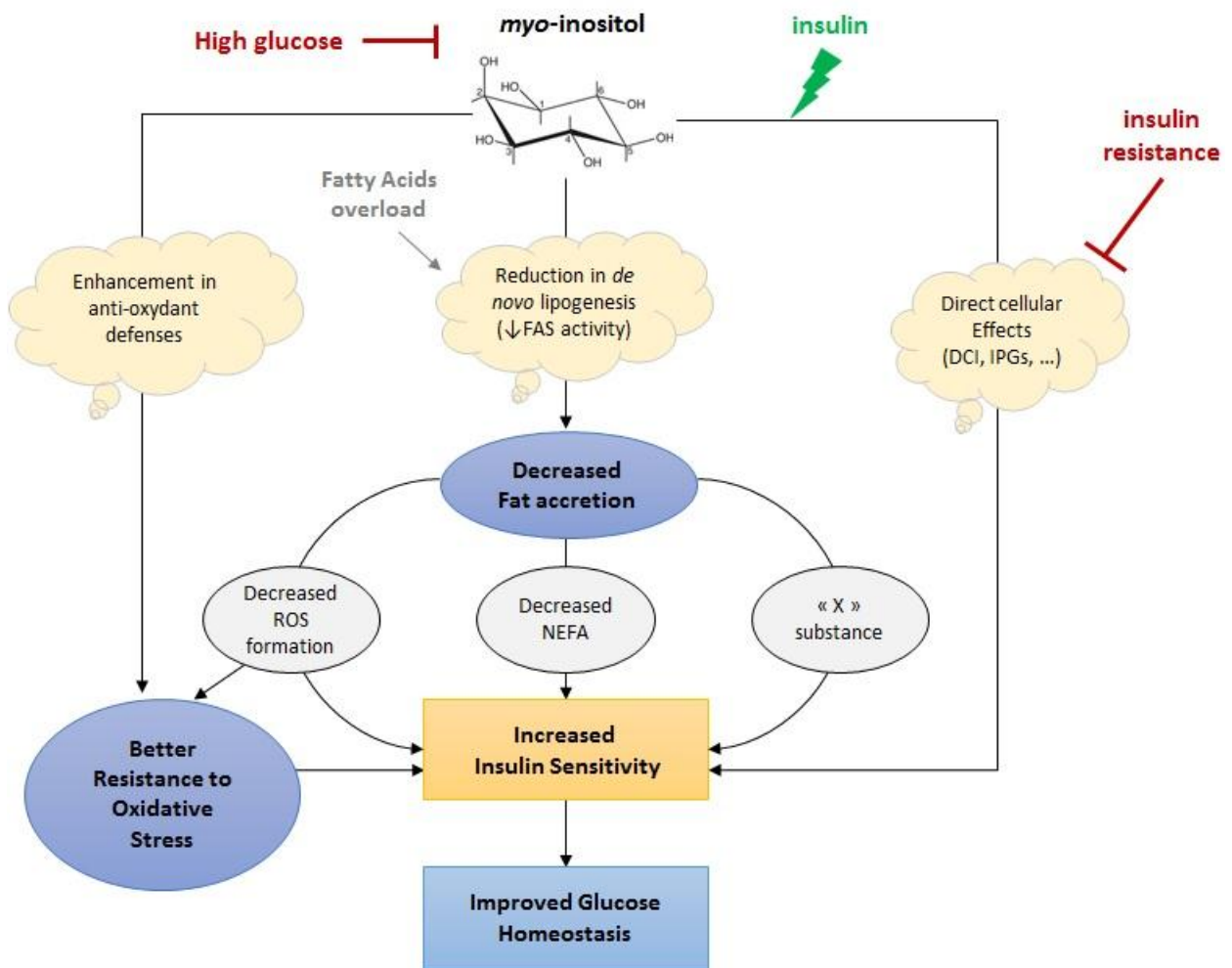
Figure 52 – Summary diagram of *myo*-inositol effects evidenced in the mice studies and putative underlying mechanisms of action. Abbreviations: DCI, D-*chiro*-inositol ; FAS, fatty acid synthase, IPGs, inositol phospho-glycans, NEFA, non-esterified fatty acids, ROS, reactive oxygen species.

References

Aguila, M.B. & Mandarim-de-Lacerda, C.A., 2003. Heart and blood pressure adaptations in Wistar rats fed with different high-fat diets for 18 months. *Nutrition (Burbank, Los Angeles County, Calif.)*, 19(4), p.347‑352.

Aguirre, V. et al., 2002. Phosphorylation of Ser307 in insulin receptor substrate-1 blocks interactions with the insulin receptor and inhibits insulin action. *The Journal of biological chemistry*, 277(2), p.1531‑1537.

Aguirre, V. et al., 2000. The c-Jun NH(2)-terminal kinase promotes insulin resistance during association with insulin receptor substrate-1 and phosphorylation of Ser(307). *The Journal of biological chemistry*, 275(12), p.9047‑9054.

Ahmad, F. et al., 1997. Alterations in skeletal muscle protein-tyrosine phosphatase activity and expression in insulin-resistant human obesity and diabetes. *The Journal of clinical investigation*, 100(2), p.449‑458.

Ahmad, F., Considine, R.V. & Goldstein, B.J., 1995. Increased abundance of the receptor-type protein-tyrosine phosphatase LAR accounts for the elevated insulin receptor dephosphorylating activity in adipose tissue of obese human subjects. *The Journal of clinical investigation*, 95(6), p.2806‑2812.

Ahmad, F. & Goldstein, B.J., 1995. Increased abundance of specific skeletal muscle protein-tyrosine phosphatases in a genetic model of insulin-resistant obesity and diabetes mellitus. *Metabolism: clinical and experimental*, 44(9), p.1175‑1184.

Alzoubi, K.H. et al., 2013. Vitamin E prevents high-fat high-carbohydrates diet-induced memory impairment: The role of oxidative stress. *Physiology & behavior*, 119C, p.72‑78.

Andrews, E.J., Ward, B.C. & Altman, N.H., 1980. *Spontaneous Animal Models of Human Disease*, Elsevier.

Andrews, P. et al., 1992. No effect of high sucrose diets on the kidneys of Wister Kyoto (WKY) rats. *Geriatric Nephrology and Urology*, 2(1), p.35‑42.

Anon, 2010. Diagnosis and Classification of Diabetes Mellitus. *Diabetes Care*, 33(Suppl 1), p.S62‑S69.

Anon, 2003. Gestational Diabetes Mellitus. *Diabetes Care*, 26(suppl 1), p.s103‑s105.

Anon, 1996. Inositol Material Safety Data Sheet. MSDS number 12480.

Ansar, H. et al., 2011. Effect of alpha-lipoic acid on blood glucose, insulin resistance and glutathione peroxidase of type 2 diabetic patients. *Saudi Medical Journal*, 32(6), p.584‑588.

Arora, S., Ojha, S.K. & Vohora, D., 2009. Characterisation of streptozotocin induced diabetes mellitus in Swiss albino mice. *Global J Pharmacol*, 3(2), p.81–84.

Artini, P.G. et al., 2013. Endocrine and clinical effects of myo-inositol administration in policystyc ovary syndrome. A randomized study. *Gynecological Endocrinology*, p.1‑5.

Asplin, I., Galasko, G. & Larner, J., 1993. chiro-inositol deficiency and insulin resistance: a comparison of the chiro-inositol- and the myo-inositol-containing insulin mediators isolated from urine, hemodialysate, and muscle of control and type II diabetic subjects. *Proceedings of the National Academy of Sciences of the United States of America*, 90(13), p.5924‑5928.

Axelsen, L.N. et al., 2010. Cardiac and metabolic changes in long-term high fructose-fat fed rats with severe obesity and extensive intramyocardial lipid accumulation. *American journal of physiology. Regulatory, integrative and comparative physiology*, 298(6), p.R1560‑1570.

Baillargeon, J.-P. et al., 2010. Uncoupling Between Insulin and Release of a D-Chiro-Inositol–Containing Inositolphosphoglycan Mediator of Insulin Action in Obese Women With Polycystic Ovary Syndrome. *Metabolic Syndrome and Related Disorders*, 8(2), p.127‑136.

Barbour, L.A. et al., 2007. Cellular Mechanisms for Insulin Resistance in Normal Pregnancy and Gestational Diabetes. *Diabetes Care*, 30(Supplement_2), p.S112‑S119.

Barg, S. et al., 2002. A subset of 50 secretory granules in close contact with L-type Ca2+ channels accounts for first-phase insulin secretion in mouse beta-cells. *Diabetes*, 51 Suppl 1, p.S74‑82.

Basciano, H., Federico, L. & Adeli, K., 2005. Fructose, insulin resistance, and metabolic dyslipidemia. *Nutrition & metabolism*, 2(1), p.5.

Bashan, N. et al., 2009. Positive and negative regulation of insulin signaling by reactive oxygen and nitrogen species. *Physiological Reviews*, 89(1), p.27‑71.

Bates, S.H., Jones, R.B. & Bailey, C.J., 2000. Insulin-like effect of pinitol. *British journal of pharmacology*, 130(8), p.1944‑1948.

Bazin, R. & Ferré, P., 2001. Assays of lipogenic enzymes. *Methods in molecular biology (Clifton, N.J.)*, 155, p.121‑127.

Becker, W. et al., 2004. Differential hepatic gene expression in a polygenic mouse model with insulin resistance and hyperglycemia: evidence for a combined transcriptional dysregulation of gluconeogenesis and fatty acid synthesis. *Journal of Molecular Endocrinology*, 32(1), p.195‑208.

Beemster, P., Groenen, P. & Steegers-Theunissen, R., 2002. Involvement of inositol in reproduction. *Nutrition reviews*, 60(3), p.80‑87.

Benjamin, J., Levine, J., et al., 1995. Double-blind, placebo-controlled, crossover trial of inositol treatment for panic disorder. *The American Journal of Psychiatry*, 152(7), p.1084‑1086.

Benjamin, J., Agam, G., et al., 1995. Inositol treatment in psychiatry. *Psychopharmacology Bulletin*, 31(1), p.167‑175.

Benjamins, J.A. & Agranoff, B.W., 1969. Distribution and properties of CDP-diglyceride:inositol transferase from brain. *Journal of neurochemistry*, 16(4), p.513‑527.

Van den Bergh, A. et al., 2008. Dyslipidaemia in type II diabetic mice does not aggravate contractile impairment but increases ventricular stiffness. *Cardiovascular research*, 77(2), p.371‑379.

Bernardis, L.L. & Patterson, B.D., 1968. Correlation between « Lee index » and carcass fat content in weanling and adult female rats with hypothalamic lesions. *The Journal of endocrinology*, 40(4), p.527‑528.

Beyer-Mears, A. et al., 1992. Myo-inositol transport in the lens of galactose-maintained rats. *Current eye research*, 11(1), p.25‑34.

Bigorgne, A.E. et al., 2008. Obesity-induced lymphocyte hyperresponsiveness to chemokines: a new mechanism of Fatty liver inflammation in obese mice. *Gastroenterology*, 134(5), p.1459‑1469.

Bocarsly, M.E. et al., 2010. High-fructose corn syrup causes characteristics of obesity in rats: increased body weight, body fat and triglyceride levels. *Pharmacology, biochemistry, and behavior*, 97(1), p.101‑106.

Boden, G. et al., 1994. Mechanisms of fatty acid-induced inhibition of glucose uptake. *The Journal of Clinical Investigation*, 93(6), p.2438‑2446.

Bogardus, C. et al., 1985. Relationship between degree of obesity and in vivo insulin action in man. *The American Journal of Physiology*, 248(3 Pt 1), p.E286‑291.

Bonner-Weir, S. et al., 1989. Compensatory growth of pancreatic beta-cells in adult rats after short-term glucose infusion. *Diabetes*, 38(1), p.49‑53.

Borg, M.L. et al., 2011. Pigment epithelium-derived factor regulates lipid metabolism via adipose triglyceride lipase. *Diabetes*, 60(5), p.1458‑1466.

Bosco, D. et al., 2010. Unique Arrangement of α- and β-Cells in Human Islets of Langerhans. *Diabetes*, 59(5), p.1202‑1210.

Bosco, D., Orci, L. & Meda, P., 1989. Homologous but not heterologous contact increases the insulin secretion of individual pancreatic B-cells. *Experimental Cell Research*, 184(1), p.72‑80.

Bray, G.A., Nielsen, S.J. & Popkin, B.M., 2004. Consumption of high-fructose corn syrup in beverages may play a role in the epidemic of obesity. *The American journal of clinical nutrition*, 79(4), p.537‑543.

Bremer, A.A., 2010. Polycystic ovary syndrome in the pediatric population. *Metabolic syndrome and related disorders*, 8(5), p.375‑394.

Brüning, J.C. et al., 1997. Development of a novel polygenic model of NIDDM in mice heterozygous for IR and IRS-1 null alleles. *Cell*, 88(4), p.561‑572.

Buettner, R. et al., 2006. Defining high-fat-diet rat models: metabolic and molecular effects of different fat types. *Journal of molecular endocrinology*, 36(3), p.485‑501.

Campbell, W.W. et al., 2004. Pinitol supplementation does not affect insulin-mediated glucose metabolism and muscle insulin receptor content and phosphorylation in older humans. *The Journal of nutrition*, 134(11), p.2998‑3003.

Cani, P.D. et al., 2007. Metabolic Endotoxemia Initiates Obesity and Insulin Resistance. *Diabetes*, 56(7), p.1761‑1772.

Carey, D.G. et al., 1996. Abdominal fat and insulin resistance in normal and overweight women: Direct measurements reveal a strong relationship in subjects at both low and high risk of NIDDM. *Diabetes*, 45(5), p.633 ‑638.

Carlomagno, G. et al., 2011. Contribution of myo-inositol and melatonin to human reproduction. *European Journal of Obstetrics & Gynecology and Reproductive Biology*, 159(2), p.267‑272.

Carlomagno, G. & Unfer, V., 2011. Inositol safety: clinical evidences. *European review for medical and pharmacological sciences*, 15(8), p.931‑936.

Chaabo, F. et al., 2010. Nutritional correlates and dynamics of diabetes in the Nile rat (Arvicanthis niloticus): a novel model for diet-induced type 2 diabetes and the metabolic syndrome. *Nutrition & metabolism*, 7, p.29.

Chang, H.-H.G., 2011. *Mechanisms underlying the abnormal inositol metabolisms in diabetes mellitus.* PhD in Mathematics. Auckland: University of Auckland. 216 pages. Available at: https://researchspace.auckland.ac.nz/handle/2292/7154 [Consulté le janvier 30, 2013].

Chang, L., Chiang, S.-H. & Saltiel, A.R., 2004. Insulin Signaling and the Regulation of Glucose Transport. *Molecular Medicine*, 10(7-12), p.65‑71.

Chang-Chen, K.J., Mullur, R. & Bernal-Mizrachi, E., 2008. β-cell failure as a complication of diabetes. *Reviews in Endocrine and Metabolic Disorders*, 9(4), p.329‑343.

Chatzigeorgiou, A. et al., 2009. The Use of Animal Models in the Study of Diabetes Mellitus. *In Vivo*, 23(2), p.245‑258.

Chau, J.F.L. et al., 2005. Sodium/myo-inositol cotransporter-1 is essential for the development and function of the peripheral nerves. *FASEB journal: official publication of the Federation of American Societies for Experimental Biology*, 19(13), p.1887‑1889.

Chen, J. et al., 2009. Rhaponticin from Rhubarb Rhizomes Alleviates Liver Steatosis and Improves Blood Glucose and Lipid Profiles in KK/Ay Diabetic Mice. *Planta Medica*, 75(05), p.472‑477.

Chen, L. et al., 2002. [The early pathological changes of KKAy mice with type 2 diabetes]. *Acta Academiae Medicinae Sinicae*, 24(1), p.71‑75.

Cheung, A. et al., 1999. Marked impairment of protein tyrosine phosphatase 1B activity in adipose tissue of obese subjects with and without type 2 diabetes mellitus. *The Journal of laboratory and clinical medicine*, 134(2), p.115‑123.

Chirala, S.S., 1992. Coordinated regulation and inositol-mediated and fatty acid-mediated repression of fatty acid synthase genes in Saccharomyces cerevisiae. *Proceedings of the National Academy of Sciences of the United States of America*, 89(21), p.10232‑10236.

Choi, K. & Kim, Y.-B., 2010. Molecular Mechanism of Insulin Resistance in Obesity and Type 2 Diabetes. *The Korean Journal of Internal Medicine*, 25(2), p.119.

Choi, M.-S. et al., 2009. Metabolic response of soy pinitol on lipid-lowering, antioxidant and hepatoprotective action in hamsters fed-high fat and high cholesterol diet. *Molecular nutrition & food research*, 53(6), p.751‑759.

Chun, M.-R. et al., 2010. Differential effects of high-carbohydrate and high-fat diet composition on muscle insulin resistance in rats. *Journal of Korean medical science*, 25(7), p.1053‑1059.

Chung, C. et al., 2008. Anti-angiogenic pigment epithelium-derived factor regulates hepatocyte triglyceride content through adipose triglyceride lipase (ATGL). *Journal of Hepatology*, 48(3), p.471‑478.

Ciotta, L. et al., 2011. Effects of myo-inositol supplementation on oocyte's quality in PCOS patients: a double blind trial. *European review for medical and pharmacological sciences*, 15(5), p.509‑514.

Clements, R.S. & Darnell, B., 1980. Myo-inositol content of common foods: development of a high-myo-inositol diet. *The American Journal of Clinical Nutrition*, 33(9), p.1954‑1967.

Clements, R.S. & Stockard, C.R., 1980. Abnormal Sciatic Nerve Myo-inositol Metabolism in the Streptozotocin-diabetic Rat: Effect of Insulin Treatment. *Diabetes*, 29(3), p.227‑235.

Coelho, M.S. et al., 2010. High sucrose intake in rats is associated with increased ACE2 and angiotensin-(1-7) levels in the adipose tissue. *Regulatory peptides*, 162(1-3), p.61‑67.

Condorelli, R.A. et al., 2011. Effects of myoinositol on sperm mitochondrial function in-vitro. *European review for medical and pharmacological sciences*, 15(2), p.129‑134.

Condorelli, R.A. et al., 2012. Myoinositol: does it improve sperm mitochondrial function and sperm motility? *Urology*, 79(6), p.1290‑1295.

Coon, P.J. et al., 1992. Role of body fat distribution in the decline in insulin sensitivity and glucose tolerance with age. *Journal of Clinical Endocrinology & Metabolism*, 75(4), p.1125 ‑1132.

Copps, K.D. & White, M.F., 2012. Regulation of insulin sensitivity by serine/threonine phosphorylation of insulin receptor substrate proteins IRS1 and IRS2. *Diabetologia*, 55(10), p.2565‑2582.

Corrado, F. et al., 2011. The effect of myoinositol supplementation on insulin resistance in patients with gestational diabetes. *Diabetic medicine: a journal of the British Diabetic Association*, 28(8), p.972‑975.

Costantino, D. et al., 2009. Metabolic and hormonal effects of myo-inositol in women with polycystic ovary syndrome: a double-blind trial. *European review for medical and pharmacological sciences*, 13(2), p.105‑110.

Couturier, K. et al., 2010. Cinnamon improves insulin sensitivity and alters the body composition in an animal model of the metabolic syndrome. *Archives of biochemistry and biophysics*, 501(1), p.158‑161.

Croze, M.L. & Soulage, C.O., 2013. Potential role and therapeutic interests of myo-inositol in metabolic diseases. *Biochimie*.

Curry, D.L., Bennett, L.L. & Grodsky, G.M., 1968. Dynamics of insulin secretion by the perfused rat pancreas. *Endocrinology*, 83(3), p.572‑584.

D'Anna, R. et al., 2013. myo-Inositol Supplementation and Onset of Gestational Diabetes Mellitus in Pregnant Women With a Family History of Type 2 Diabetes: A prospective, randomized, placebo-controlled study. *Diabetes care*.

Dai, Z. et al., 2011. Sodium/myo-inositol cotransporter 1 and myo-inositol are essential for osteogenesis and bone formation. *Journal of bone and mineral research: the official journal of the American Society for Bone and Mineral Research*, 26(3), p.582‑590.

Dang, N.T. et al., 2010. D-pinitol and myo-inositol stimulate translocation of glucose transporter 4 in skeletal muscle of C57BL/6 mice. *Bioscience, biotechnology, and biochemistry*, 74(5), p.1062‑1067.

Daughaday, W.H. & Larner, J., 1954. The renal excretion of inositol in normal and diabetic human beings. *The Journal of clinical investigation*, 33(3), p.326‑332.

Daughaday, W.H., Larner, J. & Houghton, E., 1954. The renal excretion of inositol by normal and diabetic rats 1. *Journal of Clinical Investigation*, 33(8), p.1075‑1080.

Davis, A. et al., 2000. Effect of pinitol treatment on insulin action in subjects with insulin resistance. *Diabetes care*, 23(7), p.1000‑1005.

Dawes, A.T., 2006. *Phosphoinositides and Rho proteins conspire to spatially regulate actin polymerization in motile cells*. PhD in Mathematics. Vancouver: University of British Columbia. 182 pages.

Deji, N. et al., 2009. Structural and functional changes in the kidneys of high-fat diet-induced obese mice. *American journal of physiology. Renal physiology*, 296(1), p.F118‑126.

Deranieh, R.M. & Greenberg, M.L., 2009. Cellular consequences of inositol depletion. *Biochemical Society transactions*, 37(Pt 5), p.1099‑1103.

Diani, A.R. et al., 1987. The KKAy Mouse: A Model for the Rapid Development of Glomerular Capillary Basement Membrane Thickening. *Journal of Vascular Research*, 24(6), p.297‑303.

Dobrzyn, P. et al., 2010. Loss of stearoyl-CoA desaturase 1 rescues cardiac function in obese leptin-deficient mice. *Journal of lipid research*, 51(8), p.2202‑2210.

Doubal, S. & Klemera, P., 1997. Practical methodology of evaluation of mortality curves and detection of aging-related interventions. *AGE*, 20(4), p.229‑233.

Dubuc, P.U., 1976. The development of obesity, hyperinsulinemia, and hyperglycemia in ob/ob mice. *Metabolism: clinical and experimental*, 25(12), p.1567‑1574.

Duckworth, W.C., Bennett, R.G. & Hamel, F.G., 1998. Insulin Degradation: Progress and Potential. *Endocrine Reviews*, 19(5), p.608‑624.

Eagle, H. et al., 1956. Myo-inositol as an essential growth factor for normal and malignant human cells in tissue culture. *Science (New York, N.Y.)*, 123(3202), p.845‑847.

Eisenberg Jr., F. & Bolden, A.H., 1963. Biosynthesis of inositol in rat testis homogenate. *Biochemical and Biophysical Research Communications*, 12(1), p.72‑77.

Eizirik, D.L., Cardozo, A.K. & Cnop, M., 2008. The Role for Endoplasmic Reticulum Stress in Diabetes Mellitus. *Endocrine Reviews*, 29(1), p.42‑61.

Etherton, T.D., Thompson, E.H. & Allen, C.E., 1977. Improved techniques for studies of adipocyte cellularity and metabolism. *Journal of Lipid Research*, 18(4), p.552‑557.

Farese, R.V. et al., 1994. Insulin-induced activation of glycerol-3-phosphate acyltransferase by a chiro-inositol-containing insulin mediator is defective in adipocytes of insulin-resistant, type II

diabetic, Goto-Kakizaki rats. *Proceedings of the National Academy of Sciences of the United States of America*, 91(23), p.11040‑11044.

Federici, M. et al., 2001. High glucose causes apoptosis in cultured human pancreatic islets of Langerhans: a potential role for regulation of specific Bcl family genes toward an apoptotic cell death program. *Diabetes*, 50(6), p.1290‑1301.

Ferrannini, E. et al., 1983. Effect of fatty acids on glucose production and utilization in man. *The Journal of Clinical Investigation*, 72(5), p.1737‑1747.

Folch, J., Lees, M. & Sloane Stanley, G.H., 1957. A simple method for the isolation and purification of total lipides from animal tissues. *The Journal of Biological Chemistry*, 226(1), p.497‑509.

Fonteles, M.C., Almeida, M.Q. & Larner, J., 2000. Antihyperglycemic effects of 3-O-methyl-D-chiro-inositol and D-chiro-inositol associated with manganese in streptozotocin diabetic rats. *Hormone and metabolic research*, 32(4), p.129‑132.

Fu, H. et al., 2012. Contributions in astrocytes of SMIT1/2 and HMIT to myo-inositol uptake at different concentrations and pH. *Neurochemistry international*, 61(2), p.187‑194.

Furukawa, S. et al., 2004. Increased oxidative stress in obesity and its impact on metabolic syndrome. *The Journal of Clinical Investigation*, 114(12), p.1752‑1761.

Gabriely, I. et al., 2002. Removal of Visceral Fat Prevents Insulin Resistance and Glucose Intolerance of Aging. *Diabetes*, 51(10), p.2951 ‑2958.

Galletta, M. et al., 2011. Bye-bye chiro-inositol - myo-inositol: true progress in the treatment of polycystic ovary syndrome and ovulation induction. *European review for medical and pharmacological sciences*, 15(10), p.1212‑1214.

Gastaldelli, A. et al., 2002. Metabolic Effects of Visceral Fat Accumulation in Type 2 Diabetes. *Journal of Clinical Endocrinology & Metabolism*, 87(11), p.5098 ‑5103.

Geethan, P.K.M.A. & Prince, P.S.M., 2008. Antihyperlipidemic effect of D-pinitol on streptozotocin-induced diabetic Wistar rats. *Journal of biochemical and molecular toxicology*, 22(4), p.220‑224.

Genazzani, A.D. et al., 2008. Myo-inositol administration positively affects hyperinsulinemia and hormonal parameters in overweight patients with polycystic ovary syndrome. *Gynecological endocrinology: the official journal of the International Society of Gynecological Endocrinology*, 24(3), p.139‑144.

Gerich, J.E., 2002. Is reduced first-phase insulin release the earliest detectable abnormality in individuals destined to develop type 2 diabetes? *Diabetes*, 51 Suppl 1, p.S117‑121.

Gerli, S. et al., 2007. Randomized, double blind placebo-controlled trial: effects of myo-inositol on ovarian function and metabolic factors in women with PCOS. *European review for medical and pharmacological sciences*, 11(5), p.347‑354.

Gerli, S., Mignosa, M. & Di Renzo, G.C., 2003. Effects of inositol on ovarian function and metabolic factors in women with PCOS: a randomized double blind placebo-controlled trial. *European review for medical and pharmacological sciences*, 7(6), p.151‑159.

Giordano, D. et al., 2011. Effects of myo-inositol supplementation in postmenopausal women with metabolic syndrome: a perspective, randomized, placebo-controlled study. *Menopause (New York, N.Y.)*, 18(1), p.102‑104.

Goncalves, A.C. da C. et al., 2009. Diabetic Hypertensive Leptin Receptor–Deficient db/db Mice Develop Cardioregulatory Autonomic Dysfunction. *Hypertension*, 53(2), p.387‑392.

González-Ortiz, L.J., Martínez-Abundis, E. & González-Ortiz, M., 2006. A new model to fit glucose concentration during the insulin tolerance test improving the predictive capability to estimate insulin sensitivity. *Nutrition, Metabolism, and Cardiovascular Diseases: NMCD*, 16(1), p.78‑79.

Goto, Y. & Kakizaki, M., 1981. The Spontaneous-Diabetes Rat: A Model of Noninsulin Dependent Diabetes Mellitus. *Proceedings of the Japan Academy, Series B*, 57(10), p.381‑384.

Graf, E., 1990. Antioxidant functions of phytic acid. *Free Radical Biology and Medicine*, 8, p.61‑69.

Greene, D.A., De Jesus, P.V., Jr & Winegrad, A.I., 1975. Effects of insulin and dietary myoinositol on impaired peripheral motor nerve conduction velocity in acute streptozotocin diabetes. *The Journal of clinical investigation*, 55(6), p.1326‑1336.

Greene, D.A. & Lattimer, S.A., 1982. Sodium- and energy-dependent uptake of myo-inositol by rabbit peripheral nerve. Competitive inhibition by glucose and lack of an insulin effect. *The Journal of clinical investigation*, 70(5), p.1009‑1018.

Van Greevenbroek, M.M.J., Schalkwijk, C.G. & Stehouwer, C.D.A., 2013. Obesity-associated low-grade inflammation in type 2 diabetes mellitus: causes and consequences. *The Netherlands journal of medicine*, 71(4), p.174‑187.

Gual, P., Le Marchand-Brustel, Y. & Tanti, J.-F., 2005. Positive and negative regulation of insulin signaling through IRS-1 phosphorylation. *Biochimie*, 87(1), p.99‑109.

Hamada, Y. et al., 2001. Insulin secretion to glucose as well as nonglucose stimuli is impaired in spontaneously diabetic Nagoya-Shibata-Yasuda mice. *Metabolism*, 50(11), p.1282‑1285.

Haneda, M. et al., 1990. Glucose inhibits myo-inositol uptake and reduces myo-inositol content in cultured rat glomerular mesangial cells. *Metabolism: clinical and experimental*, 39(1), p.40‑45.

Hansen, B.C., Greene, H.L. & Ortmeyer, H.K., 1998. Treatment of diabetes by myo-inositol administration. US Patent Number 5,763,392.

Hauser, G. & Finelli, V.N., 1963. The biosynthesis of free and phosphatide myo-inositol from glucose by mammalian tissue slices. *The Journal of biological chemistry*, 238, p.3224‑3228.

Hecht, M.-L. et al., 2010. Synthetic inositol phosphoglycans related to GPI lack insulin-mimetic activity. *ACS Chemical Biology*, 5(11), p.1075‑1086.

Henquin, J.-C., Boitard, C., et al., 2002. Insulin secretion: movement at all levels. *Diabetes*, 51 Suppl 1, p.S1‑2.

Henquin, J.-C., Ishiyama, N., et al., 2002. Signals and pools underlying biphasic insulin secretion. *Diabetes*, 51 Suppl 1, p.S60‑67.

Hipps, P.P., Holland, W.H. & Sherman, W.R., 1977. Interconversion of myo- and scyllo-inositol with simultaneous formation of neo-inositol by an NADP+ dependent epimerase from bovine brain. *Biochemical and Biophysical Research Communications*, 77(1), p.340‑346.

Hoffman-Kuczynski, B. & Reo, N.V., 2005. Administration of myo-inositol plus ethanolamine elevates phosphatidylethanolamine plasmalogen in the rat cerebellum. *Neurochemical Research*, 30(1), p.47‑60.

Holland, W.L. et al., 2007. Inhibition of Ceramide Synthesis Ameliorates Glucocorticoid-, Saturated-Fat-, and Obesity-Induced Insulin Resistance. *Cell Metabolism*, 5(3), p.167‑179.

Holub, B.J., 1986. Metabolism and function of myo-inositol and inositol phospholipids. *Annual review of nutrition*, 6, p.563‑597.

Hori, H. et al., 2002. Association of SH2-containing inositol phosphatase 2 with the insulin resistance of diabetic db/db mice. *Diabetes*, 51(8), p.2387‑2394.

Howard, C.F., Jr & Anderson, L., 1967. Metabolism of myo-inositol in animals. II. Complete catabolism of myo-inositol-14C by rat kidney slices. *Archives of biochemistry and biophysics*, 118(2), p.332‑339.

Hsu, C.-L. et al., 2009. Phenolic compounds rutin and o-coumaric acid ameliorate obesity induced by high-fat diet in rats. *Journal of agricultural and food chemistry*, 57(2), p.425‑431.

Hu, E. et al., 2000. Identification of a novel kidney-specific gene downregulated in acute ischemic renal failure. *American journal of physiology. Renal physiology*, 279(3), p.F426‑439.

Huang, L.C. et al., 1993. Chiroinositol deficiency and insulin resistance. III. Acute glycogenic and hypoglycemic effects of two inositol phosphoglycan insulin mediators in normal and streptozotocin-diabetic rats in vivo. *Endocrinology*, 132(2), p.652‑657.

Huang, W. et al., 2010. Depletion of liver Kupffer cells prevents the development of diet-induced hepatic steatosis and insulin resistance. *Diabetes*, 59(2), p.347‑357.

Igel, M. et al., 1997. Hyperleptinemia, Leptin Resistance, and Polymorphic Leptin Receptor in the New Zealand Obese Mouse. *Endocrinology*, 138(10), p.4234‑4239.

Isabella, R. & Raffone, E., 2012. Does ovary need D-chiro-inositol? *Journal of ovarian research*, 5(1), p.14.

Iuorno, M.J. et al., 2002. Effects of d-chiro-inositol in lean women with the polycystic ovary syndrome. *Endocrine Practice: Official Journal of the American College of Endocrinology and the American Association of Clinical Endocrinologists*, 8(6), p.417‑423.

Jiang, W.-D. et al., 2011. Myo-inositol prevents copper-induced oxidative damage and changes in antioxidant capacity in various organs and the enterocytes of juvenile Jian carp (Cyprinus carpio var. Jian). *Aquatic Toxicology (Amsterdam, Netherlands)*, 105(3-4), p.543‑551.

Jones, D.R. & Varela-Nieto, I., 1999. Diabetes and the role of inositol-containing lipids in insulin signaling. *Molecular medicine (Cambridge, Mass.)*, 5(8), p.505‑514.

Jornayvaz, F.R. et al., 2011. Hepatic insulin resistance in mice with hepatic overexpression of diacylglycerol acyltransferase 2. *Proceedings of the National Academy of Sciences of the United States of America*, 108(14), p.5748‑5752.

Kagawa, S. et al., 2008. Impact of transgenic overexpression of SH2-containing inositol 5'-phosphatase 2 on glucose metabolism and insulin signaling in mice. *Endocrinology*, 149(2), p.642‑650.

Kahn, S.E., 2003. The relative contributions of insulin resistance and beta-cell dysfunction to the pathophysiology of Type 2 diabetes. *Diabetologia*, 46(1), p.3‑19.

Kanarek, R.B. et al., 1987. Sucrose-induced obesity: effect of diet on obesity and brown adipose tissue. *The American journal of physiology*, 253(1 Pt 2), p.R158‑166.

Kaneki, M. et al., 2007. Nitrosative stress and pathogenesis of insulin resistance. *Antioxidants & redox signaling*, 9(3), p.319‑329.

Kang, M.-J. et al., 2006. Pinitol from soybeans reduces postprandial blood glucose in patients with type 2 diabetes mellitus. *Journal of medicinal food*, 9(2), p.182‑186.

Kanwar, Y.S. et al., 2008. Diabetic nephropathy: mechanisms of renal disease progression. *Experimental biology and medicine (Maywood, N.J.)*, 233(1), p.4‑11.

Kawa, J.M., Przybylski, R. & Taylor, C.G., 2003. Urinary chiro-inositol and myo-inositol excretion is elevated in the diabetic db/db mouse and streptozotocin diabetic rat. *Experimental biology and medicine (Maywood, N.J.)*, 228(8), p.907‑914.

Kawa, J.M., Taylor, C.G. & Przybylski, R., 2003. Buckwheat concentrate reduces serum glucose in streptozotocin-diabetic rats. *Journal of agricultural and food chemistry*, 51(25), p.7287‑7291.

Kawano, K. et al., 1994. OLETF (Otsuka Long-Evans Tokushima Fatty) rat: a new NIDDM rat strain. *Diabetes research and clinical practice*, 24 Suppl, p.S317‑320.

Kawasaki, T. et al., 2009. Rats fed fructose-enriched diets have characteristics of nonalcoholic hepatic steatosis. *The Journal of nutrition*, 139(11), p.2067‑2071.

Kelly, K.L. et al., 1987. A phospho-oligosaccharide mimics the effect of insulin to inhibit isoproterenol-dependent phosphorylation of phospholipid methyltransferase in isolated adipocytes. *The Journal of biological chemistry*, 262(31), p.15285‑15290.

Kemmochi, Y. et al., 2013. Metabolic Disorders and Diabetic Complications in Spontaneously Diabetic Torii Leprfa Rat: A New Obese Type 2 Diabetic Model. *Journal of Diabetes Research*, 2013. Available at: http://www.ncbi.nlm.nih.gov/pmc/articles/PMC3647577/ [Consulté le juillet 28, 2013].

Kennington, A.S. et al., 1990. Low urinary chiro-inositol excretion in non-insulin-dependent diabetes mellitus. *The New England journal of medicine*, 323(6), p.373‑378.

Kim, J.-I. et al., 2005. Effects of pinitol isolated from soybeans on glycaemic control and cardiovascular risk factors in Korean patients with type II diabetes mellitus: a randomized controlled study. *European journal of clinical nutrition*, 59(3), p.456‑458.

Kim, J.K. et al., 2001. Prevention of fat-induced insulin resistance by salicylate. *Journal of Clinical Investigation*, 108(3), p.437‑446.

Kim, M.J. et al., 2007. Effect of pinitol on glucose metabolism and adipocytokines in uncontrolled type 2 diabetes. *Diabetes research and clinical practice*, 77 Suppl 1, p.S247‑251.

Kim, M.-K. et al., 2012. Endoplasmic reticulum stress and insulin biosynthesis: a review. *Experimental diabetes research*, 2012, p.509437.

Kim, S.M. et al., 2010. Modulatory Effect of Rice Bran and Phytic Acid on Glucose Metabolism in High Fat-Fed C57BL/6N Mice. *Journal of clinical biochemistry and nutrition*, 47(1), p.12‑17.

Klemera, P. & Doubal, S., 2000. Gompertz — A program for evaluation and comparison of survival curves. *AGE*, 23(3), p.129‑132.

Kluge, R. et al., 2012. Pathophysiology and Genetics of Obesity and Diabetes in the New Zealand Obese Mouse: A Model of the Human Metabolic Syndrome. In H.-G. Joost, H. Al-Hasani, & A. Schürmann, éd. *Animal Models in Diabetes Research*. Methods in Molecular Biology. Humana Press, p. 59‑73. Available at: http://link.springer.com/protocol/10.1007/978-1-62703-068-7_5 [Consulté le août 7, 2013].

Kobayasi, R. et al., 2010. Oxidative stress and inflammatory mediators contribute to endothelial dysfunction in high-fat diet-induced obesity in mice. *Journal of hypertension*, 28(10), p.2111‑2119.

Kohli, R. et al., 2010. High-fructose, medium chain trans fat diet induces liver fibrosis and elevates plasma coenzyme Q9 in a novel murine model of obesity and nonalcoholic steatohepatitis. *Hepatology (Baltimore, Md.)*, 52(3), p.934‑944.

Koppe-Guichard, L., 2013. Rôle d'une toxine urémique, le p-crésyl-sulfate, dans la physiopathologie de l'insulino-résistance associée à la maladie rénale chronique. PhD in Physiology. Lyon : Claude Bernard University of Lyon. 153 pages.

Koracevic, D. et al., 2001. Method for the measurement of antioxidant activity in human fluids. *Journal of Clinical Pathology*, 54(5), p.356‑361.

Labarca, C. & Paigen, K., 1980. A simple, rapid, and sensitive DNA assay procedure. *Analytical Biochemistry*, 102(2), p.344‑352.

Lam, S. et al., 2006. A phase I study of myo-inositol for lung cancer chemoprevention. *Cancer epidemiology, biomarkers & prevention*, 15(8), p.1526‑1531.

Larner, J. et al., 1988. Insulin mediators: structure and formation. *Cold Spring Harbor symposia on quantitative biology*, 53 Pt 2, p.965‑971.

Larner, J. et al., 2003. Isolation, structure, synthesis, and bioactivity of a novel putative insulin mediator. A galactosamine chiro-inositol pseudo-disaccharide Mn2+ chelate with insulin-like activity. *Journal of medicinal chemistry*, 46(15), p.3283‑3291.

Larner, J., Brautigan, D.L. & Thorner, M.O., 2010. D-chiro-inositol glycans in insulin signaling and insulin resistance. *Molecular medicine (Cambridge, Mass.)*, 16(11-12), p.543‑552.

Larner, J. & Craig, J.W., 1996. Urinary myo-inositol-to-chiro-inositol ratios and insulin resistance. *Diabetes care*, 19(1), p.76‑78.

Larner, J. & Huang, L.C., 1999. Identification of a novel inositol glycan signaling pathway with significant therapeutic relevance to insulin resistance: an insulin signaling model using both tyrosine kinase and G-proteins. *Diabetes Reviews*, 7(3), p.217.

Lebrun, P. & Van Obberghen, E., 2008. SOCS proteins causing trouble in insulin action. *Acta physiologica (Oxford, England)*, 192(1), p.29‑36.

Lee, M.O., 1929. Determination of the Surface Area of the White Rat with Its Application to the Expression of Metabolic Results. *American Journal of Physiology -- Legacy Content*, 89(1), p.24‑33.

Lei, F. et al., 2007. Evidence of anti-obesity effects of the pomegranate leaf extract in high-fat diet induced obese mice. *International journal of obesity (2005)*, 31(6), p.1023‑1029.

Lenzen, S., 2008. The mechanisms of alloxan- and streptozotocin-induced diabetes. *Diabetologia*, 51(2), p.216‑226.

Leonard, B.L. et al., 2005. Insulin resistance in the Zucker diabetic fatty rat: a metabolic characterisation of obese and lean phenotypes. *Acta diabetologica*, 42(4), p.162‑170.

Letexier, D. et al., 2003. Comparison of the expression and activity of the lipogenic pathway in human and rat adipose tissue. *Journal of Lipid Research*, 44(11), p.2127‑2134.

Lewin, L.M. et al., 1976. Studies on the metabolic role of myo-inositol. Distribution of radioactive myo-inositol in the male rat. *The Biochemical journal*, 156(2), p.375‑380.

Li, Y. et al., 2004. Protein kinase C Theta inhibits insulin signaling by phosphorylating IRS1 at Ser(1101). *The Journal of biological chemistry*, 279(44), p.45304‑45307.

Lim, J.S. et al., 2010. The role of fructose in the pathogenesis of NAFLD and the metabolic syndrome. *Nature reviews. Gastroenterology & hepatology*, 7(5), p.251‑264.

Lin, X. et al., 2009. Human sodium/inositol cotransporter 2 (SMIT2) transports inositols but not glucose in L6 cells. *Archives of biochemistry and biophysics*, 481(2), p.197‑201.

Lipson, K.L. et al., 2006. Regulation of insulin biosynthesis in pancreatic beta cells by an endoplasmic reticulum-resident protein kinase IRE1. *Cell metabolism*, 4(3), p.245‑254.

Liu, L. et al., 2007. Upregulation of myocellular DGAT1 augments triglyceride synthesis in skeletal muscle and protects against fat-induced insulin resistance. *Journal of Clinical Investigation*, 117(6), p.1679‑1689.

Lizcano, J.M. & Alessi, D.R., 2002. The insulin signalling pathway. *Current biology: CB*, 12(7), p.R236‑238.

Llewelyn, J.G., 2003. The diabetic neuropathies: types, diagnosis and management. *Journal of neurology, neurosurgery, and psychiatry*, 74 Suppl 2, p.ii15‑ii19.

Lomba, A. et al., 2010. Obesity induced by a pair-fed high fat sucrose diet: methylation and expression pattern of genes related to energy homeostasis. *Lipids in health and disease*, 9, p.60.

Lombardo, Y.B. et al., 1996. Long-term administration of a sucrose-rich diet to normal rats: relationship between metabolic and hormonal profiles and morphological changes in the endocrine pancreas. *Metabolism: clinical and experimental*, 45(12), p.1527‑1532.

De Luca, C. & Olefsky, J.M., 2008. Inflammation and insulin resistance. *FEBS Letters*, 582(1), p.97‑105.

Lundbaek, K., 1962. Intravenous glucose tolerance as a tool in definition and diagnosis of diabetes mellitus. *British Medical Journal*, 1(5291), p.1507‑1513.

Ma, M.M. et al., 2007. Sphingosine kinase 1 participates in insulin signalling and regulates glucose metabolism and homeostasis in KK/Ay diabetic mice. *Diabetologia*, 50(4), p.891‑900.

Machicao, F. et al., 1990. Mannose, glucosamine and inositol monophosphate inhibit the effects of insulin on lipogenesis. Further evidence for a role for inositol phosphate-oligosaccharides in insulin action. *The Biochemical journal*, 266(3), p.909‑916.

Maeba, R. et al., 2008. Myo-inositol treatment increases serum plasmalogens and decreases small dense LDL, particularly in hyperlipidemic subjects with metabolic syndrome. *Journal of Nutritional Science and Vitaminology*, 54(3), p.196‑202.

Mark, A.L. et al., 1999. Contrasting blood pressure effects of obesity in leptin-deficient ob/ob mice and agouti yellow obese mice. *Journal of hypertension*, 17(12 Pt 2), p.1949‑1953.

Massiera, F. et al., 2010. A Western-like fat diet is sufficient to induce a gradual enhancement in fat mass over generations. *Journal of lipid research*, 51(8), p.2352‑2361.

Matarrelli, B. et al., 2013. Effect of dietary myo-inositol supplementation in pregnancy on the incidence of maternal gestational diabetes mellitus and fetal outcomes: a randomized controlled trial. *The journal of maternal-fetal & neonatal medicine: the official journal of the European Association of Perinatal Medicine, the Federation of Asia and Oceania Perinatal Societies, the International Society of Perinatal Obstetricians*.

Matsui, K. et al., 2008. Diabetes-associated complications in Spontaneously Diabetic Torii fatty rats. *Experimental animals / Japanese Association for Laboratory Animal Science*, 57(2), p.111‑121.

McLaurin, J. et al., 2000. Inositol stereoisomers stabilize an oligomeric aggregate of Alzheimer amyloid beta peptide and inhibit abeta -induced toxicity. *The Journal of Biological Chemistry*, 275(24), p.18495‑18502.

Melez, K.A. et al., 1980. Diabetes is Associated with Autoimmunity in the New Zealand Obese (NZO) Mouse. *Diabetes*, 29(10), p.835‑840.

Ménard, S.L. et al., 2010. Abnormal in vivo myocardial energy substrate uptake in diet-induced type 2 diabetic cardiomyopathy in rats. *American journal of physiology. Endocrinology and metabolism*, 298(5), p.E1049‑1057.

Meng, P.H. et al., 2009. Crosstalks between myo-inositol metabolism, programmed cell death and basal immunity in Arabidopsis. *PloS one*, 4(10), p.e7364.

Miatello, R. et al., 2005. Chronic administration of resveratrol prevents biochemical cardiovascular changes in fructose-fed rats. *American journal of hypertension*, 18(6), p.864‑870.

Minozzi, M., Nordio, M. & Pajalich, R., 2013. The Combined therapy myo-inositol plus D-Chiro-inositol, in a physiological ratio, reduces the cardiovascular risk by improving the lipid profile in PCOS patients. *European review for medical and pharmacological sciences*, 17(4), p.537‑540.

Moe, G.W. et al., 2004. In vivo TNF-alpha inhibition ameliorates cardiac mitochondrial dysfunction, oxidative stress, and apoptosis in experimental heart failure. *American journal of physiology. Heart and circulatory physiology*, 287(4), p.H1813‑1820.

Mohamed-Ali, V., Pinkney, J.H. & Coppack, S.W., 1998. Adipose tissue as an endocrine and paracrine organ. *International Journal of Obesity and Related Metabolic Disorders: Journal of the International Association for the Study of Obesity*, 22(12), p.1145‑1158.

Molitoris, B.A., Karl, I.E. & Daughaday, W.H., 1980. Concentration of myo-inositol in skeletal muscle of the rat occurs without active transport. *The Journal of clinical investigation*, 65(4), p.783‑788.

Moran, T.H. & Bi, S., 2006. Hyperphagia and obesity in OLETF rats lacking CCK-1 receptors. *Philosophical Transactions of the Royal Society B: Biological Sciences*, 361(1471), p.1211‑1218.

Moroki, T. et al., 2013. Morphological Characterization of Systemic Changes in KK-Ay Mice as an Animal Model of Type 2 Diabetes. *In vivo (Athens, Greece)*, 27(4), p.465‑472.

Muglia, L. & Locker, J., 1984. Extrapancreatic insulin gene expression in the fetal rat. *Proceedings of the National Academy of Sciences of the United States of America*, 81(12), p.3635‑3639.

Murase, T. et al., 2001. Dietary diacylglycerol suppresses high fat and high sucrose diet-induced body fat accumulation in C57BL/6J mice. *Journal of lipid research*, 42(3), p.372‑378.

Nakagawa, T. et al., 2005. Hypothesis: fructose-induced hyperuricemia as a causal mechanism for the epidemic of the metabolic syndrome. *Nature clinical practice. Nephrology*, 1(2), p.80‑86.

Nakamura, T. et al., 2010. Double-stranded RNA-dependent protein kinase links pathogen sensing with stress and metabolic homeostasis. *Cell*, 140(3), p.338‑348.

Nakayama, T. et al., 2010. Dietary fructose causes tubulointerstitial injury in the normal rat kidney. *American journal of physiology. Renal physiology*, 298(3), p.F712‑720.

Nascimento, N.R.F. et al., 2006. Inositols prevent and reverse endothelial dysfunction in diabetic rat and rabbit vasculature metabolically and by scavenging superoxide. *Proceedings of the National Academy of Sciences of the United States of America*, 103(1), p.218‑223.

Nayak, B. et al., 2005. Modulation of renal-specific oxidoreductase/myo-inositol oxygenase by high-glucose ambience. *Proceedings of the National Academy of Sciences of the United States of America*, 102(50), p.17952‑17957.

Nayak, B. et al., 2011. Transcriptional and Post-translational Modulation of myo-Inositol Oxygenase by High Glucose and Related Pathobiological Stresses. *Journal of Biological Chemistry*, 286(31), p.27594‑27611.

Needham, J., 1924. Studies on Inositol: The Synthesis of Inositol in the Animal Body. *The Biochemical journal*, 18(5), p.891‑904.

Nestler, J.E. et al., 1999. Ovulatory and metabolic effects of D-chiro-inositol in the polycystic ovary syndrome. *The New England Journal of Medicine*, 340(17), p.1314‑1320.

Noda, K. et al., 2010. An animal model of spontaneous metabolic syndrome: Nile grass rat. *FASEB journal: official publication of the Federation of American Societies for Experimental Biology*, 24(7), p.2443‑2453.

Ogawa, W., Matozaki, T. & Kasuga, M., 1998. Role of binding proteins to IRS-1 in insulin signalling. *Molecular and cellular biochemistry*, 182(1-2), p.13‑22.

Ohashi, K. et al., 2006. Adiponectin Replenishment Ameliorates Obesity-Related Hypertension. *Hypertension*, 47(6), p.1108‑1116.

Ohta, T., Miyajima, K. & Yamada, T., 2011. Pathophysiological Changes in Pre-Diabetic Stage of Spontaneously Diabetic Torii (SDT) Rats. *Journal of Animal and Veterinary Advances*, 10(7), p.813‑817.

Oishi, K., Zheng, B. & Kuo, J.F., 1990. Inhibition of Na,K-ATPase and sodium pump by protein kinase C regulators sphingosine, lysophosphatidylcholine, and oleic acid. *The Journal of biological chemistry*, 265(1), p.70‑75.

Olgemöller, B. et al., 1990. Competitive inhibition by glucose of myo-inositol incorporation into cultured porcine aortic endothelial cells. *Biochimica et biophysica acta*, 1052(1), p.47‑52.

Ortlepp et al., 2000. A metabolic syndrome of hypertension, hyperinsulinaemia and hypercholesterolaemia in the New Zealand obese mouse. *European Journal of Clinical Investigation*, 30(3), p.195–202.

Ortlepp, J.. et al., 2002. Inhibition of the renin–angiotensin system ameliorates genetically determined hyperinsulinemia. *European Journal of Pharmacology*, 436(1–2), p.145‑150.

Ortmeyer, H K et al., 1993. Chiroinositol deficiency and insulin resistance. I. Urinary excretion rate of chiroinositol is directly associated with insulin resistance in spontaneously diabetic rhesus monkeys. *Endocrinology*, 132(2), p.640‑645.

Ortmeyer, H. K. et al., 1993. Chiroinositol deficiency and insulin resistance. II. Acute effects of D-chiroinositol administration in streptozotocin-diabetic rats, normal rats given a glucose load, and spontaneously insulin-resistant rhesus monkeys. *Endocrinology*, 132(2), p.646.

Ortmeyer, H.K., 1996. Dietary myoinositol results in lower urine glucose and in lower postprandial plasma glucose in obese insulin resistant rhesus monkeys. *Obesity research*, 4(6), p.569‑575.

Ortmeyer, H.K., Larner, J. & Hansen, B.C., 1995. Effects of D-chiroinositol added to a meal on plasma glucose and insulin in hyperinsulinemic rhesus monkeys. *Obesity research*, 3 Suppl 4, p.605S‑608S.

Ozcan, U. et al., 2004. Endoplasmic reticulum stress links obesity, insulin action, and type 2 diabetes. *Science (New York, N.Y.)*, 306(5695), p.457‑461.

Özcan, U. et al., 2006. Chemical Chaperones Reduce ER Stress and Restore Glucose Homeostasis in a Mouse Model of Type 2 Diabetes. *Science*, 313(5790), p.1137‑1140.

Pak, Y. et al., 1998. In vivo chiro-inositol metabolism in the rat: a defect in chiro-inositol synthesis from myo-inositol and an increased incorporation of chiro-[3H]inositol into phospholipid in the Goto-Kakizaki (G.K) rat. *Molecules and Cells*, 8(3), p.301‑309.

Pak, Y. et al., 1992. In vivo conversion of [3H]myoinositol to [3H]chiroinositol in rat tissues. *The Journal of biological chemistry*, 267(24), p.16904‑16910.

Pak, Y. et al., 1993. Insulin stimulates the biosynthesis of chiro-inositol-containing phospholipids in a rat fibroblast line expressing the human insulin receptor. *Proceedings of the National Academy of Sciences of the United States of America*, 90(16), p.7759‑7763.

Panchal, S.K. et al., 2011. High-carbohydrate, high-fat diet-induced metabolic syndrome and cardiovascular remodeling in rats. *Journal of cardiovascular pharmacology*, 57(5), p.611‑624.

Panchal, S.K. & Brown, L., 2010. Rodent Models for Metabolic Syndrome Research. *BioMed Research International*, 2011. Available at: http://www.hindawi.com/journals/bmri/2011/351982/abs/ [Consulté le juillet 11, 2013].

Paolisso, G. et al., 1995. Metabolic benefits deriving from chronic vitamin C supplementation in aged non-insulin dependent diabetics. *J Am Coll Nutr*, 14(4), p.387‑392.

Papaleo, E. et al., 2007. Myo-inositol in patients with polycystic ovary syndrome: a novel method for ovulation induction. *Gynecological endocrinology: the official journal of the International Society of Gynecological Endocrinology*, 23(12), p.700‑703.

Parekh, P.I. et al., 1998. Reversal of diet-induced obesity and diabetes in C57BL/6J mice. *Metabolism: clinical and experimental*, 47(9), p.1089‑1096.

Park, H.J. et al., 2011. Green tea extract attenuates hepatic steatosis by decreasing adipose lipogenesis and enhancing hepatic antioxidant defenses in ob/ob mice. *The Journal of Nutritional Biochemistry*, 22(4), p.393‑400.

Park, S.Y., Ryu, J. & Lee, W., 2005. O-GlcNAc modification on IRS-1 and Akt2 by PUGNAc inhibits their phosphorylation and induces insulin resistance in rat primary adipocytes. *Experimental & molecular medicine*, 37(3), p.220‑229.

Patel, J., Iyer, A. & Brown, L., 2009. Evaluation of the chronic complications of diabetes in a high fructose diet in rats. *Indian journal of biochemistry & biophysics*, 46(1), p.66‑72.

Pederson, T.M., Kramer, D.L. & Rondinone, C.M., 2001. Serine/threonine phosphorylation of IRS-1 triggers its degradation: possible regulation by tyrosine phosphorylation. *Diabetes*, 50(1), p.24‑31.

Petit, V. et al., 2007. Chronic high-fat diet affects intestinal fat absorption and postprandial triglyceride levels in the mouse. *Journal of lipid research*, 48(2), p.278‑287.

Pettegrew, J.W. et al., 2001. Chronic myo-inositol increases rat brain phosphatidylethanolamine plasmalogen. *Biological Psychiatry*, 49(5), p.444‑453.

Pieczenik, S.R. & Neustadt, J., 2007. Mitochondrial dysfunction and molecular pathways of disease. *Experimental and molecular pathology*, 83(1), p.84‑92.

Pillon, N.J., 2010. Rôle des hydroxy-alkénals, dérivés de peroxydation lipidique, dans la physiopathologie de l'insulino-résistance. PhD in Biochemistry. Lyon: INSA de Lyon. 147 pages.

Poitout, V. et al., 2006. Regulation of the Insulin Gene by Glucose and Fatty Acids. *The Journal of Nutrition*, 136(4), p.873‑876.

Poitout, V. & Robertson, R.P., 2008. Glucolipotoxicity: Fuel Excess and β-Cell Dysfunction. *Endocrine Reviews*, 29(3), p.351‑366.

Popa, S. & Mot, M., 2013. Beta-Cell Function and Failure in Type 2 Diabetes. In K. Masuo, éd. *Type 2 Diabetes*. InTech. Available at: http://www.intechopen.com/books/type-2-diabetes/beta-cell-function-and-failure-in-type-2-diabetes [Consulté le septembre 23, 2013].

Portha, B. et al., 1974. Diabetogenic Effect of Streptozotocin in the Rat During the Perinatal Period. *Diabetes*, 23(11), p.889‑895.

Powell, D.J. et al., 2003. Ceramide disables 3-phosphoinositide binding to the pleckstrin homology domain of protein kinase B (PKB)/Akt by a PKCzeta-dependent mechanism. *Molecular and cellular biology*, 23(21), p.7794‑7808.

Puigserver, P. et al., 2003. Insulin-regulated hepatic gluconeogenesis through FOXO1-PGC-1alpha interaction. *Nature*, 423(6939), p.550‑555.

Raffone, E., Rizzo, P. & Benedetto, V., 2010. Insulin sensitiser agents alone and in co-treatment with r-FSH for ovulation induction in PCOS women. *Gynecological endocrinology: the official journal of the International Society of Gynecological Endocrinology*, 26(4), p.275‑280.

Randle, P.J. et al., 1963. The glucose fatty-acid cycle. Its role in insulin sensitivity and the metabolic disturbances of diabetes mellitus. *Lancet*, 1(7285), p.785‑789.

Reddy, V.N. et al., 1992. Study of the polyol pathway and cell permeability changes in human lens and retinal pigment epithelium in tissue culture. *Investigative ophthalmology & visual science*, 33(7), p.2334‑2339.

Ritzel, R.A. et al., 2007. Human islet amyloid polypeptide oligomers disrupt cell coupling, induce apoptosis, and impair insulin secretion in isolated human islets. *Diabetes*, 56(1), p.65‑71.

Roberts, C.K., Hevener, A.L. & Barnard, R.J., 2013. Metabolic Syndrome and Insulin Resistance: Underlying Causes and Modification by Exercise Training. *Comprehensive Physiology*, 3(1), p.1‑58.

Romero, G. et al., 1990. Anti-inositolglycan antibodies selectively block some of the actions of insulin in intact BC3H1 cells. *Proceedings of the National Academy of Sciences of the United States of America*, 87(4), p.1476‑1480.

Romero, G., Garmey, J.C. & Veldhuis, J.D., 1993. The involvement of inositol phosphoglycan mediators in the modulation of steroidogenesis by insulin and insulin-like growth factor-I. *Endocrinology*, 132(4), p.1561‑1568.

Rudich, A. et al., 1999. Lipoic acid protects against oxidative stress induced impairment in insulin stimulation of protein kinase B and glucose transport in 3T3-L1 adipocytes. *Diabetologia*, 42(8), p.949‑957.

Rui, L. et al., 2001. Insulin/IGF-1 and TNF-alpha stimulate phosphorylation of IRS-1 at inhibitory Ser307 via distinct pathways. *The Journal of clinical investigation*, 107(2), p.181‑189.

Rutkowski, D.T. & Hegde, R.S., 2010. Regulation of basal cellular physiology by the homeostatic unfolded protein response. *The Journal of Cell Biology*, 189(5), p.783‑794.

Rutledge, A.C. & Adeli, K., 2007. Fructose and the metabolic syndrome: pathophysiology and molecular mechanisms. *Nutrition reviews*, 65(6 Pt 2), p.S13‑23.

Saltiel, A.R. & Cuatrecasas, P., 1986. Insulin stimulates the generation from hepatic plasma membranes of modulators derived from an inositol glycolipid. *Proceedings of the National Academy of Sciences*, 83(16), p.5793‑5797.

Saltiel, A.R. & Kahn, C.R., 2001. Insulin signalling and the regulation of glucose and lipid metabolism. *Nature*, 414(6865), p.799‑806.

Samols, E. & Stagner, J.I., 1988. Intra-islet regulation. *The American journal of medicine*, 85(5A), p.31‑35.

Samols, E. & Stagner, J.I., 1990. Islet somatostatin--microvascular, paracrine, and pulsatile regulation. *Metabolism: clinical and experimental*, 39(9 Suppl 2), p.55‑60.

Samuel, V.T. & Shulman, G.I., 2012. Mechanisms for Insulin Resistance: Common Threads and Missing Links. *Cell*, 148(5), p.852‑871.

Santamaria, A. et al., 2012. One-year effects of myo-inositol supplementation in postmenopausal women with metabolic syndrome. *Climacteric: the journal of the International Menopause Society*, 15(5), p.490‑495.

Santuré, M. et al., 2002. Induction of insulin resistance by high-sucrose feeding does not raise mean arterial blood pressure but impairs haemodynamic responses to insulin in rats. *British journal of pharmacology*, 137(2), p.185‑196.

Sasase, T. et al., 2007. Increased fat absorption and impaired fat clearance cause postprandial hypertriglyceridemia in Spontaneously Diabetic Torii rat. *Diabetes Research and Clinical Practice*, 78(1), p.8‑15.

Sasase, T. et al., 2013. The spontaneously diabetic torii rat: an animal model of nonobese type 2 diabetes with severe diabetic complications. *Journal of diabetes research*, 2013, p.976209.

Sato, A. et al., 2010. Antiobesity effect of eicosapentaenoic acid in high-fat/high-sucrose diet-induced obesity: importance of hepatic lipogenesis. *Diabetes*, 59(10), p.2495‑2504.

Schlemmer, U. et al., 2009. Phytate in foods and significance for humans: food sources, intake, processing, bioavailability, protective role and analysis. *Molecular nutrition & food research*, 53 Suppl 2, p.S330‑375.

Schnedl, W.J. et al., 1994. STZ Transport and Cytotoxicity: Specific Enhancement in GLUT2-Expressing Cells. *Diabetes*, 43(11), p.1326‑1333.

Schweiger, M. et al., 2006. Adipose triglyceride lipase and hormone-sensitive lipase are the major enzymes in adipose tissue triacylglycerol catabolism. *The Journal of biological chemistry*, 281(52), p.40236‑40241.

Schweiger, M. et al., 2012. G0/G1 switch gene-2 regulates human adipocyte lipolysis by affecting activity and localization of adipose triglyceride lipase. *Journal of lipid research*, 53(11), p.2307‑2317.

Seino, S., Shibasaki, T. & Minami, K., 2011. Dynamics of insulin secretion and the clinical implications for obesity and diabetes. *Journal of Clinical Investigation*, 121(6), p.2118‑2125.

Seo, H.-Y. et al., 2008. Endoplasmic Reticulum Stress-Induced Activation of Activating Transcription Factor 6 Decreases Insulin Gene Expression via Up-Regulation of Orphan Nuclear Receptor Small Heterodimer Partner. *Endocrinology*, 149(8), p.3832‑3841.

Sharma, N. et al., 2008. High-sugar diets increase cardiac dysfunction and mortality in hypertension compared to low-carbohydrate or high-starch diets. *Journal of hypertension*, 26(7), p.1402‑1410.

Shen, H. et al., 2012. Herbal constituent sequoyitol improves hyperglycemia and glucose intolerance by targeting hepatocytes, adipocytes, and β-cells. *American Journal of Physiology - Endocrinology And Metabolism*, 302(8), p.E932‑E940.

Shinohara, M. et al., 2000. A new spontaneously diabetic non-obese Torii rat strain with severe ocular complications. *International journal of experimental diabetes research*, 1(2), p.89‑100.

Sima, A.A., Thomas, P.K., et al., 1997. Diabetic neuropathies. *Diabetologia*, 40 Suppl 3, p.B74‑77.

Sima, A.A., Dunlap, J.A., et al., 1997. Supplemental myo-inositol prevents L-fucose-induced diabetic neuropathy. *Diabetes*, 46(2), p.301‑306.

Simon, C. & Brandenberger, G., 2002. Ultradian oscillations of insulin secretion in humans. *Diabetes*, 51 Suppl 1, p.S258‑261.

Sivakumar, S., Palsamy, P. & Subramanian, S.P., 2010a. Attenuation of oxidative stress and alteration of hepatic tissue ultrastructure by D-pinitol in streptozotocin-induced diabetic rats. *Free radical research*, 44(6), p.668‑678.

Sivakumar, S., Palsamy, P. & Subramanian, S.P., 2010b. Impact of D-pinitol on the attenuation of proinflammatory cytokines, hyperglycemia-mediated oxidative stress and protection of kidney tissue ultrastructure in streptozotocin-induced diabetic rats. *Chemico-biological interactions*, 188(1), p.237‑245.

Sivakumar, S. & Subramanian, Sorimuthu P, 2009. D-pinitol attenuates the impaired activities of hepatic key enzymes in carbohydrate metabolism of streptozotocin-induced diabetic rats. *General physiology and biophysics*, 28(3), p.233‑241.

Sivakumar, S. & Subramanian, Sorimuthu Pillai, 2009. Pancreatic tissue protective nature of D-Pinitol studied in streptozotocin-mediated oxidative stress in experimental diabetic rats. *European journal of pharmacology*, 622(1-3), p.65‑70.

Skyler JS, S.J., 2013. THe evolution of type 1 diabetes. *JAMA*, 309(23), p.2491‑2492.

Srinivasan, K. & Ramarao, P., 2007. Animal models in type 2 diabetes research: an overview. *The Indian journal of medical research*, 125(3), p.451‑472.

Sugita, H. et al., 2005. Inducible Nitric-oxide Synthase and NO Donor Induce Insulin Receptor Substrate-1 Degradation in Skeletal Muscle Cells. *Journal of Biological Chemistry*, 280(14), p.14203‑14211.

Sun, T. et al., 2002. Both myo-inositol to chiro-inositol epimerase activities and chiro-inositol to myo-inositol ratios are decreased in tissues of GK type 2 diabetic rats compared to Wistar controls. *Biochemical and biophysical research communications*, 293(3), p.1092‑1098.

Sutherland, L.N. et al., 2008. Time course of high-fat diet-induced reductions in adipose tissue mitochondrial proteins: potential mechanisms and the relationship to glucose intolerance. *American journal of physiology. Endocrinology and metabolism*, 295(5), p.E1076‑1083.

Suzuki, S. et al., 1991. Molecular mechanism of insulin resistance in spontaneous diabetic GK (Goto-Kakizaki) rats. *New Directions in Research and Clinical Works for Obesity and Diabetes Mellitus. New York: Elsevier Science*, p.197‑203.

Sweazea, K.L., Lekic, M. & Walker, B.R., 2010. Comparison of mechanisms involved in impaired vascular reactivity between high sucrose and high fat diets in rats. *Nutrition & metabolism*, 7, p.48.

Swierczynski, J. et al., 2000. Comparative study of the lipogenic potential of human and rat adipose tissue. *Metabolism, Clinical and Experimental*, 49(5), p.594‑599.

Takenawa, T. & Egawa, K., 1977. CDP-diglyceride:inositol transferase from rat liver. Purification and properties. *The Journal of biological chemistry*, 252(15), p.5419‑5423.

Tappy, L. et al., 2010. Fructose and metabolic diseases: new findings, new questions. *Nutrition (Burbank, Los Angeles County, Calif.)*, 26(11-12), p.1044‑1049.

Teruel, T., Hernandez, R. & Lorenzo, M., 2001. Ceramide mediates insulin resistance by tumor necrosis factor-alpha in brown adipocytes by maintaining Akt in an inactive dephosphorylated state. *Diabetes*, 50(11), p.2563‑2571.

Tran, L.T., Yuen, V.G. & McNeill, J.H., 2009. The fructose-fed rat: a review on the mechanisms of fructose-induced insulin resistance and hypertension. *Molecular and cellular biochemistry*, 332(1-2), p.145‑159.

Trayhurn, P. & Wood, I.S., 2004. Adipokines: inflammation and the pleiotropic role of white adipose tissue. *The British Journal of Nutrition*, 92(3), p.347‑355.

Ueda, H. et al., 2000. Paternal-maternal effects on phenotypic characteristics in spontaneously diabetic Nagoya-Shibata-Yasuda mice. *Metabolism*, 49(5), p.651‑656.

Ueda, H. et al., 1995. The NSY mouse: a new animal model of spontaneous NIDDM with moderate obesity. *Diabetologia*, 38(5), p.503‑508.

Unfer, V. et al., 2012. Effects of myo-inositol in women with PCOS: a systematic review of randomized controlled trials. *Gynecological endocrinology: the official journal of the International Society of Gynecological Endocrinology*, 28(7), p.509‑515.

Unfer, V. et al., 2011. Myo-inositol rather than D-chiro-inositol is able to improve oocyte quality in intracytoplasmic sperm injection cycles. A prospective, controlled, randomized trial. *European review for medical and pharmacological sciences*, 15(4), p.452‑457.

Varela, I. et al., 1990. Asymmetric distribution of the phosphatidylinositol-linked phospho-oligosaccharide that mimics insulin action in the plasma membrane. *European journal of biochemistry / FEBS*, 188(2), p.213‑218.

Velussi, M. et al., 1997. Long-term (12 months) treatment with an anti-oxidant drug (silymarin) is effective on hyperinsulinemia, exogenous insulin need and malondialdehyde levels in cirrhotic diabetic patients. *Journal of Hepatology*, 26(4), p.871‑879.

Venturella, R. et al., 2012. [Assessment of the modification of the clinical, endocrinal and metabolical profile of patients with PCOS syndrome treated with myo-inositol]. *Minerva ginecologica*, 64(3), p.239‑243.

Veroni, M.C., Proietto, J. & Larkins, R.G., 1991. Evolution of insulin resistance in New Zealand obese mice. *Diabetes*, 40(11), p.1480‑1487.

Vogel, H. et al., 2013. Estrogen Deficiency Aggravates Insulin Resistance and Induces β-Cell Loss and Diabetes in Female New Zealand Obese Mice. *Hormone and Metabolic Research*, 45(06), p.430‑435.

Wada, T. et al., 2010. Spironolactone improves glucose and lipid metabolism by ameliorating hepatic steatosis and inflammation and suppressing enhanced gluconeogenesis induced by high-fat and high-fructose diet. *Endocrinology*, 151(5), p.2040‑2049.

Wang, Y. et al., 2013. Spontaneous Type 2 Diabetic Rodent Models. *Journal of Diabetes Research*, 2013. Available at: http://www.hindawi.com/journals/jdr/2013/401723/abs/ [Consulté le juillet 11, 2013].

Wang, Y., Nishina, P.M. & Naggert, J.K., 2009. Degradation of IRS1 leads to impaired glucose uptake in adipose tissue of the type 2 diabetes mouse model TALLYHO/Jng. *Journal of Endocrinology*, 203(1), p.65‑74.

Wei, X. et al., 2011. Cyanidin-3-O-β-glucoside improves obesity and triglyceride metabolism in KK-Ay mice by regulating lipoprotein lipase activity. *Journal of the science of food and agriculture*, 91(6), p.1006‑1013.

Weir, G.C. et al., 1981. Islet Secretion in a New Experimental Model for Non-insulin-dependent Diabetes. *Diabetes*, 30(7), p.590‑595.

Whiting, P.H., Palmano, K.P. & Hawthorne, J.N., 1979. Enzymes of myo-inositol and inositol lipid metabolism in rats with streptozotocin-induced diabetes. *Biochemical Journal*, 179(3), p.549‑553.

Wilcox, G., 2005. Insulin and Insulin Resistance. *Clinical Biochemist Reviews*, 26(2), p.19‑39.

Winegrad, A.I., 1987. Banting lecture 1986. Does a common mechanism induce the diverse complications of diabetes? *Diabetes*, 36(3), p.396‑406.

Wisse, B.E., 2004. The inflammatory syndrome: the role of adipose tissue cytokines in metabolic disorders linked to obesity. *Journal of the American Society of Nephrology: JASN*, 15(11), p.2792‑2800.

Woods, S.C. et al., 2003. A controlled high-fat diet induces an obese syndrome in rats. *The Journal of nutrition*, 133(4), p.1081‑1087.

Xie, Y. et al., 2010. [Dracorhodin perchlorate inhibit high glucose induce serum and glucocorticoid induced protein kinase 1 and fibronectin expression in human mesangial cells]. *China journal of Chinese materia medica*, 35(15), p.1996‑2000.

Xu, X. et al., 2008. The CUL7 E3 Ubiquitin Ligase Targets Insulin Receptor Substrate 1 for Ubiquitin-Dependent Degradation. *Molecular cell*, 30(4), p.403‑414.

Yamashita, Y. et al., 2013. Detection of orally administered inositol stereoisomers in mouse blood plasma and their effects on translocation of glucose transporter 4 in skeletal muscle cells. *Journal of agricultural and food chemistry*, 61(20), p.4850‑4854.

Yang, X. et al., 2010. The G(0)/G(1) switch gene 2 regulates adipose lipolysis through association with adipose triglyceride lipase. *Cell metabolism*, 11(3), p.194‑205.

Yao, Y. et al., 2008. D-chiro-inositol-enriched tartary buckwheat bran extract lowers the blood glucose level in KK-Ay mice. *Journal of agricultural and food chemistry*, 56(21), p.10027‑10031.

Yap, A. et al., 2007. Rat L6 myotubes as an in vitro model system to study GLUT4-dependent glucose uptake stimulated by inositol derivatives. *Cytotechnology*, 55(2-3), p.103‑108.

Yorek, M.A. & Dunlap, J.A., 1989. The effect of elevated glucose levels on myo-inositol metabolism in cultured bovine aortic endothelial cells. *Metabolism: clinical and experimental*, 38(1), p.16‑22.

Yorek, M.A., Stefani, M.R. & Moore, S.A., 1991. Acute and chronic exposure of mouse cerebral microvessel endothelial cells to increased concentrations of glucose and galactose: effect on myo-inositol metabolism, PGE2 synthesis, and Na+/K(+)-ATPase transport activity. *Metabolism: clinical and experimental*, 40(4), p.347‑358.

Yuan, M. et al., 2001. Reversal of Obesity- and Diet-Induced Insulin Resistance with Salicylates or Targeted Disruption of Ikkβ. *Science*, 293(5535), p.1673‑1677.

Zaman, A.K.M.T. et al., 2004. Salutary effects of attenuation of angiotensin II on coronary perivascular fibrosis associated with insulin resistance and obesity. *Journal of molecular and cellular cardiology*, 37(2), p.525‑535.

Zarrouki, B. et al., 2010. Cirsimarin, a potent antilipogenic flavonoid, decreases fat deposition in mice intra-abdominal adipose tissue. *International Journal of Obesity (2005)*, 34(11), p.1566‑1575.

Zechner, R. et al., 2012. FAT SIGNALS - Lipases and Lipolysis in Lipid Metabolism and Signaling. *Cell Metabolism*, 15(3), p.279‑291.

Supplements

Supplementary Table 1 – Eligible RCTs where MI has been evaluated for the treatment of PCOS patients. From (Unfer et al. 2012)

Reference	Study design	Duration	Intervention	N° of subjects	Inclusion criteria	Exclusion criteria	Assessment of the response	Results
34	Randomized, controlled vs. folic acid	12 weeks	MYO 2 g FA 200 mg/day	N= 20 Treatment: 10 Placebo: 10	Presence of micropolycystic ovaries at ultrasound; mild-to-severe hirsutism and/or acne; oligomenorrhoea or amenorrhoea; absence of enzymatic adrenal deficiency and/or other endocrine diseases; normal PRL levels (range 5–25 ng/ml); no hormonal treatment for at least 6 months before the study.	Not described	LH, FSH, PRL, E2, A, 17OHP, T, insulin, cortisol, OGTT for insulin, glucose, C-peptide determinations, vaginal ultrasound examination Ferriman–Gallway score, BMI, HOMA	LH, PRL, T, insulin levels, LH/FSH results were significantly reduced. Insulin sensitivity results were significantly improved. Menstrual cyclicity was restored in all amenorrheic and oligomenorrheic subjects.
35	Double-blind, randomized, controlled vs. folic acid	12–16 weeks	MYO 4 g FA 400 mg/day	N°= 42 Treatment: 23 Placebo: 19	Presence of oligomenorrhea, high serum-free testosterone level and/or hirsutism presence of micropolycystic ovaries at ultrasound	Not described	Systolic/diastolic blood pressure, triglycerides, cholesterol, BMI, waist-to-hip ratio, plasma glucose and insulin sensitivity, total/free T, DHEAS, SHBG, A, progesterone peak value	MI increased insulin sensitivity, improved glucose tolerance and decreased glucose-stimulated insulin release. There was a decrement in serum total T and serum-free T concentrations. In addition, there was a decrement in systolic and diastolic blood pressure. Plasma triglycerides and total cholesterol concentration decreased.
21	Prospective, randomized, controlled vs. folic acid	During ovulation induction for ICSI	MYO 4 g FA 200 mg/day	N°= 60 Treatment: 30 Placebo: 30	Age: <40 years PCOS women diagnosed by oligo amenorrhea, hyperandrogenism or thyperandrogenism and typical features of ovaries on ultrasound scan	Other medical conditions causing ovulatory disorders: hyperinsulinemia, hyperprolactinemia, hypothyroidism, or androgen excess, such as adrenal hyperplasia or Cushing syndrome	Number of morphologically mature oocytes retrieved, embryo quality, pregnancy and implantation rates. Total number of days of FSH stimulation, total dose of gonadotropin administered, E2 level on the day of hCG administration, fertilization rate per number of retrieved oocytes, embryo cleavage rate, live birth and miscarriage rate, cancellation rate, and incidence of moderate or severe ovarian hyperstimulation syndrome	Total r-FSH units and number of days of stimulation were significantly reduced in the myo-inositol group. Peak E2 levels at hCG administration were significantly lower in patients receiving myo-inositol. The mean number of oocytes retrieved did not differ in the two groups, whereas in the group cotreated with myo-inositol the mean number of germinal vesicles and degenerated oocytes was significantly reduced, with a trend for increased percentage of oocytes in metaphase II
22	Double-blind, randomized, controlled vs. folic acid	16 weeks	MYO 4 g FA 200 mg/day	N°= 92 Treatment: 45 Placebo: 47	Age: <35 years women with oligoamenorrhea, amenorrhea and PCOS ovaries. Ovaries were described as polycystic (PCOs) about the criteria of Adams et al.[a]	Patients with significant hyperprolactinemia, abnormal thyroid function tests and congenital adrenal hyperplasia	Ovarian activity was monitored using serum E2, P and LH. Ovulation frequency was calculated using the ratio of luteal phase weeks to observation weeks. Inibin-b, fasting glucose, fasting insulin, or insulin AUC, VLDL, LDL, HDL, total cholesterol, triglycerides, BMI.	Beneficial effect of MYO treatment upon ovarian function, anthropometric measures and lipid profiles
36	Randomized, controlled vs. metformin	Until the end of the study or positive pregnancy test	MYO 4 g FA 400 mg/day	N°= 120 Treatment: 60 Placebo: 60	Age: <35 years Women with PCOS defined by Rotterdam Criteria	Other medical condition causing ovulatory dysfunction, tubal defects, semen parameters defects.	Restoration of spontaneous ovarian activity by weekly serum P dosage and a transvaginal ultrasound scan documenting the presence of follicular growth or luteal cyst	Both metformin and MYO can be considered as first-line treatment for restoring normal menstrual cycles in most patients with PCOS, even if MI treatment seems to be more effective than metformin
37	Double-blind, randomized, controlled vs. placebo	16 weeks	Inositol 200 mg/day	N°= 283 Treatment: 136 Placebo: 147	Age: <35 years Women with oligomenorrhea, amenorrhea and PCOS ovaries. Ovaries were described as polycystic(PCOs) about the criteria of Adams et al[b]	Patients with significant hyperprolactinemia, abnormal thyroid function tests and congenital adrenal hyperplasia	Ovarian activity was monitored using serum E2, P and LH. Ovulation frequency was calculated using the ratio of luteal phase weeks to observation weeks. Inibin-b, fasting glucose, fasting insulin, or insulin AUC, VLDL, LDL, HDL, total cholesterol, triglycerides, BMI.	effective than metformin

FA, folic acid; PRL, prolactin; E2, oestradiol; A, androstenedione; 17OHP, 17-hydroxy-progesterone; T, testosterone; P, progesterone; OGTT, oral glucose tolerance; BMI, body mass index; LH, luteinizing hormone; FSH, follicle stimulating hormone; DHEAS, dehydroepiandrosterone; SHBG, sex hormone binding globulin; AUC, area under the curve of OGTT; VLDL, very-low-density lipoprotein; LDL, low-density lipoprotein; HDL, high-density lipoprotein.

[a]OGTT performed sampling 15 minutes before and 30, 60, 90, 120 and 240 minutes after the oral assumption of 75 g of glucose.

[b]Adams J, Polson JW, Franks S. Prevalence of polycystic ovaries in women with anovulation and idiopathic hirsutism. Br Med J 1986;293:355–359.

References : 21,(Papaleo et al. 2007) ; 22, (Gerli et al. 2007) ; 34, (Genazzani et al. 2008) ; 35, (Costantino et al. 2009) ; 36, (Raffone et al. 2010) ; 37, (Gerli et al. 2003).

Supplementary Table 2 – Clinical trials in which MI supplementation has been evaluated for the treatment of metabolic diseases (PCOS excluded)

Reference	Study design	Duration	Treatment	N° of subjects	Inclusion criteria	Exclusion criteria	Assessment of the response	Results
D'Anna et al, 2013	randomized, controlled vs. placebo (FA 200µg twice/day), open-label	from the 1st trimester through the whole pregnancy	2g MI + 200µg FA twice/day	N=220 Placebo : 110 MI : 110	1) first-degree relatives (mother, father or both) affected by T2D; 2) prepregnancy BMI <30kg/m²; 3) fasting plasma glucose <126mg/dL and random glycemia < 200mg/dL; 4) single pregnancy; 5) Caucasian race	1) prepregnancy BMI ≥ 30 kg/m²; 2) previous GDM ; 3) pre-gestational diabetes ; 4) first trimester glycosuria ; 5) first-degree relatives not affected by T2D ; 6) fasting and random glycemia ≥ 126 and 200 mg/dL respectively 7) twin pregnancies ; 8) associated therapy with corticosteroids ; 9) not Caucasian race ; 10) PCOS women	**Main outcome** : Incidence of gestational diabetes (diagnosed with IADPSG recommendations) ; **Secondary outcomes** : prevalence of fetal macrosomia (fetal weight > 4,000 g at delivery), caesarean section, gestational hypertension, preterm delivery, neonatal hypoglycemia (<45mg/dL), shoulder distocia and distress respiratory syndrome.	Incidence of gestational diabetes significantly reduced in the MI group compared with the placebo group: 6 vs. 15.3%, respectively (P = 0.04) and reduction of gestational diabetes risk occurrence (odds ratio 0.35). Significantly reduced fasting (p<0,001) and 1h-glycemia (p<0,02) at OGTT in the MI group. A statistically significant reduction of mean fetal weight at delivery in MI group and absence of fetal macrosomia (vs 7 cases in placebo group). No difference between the groups for the other secondary outcomes studied.
Matarrelli et al, 2013	randomized, controlled vs. placebo, double-blind	for the entire pregnancy period	2g MI + 200µg FA twice/day taken with at least 6 hours interval	N=75 Placebo : 39 MI : 36	Consecutive singleton pregnant women with an elevated fasting glucose (glycemia ≥5.1 mmol/L or 92 mg/dL and ≤7.0 mmol/L or 1.26 mg/dL) in the 1st or early 2nd trimester	Pregestational obesity (BMI above 35) and refusal to participate were the only exclusion criteria	OGTT at 24 to 28 weeks' gestation. BMI, need for maternal insulin therapy, macrosomia, polyhydramnios, neonatal birth weight and hypoglycaemia	The incidence of gestational diabetes in mid pregnancy was significantly reduced (p=0.001) in women who received MI compared to placebo (relative risk 0.127). Women supplemented with MI required less insulin therapy, delivered at a later gestational age, had significantly smaller babies with fewer episodes of neonatal hypoglycaemia.
Santamaria et al, 2012	randomized, controlled vs. placebo	12 months	MI 2g /day	N=80 Placebo : 40 MI : 40	Postmenopausal women with MetS (at least 3 criteria of the ATP III of the National Cholesterol Education Programme) ; Age between 50 and 60 years old and at least a 12-month period from the last menstruation	Use of glucose-lowering drugs and/or lipid-lowering drugs	serum glucose, insulin, HOMA-IR, TG, total and HDL- CST, BMI, WC and BP at baseline and after 6 and 12 months of treatment.	Serum glucose, insulin, HOMA-IR, TG, total and HDL-CST and BP significantly improved with MI compared to placebo. A significant difference from basal values was highlighted only in the MI group (p < 0.0001) for both BMI and WC at 12 months. In the MI group, the number of women without MetS was eight (20%) vs. only one in the control group after 12 months of diet.
Giordano et al, 2011	randomized, controlled vs. placebo	6 months	MI 2g/day	N=80 Placebo : 40 MI : 40	Postmenopausal women with MetS (at least 3 criteria of the ATP III of the National Cholesterol Education Programme) ; Age between 50 and 60 years old and at least a 12-month period from the last menstruation	Use of glucose-lowering drugs and/or lipid-lowering drugs	serum glucose, insulin, HOMA-IR, TG, total and HDL- CST and BP at baseline and after 6 and 12 months of treatment.	In the group treated with MI, significant improvements in diastolic BP (−11%), HOMA index (−75%), serum TG (−20%) and in HDL cholesterol (+22%) were observed.
Corrado et al, 2011	randomized, controlled vs. folic acid (FA) 400µg/day, open label	8 weeks	2g MI + 200µg FA twice/day – Inofolic® (MI + FA)	N=69 Placebo : 45 MI : 24	Gestational diabetes (diagnosed with an OGTT perfomed between 24-28 weeks of gestation)	Insulin therapy ; premature delivery (before 35 weeks of gestation)	Fasting HOMA-IR and adiponectin blood level	Fasting glucose and insulin, and consequently HOMA-IR, decreased in both groups (50% in the MI group vs. 29% in the control group), but the decline in the MI group was significantly greater than that in the control group (P = 0.0001). Adiponectin increased in the MI group while it decreased in the control group (P = 0.009).
Maeba et al, 2008	not a placebo controlled study	2 weeks	5g MI/day the 1st week, 10g MI/day the 2nd week	N = 17	Male (n=15) or female (n=2) hyperlipidemic subjects with (N=8) or without (N=9) MetS defined according to Japanese guidelines	Medications	Fasting Serum Plasmalogens, TG, Total-, LDL-, HDL- and sdLDL- cholesterol levels and fasting blood glucose levels.	After MI treatment, significant increase in plasmalogen-related parameters, and significant decrease in atherogenic cholesterols including sdLDL, were observed. Among the hyperlipidemic subjects treated with MI, subjects with MetS had a significant increase in plasmalogens and a tendency towards reduced sdLDL, hsCRP and blood glucose levels compared to subjects without MetS.

Search procedure : we searched in the MedLine ® database (using PubMed as a search engine) with the thesaurus terms "myo-inositol", "myo-inositol supplementation" or "dietary myo-inositol" in combination with "insulin", "diabetes", "metabolic syndrome" and/or "clinical trials". Papers were restricted to those published in English. Studies on women with polycystic ovary syndrome were excluded. Preference was given to randomized controlled trials. Abbreviations : ATP, Adult Treatment Panel ; BMI, Body Mass Index ; BP, Blood Pressure ; CST, cholesterol ; FA, Folic Acid ; HDL, High Density Lipoprotein ; HOMA-IR, HOmeostasis Model Assessment of Insulin Resistance ; IADPSG, International Association of Diabetes in Pregnancy Study Group ; LDL, Low Density Lipoprotein ; MetS, Metabolic Syndrome ; MI, myo-inositol ; OGTT, Oral Glucose Tolerance Test ; sdLDL, small dense LDL ; TG, triglycerides ; WC, Waist Circumference.

1

THESE SOUTENUE DEVANT L'INSTITUT NATIONAL DES SCIENCES APPLIQUEES DE LYON

NOM : CROZE   DATE de SOUTENANCE : 27 Novembre 2013
(avec précision du nom de jeune fille, le cas échéant)

Prénoms : Marine

TITRE :

Study of the insulin-sensitizing effect of *myo*-inositol in mouse :
Evaluation of the nutritional interest of a myo-inositol supplementation

NATURE : Doctorat   Numéro d'ordre : 2013ISAL0139

Ecole doctorale : Ecole Doctorale Interdisciplinaire Science Santé (ED205)

Spécialité : Biochimie

RESUME :

Insulin resistance is the first step in the development of type 2 diabetes thus finding insulin-sensitizing strategies is challenging for scientists. Some inositol isomers or derivatives have been reported to exert insulin-mimetic activity. *myo*-Inositol being the most abundant stereoisomeric form of inositol in foodstuffs, we tested its insulin-mimetic potential in the long term and as a nutritional strategy for insulin resistance prevention and/or treatment.

This study demonstrates that chronic *myo*-inositol treatment improves insulin sensitivity and reduces white adipose tissue accretion in mice. The insulin-sensitizing effect seems to be related to a direct effect on insulin signaling pathway. Reduction in adipose tissue mass also probably contribute to the long term effect of *myo*-inositol on insulin sensitivity.

myo-Inositol supplementation also improved insulin sensitivity and reduced white adipose tissue deposition in mice fed a high fat diet, but did not prevent insulin-resistance or obesity development. On one year-old mice with established obesity and altered glycemic control, *myo*-inositol supplementation showed no beneficial effect. *myo*-Inositol apparently acts on adipose tissue through reduction of *de novo* lipogenesis rather than stimulation of lipolysis. This may explain the lack or loss of *myo*-inositol efficiency in reducing adipose tissue mass in contexts of already well-established obesity (old mice) or reduced *de novo* lipogenesis (high fat diet feeding). Generation of inositol glycan putative insulin second messengers is probably reduced in context of insulin resistance which may explain the reduced effect of *myo*-inositol in both obese mice models. Moreover, *myo*-Inositol did not prevent lipotoxicity and so the associated insulin-resistance in high fat diet fed mice.

In conclusion, *myo*-inositol alone and/or in a context of overnutrition is not a suitable strategy for the prevention or treatment of insulin resistance. Combining it with other insulin sentitizing strategies may however potentiate their action and help reducing insulin-sensitizing drugs use.

MOTS-CLES : inositol, insulin, diabetes, obesity, skeletal muscle, white adipose tissue, high fat diet, *de novo* lipogenesis.

Laboratoire (s) de recherche :

INSERM U1060 / INSA de Lyon
« Cardiovascular, Metabolism, diabetologia and Nutrition » (CarMeN)

Directeur de thèse: Dr. Christophe SOULAGE et Pr. Michel GUICHARDANT

Président de jury : Dr. Hubert VIDAL

Composition du jury :   Dr. Karine COUTURIER, Examinateur
Pr. Michel GUICHARDANT, Directeur de thèse
Pr. Béatrice MORIO, Rapporteur
Pr. Michel NARCE, Rapporteur
Dr. Christophe SOULAGE, Directeur de thèse